NATURAL PRODUCTS AS LESS TOXIC ANTITUMORAL/ANTIANGIOGENIC AGENTS COMPARED TO SYNTHETIC CONVENTIONAL CHEMOTHERAPY

EDITED BY: Cecilia Veronica Nunez, Laura Alaniz and Marne Carvalho de Vasconcellos

PUBLISHED IN: Frontiers in Pharmacology and Frontiers in Oncology

frontiers Research Topics

frontiers

ISSN 1664-8714
ISBN 978-2-83250-706-3
DOI 10.3389/978-2-83250-706-3

About Frontiers

Frontiers is more than just an open-access publisher of scholarly articles: it is a pioneering approach to the world of academia, radically improving the way scholarly research is managed. The grand vision of Frontiers is a world where all people have an equal opportunity to seek, share and generate knowledge. Frontiers provides immediate and permanent online open access to all its publications, but this alone is not enough to realize our grand goals.

Frontiers Journal Series

The Frontiers Journal Series is a multi-tier and interdisciplinary set of open-access, online journals, promising a paradigm shift from the current review, selection and dissemination processes in academic publishing. All Frontiers journals are driven by researchers for researchers; therefore, they constitute a service to the scholarly community. At the same time, the Frontiers Journal Series operates on a revolutionary invention, the tiered publishing system, initially addressing specific communities of scholars, and gradually climbing up to broader public understanding, thus serving the interests of the lay society, too.

Dedication to Quality

Each Frontiers article is a landmark of the highest quality, thanks to genuinely collaborative interactions between authors and review editors, who include some of the world's best academicians. Research must be certified by peers before entering a stream of knowledge that may eventually reach the public - and shape society; therefore, Frontiers only applies the most rigorous and unbiased reviews.
Frontiers revolutionizes research publishing by freely delivering the most outstanding research, evaluated with no bias from both the academic and social point of view. By applying the most advanced information technologies, Frontiers is catapulting scholarly publishing into a new generation.

What are Frontiers Research Topics?

Frontiers Research Topics are very popular trademarks of the Frontiers Journals Series: they are collections of at least ten articles, all centered on a particular subject. With their unique mix of varied contributions from Original Research to Review Articles, Frontiers Research Topics unify the most influential researchers, the latest key findings and historical advances in a hot research area! Find out more on how to host your own Frontiers Research Topic or contribute to one as an author by contacting the Frontiers Editorial Office: frontiersin.org/about/contact

NATURAL PRODUCTS AS LESS TOXIC ANTITUMORAL/ANTIANGIOGENIC AGENTS COMPARED TO SYNTHETIC CONVENTIONAL CHEMOTHERAPY

Topic Editors:
Cecilia Veronica Nunez, National Institute of Amazonian Research (INPA), Brazil
Laura Alaniz, CONICET Northwest Research and Transfer Center of the Province of Buenos Aires (CIT NOBA), Argentina
Marne Carvalho de Vasconcellos, Federal University of Amazonas, Brazil

Citation: Nunez, C. V., Alaniz, L., de Vasconcellos, M. C., eds. (2022). Natural Products as Less Toxic Antitumoral/Antiangiogenic Agents Compared to Synthetic Conventional Chemotherapy. Lausanne: Frontiers Media SA.
doi: 10.3389/978-2-83250-706-3

Table of Contents

frontiers | Frontiers in Pharmacology

TYPE Editorial
PUBLISHED 21 October 2022
DOI 10.3389/fphar.2022.1055516

OPEN ACCESS

EDITED AND REVIEWED BY
Olivier Feron,
Université catholique de Louvain,
Belgium

*CORRESPONDENCE
Cecilia Veronica Nunez,
cecilia@inpa.gov.br

SPECIALTY SECTION
This article was submitted to Renal Pharmacology,
a section of the journal
Frontiers in Pharmacology

RECEIVED 27 September 2022
ACCEPTED 12 October 2022
PUBLISHED 21 October 2022

CITATION
Nunez CV, Vasconcellos MCd and Alaniz L (2022), Editorial: Are natural products, used as antitumoral/antiangiogenic agents, less toxic than synthetic conventional chemotherapy? *Front. Pharmacol.* 13:1055516.
doi: 10.3389/fphar.2022.1055516

Editorial: Are natural products, used as antitumoral/ antiangiogenic agents, less toxic than synthetic conventional chemotherapy?

Cecilia Veronica Nunez[1]*, Marne Carvalho de Vasconcellos[2] and Laura Alaniz[3]

[1]Bioprospection and Biotechnology Laboratory, National Institute of Amazonian Research (INPA), Manaus, Brazil, [2]Faculty of Pharmaceutical Sciences, Federal University of Amazonas (UFAM), Manaus, Brazil, [3]CIBA, Northwest Research and Transfer Center of the Province of Buenos Aires (UNNOBA), CIT NOBA (UNNOBA-UNSAdA-CONICET), Junin, Bs.As., Argentina

KEYWORDS

natural products, antitumoral, antiangiogenic, new drugs, mechanisms of action

Editorial on the Research Topic
Are natural products, used as antitumoral/antiangiogenic agents, less toxic than synthetic conventional chemotherapy?

Natural products can be isolated from several biological sources, such as plants, fungi, animals, plant cell cultures, among others. Some of these compounds can reduce tumor growth and the spreading of tumor cells by blocking their migration or preventing blood vessel formation that contribute to the colonization of distant tissues. A high percentage of drugs derived from natural products are published, however, most of them fail to gain approval for treating cancer by the European Medicines Agency in Europe or national regulatory authorities of regional reference in the Americas. It has been shown that combination of natural products with conventional clinical chemotherapy and radiotherapy in antitumoral and antiangiogenic treatments reduced the toxicity of the therapy (Tuorkey, 2015; Braicu et al., 2017). The major challenge is the lack of scientific evidence to support their approbation and determine the if it is beneficial to be used as monotherapy or if the combination with conventional therapies. Their use and approval require research that defines that these natural products offer adequate therapeutic action, are less toxic or have a synergistic effect and reduce toxicity in combination with chemotherapy and radiotherapy in combination.

In this special issue, several articles and reviews discuss the beneficial use of natural products as antitumoral/antiangiogenic agents compared or in combination with synthetic conventional chemotherapy.

The original article by Liang and collaborators discusses the use of a flavonoid isolated from the rhizome of *Alpinia officinarum*: galangin. The authors used *in vitro* and *in vivo* gastric tumor models, demonstrating that this compound inhibited tumor growth by modulating different signals, such as p-JAK2, p-STAT3, Bcl-2, cleaved caspase-3, cleaved PARP, and Ki67. Specifically, galangin appears to induce apoptosis and decrease cell proliferation, by modulating STAT3/ROS axis, demonstrating the potential application of galangin for gastric cancer therapy.

Vitale and collaborators' review provides an overview of 4-methylumbelliferone (4-MU), an orally available dietetic product, derivative of coumarin and mainly found in the plant family Umbelliferae or Apiaceae, focusing on its utility in different solid and hematological cancer. The authors discuss 4-MU mechanisms of action observed in tumors in different human models. They discuss different molecular mechanisms of 4-MU associated with its capacity to inhibit hyaluronan molecules in the tumor extracellular matrix and the biological impact on different cells of the tumor microenvironment. Finally, the authors comment about the possibility of 4-MU use as a co-adjuvant drug in conventional antineoplastic therapies. And since 4-MU, originally identified as a hepatoprotective component approved in European countries, could be considered its repositioning as an antitumor drug.

The original work of Zhang and collaborators discusses the role of Saikosaponin A (SSA), a main triterpenoid saponin component from *Radix bupleurum*. Their findings first revealed that SSA possesses potent antiangiogenic activities, thereby suppressing tumor growth by blocking VEGFR2 signaling pathways.

Wang and collaborators' original article show a gut microbiota study in which they report the identification of one anticancer gut bacterial strain (AD16). Five new compounds were isolated and identified (streptonaphthalenes A and B (1–2), pestaloficins F and G (3–4), and eudesmanetetraiol A (5)), together with nine previously known compounds, were isolated from the effective fractions of AD16. The analysis of network pharmacology suggested that three compounds could be the key components for the anti-NSCLC (non-small cell lung cancer) activity of AD16. In addition to the PI3K–Akt signaling pathway, the proteoglycans in the cancer pathway could be involved in the anti-NSCLC action of AD16.

Yangbo and collaborators showed that the combination of sodium butyrate with cisplatin enhanced the apoptosis in gastrointestinal cancer cells through the mitochondrial apoptosis-related pathways *in vitro* and *in vivo*. Their combination produced a synergic effect. Sodium butyrate showed to be an alternative to other conventional chemotherapeutic drugs because it causes less cytotoxic effects, since it acts by modulating the intestinal microbiota, with studies already proving both its improvement the patient's immune system and its effective use in other types of cancer. This, suggests that this combination may be an alternative for the treatment of a gastrointestinal cancer.

In another original paper, Liu and collaborators studied the effects of gracillin against gastric carcinoma cell line. They demonstrated that gracillin acted as inducer of the endogenous apoptosis, inhibiting cell migration and EMT (epithelial-mesenchymal transition process) pathway in BGC-823 cell line, through the tumor necrosis factor–α inducible protein-8, also called TIPE2. The EMT process is involved in tumor metastasis, characterized by high expression of N-cadherin and vimentin and low expression of E-cadherin. Thus, the authors demonstrated that gracillin has the potential to suppress tumor cell migration through the EMT process in the researched cell line, contributing to the emergence of another possible molecule to act against gastric cancer, currently the third most common cause of cancer in the world.

Zhan and collaborators reviewer the effects and mechanisms of OSW-1 (isolated from *Ornithogalum saundersiae*) against cancer *in vitro* and *in vivo*. OWS-1 was tested in the U.S National Cancer Institute in 60-cell lines *in vitro* screening panel and from these results its mechanism of action was explored. It has been shown to be cytotoxic against neoplastic cells of the ovary, breast, cervix, colon, leukemia, hepatocellular carcinoma and other cancer cells. *In vitro*, OSW-1 had activity on the inhibition of cell proliferation, acting to stop the cell cycle, inducing cell death by apoptosis and, at high concentrations, by necrosis and Golgi stress response. *In vivo* it was effective in inhibiting the growth of tumors such as breast cancer, colon cancer and leukemia. In general, it was able to inhibit tumor growth with a reduction in tumor size and weight, less metastatic nodules in the lungs and longer survival. In the case of the NFATc2 knockdown model, the NFATc2 may be related to suppression of migration and tumor invasion. The compound regulated the action on angiogenesis and the regulation of miRNA expression and various signaling pathways.

Cháirez-Ramírez et al. article reviews the role of the most studied polyphenols in the regulation of key elements of cancer signaling pathways and highlights the importance of a profound understanding of these regulations in order to improve cancer treatment and control with natural products.

Chang and collaborators reviewer the bibliographic background of herbal compounds from traditional Chinese medicine (TCM) applied for treating colorectal cancer (CRC). The authors focused their discussion on the Wnt/β-catenin signaling pathway since it plays a vital role in the initiation and progression of CRC. Also, how these natural

compounds can be used in different stages of tumor disease, from precancerous lesions such as polyps, carcinoma *in situ* to metastatic cancer. Besides, they make an extensive comparison between TCM with small molecules or new drugs targeting Wnt/β-catenin used in combination with traditional chemotherapy that are under preclinical, clinical phase or FDA approved.

Author contributions

All authors listed have made a substantial, direct, and intellectual contribution to the work and approved it for publication.

Conflict of interest

The authors declare that the research was conducted in the absence of any commercial or financial relationships that could be construed as a potential conflict of interest.

Publisher's note

References

Braicu, C., Mehterov, N., Vladimirov, B., Sarafian, V., Nabavi, S. M., Atanasov, A. G., et al. (2017). Nutrigenomics in cancer: Revisiting the effects of natural compounds. *Semin. Cancer Biol.* 46, 84–106. doi:10.1016/j.semcancer.2017.06.011

Tuorkey, M. J. (2015). Cancer therapy with phytochemicals: Present and future perspectives. *Biomed. Environ. Sci.* 28 (11), 808–819. doi:10.3967/bes2015.112

frontiers in Pharmacology

ORIGINAL RESEARCH
published: 26 April 2021
doi: 10.3389/fphar.2021.646628

Galangin Inhibits Gastric Cancer Growth Through Enhancing STAT3 Mediated ROS Production

Xiaohui Liang, Ping Wang, Chun Yang, Fei Huang, Hui Wu, Hailian Shi and Xiaojun Wu**

Shanghai Key Laboratory of Compound Chinese Medicines, The Ministry of Education (MOE) Key Laboratory for Standardization of Chinese Medicines, The SATCM Key Laboratory for New Resources and Quality Evaluation of Chinese Medicines, Institute of Chinese Materia Medica, Shanghai University of Traditional Chinese Medicine, Shanghai, China

Galangin, a flavonoid isolated from the rhizome of *Alpinia officinarum* (Hance), exerts anticancer activities against many cancer cells such as liver cancer, breast cancer, lung cancer and esophageal cancer. However, the effect, as well as the underlying molecular mechanism of galangin on gastric cancer remains to be elucidated. In the present study, galangin inhibited cell viability of MGC 803 cells but not normal gastric mucosal epithelial GES-1 cells. It suppressed cell proliferation accompanied by reduced Ki67 and PCNA expression, promoted apoptosis shown by decreased Bcl-2 and elevated cleaved caspase-3 and cleaved PARP. And, galangin significantly inactivated JAK2/STAT3 pathway. When STAT3 was overexpressed, the proliferation inhibition and apoptosis promotion induced by galangin were abrogated. Meanwhile, galangin increased ROS accumulation, and reduced Nrf2 and NQO-1, but elevated HO-1 in MGC 803 cells. NAC, a ROS scavenger, rescued ROS over-accumulation and proliferation inhibition of galangin. STAT3 overexpression also counteracted excessive ROS accumulation induced by galangin. Consistent with the *in vitro* experiments, in nude mice exnografted with MGC 803 cells, galangin inhibited tumor growth and reversed the abnormally expressed proteins, such as p-JAK2, p-STAT3, Bcl-2, cleaved caspase-3, cleaved PARP, and Ki67. Taken together, galangin was suggested to inhibit the growth of MGC 803 cells through inducing apoptosis and decreasing cell proliferation, which might be mediated by modulating STAT3/ROS axis. Our findings implicate a potential application of galangin for gastric cancer therapy possibly with low toxicity.

Keywords: galangin, gastric cancer, apoptosis, proliferation, ROS, stat3

OPEN ACCESS

Edited by:
Marne Carvalho de Vasconcellos, Federal University of Amazonas, Brazil

Reviewed by:
Agnieszka Zdzisława Robaszkiewicz, University of Łódź, Poland
Ran Zhao, Zhengzhou University, China

****Correspondence:***
Hailian Shi
shihailian2003@163.com
Xiaojun Wu
xiaojunwu320@126.com

Specialty section:
This article was submitted to Pharmacology of Anti-Cancer Drugs, a section of the journal Frontiers in Pharmacology

Received: *27 December 2020*
Accepted: *08 April 2021*
Published: *26 April 2021*

Citation:
Liang X, Wang P, Yang C, Huang F, Wu H, Shi H and Wu X (2021) Galangin Inhibits Gastric Cancer Growth Through Enhancing STAT3 Mediated ROS Production. Front. Pharmacol. 12:646628. doi: 10.3389/fphar.2021.646628

INTRODUCTION

Gastric cancer caused death ranks third among all cancer-related deaths worldwide, and the 5-year survival rate of cancer patients is still less than 5% (Digklia and Wagner, 2016; Wang et al., 2019). Surgery is currently considered to be the only radical treatment. However, chemotherapy almost runs through the treatment of middle- and late-stage gastric cancer after surgery (Amedei et al., 2011; Corso et al., 2013). Unfortunately, its side effects gravely reduce the life quality of cancer patients and

Abbreviations: DCFH-DA, 2′,7′-dichlorofluorescin diacetate; JAK2, Janus associated kinase; HIF1α, hypoxia-inducible factor 1α; HO-1, heme oxygenase-1; MMP, Mitochondrial membrane potential; NF-κB, nuclear factor-kappa B; NQO1, NAD(P)H quinone oxidoreductase 1; Nrf2, NF-E2-related factor 2; PARP, poly (adenosine diphosphate-ribose) polymerase; ROS, reactive oxygen species; STAT3, signal transducer and activator of transcription 3; 5-FU, 5-Fluorouracil.

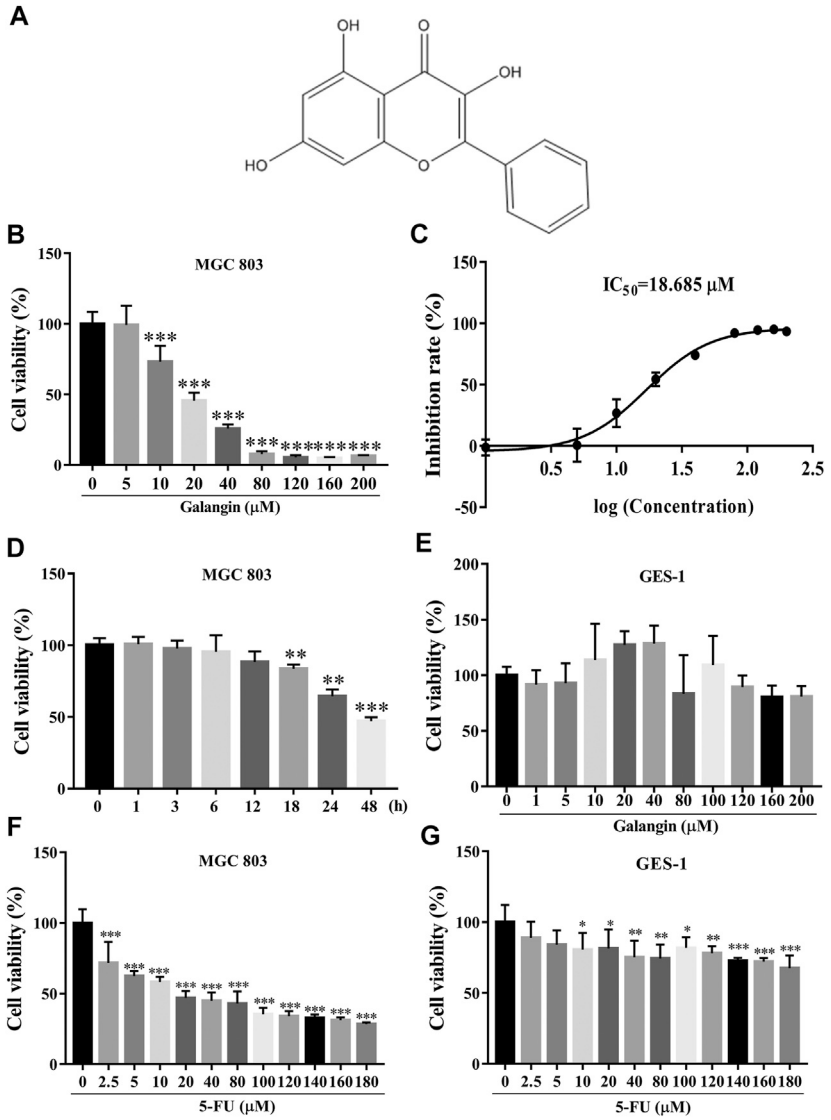

FIGURE 1 | Galangin inhibits cell viability of MGC 803 cells. **(A)** Chemical structure of Galangin. **(B)** Galangin reduced cell viability of MGC 803 cells in a dose-dependent manner after treatment for 48 h. **(C)** IC_{50} of galangin for 48 h in MGC 803 cells. **(D)** Galangin (20 μM) inhibited cell viability of MGC 803 cells in a time-dependent manner. **(E)** Galangin showed no significant effect on GES-1 cells (48 h), a normal gastric mucosal epithelial cell line. **(F)** 5-FU inhibited cell viability of MGC 803 cells (48 h). **(G)** 5-FU inhibited cell viability of GES-1 cells (48 h). All of the data were shown as mean ± SD, and differences among ≥3 groups **(Figures 1B,D,E)** were analyzed via one-way ANOVA with Dunnett test by using GraphPad 7.0 software; $^{*}p < 0.05$; $^{**}p < 0.01$; $^{***}p < 0.001$, compared with control group. n ≥ 3.

limit its clinical efficacy as well. Furthermore, patients with gastric cancer in advanced stages often poorly respond to chemotherapy. Therefore, it is still urgent to develop new chemotherapeutic drug with low toxicity against gastric cancer.

Many oncogenic proteins involve in the cancer progression including signal transducer and activator of transcription 3 (STAT3), an oncogenic transcription factor, which participates in the cell apoptosis (Kim and Park, 2018; Wu et al., 2019), proliferation and autophagy (You et al., 2015; Furtek et al., 2016; Kim et al., 2017; Fathi et al., 2018; Li et al., 2018). Janus associated kinase (JAK)2, an important tyrosine kinase, belongs to the Janus family and plays a positive feedback regulatory role in the expression of STAT3 (Kaptein et al., 1996; Justicia et al., 2000). Suppression of JAK/STAT3 pathway, for instance, by piperlongumine, results in gastric cancer inhibition (Justicia et al., 2000; Song et al., 2016). Therefore, STAT3 should be a valuable target for cancer therapy.

Reactive oxygen species (ROS) is a double-edged sword for cancer cells, and plays different roles in different stages of cancer (Prasad et al., 2017). ROS promotes proliferation and growth of cancer cells through activating various cell signaling pathways, which are primarily mediated through the transcription factors nuclear factor-kappa B (NF-κB) and STAT3, hypoxia-inducible factor 1α (HIF1α), kinases, growth factors, cytokines and other

proteins (Prasad et al., 2017). However, excessive accumulation of ROS can cause cell damage and apoptosis (Kudryavtseva et al., 2016; Ismail et al., 2019).

Galangin, named as 3, 5, 7-trihydroxyflavone (**Figure 1A**), is a natural flavonoid compound, mainly present in the rhizome of *Alpinia officinarum* Hance (Zingiberaceae) (Liu et al., 2018). It showed anti-tumor activity against several cancer cells except gastric cancer, such as liver cancer (Zhang et al., 2010), breast cancer (Liu et al., 2018), lung cancer (Yu et al., 2018) and esophageal cancer (Ren et al., 2016) *in vitro*. In this study, the effect and the underlying molecular mechanism of galangin on gastric cancer cells were investigated, which may extend its potential clinical application.

MATERIALS AND METHODS

Cell Culture

Gastric cancer cell line MGC 803 and mucosal epithelial cell line GES-1 were obtained from Cell Bank, Type Culture Collection of Chinese Academy of Sciences (Shanghai, China). The cells were cultured in RPMI 1640 medium (Meilunbio, Cat. No.: MA 0215) supplemented with 10% fetal bovine serum (FBS, Gibco, Cat. No.: 10099–141), and 1% penicillin and streptomycin (Meilunbio, Cat. No.:MA0110) in a humidified incubator with 5% CO_2 at 37°C.

Cell Viability Assay

After treatment with galangin at different concentrations for 0–48 h, the cells were incubated with 20 μL CCK-8 solution (Cell Counting Kit-8, DOJINDO Laboratories, Cat. No.: CK04) for another 1 h at 37°C. Absorbance of the medium was detected at 450 nm on a Thermo Scientific Varioskan Flash microplate reader (Thermo, United States). The cell viability rate was calculated as follows (absorbance of drug-treated sample/ absorbance of control sample) × 100.

Immunocytochemistry

MGC 803 cells were cultured on coverslips in 24-well plate for 12 h, followed by galangin treatment (20 μM) for 48 h. After washed once with 1 × PBS solution, the cells were fixed with 4% paraformaldehyde (PFA), permeabilized with 0.3% Triton-X-100 and blocked with 10% donkey serum. Then they were incubated with primary antibody against Ki67 (Cat. No. ab16667) overnight at 4°C. Then they were incubated with secondary antibody conjugated with Alexa-488 fluorophore for 1 h at room temperature (RT). After washed with 1 × PBS solution twice, the coverslips with cells were mounted on glass slides with mounting medium containing DAPI. Immunofluorescence images were acquired by an inverted fluorescence microscope (IX81, Olympus, Japan).

Annexin V/PI Staining

After galangin treatment at 20 μM for 48 h, MGC 803 cells were harvested by trypsin without EDTA, and washed twice with 1 × PBS solution. Consequently, the cells were double stained with Annexin V/PI according to manufacturer's protocol, and detected on a Guava flow cytometer (Guava easycyte HT, Millipore, Germany).

Hoechst 33258 Staining

After galangin (20 μM) treatment for 48 h, MGC 803 cells were fixed with 4% PFA for 10 min. Then the cells were gently rinsed with 1 × PBS solution and stained with 10 μg/ml Hoechst 33258 solution for another 15 min. Finally, the cells were washed with 1 × PBS solution, and observed under a fluorescence microscope (IX81).

EdU Staining

MGC 803 cells were plated at a density of 8.0×10^4 cells/ml on a 96-well plate and allowed to adhere to plates overnight. EdU staining was carried out using the EdU imaging kit (RiboBio Co., China). Briefly, cells treated with galangin (20 μM) were first labeled with 50 μM EdU at 37°C for 2 h. Subsequently, they were fixed with 4% PFA for another 30 min, and incubated with 1 × PBS solution containing 0.5% Triton X-100 for 10 min. After washed with 1 × PBS solution, the cells were incubated with 100 μL dying solution for 30 min in the dark. Finally, the nuclei were stained with Hoechst 33342 solution for another 30 min. Fluorescent images were captured by fluorescence microscopy (IX81). Data were analyzed by using ImageJ software.

Mitochondrial Membrane Potential Measurement

MMP was measured by using fluorescent probe JC-1 (Santa Cruz, Cat. No.: sc-364, 116). After galangin (20 μM) treatment for 24 and 48 h, MGC 803 cells were rinsed with 1×HBSS solution (Gibco, Cat. No.: 14025–092) and incubated with JC-1 (10 μM) at 37°C for another 30 min. After that, the cells were rinsed with 1 × HBSS solution once again, and the fluorescent intensity of the JC-1 monomers and aggregates was detected under different conditions (Ex (λ) 485 nm, Em (λ) 530 nm for monomers; Ex (λ) 530 nm, Em (λ) 590 nm for aggragates) on a microplate reader (Varioskan Flash, Thermo Scientific, United States). Fluorescent images were captured under a fluorescent microscope (IX81).

Western Blotting Analysis

MGC 803 cells or tumor tissues were lyzed in CelLytic™ MT Cell Lysis Reagent (Sigma, Cat. No.: C3228) containing protease and phosphatase inhibitors (Roche, Cat. No.: 04693116001, 04906837001) for 30 min on ice. After centrifugation at 12,000 rpm at 4°C for 15 min, the supernatant was collected and the protein concentration was quantified by using BCA assay. Totally, 30 μg proteins from each samples were separated by SDS-PAGE (10%) and transferred onto PVDF membrane by wet transfer. Afterward, the membranes were blocked with 0.5% BSA solution for 1 h and incubated with primary antibodies against JAK2 (1:1,000, D2E12, #3230, CST, United States), p-JAK2 (1: 1,000, C80C3, #3776, CST, United States), STAT3 (1:1,000, 124H6, #9139, CST, United States), p-STAT3 (1:2000, D3A7, #9145, CST, United States), Ki67 (1:500, sp6, #ab16667, Abcam, United States), Bcl-2 (1:1,000, 50E3, #2870, CST, United States), Bax (1:1,000, D2E11, #5023, CST, United States), Cleaved caspase-3 (1:1,000, 5A1E, #9664, CST, United States), Caspase-3 (1:1,000, D3R6Y

TABLE 1 | Primers used in qPCR analysis.

Genes	Forward primer	Reverse primer
Ki67	5′-CAGACATCAGGAGAGACTACAC-3′	5′-AAGAAGTTCAGGTACCTCAGTG-3′
PCNA	5′-TAATTTCCTGTGCAAAAGACGG-3′	5′-AAGAAGTTCAGGTACCTCAGTG-3′
GAPDH	5′- GCACCGTCAAGGCTGAGAAC-3′	5′- TGGTGAAGACGCCAGTGGA-3′

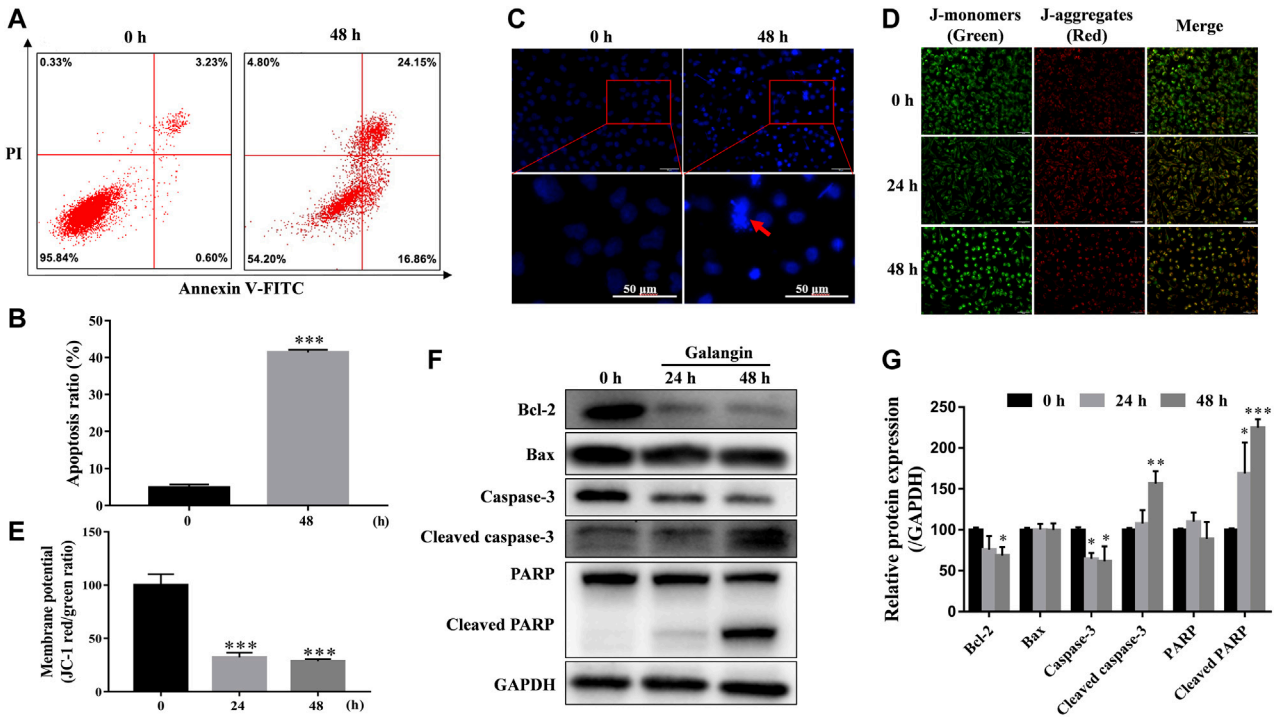

FIGURE 2 | Galangin promotes cell apoptosis. **(A–B)** Glangin enhanced cell apoptosis after treatment for 24 h in MGC 803 cells detected by Annexin V-FITC/PI staining. **(C)** Galangin (20 μM) induced chromatin condensation and nuclear shrinkage or fragmentation in MGC 803 cells after 48 h treatment stained with Hoechst 33,258. **(D–E)** Galangin (20 μM) treatment decreased mitochondrial membrane potential (MMP) in MGC 803 cells after treatment for 24 and 48 h, detected by JC-1 (10 μM) staining. The staining of MGC 803 cells by JC-1 is visible as green for J-monomers (emission maximum of ~529 nm) or red for J-aggregates (with a specific red fluorescence emission maximum at 590 nm). **(F–G)** Galangin (20 μM) modulated protein expression of apoptosis-related proteins in MGC 803 cells after treatment for 24 and 48 h analyzed by Western blotting analysis. All of the data were shown as mean ± SD, and differences among two groups (**Figure 2B**) were analyzed by the Student's *t*-test, and differences among ≥3 groups (**Fig.2E and G**) were analyzed via one-way ANOVA with Dunnett test by using GraphPad 7.0 software; $^{*}p < 0.05$; $^{**}p < 0.01$; $^{***}p < 0.001$, compared with control group. n ≥ 3. Scale bar: 50 μm.

#14220, CST, United States), LaminB1(1:3,000, # 6,581–1 Epitomics United States), Nrf2 (1:500, sc-722, Santa Cruz, United States), NQO1 (1:500, sc-32793, Santa Cruz, United States), HO-1 (1:500, sc136960, Santa Cruz, United States), PARP (1:1,000, 9532s, Santa Cruz, United States), and GAPDH (1:200,000, D16H11, #5174, CST, United States) overnight at 4°C. After washed with 1 × PBST, the membranes were incubated with respective secondary antibodies conjugated with horseradish peroxidase for another 1 h at RT. The protein bands were visualized with Immobilon™ Western Chemiluminescent HRP Substrate (Millipore Corporation, Cat. No.: WBKLS0500), and the images were taken under the visualization instrument Tanon-5200 (Tanon, China).

Real-Time Quantitative PCR

Total RNA was isolated from the harvested MGC 803 cells by using TRIzol Reagent (Ambion, REF: 15596018). cDNA was reversely transcribed from RNA (2 μg) by using Revert Aid First Strand cDNA Synthesis Kit (Thermo, Cat. No.: K1622) according to the manufacturer's protocol. Real-time quantitative PCR was performed with SYBR reagent (VazymE, L/N 7E141I7, Cat. No.: Q111–02) on Quant Studio six Flex System (Life technologies, Cat. No.: 20170777). Quantification of target genes was determined by the $2^{-\Delta\Delta Ct}$ method. And the relative expression of individual genes was normalized to that of GAPDH in the same sample. The sequences of the primers (GeneRay, China) used were listed in **Table 1**.

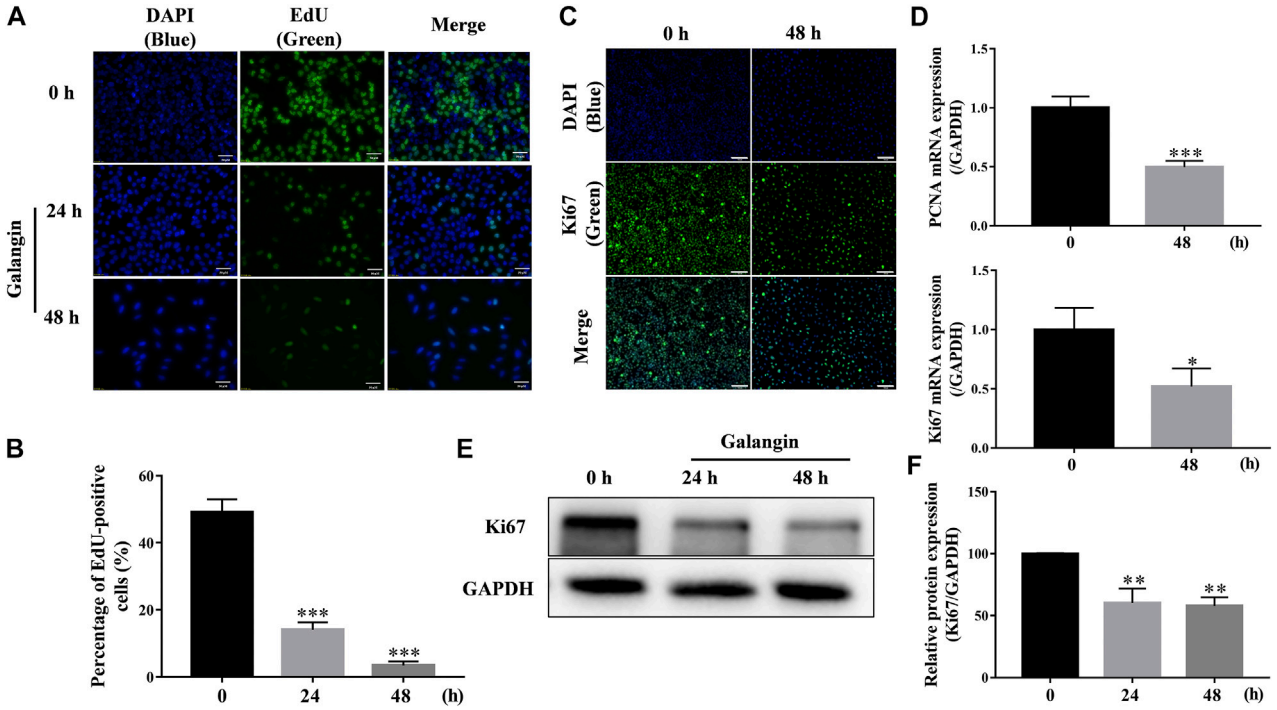

FIGURE 3 | Galangin inhibits proliferation of MGC 803 cells. **(A–B)** Galangin (20 μM) decreased cell proliferation of MGC 803 cells after treatment for 24 and 48 h detected by EdU staining. Scale bar, 50 μm. **(C)** Galangin (20 μM) inhibited protein expression of Ki67 in MGC 803 cells detected by ICC staining. Scale bar, 100 μm. **(D)** Galangin (20 μM) downregulated mRNA expression of PCNA and Ki67 after treatment for 48 h. **(E–F)** Galangin (20 μM) decreased protein expression of Ki67 in MGC 803 cells after treatment for 24 and 48 h analyzed by Western blotting analysis. All of the data were shown as mean ± SD, and differences among two groups (**Figure 3D**) were analyzed by the Student's *t*-test, and differences among ≥3 groups (**Figures 3B,F**) were analyzed via one-way ANOVA with Dunnett test by using GraphPad 7.0 software; $^{*}p < 0.05$; $^{**}p < 0.01$; $^{***}p < 0.001$, compared with control group. n ≥ 3.

ROS Level Measurement

The intracellular ROS production in MGC 803 cells was measured by the oxidation-sensitive fluorescent probe 2′,7′-dichlorofluorescin diacetate (DCFH-DA). In brief, after galangin (20 μM) treatment for 12, 18, 24, and 48 h, MGC 803 cells were gently washed with 1 × HBSS solution and incubated with DCFH-DA (10 μM) for 30 min at 37°C. Fluorescence was immediately measured on a Varioskan Flash microplate reader (Ex (λ) 485 nm, Em (λ) 535 nm, Thermo, United States).

STAT3 Transient Transfection

STAT3 was over-expressed by transiently transfecting p-CMV-STAT3 plasmid in MGC 803 cells. The cells are seeded in a medium dish until growing to 50% confluency, then transiently transfected with p-CMV-STAT3 plasmid or p-CMV plasmid for 24 h by using NEOFECT DNA transfection reagent (Neofect Beijing Biotech, China). After treatment with galangin (20 μM) for 48 h, MGC 803 cells were subjected to CCK-8 assay and western blotting assay.

Animals and Treatments

Healthy 4-week-old male nude mice (12 ± 2 g) were obtained from Shanghai Slake Experimental Animal Co., Ltd. and kept under SPF animal rooms. All animal experiments were carried out in accordance with the protocol approved by the Animal Ethics Committee in Shanghai University of Traditional Chinese Medicine (SHUTCM), which complies with international rules and policies for laboratory animal use and care as found in the European Community guidelines (EEC Directive of 1986; 86/609/EEC). All animal experiments were approved by the institutional Ethics Committee of SHUTCM (PZSHUTCM200724009).

After one week habituation, the mice were inoculated subcutaneously with MGC 803 cells (5×10^6 cells in 200 μL PBS per mouse). Body weight and tumor volume were measured every three days. When the tumor volume reached approximately 50 mm^3, the mice were randomly divided into three groups, namely Control group, Galangin group and 5-Fluorouracil (5-FU) group. Galangin was dissolved in 0.5% sodium carboxylmethylcellulose. 5-Fu was dissolved in 1 × PBS solution. Control mice were intraperitoneally injected with 0.5% sodium carboxylmethylcellulose solution. Galangin-treated mice were administered with galangin (120 mg/kg) by oral gavage once a day. Meanwhile, 5-FU-treated mice were intraperitoneally injected with 5-FU (50 mg/kg) twice a week. Tumor volume was calculated according to the formula [length × $(width)^2$]/2. Three weeks after treatment, all the nude mice were sacrificed, and the isolated tumors were weighted and then cut into several parts which were either fixed in 4% PFA or stored at −80°C for further analysis.

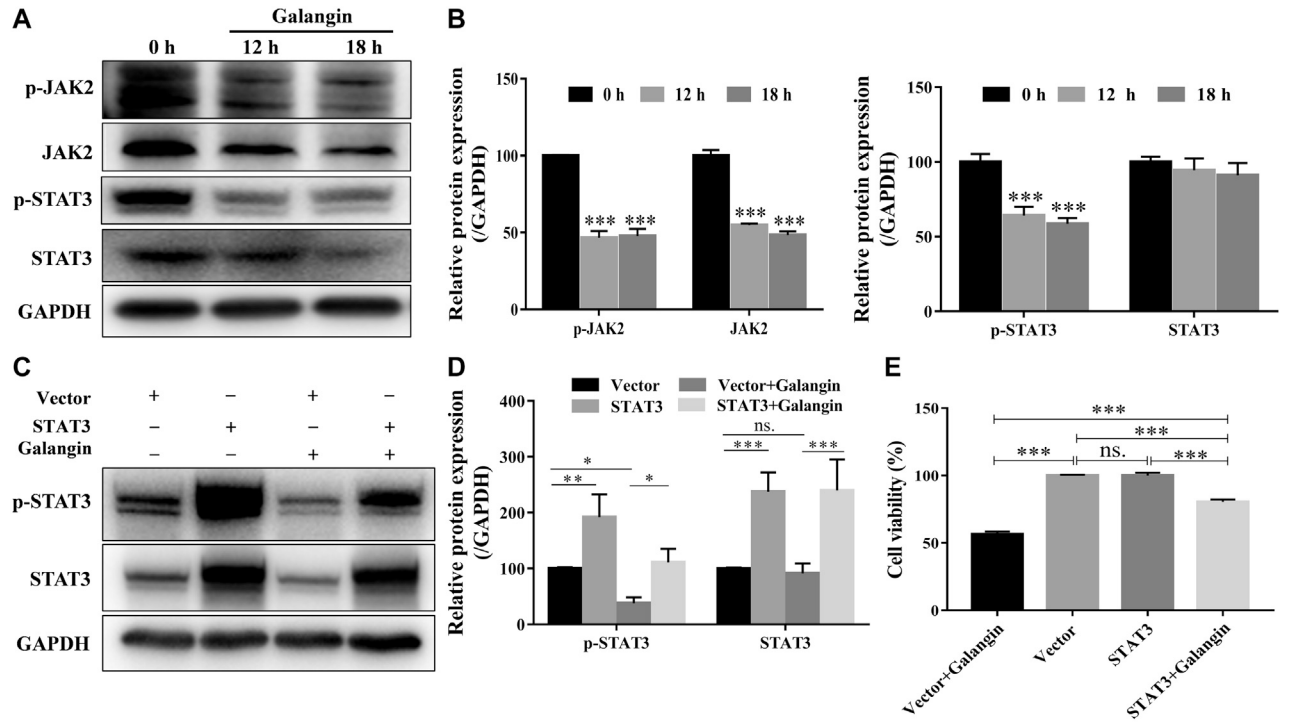

FIGURE 4 | Galangin inhibits overactivation of JAK2/STAT3 signaling pathway. **(A–B)** Galangin (20 μM) decreased protein expression of JAK2, p-JAK2, STAT3, and p-STAT3 in MGC 803 cells after treatment for 12 and 18 h. **(C–D)** Overexpression of STAT3 reversed the inhibitory effect of galangin (20 μM) on the protein expression of p-STAT3 and STAT3 in MGC 803 cells after treatment for 48 h. **(E)** Overexpression of STAT3 reversed the inhibitory effect of galangin (20 μM) on the cell viability of MGC 803 cells after treatment for 48 h. All of the data were shown as mean ± SD, and differences among ≥3 groups were analyzed via one-way ANOVA with Dunnett test (**Figure 4B**, compared with control (0 h) group) or Tukey test (**Figures 4D,E**) by using GraphPad 7.0 software; $^{*}p < 0.05$; $^{**}p < 0.01$; $^{***}p < 0.001$. n ≥ 3.

Statistical Analysis

All of the data were presented as the mean ± standard deviation (SD). Differences between two groups were analyzed by the Student's *t*-test. Differences among more than two groups were analyzed by one-way ANOVA with Dunnett or Tukey test using GraphPad 7.0 software (La Jolla, CA, United States). The value of $p < 0.05$ was considered to indicate a statistically significant difference.

RESULTS

Galangin Reduced Cell Viability of MGC 803 Cells *In Vitro*

As shown in **Figures 1B,C**, galangin significantly reduced the cell viability of MGC 803 cells after treatment for 48 h. The IC_{50} value of galangin on MGC 803 cells for 48 h was 18.685 μM. Galangin inhibited cell viability of MGC 803 cells as early as 18 h after treatment. The cell viability of MGC 803 cells inhibited by galangin (20 μM) were 16.34, 35.57, and 52.97%, respectively, after treatment for 18, 24, and 48 h (**Figure 1D**). In contrast, after treatment for 48 h, galangin used below 200 μM had no significant cytotoxicity to GES-1 cells (**Figure 1E**), suggesting its low cytotoxicity to normal cells. 5-FU (≥2.5 μM) treatment for 48 h significantly inhibited cell viability of MGC 803 cells (**Figure 1F**), however, it (≥10 μM) also significantly suppressed cell viability of GES-1 cells after treatment for 48 h (**Figure 1G**). These results indicated that galangin inhibited gastric cancer cell viability with lower toxicity than 5-FU.

Galangin Induced Apoptosis of MGC 803 Cells

As shown in **Figures 2A,B**, compared with the untreated cells, galangin (20 μM) prominently increased the percentages of the early and late apoptotic cells by 41.41% after treatment for 48 h ($p < 0.001$). And it significantly induced chromatin condensation and nuclear shrinkage or fragmentation in MGC 803 cells (**Figure 2C**). MMP decrease is an early manifestation of cell apoptosis. Compared with the control, galangin significantly reduced the density ratio of JC-1 red/green fluorescence in MGC 803 cells, suggesting that galangin decreased MMP after treatment for 24 and 48 h (**Figures 2D,E**, $p < 0.001$). As shown in **Figures 2F,G**, after treatment for 48 h, compared with the control, galangin significantly decreased the protein expression of Bcl-2 and caspase-3, and up-regulated the protein expression of cleaved caspase 3 and cleaved poly (adenosine diphosphate-ribose) polymerase (PARP) ($p < 0.05$, $p < 0.01$ or $p < 0.001$). However, galangin did not change the expression of Bax in MGC 803 cells. These results indicated that galangin induced significant apoptosis of MGC 803 cells.

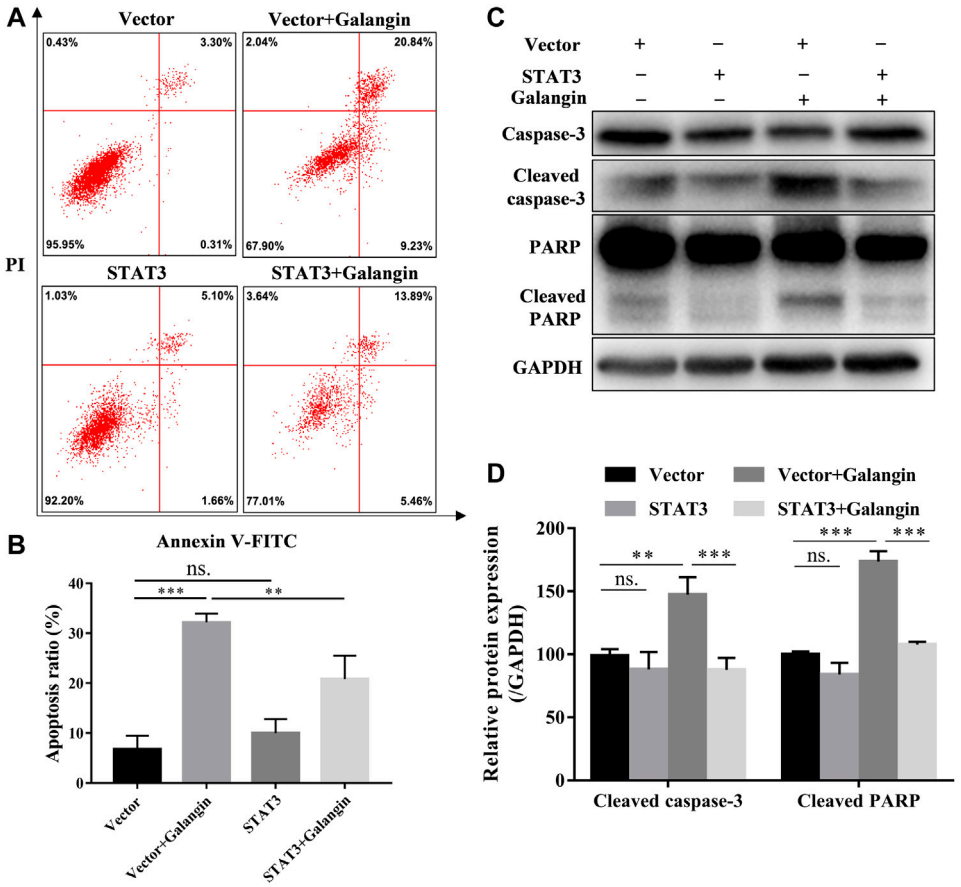

FIGURE 5 | STAT3 overexpression counteractes the effect of galangin on cell apoptosis in MGC 803 cells. **(A–B)** STAT3 overexpression abolished the effect of galangin (20 μM) on cell apoptosis of MGC 803 cells after treatment for 48 h, detected by Annexin V/PI staining. **(C–D)** Overexpression of STAT3 reversed the effect of galangin (20 μM) on protein expression of cleaved caspase-3 and cleaved PARP in MGC 803 cells. All of the data were shown as mean ± SD, and differences among ≥3 groups (**Figures 5B,D**) were analyzed by one-way ANOVA with Tukey test by using GraphPad 7.0 software; $^{**}p < 0.01$; $^{***}p < 0.001$. n ≥ 3.

Galangin Inhibited Proliferation of MGC 803 Cells

As shown in **Figures 3A,B**, after treatment for 24 and 48 h, galangin significantly decreased the number of EdU-positive cells ($p < 0.001$), compared with the control. Ki67, a nuclear antigen, is a marker for cell proliferation. As shown in **Figure 3C**, compared with the control, galangin reduced the immuno-fluorescent intensity of Ki67 in MGC 803 cells. Meanwhile, galangin significantly inhibited the mRNA expression of PCNA, and suppressed the expression of Ki67 at both mRNA and protein levels (**Figures 3D–F**, $p < 0.05$, $p < 0.01$ or $p < 0.001$). These results implicated that galangin could inhibit the proliferaton of MGC 803 cells.

Galangin Inhibited Cell Viability by Suppressing STAT3 Activation in MGC 803 Cells

As displayed in **Figures 4A,B**, galangin reduced the protein expression of *p*-JAK2, and p-STAT3 after treatment for 12 and 18 h in MGC 803 cells. When STAT3 was overexpressed, the inhibitory effect of galangin on the protein expressions of p-STAT3 and STAT3 was abolished (**Figures 4C,D**). Meanwhile, the cell viability inhibited by galangin on MGC 803 cells was counteracted by the overexpression of STAT3 (**Figure 4E**, $p < 0.001$). These results indicated that galangin inhibited the cell viability of MGC 803 cells through modulating the activation of STAT3.

STAT3 Overexpression Counteracted Apoptosis Induced by Galangin in MGC 803 Cells

To confirm the role of STAT3 in the effect of galangin on cell apoptosis, the STAT3 overexpressed cells treated with galangin were subjected to Annexin V/PI staining. As shown in **Figures 5A,B**, overexpression of STAT3 significantly mitigated the ratio of apoptotic cells induced by galangin in MGC 803 cells ($p < 0.01$). Furthermore, STAT3 overexpression counteracted the inductive effect of galangin on the protein expression of cleaved caspase-3 and cleaved PARP in MGC 803 cells after treatment for 48 h (**Figures 5C,D**). These results clearly clarified the essential role of STAT3 in galangin induced apoptosis of MGC 803 cells.

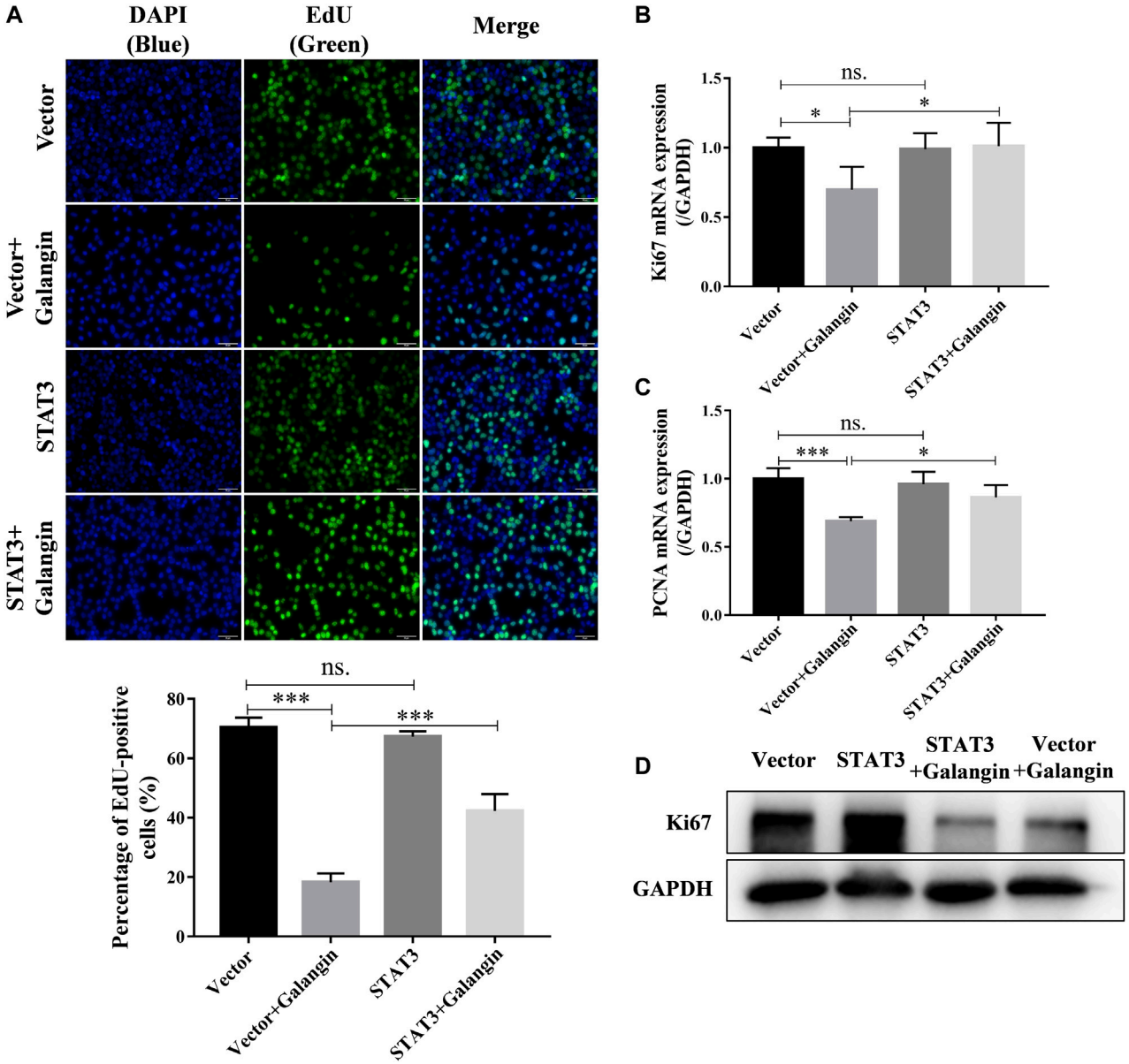

FIGURE 6 | Overexpression of STAT3 counteractes the inhibition of galangin (20 μM) on cell proliferation of MGC 803 after treatment for 48 h. **(A)** STAT3 overexpression counteracted the inhibitory effect of galangin (20 μM) on cell proliferation of MGC 803 cells after treatment for 48 h, detected by EdU staining. **(B–C)** Overexpression of STAT3 reversed the effect of galangin on the mRNA expression of PCNA and Ki67 after treatment for 48 h in MGC 803 cells detected by qPCR assay. **(D)** Overexpression of STAT3 reversed the effect of galangin on protein expression of Ki67 in MGC 803 cells after treatment for 48 h. All of the data were shown as mean ± SD, and differences among ≥3 groups (**Figures 6A–C**) were analyzed by one-way ANOVA with Tukey test by using GraphPad 7.0 software; *$p < 0.05$; ***$p < 0.001$. n ≥ 3. Scale bar, 50 μm.

Overexpression of STAT3 Reduced the Inhibitory Effect of Galangin on Cell Proliferation of MGC 803 Cells

To confirm the role of STAT3 in the inhibition effect of galangin on cell proliferation, qPCR assay, Western blot method, and EdU staining were used to examine the effect of galangin on cell proliferation in STAT3 overexpressed MGC 803 cells. As shown in **Figure 6A**, overexpression of STAT3 markedly increased the pencentage of EdU positive cells treated by galangin ($p < 0.001$). Furthermore, STAT3 overexpression also reversed the inhibitory effect of galangin on the mRNA expression of PCNA and Ki67 as well as the protein expression of Ki67 (**Figures 6B–D**).

Galangin Enhanced ROS Accumulation in MGC 803 Cells

As shown in **Figure 7A**, as early as 12 h after treatment, galangin (20 μM) significantly increased the ROS level in a time-dependent manner in MGC 803 cells. However, significantly decreased cell

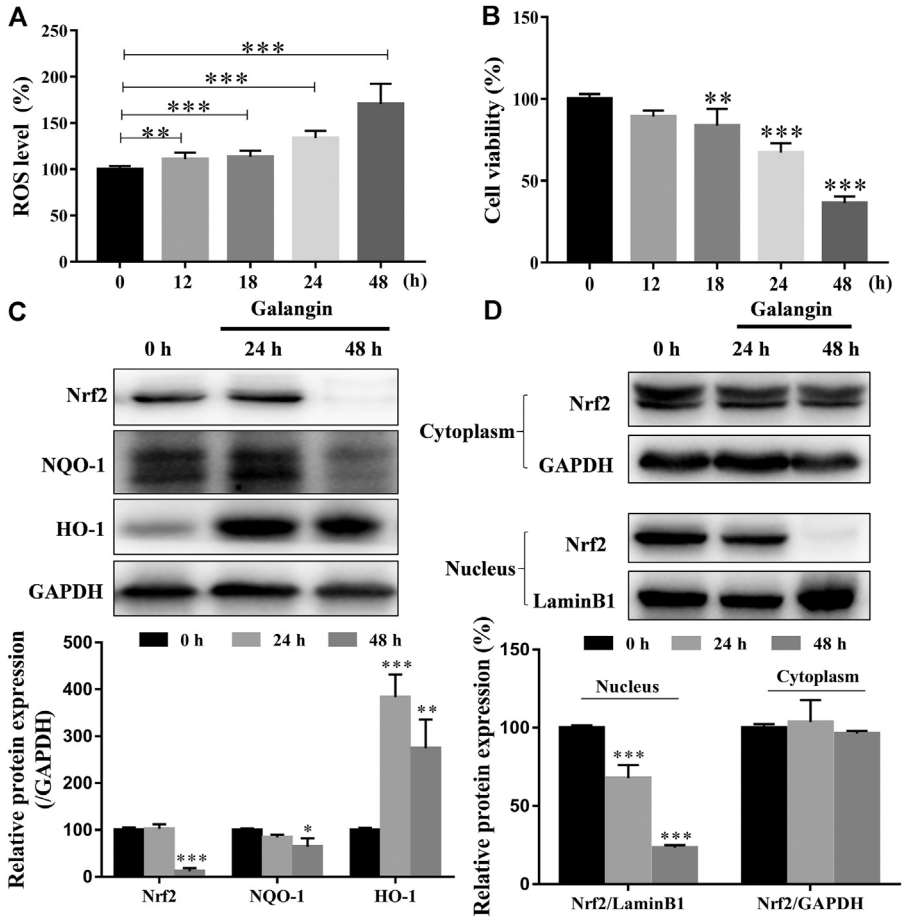

FIGURE 7 | Galangin enhances ROS accumulation and reduces activation of Nrf2-mediated antioxidant system in MGC 803 cells. **(A–B)** Galangin (20 μM) promoted ROS levels in MGC 803 cells after treatment for 12, 18, 24, and 48 h. **(C)** Galangin (20 μM) reduced protein expression of Nrf2 and NQO-1, and enhanced protein expression of HO-1 after treatment for 48 h in MGC 803 cells. **(D)** Galangin (20 μM) inhibited Nrf2 translocation into nucleus of MGC 803 cells after treatment for 48 h. All of the data were shown as mean ± SD, and differences among ≥3 groups were analyzed by one-way ANOVA with Dunnett test by using GraphPad 7.0 software; $^{**}p < 0.01$; $^{***}p < 0.001$, compared with control group. n ≥ 3.

viability was observed after treated with galangin after 18 h (**Figure 7B**). In MGC 803 cells treated with galangin for 48 h, the protein expression of NF-E2-related factor 2 (Nrf2) and NAD(*p*)H quinone oxidoreductase 1 (NQO-1) were reduced, while the protein expression of heme oxygenase-1 (HO-1) was elevated (**Figure 7C**). Furthermore, the translocation of Nrf2 into nucleus was reduced significantly after treated by galangin for 48 h (**Figure 7D**). These results indicated that over-produced ROS and dysfunctioned antioxidant system might finally account for the inhibitory effect of galangin on the growth of MGC 803 cells.

STAT3/ROS *Axis* Mediated the Inhibition of Galangin on Cell Proliferation of MGC 803 Cells

To explore the possible role of the production of ROS in galangin-treated MGC 803 cells, NAC, a ROS scavenger, was used. As displayed in **Figure 8A**, addition of NAC markedly reduced ROS level in galangin treated MGC 803 cells ($p < 0.001$). Correspondingly, compared with cells treated with only galangin, the percentage of EdU positive cells were increased significantly in NAC and galangin co-treated cells (**Figure 8B**, $p < 0.01$ or $p < 0.001$). To further investigate the relationship between STAT3 activation and ROS production, the ROS level in STAT3 overexpressed cells was examined. As shown in **Figure 8C**, overexpression of STAT3 did not change the ROS production in MGC 803 cells. However, STAT3 overexpression reduced the ROS accumulation induced by galangin treatment in cells (**Figure 8C**, $p < 0.001$). These results suggested that galangin suppressed the activation of STAT3, thereby increased the generation of ROS, finally leading to the decrease of cell proliferation of gastric cancer cells.

Galangin Inhibited Tumor Growth *In Vivo*

To verify the inhibitory effect of galangin on gastric cancer growth *in vivo*, the MGC 803 cell xenograft mouse model was established. Compared with the control, galangin and 5-FU treatment significantly inhibited the increase of tumor weight

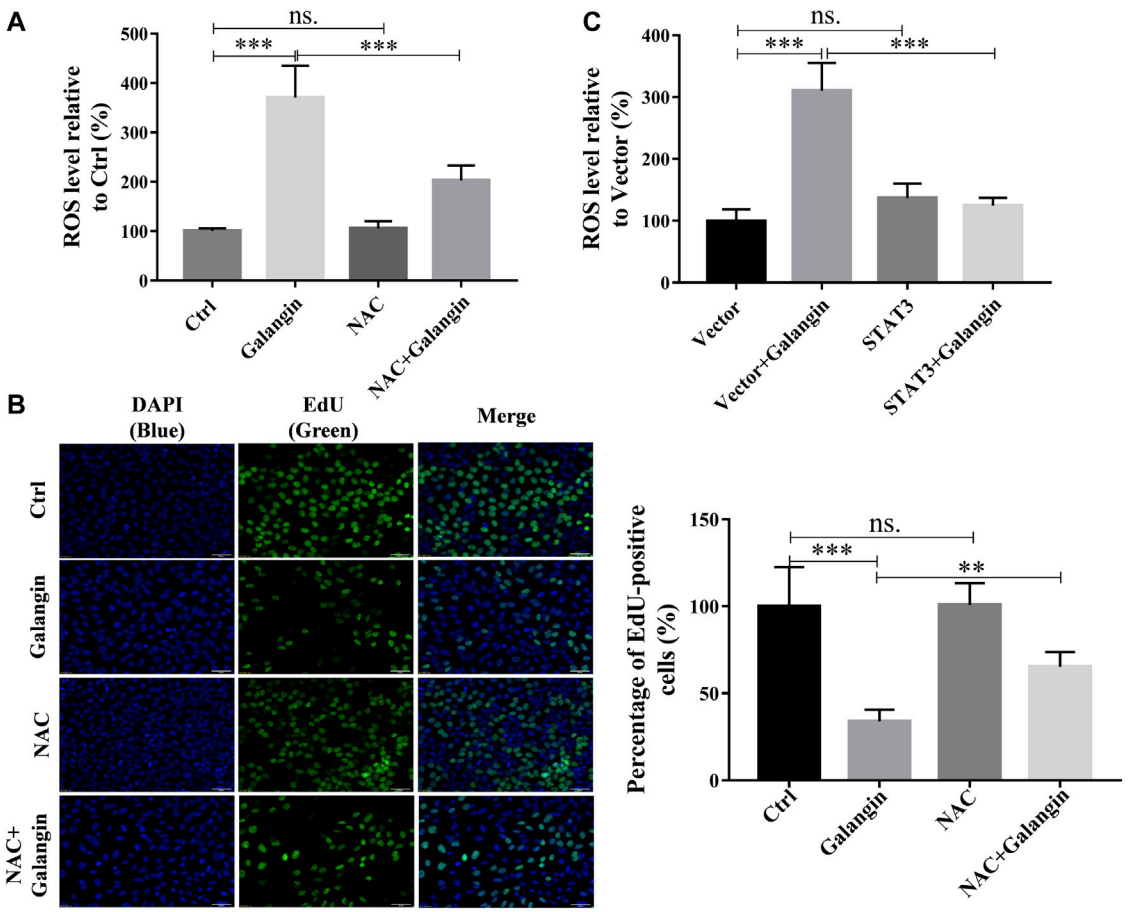

FIGURE 8 | The inhibition of galangin on cell proliferation is associated with ROS generation. **(A)** NAC (ROS scavenger) abolished the enhanced ROS accumulation in MGC 803 cells induced by galangin (20 μM) after treatment for 48 h. **(B)** NAC counteracted the inhibited cell proliferation induced by galangin (20 μM) after treatment for 48 h detected by EdU staining in MGC 803 cells. **(C)** STAT3 overexpression reversed the enhanced ROS accumulation in MGC 803 cells induced by galangin (20 μM) after treatment for 48 h. All of the data were shown as mean ± SD, and differences among ≥3 groups were analyzed by one-way ANOVA with Tukey test by using GraphPad 7.0 software; $^{**}p < 0.01$; $^{***}p < 0.001$. n ≥ 3. Scale bar: 50 μm.

and volume *in vivo* (**Figures 9A–C**, $p < 0.05$ or $p < 0.001$). Nevertheless, as shown in **Figure 9D**, galangin showed no significant effect on body weight of nude mice. In contrast, 5-FU significantly decreased the body weight of nude mice ($p < 0.001$). In tumor tissues from galangin treated mice, the ratios of *p*-JAK2/JAK2 and p-STAT3/STAT3, as well as the protein expressions of Bcl-2, caspase-3 and Ki67 were all reduced remarkably (**Figures 9E,F**, $p < 0.01$ or $p < 0.001$). Conversely, the protein expressions of cleaved caspase-3 and cleaved PARP were increased markedly by galangin treatment ($p < 0.001$). These results suggested that galangin could inhibit gastric cancer growth *in vivo*.

DISCUSSION

Flavonoids are widely distributed in nature, and often can be found in food. Galangin, a natural flavonoid compound mainly present in the rhizome of *Alpinia officinarum* Hance (Zingiberaceae) (Liu et al., 2018), shows extensive anti-tumor activities except in gastric cancer. Impaired proliferation and apoptosis commonly account for the cancer progression (Goldar et al., 2015; White, 2015). In the present study, galangin was found to significantly suppress the proliferation, while induced the apoptosis of MGC 803 cells both *in vitro* and *in vivo*. Moreover, it showed no toxicity on normal gastric mucosal epithelial cell line (GES-1 cells) and induced no body weight loss in nude mice, suggesting its potential clinical application for the treatment of gastric cancer possibly with low toxicity.

STAT3 dysfunction accounts for the impaired cell proliferation and apoptosis in cancer cells (Fathi et al., 2018; Liang and Yang, 2020). JAK-medicated tyrosine phosphorylation enhances the dimerization of STATs. In the present study, galangin reduced the phosphorylated JAK2 and STAT3 in MGC 803 cells at 12 h, and the inhibitory effect of galangin on cell viability of MGC 803 cells was counteracted by STAT3 overexpression, indicating galangin inhibited gastric cancer in a STAT3-dependent manner.

Mitochondrial-dependent apoptosis plays an important role in cell death. Bcl-2 inhibits cell apoptosis, however, Bax promotes cell apoptosis (Mao et al., 2007). Both activated caspase-8 and caspase-9

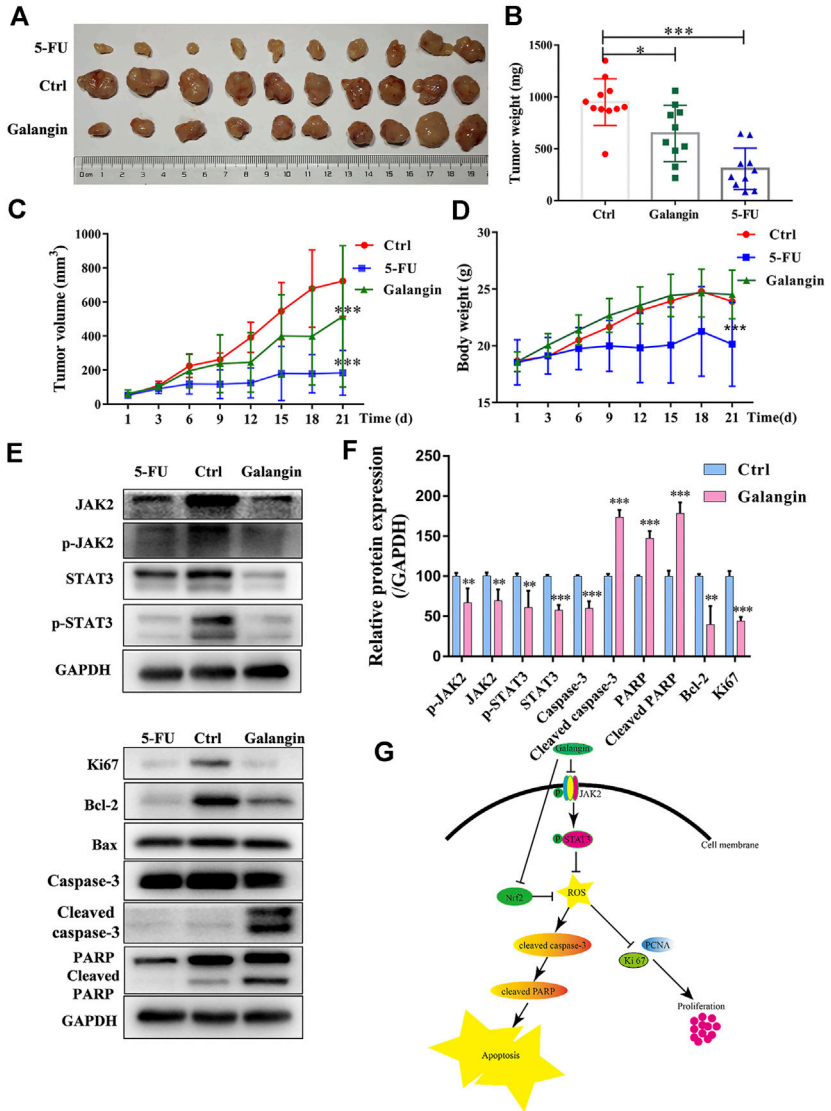

FIGURE 9 | Galangin inhibits tumor growth in the MGC 803 cell xenograft model. **(A–B)** Galangin (120 mg/kg) significantly inhibited tumor growth (n = 10). **(C)** Galangin (120 mg/kg) significantly inhibited tumor volume (n = 10). **(D)** Body weight changes (n = 10). **(E-F)** Galangin modulated protein expression of JAK2, p-JAK2, STAT3, p-STAT3, Bcl-2, Caspase-3, Cleaved caspase-3, PARP, Cleaved PARP, and Ki67 in tumor tissues (n = 6). **(G)** Schematic illustration of possible underlying molecular mechanism of the inhibitory effect of galangin on MGC 803 cells. All of the data were shown as mean ± SD, and differences among ≥3 groups (**Figures 9B–F**) were analyzed by one-way ANOVA with Dunnett test by using GraphPad 7.0 software; $^{*}p < 0.05$, $^{**}p < 0.01$; $^{***}p < 0.001$, compared with control group.

can activate caspase-3 which is the central link of apoptosis (Zheng et al., 2006). Then caspase-3 cleaves several cellular proteins, including PARP, causing morphological changes and DNA breaks, and ultimately leading to apoptosis (Zheng et al., 2006; Yang et al., 2017). In the present study, galangin significantly decreased Bcl-2 and increased cleaved caspase-3 and cleaved PARP. STAT3 overexpression counteracted the enhanced apoptosis induced by galangin, and reversed the inductive effect of glangin on cleaved caspase-3 and cleaved PARP, indicating that galangin induced apoptosis in a STAT3-dependent manner through enhancing cleavage of caspase-3 and its downstream PARP in MGC 803 cells. Meanwhile, STAT3 overexpression abolished the inhibitory effect of galangin on cell proliferation as well as Ki67 and PCNA expression, indicating galangin inhibited cell proliferation also in a STAT3-dependent manner.

Low concentration of ROS can activate transcription factors to promote cell proliferation and differentiation, but excessive ROS can induce depolarization of the mitochondrial membrane, thereby promote the increase of other pro-apoptotic molecules in the cells, reduce the proliferation and survival of tumor cells, and promote cell apoptosis (Leanza et al., 2017; Prasad et al., 2017). In the present study, galangin increased intracellular ROS accumulation of MGC 803 cells in a time-dependent manner. Meanwhile, Nrf2-mediated antioxidant system was significantly decreased, as evidenced by the decreased Nrf2 and NQO-1 in MGC 803 cells. Furthermore, galangin also suppressed Nrf2 translocation into nucleus, indicating galangin

increased ROS level by suppressing Nrf2 mediated antioxidant system. NAC could abolish galangin-induced ROS accumulation and block the inhibitory effect of galangin on cell proliferation, indicating galangin suppressed cell proliferation in a ROS-dependent manner. Furthermore, STAT3 overexpression almost completely abolished the ROS accumulation induced by galangin treatment, indicating galangin induced ROS generation through STAT3 suppression. Many researches have proved that ROS enhanced cell apoptosis (Cui et al., 2018; Dong et al., 2019), however, it has not been found that STAT3 also modulates ROS levels. Our results demonstrated that STAT3 activation inhibited ROS overload. Therefore, galangin might inhibit cell proliferation and enhance apoptosis by modulating STAT3/ROS axis in MGC 803 cells. 5-FU is a first-line chemotherapeutic drug for gastric cancer in clinic, that's why we choose 5-FU as the positive drug in our study. However, it has serious adverse effects including bone marrow suppression, digestive tract toxicity and drug resistance (Wang et al., 2020). Galangin showed no obvious cytotoxicity on normal gastric mucosal epithelial cell line, GES-1 cells. In contrast, 5-FU (≥10 μM) significantly inhibited cell viability of GES-1 cells. Body weight loss is an important indicator of *in vivo* toxicity (Cai et al., 2020). Galangin did not reduce the body weight of nude mice. However, 5-FU showed the negative effect. Thus, galangin inhibited gastric tumor growth possibly with low toxicity. However, the low toxicity and its underlying molecular mechanism of galangin on normal cells still need further study.

In summary, galangin inhibited MGC 803 cells growth through enhancing apoptosis and decreasing cell proliferation, which was mediated by modulating STAT3/ROS axis. Our findings suggest that galangin is a potential drug for gastric cancer treatment with possibly low toxicity.

DATA AVAILABILITY STATEMENT

The original contributions presented in the study are included in the article/Supplementary Material, further inquiries can be directed to the corresponding authors.

ETHICS STATEMENT

The animal study was reviewed and approved by The Animal Ethics Committee in Shanghai University of Traditional Chinese Medicine (SHUTCM).

AUTHOR CONTRIBUTIONS

XL did most of experiments and wrote the original draft. PW and CY took part in cell culture and western blotting assay. FH and HW took part in Annexin/PI staining and qPCR assay. HS and XW designed experiments and wrote the manuscript. All authors read and approved the final manuscript.

FUNDING

This study and open access publication fees were supported by Educational Commission of Shanghai of China (2020LK014); the National Natural Science Foundation of China (81603354); Graduate Student Innovation Ability Project of Shanghai University of Traditional Chinese Medicine (Y2020030).

REFERENCES

Amedei, A., Benagiano, M., della Bella, C., Niccolai, E., and D'Elios, M. M. (2011). Novel Immunotherapeutic Strategies of Gastric Cancer Treatment. *J. Eng. Sci. Med. Diagn. Ther.* 2011, 437348. doi:10.1155/2011/437348

Cai, X.-j., Fei, W.-d., Xu, Y.-y., Xu, H., Yang, G.-y., Cao, J.-w., et al. (2020). Combination of Metronomic Administration and Target Delivery Strategies to Improve the Anti-angiogenic and Anti-tumor Effects of Triptolide. *Drug Deliv. Transl. Res.* 10, 93–107. doi:10.1007/s13346-019-00665-8

Corso, G., Roncalli, F., Marrelli, D., Carneiro, F., and Roviello, F. (2013). History, Pathogenesis, and Management of Familial Gastric Cancer: Original Study of John XXIII's Family. *Biomed. Res. Int.* 2013, 385132. doi:10.1155/2013/385132

Cui, Q., Wang, J.-Q., Assaraf, Y. G., Ren, L., Gupta, P., Wei, L., et al. (2018). Modulating ROS to Overcome Multidrug Resistance in Cancer. *Drug Resist. Updates* 41, 1–25. doi:10.1016/j.drup.2018.11.001

Digklia, A., and Wagner, A. D. (2016). Advanced Gastric Cancer: Current Treatment Landscape and Future Perspectives. *Wjg* 22, 2403–2414. doi:10.3748/wjg.v22.i8.2403

Dong, K., Lei, Q., Guo, R., Wu, X., Zhang, Y., Cui, N., et al. (2019). Regulating Intracellular ROS Signal by a Dual pH/reducing-Responsive Nanogels System Promotes Tumor Cell Apoptosis. *Ijn* 14, 5713–5728. doi:10.2147/ijn.s208089

Fathi, N., Rashidi, G., Khodadadi, A., Shahi, S., and Sharifi, S. (2018). STAT3 and Apoptosis Challenges in Cancer. *Int. J. Biol. Macromolecules* 117, 993–1001. doi:10.1016/j.ijbiomac.2018.05.121

Furtek, S. L., Backos, D. S., Matheson, C. J., and Reigan, P. (2016). Strategies and Approaches of Targeting STAT3 for Cancer Treatment. *ACS Chem. Biol.* 11, 308–318. doi:10.1021/acschembio.5b00945

Goldar, S., Khaniani, M. S., Derakhshan, S. M., and Baradaran, B. (2015). Molecular Mechanisms of Apoptosis and Roles in Cancer Development and Treatment. *Asian Pac. J. Cancer Prev.* 16, 2129–2144. doi:10.7314/apjcp.2015.16.6.2129

Ismail, T., Kim, Y., Lee, H., Lee, D.-S., and Lee, H.-S. (2019). Interplay between Mitochondrial Peroxiredoxins and ROS in Cancer Development and Progression. *Ijms* 20, 4407. doi:10.3390/ijms20184407

Justicia, C., Gabriel, C. l., and Planas, A. M. (2000). Activation of the JAK/STAT Pathway Following Transient Focal Cerebral Ischemia: Signaling through Jak1 and Stat3 in Astrocytes. *Glia* 30, 253–270. doi:10.1002/(sici)1098-1136(200005)30:3<253::aid-glia5>3.0.co;2-o

Kaptein, A., Paillard, V., and Saunders, M. (1996). Dominant Negative Stat3 Mutant Inhibits Interleukin-6-Induced Jak-STAT Signal Transduction. *J. Biol. Chem.* 271, 5961–5964. doi:10.1074/jbc.271.11.5961

Kim, B., and Park, B. (2018). Saffron Carotenoids Inhibit STAT3 Activation and Promote Apoptotic Progression in IL-6-stimulated Liver Cancer Cells. *Oncol. Rep.* 39, 1883–1891. doi:10.3892/or.2018.6232

Kim, D.-H., Park, J. E., Chae, I. G., Park, G., Lee, S., and Chun, K.-S. (2017). Isoliquiritigenin Inhibits the Proliferation of Human Renal Carcinoma Caki Cells through the ROS-Mediated Regulation of the Jak2/STAT3 Pathway. *Oncol. Rep.* 38, 575–583. doi:10.3892/or.2017.5677

Kudryavtseva, A. V., Krasnov, G. S., Dmitriev, A. A., Alekseev, B. Y., Kardymon, O. L., Sadritdinova, A. F., et al. (2016). Mitochondrial Dysfunction and Oxidative Stress in Aging and Cancer. *Oncotarget* 7, 44879–44905. doi:10.18632/oncotarget.9821

Leanza, L., Romio, M., Becker, K. A., Azzolini, M., Trentin, L., Managò, A., et al. (2017). Direct Pharmacological Targeting of a Mitochondrial Ion Channel Selectively Kills Tumor Cells In Vivo. *Cancer cell* 31, 516–531. doi:10.1016/j.ccell.2017.03.003

Li, H., Chen, L., Li, J. J., Zhou, Q., Huang, A., Liu, W. W., et al. (2018). miR-519a Enhances Chemosensitivity and Promotes Autophagy in Glioblastoma by Targeting STAT3/Bcl2 Signaling Pathway. *J. Hematol. Oncol.* 11, 70. doi:10.1186/s13045-018-0618-0

Liang, J.-R., and Yang, H. (2020). Ginkgolic Acid (GA) Suppresses Gastric Cancer Growth by Inducing Apoptosis and Suppressing STAT3/JAK2 Signaling Regulated by ROS. *Biomed. Pharmacother.* 125, 109585. doi:10.1016/j.biopha.2019.109585

Liu, D., You, P., Luo, Y., Yang, M., and Liu, Y. (2018). Galangin Induces Apoptosis in MCF-7 Human Breast Cancer Cells through Mitochondrial Pathway and Phosphatidylinositol 3-Kinase/Akt Inhibition. *Pharmacology* 102, 58–66. doi:10.1159/000489564

Mao, W.-P., Ye, J.-L., Guan, Z.-B., Zhao, J.-M., Zhang, C., Zhang, N.-N., et al. (2007). Cadmium Induces Apoptosis in Human Embryonic Kidney (HEK) 293 Cells by Caspase-dependent and -independent Pathways Acting on Mitochondria. *Toxicol. Vitro* 21, 343–354. doi:10.1016/j.tiv.2006.09.004

Prasad, S., Gupta, S. C., and Tyagi, A. K. (2017). Reactive Oxygen Species (ROS) and Cancer: Role of Antioxidative Nutraceuticals. *Cancer Lett.* 387, 95–105. doi:10.1016/j.canlet.2016.03.042

Ren, K., Zhang, W., Wu, G., Ren, J., Lu, H., Li, Z., et al. (2016). Synergistic Anti-cancer Effects of Galangin and Berberine through Apoptosis Induction and Proliferation Inhibition in Oesophageal Carcinoma Cells. *Biomed. Pharmacother.* 84, 1748–1759. doi:10.1016/j.biopha.2016.10.111

Song, B., Zhan, H., Bian, Q., and Gu, J. (2016). Piperlongumine Inhibits Gastric Cancer Cells via Suppression of The JAK1,2/STAT3 Signaling Pathway. *Mol. Med. Rep.* 13, 4475–4480. doi:10.3892/mmr.2016.5091

Wang, X., Guo, J., Dai, M., Wang, T., Yang, T., Xiao, X., et al. (2020). PLOD2 Increases Resistance of Gastric Cancer Cells to 5-fluorouracil by Upregulating BCRP and Inhibiting Apoptosis. *J. Cancer* 11, 3467–3475. doi:10.7150/jca.41828

Wang, Z., Tang, X., Wu, X., Yang, M., Wang, W., Wang, L., et al. (2019). Cardamonin Exerts Anti-gastric Cancer Activity via Inhibiting LncRNA-PVT1-STAT3 axis. *Biosci. Rep.* 39, BSR20190357. doi:10.1042/bsr20190357

White, E. (2015). The Role for Autophagy in Cancer. *J. Clin. Invest.* 125, 42–46. doi:10.1172/jci73941

Wu, D., Wang, X.-P., and Zhang, W. (2019). Sesamolin Exerts Anti-proliferative and Apoptotic Effect on Human Colorectal Cancer Cells via Inhibition of JAK2/STAT3 Signaling Pathway. *Cel Mol Biol (Noisy-le-grand)* 65, 96–100. doi:10.14715/cmb/2019.65.6.16

Yang, Y., Yu, Y., Wang, J., Li, Y., Li, Y., Wei, J., et al. (2017). Silica Nanoparticles Induced Intrinsic Apoptosis in Neuroblastoma SH-Sy5y Cells via CytC/Apaf-1 Pathway. *Environ. Toxicol. Pharmacol.* 52, 161–169. doi:10.1016/j.etap.2017.01.010

You, L., Wang, Z., Li, H., Shou, J., Jing, Z., Xie, J., et al. (2015). The Role of STAT3 in Autophagy. *Autophagy* 11, 729–739. doi:10.1080/15548627.2015.1017192

Yu, S., Gong, L.-S., Li, N.-F., Pan, Y.-F., and Zhang, L. (2009). Galangin (GG) Combined with Cisplatin (DDP) to Suppress Human Lung Cancer by Inhibition of STAT3-Regulated NF-κB and Bcl-2/Bax Signaling Pathways. *Biomed. Pharmacother.* 97, 213–224. doi:10.1016/j.biopha2017.10.059

Zhang, H.-T., Luo, H., Wu, J., Lan, L. B., Fan, D. H., Zhu, K. D., et al. (2010). Galangin Induces Apoptosis of Hepatocellular Carcinoma Cellsviathe Mitochondrial Pathway. *Wjg* 16, 3377–3384. doi:10.3748/wjg.v16.i27.3377

Zheng, L., Zheng, J., Wu, L.-J., and Zhao, Y.-Y. (2006). Julibroside J 8 -induced HeLa Cell Apoptosis through Caspase Pathway. *J. Asian Nat. Prod. Res.* 8, 457–465. doi:10.1080/10286020500173309

Conflict of Interest: The authors declare that the research was conducted in the absence of any commercial or financial relationships that could be construed as a potential conflict of interest.

frontiers in Pharmacology

REVIEW
published: 26 July 2021
doi: 10.3389/fphar.2021.690501

Potential Role of Traditional Chinese Medicines by Wnt/β-Catenin Pathway Compared With Targeted Small Molecules in Colorectal Cancer Therapy

Jinrong Chang[1], Hoileong Wong Xavier[2], Dongfeng Chen[1], Yamei Liu[1], Hui Li[1] and Zhaoxiang Bian[2]**

[1]School of Basic Medical Sciences, Guangzhou University of Chinese Medicine, Guangzhou, China, [2]School of Chinese Medicine, Hong Kong Baptist University, Hong Kong, China

OPEN ACCESS

Edited by:
Cecilia Veronica Nunez,
National Institute of Amazonian Research (INPA), Brazil

Reviewed by:
Zhaofeng Liang,
Jiangsu University, China
Mei cun Yao,
Sun Yat-Sen University, China
Qiuhua Lai,
Southern Medical University, China

***Correspondence:**
Zhaoxiang Bian
bianzxiang@gmail.com
Hui Li
lihui@gzucm.edu.cn

Specialty section:
This article was submitted to Pharmacology of Anti-Cancer Drugs, a section of the journal Frontiers in Pharmacology

Received: 03 April 2021
Accepted: 02 July 2021
Published: 26 July 2021

Citation:
Chang J, Xavier HW, Chen D, Liu Y, Li H and Bian Z (2021) Potential Role of Traditional Chinese Medicines by Wnt/β-Catenin Pathway Compared With Targeted Small Molecules in Colorectal Cancer Therapy. Front. Pharmacol. 12:690501. doi: 10.3389/fphar.2021.690501

Colorectal cancer (CRC) has become a global public health problem because of its high incidence and mortality rate worldwide. The previous clinical treatment for CRC mainly involves conventional surgery, chemotherapy, and radiotherapy. With the development of tumor molecular targeted therapy, small molecule inhibitors present a great advantage in improving the survival of patients with advanced CRC. However, various side effects and drug resistance induced by chemotherapy are still the major obstacles to improve the clinical benefit. Thus, it is crucial to find new and alternative drugs for CRC treatment. Traditional Chinese medicines (TCMs) have been proved to have low toxicity and multi-target characteristics. In the last few decades, an increasing number of studies have demonstrated that TCMs exhibit strong anticancer effects in both experimental and clinical models and may serve as alternative chemotherapy agents for CRC treatment. Notably, Wnt/β-catenin signaling pathway plays a vital role in the initiation and progression of CRC by modulating the stability of β-catenin in the cytoplasm. Targeting Wnt/β-catenin pathway is a novel direction for developing therapies for CRC. In this review, we outlined the anti-tumor effects of small molecular inhibitors on CRC through Wnt/β-catenin pathway. More importantly, we focused on the potential role of TCMs against tumors by targeting Wnt/β-catenin signaling at different stages of CRC, including precancerous lesions, early stage of CRC and advanced CRC. Furthermore, we also discussed perspectives to develop potential new drugs from TCMs *via* Wnt/β-catenin pathway for the treatment of CRC.

Keywords: traditional Chinese medicines, colorectal cancer, Wnt/β-catenin, potential role, small molecules, therapeutic mechanism

INTRODUCTION

Colorectal cancer (CRC) is the third cause of cancer-related death worldwide according to the latest statistics of the International Agency for Research on Cancer (IARC) of the World Health Organization (WHO) (Authors Anonymous, 2021a). It estimated that there are 1.8 million new CRC cases and 880,792 CRC-related deaths in 2018 (Yang et al., 2020). Moreover, the incidence of CRC in some countries is on the rise gradually. Approximately 70% CRC cases are sporadic and

develop through the adenoma-carcinoma sequence (De Filippo et al., 2002; Fodde, 2002). Tumorigenesis is usually driven by multiple genetic and molecular alterations in the different stages. The mutations of adenomatous polyposis *coli* (APC) gene, were first discovered as the underlying cause of the hereditary colon cancer syndrome termed familial adenomatous polyposis (FAP); in 1991 (Kinzler et al., 1991; Nishisho et al., 1991). Then some researchers found that APC gene could interact with ß-catenin and loss of APC function results in overactive T-cell factor 4 (TCF4)/β-catenin signaling. These findings establish a direct link between Wnt/β-catenin signaling pathway and human CRC. Furthermore, more than 90% of sporadic CRCs has been identified to carry mutations of one or more components of the Wnt/β-catenin signaling pathway including APC based on the genome-scale analysis (Network, 2012). Therefore, the canonical Wnt pathway plays an pivatal role in the development of CRC and may be a significant potential target for CRC treatment.

In clinical practice, standard conventional treatments for CRC are surgery, chemo-therapy and radiotherapy. Currently, with the development of tumor molecular targeted therapy, small molecule inhibitors present a great advantage in improving the survival of patients with advanced CRC. Moreover, long-term application of these therapies can lead to various side effects and toxicities, consisting of nausea, vomiting, mucositis, peripheral neuropathy, and diarrhea (Mcquade et al., 2017). Thus, it is urgent to identify new and more effective drugs for CRC treatment. TCMs have been used for more than 2000 years in China. Owing to the low toxicity and the multi-target capacity (So et al., 2019), TCMs are attracting increasing attention and acceptance for the treatment of CRC as it can alleviate chemotherapy-induced side effects and improve the quality of life of patients with CRC. Previous studies have shown that diverse TCMs exhibit excellent anti-tumor activities in both experimental models and clinical cases. In this review, we focused on ongoing strategies of TCMs used to target aberrant Wnt/β-catenin pathway compared with targeted small molecules as a novel therapeutic intervention in different stages of CRC. Taken together, TCMs will become promising alternative drugs to treat cancer with less toxicity and also be used as an adjunctive treatment together with classic drugs for improving therapeutic outcomes in CRC patients.

Wnt/β-Catenin Pathway and CRC

Wnt signaling pathway is a highly conserved signaling pathway in eukaryotes and commonly divided into canonical (β-catenin dependent) and non-canonical (β-catenin independent) pathways (Polakis, 2012). Originally, many components of the Wnt signaling were identified as key mediators of patterning decisions during embryonic development by genetic screening (Mazzotta et al., 2016). In the last decade, aberrant Wnt/β-catenin pathway activation in carcinogenesis has most prominently been described for CRC. Data from the Cancer Genome Atlas (TCGA) suggests that Wnt/β-catenin pathway is activated in 93% of nonhypermutated CRC and 97% of hypermutated CRC (Li et al., 2012; Sebio et al., 2014; Voorneveld et al., 2015). The status of Wnt/ß-catenin pathway is mainly related to the stability of ß-catenin controlled by the ß-catenin destruction complex that is comprised of scaffolding proteins APC, Axin and the kinases casein kinase 1 (CK1) and Glycose synthase kinase 3β (GSK3β). Absence of Wnt ligands stimuli, the cytosolic ß-catenin is phosphorylated by GSK3β, ubiquitinated by ß-TrCP^{200} and targeted for proteasomal degradation. The ligand Wnt binds to the cell surface receptor Frizzled and low-density lipoprotein receptor-related protein 5/6 (LRP5/6) to form a trimer, which recruits the Dishevelled (Dvl) protein to the plasma membrane, leading to dissociation of the destruction complex followed by cytosolic accumulation of ß-catenin. Consequently, the ß-catenin translocates to the nucleus where nuclear ß-catenin cooperates with TCF/LEF family transcription factors to active target genes such as c-myc, MMP-7, SNAIL and EGFR (Zhan et al., 2017). The activation of Wnt/β-catenin signaling is indispensable for the progression of CRC (**Figure 1**).

The best-known mutation of APC is the major driver of Wnt pathway in colorectal tumorigenesis which functions as a negative regulator and its importance was further highlighted by several recent studies (Hankey et al., 2018). By using the CRISPR/Cas9 technique to introduce APC mutation into human intestinal organoids, the tumorigenesis of CRC could be modeled *in vivo* (Drost et al., 2015; Matano et al., 2015). Moreover, these studies in human and mouse models indicated that the genotypes of APC mutations are consistent with the distinct levels of canonical Wnt pathway and these alterations are associated with characteristic tumor locations within the large intestine (Buchert et al., 2010; Christie et al., 2013). Besides APC, ring finger protein 43 (RNF43) mutations and R-spondin translocations are noted in over 18 and 9% patients with CRC respectively by preventing removal of Wnt receptor. Both RNF43 and R-spondin fusion are completely opposite to APC mutations (Schatoff et al., 2017). In addition to the well-established function of Wnt/ß-catenin in CRC, there is accumulating evidence indicating that the KRAS is also an important and frequently mutant gene during colorectal cancinogenesis. Up to 40% of KRAS mutations occur in patients with CRC (Arrington et al., 2012). The discovery of small-molecule RAS inhibitors or a siRNA targeting RAS displayed anti-proliferative activity on xenografts of human CRC cell line SW480 (Song et al., 2020). The mutations of KRAS result in the hyper-activation of RAS-extracellular signal-regulated kinase (ERK) pathway involving transformation of cells and tumorigenesis. Series of studies confirmed the regulation of the RAS-ERK pathway by Wnt/β-catenin signaling and its roles, such as Axin, APC, and GSK3β, and so on (Vincan and Barker, 2008). The crosstalk of RAS and Wnt/β-catenin pathways relies on the phosphorylation of RAS mediated by GSK3β. GSK3β, a key component of the ß-catenin destruction complex, is identified as a kinase inducing phosphorylations of ß-catenin and RAS at the different sites of the threonine, and subsequently recruits the ß-TrCP E3 linker for the proteasomal degradation. Inactivation of GSK3β caused by Wnt stimuli or APC loss further leads to high concentration of cytoplasmic ß-catenin and KRAS (Lee et al., 2018a). Therefore, both mutations of APC and KRAS have a positive connection with the Wnt/β-catenin pathway in colorectal tumorigenesis (**Figure 1**).

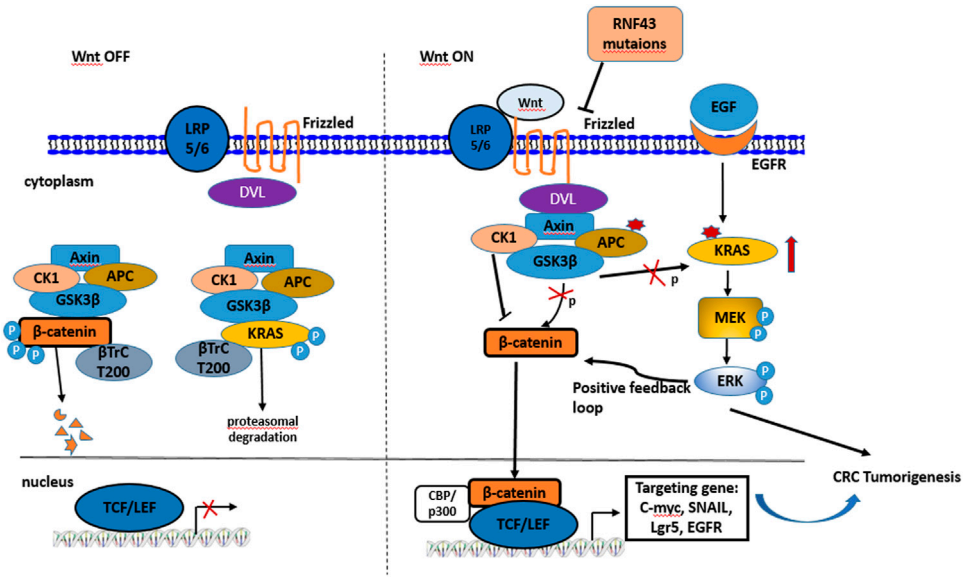

FIGURE 1 | Schematic illustration of the Wnt/β-catenin signaling pathway in CRC. **(A)** Inactive Wnt/β-catenin pathway. In the absence of Wnt ligands, destruction complex phosphylates *β*-catenin and KRAS for ubiquitination and proteolytic degradation; **(B)** Active *β*-catenin pathway and crosstalk with KRAS/ERK pathway. In the Wnt stimuli or APC loss, GSK3β becomes inactive status, leading to the high levels of cytoplasmic *β*-catenin and KRAS. While KRAS mutations have a positive feedback loop with the level of cytoplasmic *β*-catenin. In addition, RNF43 mutations can relieve the degradation of fizzled protein and activate Wnt/β-catenin pathway.

Metastasis is a hallmark of advanced cancer and a major challenge to clinic treatment. Epithelial-mesenchymal transition (EMT) is a crucial process by which epithelial cells lose cell polarity and cell-cell adhesion, and closely associate with invasion and metastasis in many types of malignancies including CRC (Spaderna et al., 2006; Vu and Datta, 2017). There is a complicated network involved in the regulation of EMT, containing different signaling pathways. Many investigations indicated that aberrant activation of the canonical Wnt pathway promotes EMT-associated dedifferentiation located at the invasive front of colorectal tumors. Enhanced Wnt/β-catenin signaling in CRC cells induces the action of E-cadherin repressors SNAIL and upregulation of matrix metalloproteinases (MMP) involving CRC invasion and metastasis (Gu et al., 2016). However, inactivating mutations of APC and AXIN2 can up-regulate the canonical Wnt pathway, thereby promoting EMT. Furthermore, *in vitro* and *in vivo* experiments showed that WNT3a overexpression induces SNAIL expression and promotes invasion (Qi et al., 2014).

In addition, increasing evidences suggest that cancer stem cells (CSCs) theory underlies tumor proliferation, differentiation and metastasis. Although there is still no consensus on the concept of cancer stemness, the vital role of the Wnt pathway for the function of normal and cancer stem cells is commonly accepted (Reya and Clevers, 2005). In the intestinal crypt, Wnt/β-catenin pathway exerts a crucial role in the self-renewal of CSCs in CRC (Yan K. S. et al., 2017). R-spondin receptor Lgr5, one putative mark of intestinal stem cells, is a direct target gene of the canonical Wnt signaling cascade and able to promote tumor proliferation after APC is deleted in these cells. The experiments in mouse models showed that the $Lgr5^{+}$ stem cells can increase additionally the population of Lgr5-positive cells and drive adenoma expanding in colon (Barker et al., 2009). CD44v6, as another CSC marker in colorectal cancer, is promoted by Wnt/β-catenin signaling and cytokines secreted from tumor-associated cells (Todaro et al., 2014). Moreover, the tumor environment has an important effect on maintenance of cancer stemness in some studies, such as hepatocyte growth factor, which is secreted by myofibroblasts in tumor micro-environment and can induce stemness features in colorectal cancer cells by improving Wnt activity (Clara et al., 2020). Recently, several studies uncovered potential relations between Wnt pathway and non-coding microRNAs in CSCs. Scientists have discovered miR-142 can inhibit stem cell-like traits by targeting APC gene whose mutations are linked to colon cancer (Isobe et al., 2014). Taken together, these findings indicate that canonical WNT signaling plays a vital role in the maintenance and expansion of CSCs in CRC.

Small Molecules Targeting Wnt/β-Catenin Pathway for CRC Treatment

Due to the importance of canonical Wnt/β-catenin signaling in human carcinogenic development, small molecule inhibitors targeting Wnt signaling have been developed for the treatment of CRC (**Table 1**). Activation of Wnt signaling through *β*-catenin is a critical event in CRC progression. Porcupine (PORCN) is a membrane-bound O-acyltransferase protein which regulates Wnt ligands secretion outside the cell membrane through palmitoylation. In recent years, PORCN has emerged as a molecular target for treating Wnt-driven cancers. ETC-159, WNT974 (LGK974) and Rxc004 has been identified as potent

TABLE 1 | List of small molecules targeting Wnt/β-catenin pathway for CRC treatment.

Small molecules	Mechanism of action	Preclinical vs. clinical trial (phase) vs. FDA approved	Reference
ETC-159	Porcupine inhibitor	Phase 1	Soo and Keller (2015)
WNT874 (LGK974)	Porcupine inhibitor	Phase 1	Shah et al. (2021)
RXC004	Porcupine inhibitor	Phase 1/2	
IWP-2	Porcupine inhibitor	Preclinical	Masaru (2017)
Pyrvinium	Binding to CK1a	FDA approved	Momtazi-Borojeni et al. (2018)
ICG-001	Binding to CBP	Preclinical	Bahrami et al. (2017)
PRI-724	CBP/β-catenin inhibitor	Phase 1b	
Windorphen	P300/β-catenin inhibitor	Preclinical	Hao et al. (2013)
NSC668036	Binding to Dishevelled	Preclinical	Shan et al. (2005)
Pen-N3	Binding to Dishevelled	Preclinical	Zhang et al. (2009)
XAV939	Tankyrases inhibitor	Preclinical	Huang et al. (2009)
JW55	Tankyrases inhibitor	Preclinical	Waaler et al. (2012)
G007-LK	Tankyrases inhibitor	Preclinical	Lau et al. (2013)
G244-LM	Tankyrases inhibitor	Preclinical	Narwal et al. (2012)
IWR-1	Tankyrases inhibitor	Preclinical	Mashima et al. (2017)
CCT031374	β-catenin inhibitor	Preclinical	Ewan et al. (2010)
CCT036477	β-catenin inhibitor	Preclinical	
CCT070535	β-catenin inhibitor	Preclinical	
iCRT3	β-catenin/Tcf	Preclinical	Gonsalves et al. (2011)
iCRT5	β-catenin/Tcf	Preclinical	
iCRT14	β-catenin/Tcf	Preclinical	
PKF115-584	β-catenin/Tcf	Preclinical	Yan M. et al. (2017)
PKF222-815	β-catenin/Tcf	Preclinical	
CGP049090	β-catenin/Tcf	Preclinical	Tian et al. (2012)
BC21	β-catenin/Tcf	Preclinical	
NC403	β-catenin/Tcf	Preclinical	He et al. (2017)
KYA1797k	GSK3β activator	Preclinical	Lee et al. (2018b)
KY1022	GSK3β activator	Preclinical	Cho et al. (2016)

inhibitors of Wnt secretion inhibiting *ß*-catenin activity in preclinical studies. ETC-159 has been proven to be remarkably efficacious in treating CRCs with R-spondin translocation *in vivo* and *in vitro* experiments (Soo and Keller, 2015). During *in vitro* studies in RNF43 mutant and R-spondin fusion CRC cell lines, Rxc004 could potently repress the cell proliferation by arresting cell cycle at G1/S and G2/M phase (Shah et al., 2021). IWP-2 is another inhibitor of PORCN. Experiments on organoid derived from CRC patients unveiled that IWP-2 is sensitive to the cancers with loss of function RNF43 mutations (Masaru, 2017). Pyrvinium, a FDA-approved drug, has been shown to bind to CK1*α* and form a degradation complex with GSK-3, APC, and Axin, resulting in the inhibition of Wnt signaling. Moreover, Pyrvinium suppresses the proliferation of CRC with mutations of APC or *ß*-catenin in HCT116 and SW480 cell lines (Momtazi-Borojeni et al., 2018). ICG-001, a selective inhibitor of Wnt/β-catenin pathway, binds to the CREB-binding protein (CBP) and down-regulates *ß*-catenin/Tcf transcription. As a consequence, ICG-001 selectively induces apoptosis in colon carcinoma cells but not in normal colonic epithelial cells, which is effective in mouse with APC mutations or nude mouse xenograft models of colon cancer. PRI-724, the second generation specific CBP/catenin antagonist for oncology, has been proved to have an acceptable safety profile in early clinical trials and is now under further clinical investigation (Bahrami et al., 2017). Windorphen (WD) is an inhibitor of Wnt/β-catenin signaling by directly targeting p300 to disrupt the association of *ß*-catenin with p300. These findings suggest that WD can selectively kill cancer cells with aberrant activation of Wnt signaling (Hao et al., 2013). Other small molecules, such as NSC668036 and Pen-N3, block the Wnt signaling pathway through binding to the Dishevelled (Dvl) PDZ domain and interrupting the receptor Frizzled (Fz)-Dvl interaction in colon cells (Shan et al., 2005; Zhang et al., 2009).

Some studies indicate that tankyrases (TNKS) are novel targets for Wnt inhibition by regulating stabilization of Axin and hence leading to increased *ß*-catenin degradation. XAV939 and JW55 have been shown to target Wnt/β-catenin pathway through inhibiting the poly-ADP-ribose polymerase (PARP) domains of TNKS in DLD-1 and SW480 cell lines *in vitro* (Huang et al., 2009). JW55 also reduces the growth of tumor in conditional APC mutation mice (Waaler et al., 2012). G007-LK and G244-LM are two other types of small-molecule tankyrase inhibitors (Lau et al., 2013). In particular, G007-LK has greater stability and displays favorable pharmacokinetic properties to inhibit Wnt/β-catenin signaling in APC-mutant CRC xenograft tumors (Tanaka et al., 2017; Katoh, 2018). IWR-1 is another tankyrase inhibitor which interacts with PARP enzyme (Mashima et al., 2017).

β-catenin is a key mediator of Wnt signaling, regulating the stabilization of the destruction complex and consequently intracellular *ß*-catenin levels. Ewan K et al. revealed that three small molecule inhibitors including CCT031374, CCT036477, and CCT070535 can block the Wnt/β-catenin signaling through reducing the level of *ß*-catenin without altering its stability, which

TABLE 2 | Effects of monomers, extracts, formula of TCMs on CRC by Wnt/β-catenin pathway.

Herbal medicine	Stage	Cell	Animal	Cellular mechanism	Wnt related targets	References
Berberine	Polyps	KM12C KM12SM KM12L4A	Apc Min/+ mice	Proliferation	β-catenin, APC	Zhang J. et al. (2013)
Genistein	Pre-neoplasia	-	SD Rat	Differentiation	Wnt5a, Sfrp1,2,5	Zhang et al. (2020)
EESB	CRC	HT29	BALB/c nude mice	Proliferation Apoptosis	APC, *β*-catenin	Wei et al. (2017)
Brucine Strychnine	CRC	DLD1, SW480, LoVe	Nude mice	Proliferation Apoptosis	APC, *β*-catenin, Dkk1	Ren et al. (2019)
Luteolin	CRC	HCT15	BALB/c mice	Proliferation	GSK-3β, *β*-catenin	Ashokkumar and Sudhandiran (2011)
C. brachycephalum	CRC	SW480	-	Proliferation	GSK-3β, *β*-catenin	Mervai et al. (2015)
PAG	CRC	HCT116	-	Proliferation, Apoptosis	GSK-3β, *β*-catenin Dvl2	Qiu et al. (2017)
Wogonin	CRC	SW480	-	Proliferation	GSK-3β, Ctnnb1	Li et al. (2020)
NG	CRC, Migration	HT29, SW620	-	Proliferation Apoptosis, Cell cycle, EMT	GSK-3β, *β*-catenin	Wen et al. (2019)
IBC	CRC	HCT116, SW480	-	Proliferation Apoptosis	GSK-3β, *β*-catenin	Li et al. (2019)
4 *β* HWE	CRC	HCT116, HT29, SW480, LoVo, CCD-CoN-841	BALB/c nude mice	Proliferation, Apoptosis	β-catenin	Ye et al. (2019)
Rg3	CRC	HCT116, SW480	Athymic nude mice	Proliferation	β-catenin	He B.-C. et al. (2011)
Isoquercitrin	CRC	HCT116, DLD-1, SW480	*Xenopus* embryos	Proliferation	β-catenin	Amado et al. (2014)
RTHF	CRC	SW620, HT29	C57Bl/6 mice	Cell cycle, Stemness, EMT	β-catenin	Wu et al. (2018)
TGG	CRC	NIH3T3, HT29	-	Apoptosis	β-catenin	Li et al. (2019)
TET	CRC, Migration	HCT116, SW480	Female athymic nude mice	Proliferation, Apoptosis	β-catenin	He B.-C. et al. (2011)
Curcumin	CRC	SW620, rHCT116	-	Proliferation Apoptosis,EMT	β-catenin, Wnt3a	Jiang X. et al. (2019)
Beta-elemene	CRC	HCT116, HT29	-	Proliferation Apoptosis	β-catenin, Wnt3a	-
Celastrol	CRC	HCT116, SW480	APC Min/+ mice	Proliferation	β-catenin, YAP, LKB1	Wang et al. (2019)
BRB	CRC	HCT116, HT29, LoVo, SW480	c57Bl/6 mice	miRNA	β-catenin, DKK3	Guo et al. (2020)
Quercetin	CRC	SW480, clone 26	-	Proliferation Apoptosis	β-catenin, Tcf4	Shan et al. (2009)
COL	CRC	DLD1, SW480, LoVe	BALB/c nude mice	Proliferation Apoptosis	β-catenin, TCF/LEF	Lei et al. (2019)
Apigenin	CRC	SW480, HCT15	-	Proliferation	β-catenin, TCF/LEF	Xu et al. (2016)
Silibinin	CRC	SW480	Athymic nude mice	Proliferation	β-catenin, Tcf4	Kaur et al. (2010)
Lonchocarpin	CRC	RKO, SW480	*Xenopus laevis*	Proliferation	β-catenin, Tcf4	Predes et al. (2019)
Henryin	CRC	HCT116, SW480, HT29	-	Proliferation	-	Li et al. (2013)
γ-Mangostin	CRC	HCT116, SW480, RKO, LS174T	Nude mice	Proliferation Apoptosis, Stemness	TCF4	Krishnamachary et al. (2019)
Huaier	CRC, Metastasis	T1,T2	-	Stemness	β-catenin, TCF/LEF	Zhang T et al. (2013)
Resveratrol	CRC, Invasion, Metstasis	HCT116, LoVo	-	MMPs	β-catenin	Ji et al. (2013)
IPM711	Invasion, Migration	HT29, HCT116, NCM460	-	Proliferation, EMT	β-catenin, FZD	Ma et al. (2019)
TKP	Invasion, Migration	DLD1, HCT116	-	MMP2, MMP9	GSK-3β	Sun et al. (2020)
Cinnamaldehyde	CRC, Migration	HCT116, SW480	BALB/c nude mice	EMT, Stemness	β-catenin, GSK-3β	Wu et al. (2019)
ZJW	CRC, Invasion, Migration	SW403	-	Proliferation, MMPs	β-catenin, Axin1, Dvl2,3, GSK-3β, Lef1,Tcf4	Pan et al. (2017)
WCA	CRC, Metastasis	HCT116	-	MMPs, EMT	β-catenin	Tao et al. (2019)
HLJDD	CID	HT29	Athymic nude mice	Stemness	Wnt3,Axin2, Fzd5,Pygo2	Chan et al. (2020)
AP	CACC	HT29, HCT116	ICR mice	Proliferation	β-catenin	Li et al. (2020)

Notes: 1. EESB, ethanol extract of Scutellaria barbata D. Don; 2. PAG, pterisolic acid G; 3. NG, Nerigoside; 4. IBC, Isobavachalcone; 5. 4 ß HWE, four ß-Hydroxywithanolide E; 6. RTHF, Radix Tetrastigma hemsleyani flavone; 7. TGG, 1,4,6-Tri-O-galloyl-β- d -glucopyranose, 8. TET, tetrandrine; 9. BRB, black raspberry; 10. COL, columbamine; 11. IPM711, 4-(1H-imidazo [4,5-f][1,10]-phenanthrolin-2-yl)-2- methoxyphenol; 12. TKP, Trichosanthes *kirilowii; 13. ZJW, Zuo Jin Wan; 14.WCA,Weichang'an; 15.HLJDD, Huanglian Jiedu Decoction; 16. AP, apple polysaccharide; 17. CID, chemotherapy-induced diarrhea.*

is different from drugs involving inhibition of TCF-dependent transcription in SW480 cells (Ewan et al., 2010). Interaction of ß-catenin with TCF binding proteins is a crucial step in the activation of target genes in response to the activation of Wnt/β-catenin pathway. A cohort of Wnt antagonists including iCRT3, iCRT5, iCRT14, PKF115-584, PKF222-815, CGP049090, and BC21 have been demonstrated to suppress the Wnt/β-catenin signaling by breaking the association between Tcf4 and ß-catenin (Gonsalves et al., 2011; Tian et al., 2012; Yan M. et al., 2017). NC043 is an inhibitor of ß-catenin/TCF4, which decreases ß-catenin/TCF4 association without affecting the cytosol-nuclear distribution of soluble ß-catenin *in vivo* and *in vitro* (He et al., 2017).

In recent years, a small molecular KYA1797K has been identified to suppress the formation of CRCs along with the mutations of APC and KRAS via activating GSK3β and subsequently reducing the level of both ß-catenin and Ras as showed both *in vitro* and *in vivo* studies. Moreover, KYA1797K can alleviate the resistant to the EGFR-targeting therapies because of KRAS mutations (Lee et al., 2018b). Whereas, KY1022 destabilizes both ß-catenin and Ras by targeting the Wnt/β-catenin signaling in the process of metastasis involving EMT, which is different from the action of KY1797K (Cho et al., 2016). As indicated above, small molecule inhibitors targeting Wnt/β-catenin pathway exhibit promising therapeutic effects on CRC. However, to the best of our knowledge, few of these small molecules has gone into clinical trials. In the future, many scientists will make great efforts to identify more small molecules targeting Wnt/β-catenin and convert them into effective therapies.

Therapeutic Mechanism of TCMs Against CRC via Wnt/β-Catenin Pathway

It is well documented that uncontrolled cell proliferation is a typical feature in many types tumor development, especially in CRC. The complex balance between proliferation and apoptosis is intimately connected with tissue homeostasis (Diwanji and Bergmann, 2018) and in general, increased cell proliferation along with reduced apoptosis, drives tumor formation. It has been found that many compounds or extracts from TCMs could inhibit colorectal tumorigenesis by targeting different molecules in Wnt/β-catenin pathway. Therefore, we summarized the single-herb and formula of TCM against the different stages of CRC via Wnt/β-catenin pathway (**Table 2**).

EFFECT OF ACTIVE COMPOUNDS ON PRECANCEROUS CRC

The presence of adenoma (polyps), is a precursor and a major risk factor for CRC (Nguyen et al., 2020). Currently, endoscopic removal is the most effective therapeutic regimen for these patients. However, TCMs also have been reported to exhibit important therapeutic effects on colon adenomas. Alkaloid berberine, which is previously used as an anti-inflammatory drug, has proximately been demonstrated to possess anti-tumor activity by reducing Wnt activity and its mechanism of action may involve inhibition of ß-catenin translocation to the nucleus by enhancing the expression of APC gene and stabilizing the complex of APC-β-catenin. Studies looking at berberine treatment *in vivo* have found that it gave rise to reduced formation of polyps accompanied with a decrease in cyclin D1 and c-myc expression in the intestinal adenoma model. Furthermore, oral administration of berberine has been confirmed to significantly reduce the size of polyps in patients with FAP (Zhang J. et al., 2013). In addition, the discovery of Aberrant crypt foci (ACF) in early colorectal adenomas provided new opportunities to explore the pathogenic mechanism of CRC. Genistein, a soya isoflavone, is capable of decreasing the number of total aberrant crypts in the colon cancer model with azoxymethane (AOM) injection by repressing the expressions of Wnt/β-catenin target genes, including Wnt5a, Sfrp1, Sfrp2, Sfrp5, and c-Myc. These results revealed a novel role for genistein as a suppressor of carcinogen-induced Wnt/β-catenin signaling and the prevention of early colon neoplasia (Zhang et al., 2020).

THERAPEUTIC MECHANISM OF ACTIVE COMPOUNDS AGAINST CRC IN SITU

Ninety-three percent of CRC cases has at least one mutation in Wnt/β-catenin pathway genes (Pearlman et al., 2017). The most frequently mutated gene in CRC is APC which may be a promising target for drug development in CRC. The ethanol extract of Scutellaria barbata D. Don (EESB), used for the treatment of various types of cancer clinically (Wei et al., 2017; Zhang et al., 2017; Liu et al., 2018), has been found to prevent the development of human CRC via increasing APC expression with a concomitant decrease in the expression of ß-catenin, leading to inactivation of the Wnt/β-catenin pathway in a CRC xenografted mouse model and HT-29 cell line. Brucine and strychnine from nux vomic have remarkable effects in improving circulatory system and relieving arthritic and traumatic pains. Recently, Ren H et al. (2019) found both two compounds can suppress the growth significantly by inducing the apoptosis of CRCs in nude mice by enhancing the expression of APC and reducing that of ß-catenin. Meanwhile, they can greatly promote DKK1 expression, which is proved to negatively regulate Wnt/β-catenin pathway. On the other hand, some monomers derived from traditional Chinese herbs such as Luteolin, C. brachycephalum, pterisolic acid G (PAG), wogonin, nerigoside (NG) and isobavachalcone (IBC), exhibit anticancer functions by affecting the phosphorylation state of GSK-3β and ß-catenin in CRC. However, nerigoside has been found to destroy the balance of proliferation and apoptosis through the ERK/GSK3β/β-catenin signaling pathways, whereas isobavachalcone exerts its anticancer effect via the AKT/GSK-3β/β-catenin pathway in CRC (Ashokkumar and Sudhandiran, 2011; Mervai et al. (2015); Qiu et al., 2017; Li et al., 2019; Tan et al., 2019; Wen et al., 2019).

There are some compounds inhibiting CRC by mediating the core molecule of canonical Wnt pathway. Ye ZN et al. discovered that the anti-tumor effect of four ß HWE is to promote the phosphorylation and degradation of ß-catenin and the subsequent inhibition of its nuclear translocation in CRC cells

(Ye et al., 2019). While, Ginsenoside Rg3 and isoquercitrin were demonstrated to inhibit Wnt/β-catenin pathway by blocking nuclear translocation of the ß-catenin protein and hence inhibiting ß-catenin/Tcf transcriptional activity (He B. et al., 2011). Moreover, some experiments *in vitro* showed that Radix Tetrastigma hemsleyani flavone (RTHF), 1,4,6-Tri-O-galloyl-β-d-glucopyranose (TGG) as well as tetrandrine (TET) could suppress colorectal tumor growth and downregulate target genes expression (He B.-C. et al., 2011; Wu et al., 2018; Li et al., 2019). Curcumin is another inhibitor of ß-catenin in many cancers (Deguchi, 2015). Previous studies illustrated caudal type homeobox-2 (CDX2) is a mediator of the Wnt signaling pathway, and curcumin can reduce cell proliferation and increase apoptosis by restoring CDX2 which inhibited the Wnt/β-catenin signaling pathway (Jiang X. et al., 2019). Besides, curcumin might exert anti-resistant effect of 5-FU on rHCT-116 cells by controlling WNT signal pathway to reverse the EMT progress (Lu et al., 2020). Beta-elemene, however, could elevate sensitivity to 5-FU through down-regulating miR-191 and preventing the Wnt/β-catenin pathway in CRC cells (Guo et al., 2018). Lately, accumulating evidence has strongly suggested Hippo signaling interacted with Wnt/β-catenin pathway. (Jiang Z. et al., 2019). found that celastrol, isolated from Tripterygium wilfordii plant, exerted antitumor effects by accelerating ß-catenin degradation via the HSF1–LKB1–AMPKα–YAP pathway in CRC. In addition, miRNA microarray analysis suggested that black raspberry (BRB) anthocyanins can reduce the expression of miR-483–3p accompanied by an increased level of DKK3 expression, which is one negative regulator of Wnt pathway (Guo et al., 2020).

Some studies revealed that quercetin and columbamine (inhibitors of the Wnt/ß-catenin pathway) could decrease nuclear lcatenin and downregulate the transcriptional activity of ß-catenin/Tcf, leading to inhibition of cell proliferation in SW480 cell lines (Pahlke et al., 2006; Lei et al., 2019). Similar to quercetin and columbamine, apigenin can suppress CRC proliferation by inhibiting ß-catenin nuclear entry and thereby prevented the expression of Wnt downstream target genes (Xu et al., 2016). Silibinin and lonchocarpin, also exert anticancer functions through the regulation of ß-catenin/Tcf transcriptional activity in animal and cell models (Kaur et al., 2010; Predes et al., 2019). Yet silibinin exhibited selective growth inhibitory effects on SW480 cells (human CRC cells), but not HCT116 cells, by inhibition of Wnt signaling. Henryin, used to control pain for a long time, has been reported to be capable of impairing the association of the ß-catenin/TCF4 trans-criptional complex through direct blockade of ß-catenin binding to TCF4, but not to affect the cytosol to nuclear distribution of soluble ß-catenin (Li et al., 2013). In addition, γ-mangostin, found in Mangosteen fruit, can interact with the transcription factor TCF4 at the ß-catenin binding domain, which results in the suppression of the expression of cyclin D1 and c-Myc. Furthermore, γ-mangostin treatment significantly decreased the levels of stem cell markers such as Lgr5, Dclk1 and CD44 in HCT116, LS174T and DLD1 cells, which also confirmed *in vivo* models (Krishnamachary et al., 2019). In the last few decades, the existence of CSCs is central to chemo-resistance and recurrence of many tumors. Some studies identified Huaier aqueous extract can take action against CRC by eradicating CSCs and the Wnt pathway may be considered as a potential target of Huaier for the treatment of CRC (Zhang T. et al., 2013).

REGULATORY MECHANISM OF ACTIVE COMPOUNDS AGAINST METASTATIC CRC

The development of distant metastases and therefore resistance to therapy, are major clinical problems in the management of the patients with advanced cancer. Recently, medical professionals have focused on TCMs as a way to resolve these issues. Resveratrol, a natural antioxidant from Polygonum cuspidatum, inhibits the invasion and metastasis of human CRC through down-regulation of Metastasis Associated Lung Adenocarcinoma Transcript1 (MALAT1) (Xu et al., 2011; Ji et al., 2013). IPM711, a structurally modified vanillin, was reported to attenuate EMT by increasing the expression of E-cadherin (Ma et al., 2019). Furthermore, a serine protease TKP has a repressive effect on CRC cell invasion and metastasis by targeting MMP2 and MMP9, and is mediated by blockade of both Wnt/β-catenin and Hedgehog/Gli1 signaling (Sun et al., 2020). In addition, cinnamaldehyde has been certified to have potential adjuvant effect on CRC cells in combination with oxaliplatin through blocking the Wnt/β-catenin pathway and enhancing the susceptibility of oxaliplatin in the hypoxic environment (Wu et al., 2019).

EFFECT OF TCM FORMULAS ON CRC

As well as the monomers and extracts derived from TCMs, an increasing body of evidence suggests that TCM formulas possess anticancer properties, too. Zuo Jin Wan (ZJW) has been used in the treatment of gastrointestinal and liver diseases in China for ages (Chao et al., 2011; Sun et al., 2019), which is composed of Rhizoma Coptidis and Evodia Rutaecarpa at a ratio of 6:1. Berberine and evodiamine are two key elements of ZJW extract and possess anti-tumorigenic activity, respectively (Ayati et al., 2017; Wang et al., 2019). Over the past few decades, many clinical studies had found that some subtypes of 5-HT receptors (5-HTRs) would enhance the proliferation of CRC cells. Recent studies showed that ZJW extracts can exert anti-tumorigenic effects by suppressing the canonical Wnt/β-catenin pathway in animal and cell experiments, similar to that seen with 5-HTR antagonists (Pan et al., 2017). Weichang' an (WCA) is a traditional Chinese medicinal formula used as an anticancer drug and the experimental data also showed the anti-metastatic function by blunting the activation of Wnt/β-catenin pathway and reducing the expression of MMP9 and the EMT-related protein ZEB1 (Tao et al., 2019). Furthermore, TCM formulations could provide an adjunct for chemotherapy in cancer patients. Huanglian Jiedu Decoction (HLJDD) has been revealed to significantly alleviate the diarrhea induced by chemotherapy in a mouse model. The experiments from the intestinal segments of 5-Fu/CPT-11-treated mice proved pre-treatment with HLJDD could activate the Wnt/β-catenin

TABLE 3 | New drugs inhibiting Wnt/β-catenin pathway for treatment CRC in clinic.

New drug	Disease or condition	Combination with	Aim or result	Phase	Recruitment status
Resveratrol	Colon cancer	-	Resveratrol represented a potential colon cancer preventive strategy in this phase I study	Phase I	completed
Genistein	Metastatic CRC	FOLFOX or FOLFOX-Avastin	Combining genistein with the standard of care chemotherapeutic regimens reduced chemotherapy resistance and improved response rates	Phase I and II	completed
Wnt 974 (LGK974)	BRAFV600-mutant Metastatic CRC	LGX818 and Cetuximab	The triple combination of WNT974, LGX818 and cetuximab could result in anti-cancer activity with the inhibition of Wnt and BRAF signals	Phase Ib/II	completed
ABT-888 (veliparib)	CRC that cannot been cured by surgery	Temozolomide	Combining veliparib and temozolomide was well-tolerated at doses up to 200 mg/m^2/day of temozolomide	Phase II	completed
Foxy5	Metastatic CRC	-	The aim is to set up the recommended drug dose for use in the subsequent clinical phase 2 study and develop Foxy-5 as a first-line drug in anti-metastatic cancer	Phase I	completed
Foxy5	CRC with low Wnt-5a	Surgery to remove the tumour and then giving treatment with FOLFOX about 6 months	In this trial the safety and tolerability of Foxy-5 will be built and early signs of anti-metastatic activity will be evaluated in subjects with resectable colon cancer	Phase II	Recruiting
Niclosamide	FAP	Placebo	Niclosamide has been indicated to have a inhibitory effect on tumorigenesis via inhibition of Wnt pathway with no significant safety issues	Phase II	Recruiting

pathway by inducing the expressions of Wnt signaling components, comprised of Wnt3, Fzd5, Axin2, and Pygo2 (Chan et al., 2020). These data suggest that HLJDD could boost the regeneration of intestinal progenitor cells after chemotherapy, probably by activating Wnt/β-catenin.

In addition, TCMs can also prevent the development of colitis associated colorectal cancer (CACC) through canonical Wnt signaling. It is showed that apple polysaccharide (AP) from apple residues could affect the activation of Wnt/β-catenin signaling pathway *in vivo*, but not *in vitro* experiments (Li et al., 2020). Previous studies showed that AP treatment could effectively decrease the proliferation of *Fusobacterium* in AOM/DSS-induced intestinal tract. Therefore, AP may restrain the activation of Wnt/β-catenin signal pathway in CACC mice through controlling the imbalance of intestinal flora.

Development of New Drugs in Clinic

CRC is often diagnosed at an advanced stage when tumor cell dissemination has already taken place and chemotherapy was one of the major methods for the treatment of CRC in the past few decades. In clinic, it is obviously clear that fluoropyrimidines, irinotecan, and oxaliplatin have been widely applied to chemotherapeutic regimens for tumors (Gustavsson et al., 2015). The recent introduction of small molecular target agents, such as anti-EGFR (cetuximab, panitumumab) and antiangiogenic molecules (bevacizumab) have led to profound improvements in the life expectancy of patients with advanced CRC (Franke et al., 2019), but with potential lethal adverse drug events and drug resistance. Therefore, it is necessary to develop new and neo-adjuvant therapies in combination with other chemotherapeutics. TCMs and their active compounds with multi-targets was reported to prevent and treat CRC patients as promising candidates, which is distinct from small molecular inhibitors that depend on single target (Yeh et al., 2020). In addition, because of relatively lower toxicity and cheaper price, TCMs can be more accepted by patients with CRC physically and psychologically.

On account of the significance of Wnt/β-catenin pathway in CRC development and metastasis, some native components of TCMs was developed as novel drugs specifically targeting this signaling pathway and are already in clinical trials (**Table 3**). Resveratrol is a naturally occurring polyphenol with antioxidant, which has been used in many diseases involving cancers. Recently, *in vitro* studies suggest that resveratrol exhibited preventative colon cancer effects and this was associated with Wnt signaling (93). In this clinical trial, patients with colon cancer were randomly provided a treatment with resveratrol, and relevant studies tested its effects directly on colon cancer and normal colonic mucosa. These results showed that resveratrol could inhibit Wnt/β-catenin signaling in the normal colonic mucosa, but not in colon cancer (Nguyen et al., 2009). Thus, resveratrol represented a potential colon cancer preventive strategy in this phase I study. Genistein is also identified to block Wnt/β-catenin signaling and has a cooperative effect with chemotherapeutic agents in lab. According to pre-clinical data, investigators found that combining genistein with standard chemotherapeutic regimens could reduce chemotherapy resistance and improve patient's response rates (Authors Anonymous, 2021b).

Besides, small molecular weight Wnt 974, a potential inhibitor of Wnt/β-catenin signaling, has been used to assess its safety and antitumor activity in combination with chemotherapeutic agents in patients with BRAF-mutant metastatic CRC and Wnt pathway mutations (Authors Anonymous, 2021c). Nevertheless, so far, the study results have not been published. ABT-888 (veliparib) has also been used in combination with chemotherapeutic drugs to inhibit the growth of metastatic CRC in phaseIandIIclinical trials (Authors Anonymous, 2021d). But it has not yet been approved

by the FDA for use in this cancer. Foxy5, identified by WntResearch, can prevent migration of epithelial cancer cells by mimicking the functions of Wnt-5a and thereby play the anti-metastatic role. The safety and tolerability of Foxy-5 were established and early signs of anti-metastatic activity were evaluated in subjects with resectable colon cancer. Further, researchers have already examined the maximum tolerated dose and dose-limiting toxicity of this drug (Authors Anonymous, 2021e). Interestingly, another small molecule niclosamide, an anti-helminthic drug, has been proved to have an obviously suppressive effect on colorectal tumorigenesis by attenuating Wnt/β-catenin signaling lately. In this experiment, investigators devised a double-blind randomized controlled trial to evaluate the effect of niclosamide on patients with FAP. Unfortunately, to date, this project is still in the recruitment stage (Authors Anonymous, 2021f).

CONCLUSIONS AND FUTURE PERPECTIVES

CRC has become a global public health problem on account of its high incidence and mortality rate worldwide. The clinical treatments for CRC mainly involve surgery-based chemotherapy. In recent years, with the application of targeting small molecules against cancer, the quality of life for CRC patients has improved. Nevertheless, chemotherapy-induced side effects and drug resistance remain a major issue for clinical practice. Numerous studies have shown that TCMs can be used to exert potential anticancer activity and alleviate the side effects associated with chemotherapy. It is confirmed that various mutations in one or more members of the canonical Wnt signaling pathway take place in the progression of CRC. Therefore, in this review, we aimed to intensively explore molecular mechanisms of TCMs against cancer at the different stages in CRC progress, including precancerous lesions, early stage CRC and CRC invasion and migration based on the inhibition of the Wnt/β-catenin signaling pathway. Cell culture and animal experiments have found that TCMs play anticancer roles by regulating APC/β-catenin, GSK-3β/β-catenin, and β-catenin/TCF4 pathways which represent the main elements of the Wnt/β-catenin pathway involved in the treatment of CRC. Thus, understanding the molecular mechanisms of action of TCMs and how they target Wnt/β-catenin may shed light on future therapies for CRC. However, it needs multi-level and multi-link comprehensive action to anti-tumor because of the complex composition of traditional Chinese medicine. This suggests that we need to investigate the crosstalk between Wnt/β-catenin signal pathway and others. In addition, there remains very few new clinical treatments under development due to lack of strict evaluation system for effectiveness and safety of TCMs. Therefore, it will hopefully pave the way for the CRC clinical treatment and may also relieve the side effects related to chemotherapy if there is a breakthrough in the study of multi-target intervention of TCM in CRC.

AUTHOR CONTRIBUTIONS

Chang JC wrote the article; ZB and HW took part in the critical revision of this article; all of the authors had no objection to the final article.

FUNDING

Supported by the Guangdong Natural Science Foundation, No. 2017A030312009.

ACKNOWLEDGMENTS

I wish to thank all members of ZB' research team in school of Chinese medicine, Hong Kong Baptist University, as well as Jianyong Xiao.

REFERENCES

Amado, N., Predes, D., Moreno, M., Carvalho, I., Mendes, F., and Abreu, J. (2014). Flavonoids and Wnt/β-Catenin Signaling: Potential Role in Colorectal Cancer Therapies. *Int. J. Mol. Sci.* 15 (7), 12094–12106. doi:10.3390/ijms150712094

Arrington, A. K., Heinrich, E. L., Lee, W., Duldulao, M., Patel, S., Sanchez, J., et al. (2012). Prognostic and Predictive Roles of KRAS Mutation in Colorectal Cancer. *Int. J. Mol. Sci.* 13 (10), 12153–12168. doi:10.3390/ijms131012153

Ashokkumar, P., and Sudhandiran, G. (2011). Luteolin Inhibits Cell Proliferation During Azoxymethane-Induced Experimental Colon Carcinogenesis *via* Wnt/Beta-Catenin Pathway. *Invest New Drugs* 29 (2), 273–284. doi:10.1007/s10637-009-9359-9

Authors Anonymous (2021a). Cancer Today. Available at: https://gco.iarc.fr/today/fact-sheets-cancers.. (accessed 6 9 2021)

Authors Anonymous (2021b). Genistein in Treatment of Metastatic Colorectal Cancer - Full Text View - ClinicalTrials.Gov. Available at: https://clinicaltrials.gov/ct2/show/NCT01985763?term=genistein&cond=Colorectal+ Cancer&draw=2&rank=1. (accessed 6 9 2021)

Authors Anonymous (2021c). Study of WNT974 in Combination with LGX818 and Cetuximab in Patients with BRAF-Mutant Metastatic Colorectal Cancer (mCRC) and Wnt Pathway Mutations-Full Text View-ClinicalTrials.Gov. Available at: https://clinicaltrials.gov/ct2/show/NCT02278133?term=wnt974& cond=colorectal+cancer&draw=2&rank=1. (accessed 6 9 2021)

Authors Anonymous (2021d). A Study of ABT-888 in Combination with Temozolomide for Colorectal Cancer - Full Text View-ClinicalTrials.Gov. Available at: https://clinicaltrials.gov/ct2/show/NCT01051596?term= ABT-888&cond=colorectal+cancer&draw=2&rank=1. (accessed 6 9 2021)

Authors Anonymous (2021e). Phase I Study to Evaluate Safety, Tolerability, Anti-tumour Activity and PK Profiles of Foxy-5 in Metastatic Breast, Colon or Prostate Cancer-Full Text View-ClinicalTrials.Gov. Available at: https://clinicaltrials.gov/ct2/show/NCT02020291?term=Foxy5&cond=colorectal+cancer&draw=2&rank=1. (accessed 6 9 2021)

Authors Anonymous (2021f). Drug Trial to Investigate the Safety and Efficacy of Niclosamide Tablets in Patients with Metastases of a Colorectal Cancer Progressing after Therapy - Full Text View - ClinicalTrials.Gov. Available at: https://clinicaltrials.gov/ct2/show/NCT02519582?term=niclosamide&cond= colorectal+cancer&draw=2&rank=1. (accessed 6 9 2021)

Ayati, S. H., Fazeli, B., Momtazi-Borojeni, A. A., Cicero, A. F. G., Pirro, M., and Sahebkar, A. (2017). Regulatory Effects of Berberine on microRNome in Cancer and Other Conditions. *Crit. Rev. Oncology/Hematology* 116, 147–158. doi:10.1016/j.critrevonc.2017.05.008

Bahrami, A., Amerizadeh, F., Shahidsales, S., Khazaei, M., Ghayour-Mobarhan, M., Sadeghnia, H. R., et al. (2017). Therapeutic Potential of Targeting Wnt/

β-Catenin Pathway in Treatment of Colorectal Cancer: Rational and Progress. *J. Cel. Biochem.* 118 (8), 1979–1983. doi:10.1002/jcb.25903

Barker, N., Ridgway, R. A., van Es, J. H., van de Wetering, M., Begthel, H., van den Born, M., et al. (2009). Crypt Stem Cells as the Cells-Of-Origin of Intestinal Cancer. *Nature* 457 (7229), 608–611. doi:10.1038/nature07602

Buchert, M., Athineos, D., Abud, H. E., Burke, Z. D., Faux, M. C., Samuel, M. S., et al. (2010). Genetic Dissection of Differential Signaling Threshold Requirements for the Wnt/β-Catenin Pathway *In Vivo*. *Plos Genet.* 6 (1), e1000816. doi:10.1371/journal.pgen.1000816

Chan, Y.-T., Cheung, F., Zhang, C., Fu, B., Tan, H.-Y., Norimoto, H., et al. (2020). Ancient Chinese Medicine Herbal Formula Huanglian Jiedu Decoction as a Neoadjuvant Treatment of Chemotherapy by Improving Diarrhea and Tumor Response. *Front. Pharmacol.* 11. doi:10.3389/fphar.2020.00252

Chao, D.-C., Lin, L.-J., Kao, S.-T., Huang, H.-C., Chang, C.-S., Liang, J.-A., et al. (2011). Inhibitory Effects of Zuo-Jin-Wan and its Alkaloidal Ingredients on Activator Protein 1, Nuclear Factor-Kb, and Cellular Transformation in HepG2 Cells. *Fitoterapia* 82 (4), 696–703. doi:10.1016/j.fitote.2011.02.009

Cho, Y.-H., Cha, P.-H., Kaduwal, S., Park, J.-C., Lee, S.-K., Yoon, J.-S., et al. (2016). KY1022, a Small Molecule Destabilizing Ras via Targeting the Wnt/β-Catenin Pathway, Inhibits Development of Metastatic Colorectal Cancer. *Oncotarget* 7 (49), 81727–81740. doi:10.18632/oncotarget.13172

Christie, M., Jorissen, R. N., Mouradov, D., Sakthianandeswaren, A., Li, S., Day, F., et al. (2013). Different APC Genotypes in Proximal and Distal Sporadic Colorectal Cancers Suggest Distinct WNT/β-catenin Signalling Thresholds for Tumourigenesis. *Oncogene* 32 (39), 4675–4682. doi:10.1038/onc.2012.486

Clara, J. A., Monge, C., Yang, Y., and Takebe, N. (2020). Targeting Signalling Pathways and the Immune Microenvironment of Cancer Stem Cells - a Clinical Update. *Nat. Rev. Clin. Oncol.* 17 (4), 204–232. doi:10.1038/s41571-019-0293-2

Deguchi, A. (2015). Curcumin Targets in Inflammation and Cancer. *Emiddt* 15 (2), 88–96. doi:10.2174/1871530315666150316120458

Diwanji, N., and Bergmann, A. (2018). An Unexpected Friend – ROS in Apoptosis-Induced Compensatory Proliferation: Implications for Regeneration and Cancer. *Semin. Cel Dev. Biol.* 80, 74–82. doi:10.1016/j.semcdb.2017.07.004

Drost, J., van Jaarsveld, R. H., Ponsioen, B., Zimberlin, C., van Boxtel, R., Buijs, A., et al. (2015). Sequential Cancer Mutations in Cultured Human Intestinal Stem Cells. *Nature* 521 (7550), 43–47. doi:10.1038/nature14415

Ewan, K., Pająk, B., Stubbs, M., Todd, H., Barbeau, O., Quevedo, C., et al. (2010). A Useful Approach to Identify Novel Small-Molecule Inhibitors of Wnt-dependent Transcription. *Cancer Res.* 70 (14), 5963–5973. doi:10.1158/0008-5472.CAN-10-1028

Filippo, C. D., Luceri, C., Caderni, G., Pacini, M., Messerini, L., Biggeri, A., et al. (2002). Mutations of the APC Gene in Human Sporadic Colorectal Cancers. *Scand. J. Gastroenterol.* 37 (9), 1048–1053. doi:10.1080/003655202320378248

Fodde, R. (2002). The APC Gene in Colorectal Cancer. *Eur. J. Cancer* 38 (7), 867–871. doi:10.1016/s0959-8049(02)00040-0

Franke, A. J., Skelton, W. P., Starr, J. S., Parekh, H., Lee, J. J., Overman, M. J., et al. (2019). Immunotherapy for Colorectal Cancer: A Review of Current and Novel Therapeutic Approaches. *J. Natl. Cancer Inst.* 111 (11), 1131–1141. doi:10.1093/jnci/djz093

Gonsalves, F. C., Klein, K., Carson, B. B., Katz, S., Ekas, L. A., Evans, S., et al. (2011). An RNAi-Based Chemical Genetic Screen Identifies Three Small-Molecule Inhibitors of the Wnt/wingless Signaling Pathway. *Proc. Natl. Acad. Sci.* 108 (15), 5954–5963. doi:10.1073/pnas.1017496108

Gu, Y., Wang, Q., Guo, K., Qin, W., Liao, W., Wang, S., et al. (2016). TUSC3 Promotes Colorectal Cancer Progression and Epithelial-Mesenchymal Transition (EMT) through WNT/β-catenin and MAPK Signalling. *J. Pathol.* 239 (1), 60–71. doi:10.1002/path.4697

Guo, J., Yang, Z., Zhou, H., Yue, J., Mu, T., Zhang, Q., et al. (2020). Upregulation of DKK3 by miR-483-3p Plays an Important Role in the Chemoprevention of Colorectal Cancer Mediated by Black Raspberry Anthocyanins. *Mol. Carcinog* 59 (2), 168–178. doi:10.1002/mc.23138

Guo, Z., Liu, Z., Yue, H., and Wang, J. (2018). Retracted : Beta-elemene Increases Chemosensitivity to 5-fluorouracil through Down-regulating microRNA-191 Expression in Colorectal Carcinoma Cells. *J. Cel. Biochem.* 119 (8), 7032–7039. doi:10.1002/jcb.26914

Gustavsson, B., Carlsson, G., Machover, D., Petrelli, N., Roth, A., Schmoll, H.-J., et al. (2015). A Review of the Evolution of Systemic Chemotherapy in the Management of Colorectal Cancer. *Clin. Colorectal Cancer* 14 (1), 1–10. doi:10.1016/j.clcc.2014.11.002

Hankey, W., Frankel, W. L., and Groden, J. (2018). Functions of the APC Tumor Suppressor Protein Dependent and Independent of Canonical WNT Signaling: Implications for Therapeutic Targeting. *Cancer Metastasis Rev.* 37 (1), 159–172. doi:10.1007/s10555-017-9725-6

Hao, J., Ao, A., Zhou, L., Murphy, C. K., Frist, A. Y., Keel, J. J., et al. (2013). Selective Small Molecule Targeting β-Catenin Function Discovered by *In Vivo* Chemical Genetic Screen. *Cel Rep.* 4 (5), 898–904. doi:10.1016/j.celrep.2013.07.047

He, B., Gao, J., Luo, X., Luo, J., Shen, J., Wang, L., et al. (2011). Ginsenoside Rg3 Inhibits Colorectal Tumor Growth through the Down-Regulation of Wnt/ß-Catenin Signaling. *Int. J. Oncol.* 38 (2), 437. doi:10.3892/ijo.2010.858

He, B.-C., Gao, J.-L., Zhang, B.-Q., Luo, Q., Shi, Q., Kim, S. H., et al. (2011). Tetrandrine Inhibits Wnt/β-Catenin Signaling and Suppresses Tumor Growth of Human Colorectal Cancer. *Mol. Pharmacol.* 79 (2), 211–219. doi:10.1124/mol.110.068668

He, X., Zhang, W., Yan, C., Nie, F., Li, C., Liu, X., et al. (2017). Chemical Biology Reveals CARF as a Positive Regulator of Canonical Wnt Signaling by Promoting TCF/β-catenin Transcriptional Activity. *Cell Discov* 3, 17003. doi:10.1038/celldisc.2017.3

Huang, S.-M. A., Mishina, Y. M., Liu, S., Cheung, A., Stegmeier, F., Michaud, G. A., et al. (2009). Tankyrase Inhibition Stabilizes Axin and Antagonizes Wnt Signalling. *Nature* 461 (7264), 614–620. doi:10.1038/nature08356

Isobe, T., Hisamori, S., Hogan, D. J., Zabala, M., Hendrickson, D. G., Dalerba, P., et al. (2014). miR-142 Regulates the Tumorigenicity of Human Breast Cancer Stem Cells through the Canonical WNT Signaling Pathway. *Elife* 3, e01977. doi:10.7554/eLife.01977

Ji, Q., Liu, X., Fu, X., Zhang, L., Sui, H., Zhou, L., et al. (2013). Resveratrol Inhibits Invasion and Metastasis of Colorectal Cancer Cells via MALAT1 Mediated Wnt/β-Catenin Signal Pathway. *PLoS One* 8 (11), e78700. doi:10.1371/journal.pone.0078700

Jiang, X., Li, S., Qiu, X., Cong, J., Zhou, J., and Miu, W. (2019). Curcumin Inhibits Cell Viability and Increases Apoptosis of SW620 Human Colon Adenocarcinoma Cells via the Caudal Type Homeobox-2 (CDX2)/Wnt/β-Catenin Pathway. *Med. Sci. Monit.* 25, 7451–7458. doi:10.12659/MSM.918364

Jiang, Z., Cao, Q., Dai, G., Wang, J., Liu, C., Lv, L., et al. (2019). Celastrol Inhibits Colorectal Cancer through TGF-β1/Smad Signaling. *Onco Targets Ther.* 12, 509–518. doi:10.2147/OTT.S187817

Katoh, M. (2018). Multi-layered P-revention and T-reatment of C-hronic I-nflammation, O-rgan F-ibrosis and C-ancer A-ssociated with C-anonical WNT/β-catenin S-ignaling A-ctivation (Review). *Int. J. Mol. Med.* 42 (2), 713–725. doi:10.3892/ijmm.2018.3689

Kaur, M., Velmurugan, B., Tyagi, A., Agarwal, C., Singh, R. P., and Agarwal, R. (2010). Silibinin Suppresses Growth of Human Colorectal Carcinoma SW480 Cells in Culture and Xenograft through Down-Regulation of β-Catenin-Dependent Signaling. *Neoplasia* 12 (5), 415–424. doi:10.1593/neo.10188

Kinzler, K., Nilbert, M., Su, L., Vogelstein, B., Bryan, T., Levy, D., et al. (1991). Identification of FAP Locus Genes from Chromosome 5q21. *Science* 253 (5020), 661–665. doi:10.1126/science.1651562

Krishnamachary, B., Subramaniam, D., Dandawate, P., Ponnurangam, S., Srinivasan, P., Ramamoorthy, P., et al. (2019). Targeting Transcription Factor TCF4 by Gamma-Mangostin, a Natural Xanthone. *Oncotarget* 10 (54), 5576–5591. doi:10.18632/oncotarget.27159

Lau, T., Chan, E., Callow, M., Waaler, J., Boggs, J., Blake, R. A., et al. (2013). A Novel Tankyrase Small-Molecule Inhibitor Suppresses APC Mutation-Driven Colorectal Tumor Growth. *Cancer Res.* 73 (10), 3132–3144. doi:10.1158/0008-5472.CAN-12-4562

Lee, S.-K., Cho, Y.-H., Cha, P.-H., Yoon, J.-S., Ro, E. J., Jeong, W.-J., et al. (2018a). A Small Molecule Approach to Degrade RAS with EGFR Repression Is a Potential Therapy for KRAS Mutation-Driven Colorectal Cancer Resistance to Cetuximab. *Exp. Mol. Med.* 50 (11), 1–12. doi:10.1038/s12276-018-0182-2

Lee, S.-K., Hwang, J.-H., and Choi, K.-Y. (2018b). Interaction of the Wnt/β-Catenin and RAS-ERK Pathways Involving Co-stabilization of Both β-catenin and RAS Plays Important Roles in the Colorectal Tumorigenesis. *Adv. Biol. Regul.* 68, 46–54. doi:10.1016/j.jbior.2018.01.001

Lei, C., Yao, Y., Shen, B., Liu, J., Pan, Q., Liu, N., et al. (2019). Columbamine Suppresses the Proliferation and Malignization of colon Cancer Cells via Abolishing Wnt/β-Catenin Signaling Pathway. *Cancer Manag Res.* 11, 8635–8645. doi:10.2147/CMAR.S209861

Li, V. S. W., Ng, S. S., Boersema, P. J., Low, T. Y., Karthaus, W. R., Gerlach, J. P., et al. (2012). Wnt Signaling through Inhibition of β-Catenin Degradation in an Intact Axin1 Complex. *Cell* 149 (6), 1245–1256. doi:10.1016/j.cell.2012.05.002

Li, W., Yang, C.-J., Wang, L.-Q., Wu, J., Dai, C., Yuan, Y.-M., et al. (2019). A Tannin Compound from Sanguisorba Officinalis Blocks Wnt/β-Catenin Signaling Pathway and Induces Apoptosis of Colorectal Cancer Cells. *Chin. Med.* 14, (1). 22. doi:10.1186/s13020-019-0244-y

Li, X., Pu, J., Jiang, S., Su, J., Kong, L., Mao, B., et al. (2013). Henryin, an Ent-Kaurane Diterpenoid, Inhibits Wnt Signaling through Interference with β-Catenin/TCF4 Interaction in Colorectal Cancer Cells. *PLoS One* 8 (7), e68525. doi:10.1371/journal.pone.0068525

Li, Y., Qin, X., Li, P., Zhang, H., Lin, T., Miao, Z., et al. (2019). Isobavachalcone Isolated From Psoralea Corylifolia Inhibits Cell Proliferation and Induces Apoptosis *via* Inhibiting the AKT/GSK-3beta/beta-catenin Pathway in Colorectal Cancer Cells. *Drug Des. Dev. Ther.* 13, 1449–1460. doi:10.2147/DDDT.S192681

Li, Y., Wang, S., Sun, Y., Xu, W., Zheng, H., Wang, Y., et al. (2020). Apple Polysaccharide Protects ICR Mice against Colitis Associated Colorectal Cancer through the Regulation of Microbial Dysbiosis. *Carbohydr. Polym.* 230, 115726. doi:10.1016/j.carbpol.2019.115726

Liu, J., Jiang, M., Li, Z., Zhang, X., Li, X., Hao, Y., et al. (2018). A Novel Systems Pharmacology Method to Investigate Molecular Mechanisms of Scutellaria Barbata D. Don for Non-small Cell Lung Cancer. *Front. Pharmacol.* 9, 1473. doi:10.3389/fphar.2018.01473

Lu, Y., Zhang, R., Zhang, X., Zhang, B., and Yao, Q. (2020). Curcumin May Reverse 5-fluorouracil Resistance on Colonic Cancer Cells by Regulating TET1-NKD-Wnt Signal Pathway to Inhibit the EMT Progress. *Biomed. Pharmacother.* 129, 110381. doi:10.1016/j.biopha.2020.110381

Ma, W., Li, X., Song, P., Zhang, Q., Wu, Z., Wang, J., et al. (2019). A Vanillin Derivative Suppresses the Growth of HT29 Cells through the Wnt/β-Catenin Signaling Pathway. *Eur. J. Pharmacol.* 849, 43–49. doi:10.1016/j.ejphar.2019.01.047

Masaru, K. (2017). Canonical and Non-canonical WNT Signaling in Cancer Stem Cells and Their Niches: Cellular Heterogeneity, Omics Reprogramming, Targeted Therapy and Tumor Plasticity (Review). *Int. J. Oncol.* 51 (5), 1357–1369. doi:10.3892/ijo.2017.4129

Mashima, T., Taneda, Y., Jang, M.-K., Mizutani, A., Muramatsu, Y., Yoshida, H., et al. (2017). mTOR Signaling Mediates Resistance to Tankyrase Inhibitors in Wnt-Driven Colorectal Cancer. *Oncotarget* 8 (29), 47902–47915. doi:10.18632/oncotarget.18146

Matano, M., Date, S., Shimokawa, M., Takano, A., Fujii, M., Ohta, Y., et al. (2015). Modeling Colorectal Cancer Using CRISPR-Cas9-Mediated Engineering of Human Intestinal Organoids. *Nat. Med.* 21 (3), 256–262. doi:10.1038/nm.3802

Mazzotta, S., Neves, C., Bonner, R. J., Bernardo, A. S., Docherty, K., and Hoppler, S. (2016). Distinctive Roles of Canonical and Noncanonical Wnt Signaling in Human Embryonic Cardiomyocyte Development. *Stem Cel Rep.* 7 (4), 764–776. doi:10.1016/j.stemcr.2016.08.008

Mcquade, R. M., Stojanovska, V., Bornstein, J. C., and Nurgali, K. (2017). Colorectal Cancer Chemotherapy: The Evolution of Treatment and New Approaches. *Curr Med Chem.* 24 (15), 1537–1557. doi:10.2174/0929867324666170111152436

Mervai, Z., Sólyomváry, A., Tóth, G., Noszál, B., Molnár-Perl, I., Baghy, K., et al. (2015). Endogenous Enzyme-Hydrolyzed Fruit of Cirsium Brachycephalum: Optimal Source of the Antiproliferative Lignan Trachelogenin Regulating the Wnt/β-Catenin Signaling Pathway in the SW480 Colon Adenocarcinoma Cell Line. *Fitoterapia* 100, 19–26. doi:10.1016/j.fitote.2014.10.017

Momtazi-Borojeni, A. A., Abdollahi, E., Ghasemi, F., Caraglia, M., and Sahebkar, A. (2018). The Novel Role of Pyrvinium in Cancer Therapy. *J. Cel. Physiol.* 233 (4), 2871–2881. doi:10.1002/jcp.26006

Narwal, M., Venkannagari, H., and Lehtio, L. (2012). Structural Basis of Selective Inhibition of Human Tankyrases. *J. Med. Chem.* 55 (3), 1360–1367. doi:10.1021/jm201510p

Network, C. G. A. (2012). Comprehensive Molecular Characterization of Human colon and Rectal Cancer. *Nature* 487 (7407), 330–337. doi:10.1038/nature11252

Nguyen, A. V., Martinez, M., Stamos, M. J., Moyer, M. P., Planutis, K., Hope, C., et al. (2009). Results of a Phase I Pilot Clinical Trial Examining the Effect of Plant-Derived Resveratrol and Grape Powder on Wnt Pathway Target Gene Expression in Colonic Mucosa and colon Cancer. *Cancer Manag. Res.* 1, 25–37.

Nguyen, L. H., Goel, A., and Chung, D. C. (2020). Pathways of Colorectal Carcinogenesis. *Gastroenterology* 158 (2), 291–302. doi:10.1053/j.gastro.2019.08.059

Nishisho, I., Nakamura, Y., Miyoshi, Y., Miki, Y., Ando, H., Horii, A., et al. (1991). Mutations of Chromosome 5q21 Genes in FAP and Colorectal Cancer Patients. *Science* 253 (5020), 665–669. doi:10.1126/science.1651563

Pahlke, G., Ngiewih, Y., Kern, M., Jakobs, S., Marko, D., and Eisenbrand, G. (2006). Impact of Quercetin and EGCG on Key Elements of the Wnt Pathway in Human Colon Carcinoma Cells. *J. Agric. Food Chem.* 54 (19), 7075–7082. doi:10.1021/jf0612530

Pan, J., Xu, Y., Song, H., Zhou, X., Yao, Z., and Ji, G. (2017). Extracts of Zuo Jin Wan, a Traditional Chinese Medicine, Phenocopies 5-HTR1D Antagonist in Attenuating Wnt/β-Catenin Signaling in Colorectal Cancer Cells. *BMC Complement. Altern. Med.* 17 (1). 506. doi:10.1186/s12906-017-2006-7

Pearlman, R., Frankel, W. L., Swanson, B., Zhao, W., Yilmaz, A., Miller, K., et al. (2017). Prevalence and Spectrum of Germline Cancer Susceptibility Gene Mutations Among Patients with Early-Onset Colorectal Cancer. *JAMA Oncol.* 3 (4), 464–471. doi:10.1001/jamaoncol.2016.5194

Polakis, P. (2012). Wnt Signaling in Cancer. *Cold Spring Harbor Perspect. Biol.* 4 (5), a008052. doi:10.1101/cshperspect.a008052

Predes, D., Oliveira, L., Ferreira, L., Maia, L. A., Delou, J., Faletti, A., et al. (2019). The Chalcone Lonchocarpin Inhibits Wnt/β-Catenin Signaling and Suppresses Colorectal Cancer Proliferation. *Cancers* 11 (12), 1968. doi:10.3390/cancers11121968

Qi, L., Sun, B., Liu, Z., Cheng, R., Li, Y., and Zhao, X. (2014). Wnt3a Expression Is Associated with Epithelial-Mesenchymal Transition and Promotes colon Cancer Progression. *J. Exp. Clin. Cancer Res.* 33, 107. doi:10.1186/s13046-014-0107-4

Qiu, S., Wu, X., Liao, H., Zeng, X., Zhang, S., Lu, X., et al. (2017). Pteisolic Acid G, a Novel Ent-Kaurane Diterpenoid, Inhibits Viability and Induces Apoptosis in Human Colorectal Carcinoma Cells. *Oncol. Lett.* 14 (5), 5540–5548. doi:10.3892/ol.2017.6889

Ren, H., Zhao, J., Fan, D., Wang, Z., Zhao, T., Li, Y., et al. (2019). Alkaloids from Nux Vomica Suppresses colon Cancer Cell Growth through Wnt/β-catenin Signaling Pathway. *Phytotherapy Res.* 33 (5), 1570–1578. doi:10.1002/ptr.6347

Reya, T., and Clevers, H. (2005). Wnt Signalling in Stem Cells and Cancer. *Nature* 434 (7035), 843–850. doi:10.1038/nature03319

Schatoff, E. M., Leach, B. I., and Dow, L. E. (2017). Wnt Signaling and Colorectal Cancer. *Curr. Colorectal Cancer Rep.* 13 (2), 101–110. doi:10.1007/s11888-017-0354-9

Sebio, A., Kahn, M., and Lenz, H.-J. (2014). The Potential of Targeting Wnt/β-Catenin in colon Cancer. *Expert Opin. Ther. Targets* 18 (6), 611–615. doi:10.1517/14728222.2014.906580

Shah, K., Panchal, S., and Patel, B. (2021). Porcupine Inhibitors: Novel and Emerging Anti-cancer Therapeutics Targeting the Wnt Signaling Pathway. *Pharmacol. Res.* 167, 105532. doi:10.1016/j.phrs.2021.105532

Shan, B., Wang, M., and Li, R. (2009). Quercetin Inhibit Human SW480 Colon Cancer Growth in Association with Inhibition of Cyclin D1 and Survivin Expression through Wnt/β-Catenin Signaling Pathway. *Cancer Invest.* 27 (6), 604–612. doi:10.1080/07357900802337191

Shan, J., Shi, D.-L., Wang, J., and Zheng, J. (2005). Identification of a Specific Inhibitor of the Dishevelled PDZ Domain†. *Biochemistry* 44 (47), 15495–15503. doi:10.1021/bi0512602

So, T.-H., Chan, S.-K., Lee, V. H.-F., Chen, B.-Z., Kong, F.-M., and Lao, L.-X. (2019). Chinese Medicine in Cancer Treatment - How Is it Practised in the East and the West?. *Clin. Oncol.* 31 (8), 578–588. doi:10.1016/j.clon.2019.05.016

Soo, Y. H., and Keller, T. H. (2015). The Use of porcupine Inhibitors to Target Wnt-Driven Cancers. *Bioorg. Med. Chem. Lett.* 25 (23), 5472–5476. doi:10.1016/j.bmcl.2015.10.032

Song, J., Seo, H., Kim, M.-R., Lee, S.-J., Ahn, S., and Song, M. (2020). Active Compound of Pharbitis Semen (Pharbitis Nil Seeds) Suppressed KRAS-Driven Colorectal Cancer and Restored Muscle Cell Function during Cancer Progression. *Molecules* 25 (12), 2864. doi:10.3390/molecules25122864

Spaderna, S., Schmalhofer, O., Hlubek, F., Berx, G., Eger, A., Merkel, S., et al. (2006). A Transient, EMT-Linked Loss of Basement Membranes Indicates Metastasis and Poor Survival in Colorectal Cancer. *Gastroenterology* 131 (3), 830–840. doi:10.1053/j.gastro.2006.06.016

Sun, M.-Y., Wang, D.-D., Sun, J., Zhao, X.-H., Cai, S., Wu, Q.-X., et al. (2019). The Zuo Jin Wan Formula Increases Chemosensitivity of Human Primary Gastric Cancer Cells by AKT Mediated Mitochondrial Translocation of Cofilin-1. *Chin. J. Nat. Medicines* 17 (3), 198–208. doi:10.1016/S1875-5364(19)30022-6

Sun, X., Xu, X., and Song, L. (2020). TKP, a Serine Protease Extracted fromTrichosanthes Kirilowii, Inhibits the Migration and Invasion of Colorectal Adenocarcinoma Cells by Targeting Wnt/β-catenin and Hedgehog/Gli1 Signalings. *Phytotherapy Res.* 34 (4), 867–878. doi:10.1002/ptr.6569

Tan, H., Li, X., Yang, W. H., and Kang, Y. (2019). A Flavone, Wogonin From Scutellaria Baicalensis Inhibits the Proliferation of Human Colorectal Cancer Cells by Inducing of Autophagy, Apoptosis and G2/M Cell Cycle Arrest *via* Modulating the PI3K/AKT and STAT3 Signalling Pathways. *J. BUON.* 24 (3), 1143–1149.

Tanaka, N., Mashima, T., Mizutani, A., Sato, A., Aoyama, A., Gong, B., et al. (2017). APC Mutations as a Potential Biomarker for Sensitivity to Tankyrase Inhibitors in Colorectal Cancer. *Mol. Cancer Ther.* 16 (4), 752–762. doi:10.1158/1535-7163.MCT-16-0578

Tao, L., Gu, Y., Zheng, J., Yang, J., and Zhu, Y. (2019). Weichang'an Suppressed Migration and Invasion of HCT116 Cells by Inhibiting Wnt/β-catenin Pathway while Upregulating ARHGAP25. *Biotechnol. Appl. Biochem.* 66 (5), 787–793. doi:10.1002/bab.1784

Tian, W., Han, X., Yan, M., Xu, Y., Duggineni, S., Lin, N., et al. (2012). Structure-Based Discovery of a Novel Inhibitor Targeting the β-Catenin/Tcf4 Interaction. *Biochemistry* 51 (2), 724–731. doi:10.1021/bi201428h

Todaro, M., Gaggianesi, M., Catalano, V., Benfante, A., Iovino, F., Biffoni, M., et al. (2014). CD44v6 Is a Marker of Constitutive and Reprogrammed Cancer Stem Cells Driving colon Cancer Metastasis. *Cell Stem Cell* 14 (3), 342–356. doi:10.1016/j.stem.2014.01.009

Vincan, E., and Barker, N. (2008). The Upstream Components of the Wnt Signalling Pathway in the Dynamic EMT and MET Associated with Colorectal Cancer Progression. *Clin. Exp. Metastasis* 25 (6), 657–663. doi:10.1007/s10585-008-9156-4

Voorneveld, P. W., Kodach, L. L., Jacobs, R. J., van Noesel, C. J. M., Peppelenbosch, M. P., Korkmaz, K. S., et al. (2015). The BMP Pathway Either Enhances or Inhibits the Wnt Pathway Depending on the SMAD4 and P53 Status in CRC. *Br. J. Cancer* 112 (1), 122–130. doi:10.1038/bjc.2014.560

Vu, T., and Datta, P. (2017). Regulation of EMT in Colorectal Cancer: A Culprit in Metastasis. *Cancers* 9 (12), 171. doi:10.3390/cancers9120171

Waaler, J., Machon, O., Tumova, L., Dinh, H., Korinek, V., Wilson, S. R., et al. (2012). A Novel Tankyrase Inhibitor Decreases Canonical Wnt Signaling in colon Carcinoma Cells and Reduces Tumor Growth in Conditional APC Mutant Mice. *Cancer Res.* 72 (11), 2822–2832. doi:10.1158/0008-5472.CAN-11-3336

Wang, D., Ge, S., Chen, Z., and Song, Y. (2019). Evodiamine Exerts Anticancer Effects via Induction of Apoptosis and Autophagy and Suppresses the Migration and Invasion of Human colon Cancer Cells. *J. BUON.* 24 (5), 1824–1829.

Wei, L.-H., Lin, J.-M., Chu, J.-F., Chen, H.-W., Li, Q.-Y., and Peng, J. (2017). Scutellaria Barbata D. Don Inhibits Colorectal Cancer Growth via Suppression of Wnt/β-Catenin Signaling Pathway. *Chin. J. Integr. Med.* 23 (11), 858–863. doi:10.1007/s11655-017-2775-3

Wen, S.-Y., Chen, Y. Y., Deng, C. M., Zhang, C. Q., and Jiang, M. M (2019). Nerigoside Suppresses Colorectal Cancer Cell Growth and Metastatic Potential Through Inhibition of ERK/GSK3beta/Beta-Catenin Signaling Pathway. *Phytomedicine.* 57, 352–363. doi:10.1016/j.phymed.2018.12.033

Wu, C.-E., Zhuang, Y.-W., Zhou, J.-Y., Liu, S.-l., Wang, R.-P., and Shu, P. (2019). Cinnamaldehyde Enhances Apoptotic Effect of Oxaliplatin and Reverses Epithelial-Mesenchymal Transition and Stemnness in Hypoxic Colorectal Cancer Cells. *Exp. Cel Res.* 383 (1), 111500. doi:10.1016/j.yexcr.2019.111500

Wu, X., Yu, N., Zhang, Y., Ye, Y., Sun, W., Ye, L., et al. (2018). Radix Tetrastigma Hemsleyani Flavone Exhibits Antitumor Activity in Colorectal Cancer via Wnt/β-Catenin Signaling Pathway. *Onco Targets Ther.* 11, 6437–6446. doi:10.2147/OTT.S172048

Xu, C., Yang, M., Tian, J., Wang, X., and Li, Z. (2011). MALAT-1: a Long Non-coding RNA and its Important 3' End Functional Motif in Colorectal Cancer Metastasis. *Int. J. Oncol.* 39 (1), 169–175. doi:10.3892/ijo.2011.1007

Xu, M., Wang, S., Song, Y., Yao, J., Huang, K., and Zhu, X. (2016). Apigenin Suppresses Colorectal Cancer Cell Proliferation, Migration and Invasion via Inhibition of the Wnt/β-Catenin Signaling Pathway. *Oncol. Lett.* 11 (5), 3075–3080. doi:10.3892/ol.2016.4331

Yan, K. S., Janda, C. Y., Chang, J., Zheng, G. X. Y., Larkin, K. A., Luca, V. C., et al. (2017). Non-equivalence of Wnt and R-Spondin Ligands during Lgr5+ Intestinal Stem-Cell Self-Renewal. *Nature* 545 (7653), 238–242. doi:10.1038/nature22313

Yan, M., Li, G., and An, J. (2017). Discovery of Small Molecule Inhibitors of the Wnt/β-Catenin Signaling Pathway by Targeting β-catenin/Tcf4 Interactions. *Exp. Biol. Med. (Maywood)* 242 (11), 1185–1197. doi:10.1177/1535370217708198

Yang, Y., Han, Z., Han, Z., Li, X., Huang, A., Shi, J., et al. (2020). Epidemiology and Risk Factors of Colorectal Cancer in China. *Chin. J. Cancer Res.* 32 (6), 729–741. doi:10.21147/j.issn.1000-9604.2020.06.06

Ye, Z.-N., Yuan, F., Liu, J.-Q., Peng, X.-R., An, T., Li, X., et al. (2019). Physalis Peruviana-Derived 4β-Hydroxywithanolide E, a Novel Antagonist of Wnt Signaling, Inhibits Colorectal Cancer *In Vitro* and *In Vivo*. *Molecules* 24 (6), 1146. doi:10.3390/molecules24061146

Yeh, M.-H., Chiu, H.-P., Wu, M.-C., Koo, M., Lin, N.-W., Liao, K.-K., et al. (2020). Integrated Chinese Herbal Medicine and Western Medicine on the Survival in Patients with Colorectal Cancer: A Retrospective Study of Medical Records. *Evidence-Based Complement. Altern. Med.* 2020, 1–10. doi:10.1155/2020/4561040

Zhan, T., Rindtorff, N., and Boutros, M. (2017). Wnt Signaling in Cancer. *Oncogene* 36 (11), 1461–1473. doi:10.1038/onc.2016.304

Zhang, J., Cao, H., Zhang, B., Cao, H., Xu, X., Ruan, H., et al. (2013). Berberine Potently Attenuates Intestinal Polyps Growth in ApcMin Mice and Familial Adenomatous Polyposis Patients through Inhibition of Wnt Signalling. *J. Cel. Mol. Med.* 17 (11), 1484–1493. doi:10.1111/jcmm.12119

Zhang, L., Ren, B., Zhang, J., Liu, L., Liu, J., Jiang, G., et al. (2017). Anti-tumor Effect of Scutellaria Barbata D. Don Extracts on Ovarian Cancer and its Phytochemicals Characterisation. *J. Ethnopharmacology* 206, 184–192. doi:10.1016/j.jep.2017.05.032

Zhang, L., Zhang, J., Gong, Y., and Lv, L. (2020). Systematic and Experimental Investigations of the Anti-colorectal Cancer Mediated by Genistein. *Biofactors* 46 (6), 974–982. doi:10.1002/biof.1677

Zhang, T., Wang, K., Zhang, J., Wang, X., Chen, Z., Ni, C., et al. (2013). Huaier Aqueous Extract Inhibits Colorectal Cancer Stem Cell Growth Partially via Downregulation of the Wnt/β-Catenin Pathway. *Oncol. Lett.* 5 (4), 1171–1176. doi:10.3892/ol.2013.1145

Zhang, Y., Appleton, B. A., Wiesmann, C., Lau, T., Costa, M., Hannoush, R. N., et al. (2009). Inhibition of Wnt Signaling by Dishevelled PDZ Peptides. *Nat. Chem. Biol.* 5 (4), 217–219. doi:10.1038/nchembio.152

Conflict of Interest: The authors declare that the research was conducted in the absence of any commercial or financial relationships that could be construed as a potential conflict of interest.

Publisher's Note: All claims expressed in this article are solely those of the authors and do not necessarily represent those of their affiliated organizations, or those of the publisher, the editors and the reviewers. Any product that may be evaluated in this article, or claim that may be made by its manufacturer, is not guaranteed or endorsed by the publisher.

frontiers in Pharmacology

ORIGINAL RESEARCH
published: 27 August 2021
doi: 10.3389/fphar.2021.708093

Combining Sodium Butyrate With Cisplatin Increases the Apoptosis of Gastric Cancer *In Vivo* and *In Vitro* via the Mitochondrial Apoptosis Pathway

Yangbo Li[1,2,3], *Pengzhan He*[1,2,3], *Yinghui Liu*[1,2,3], *Mingming Qi*[1,2,3] *and Weiguo Dong*[1,2,3]*

[1]*Department of Gastroenterology, Renmin Hospital of Wuhan University, Wuhan, China,* [2]*Central Laboratory, Renmin Hospital of Wuhan University, Wuhan, China,* [3]*Key Laboratory of Hubei Province for Digestive System Disease, Wuhan, China*

Introduction: The gastrointestinal malignancy, gastric cancer (GC), has a high incidence worldwide. Cisplatin is a traditional chemotherapeutic drug that is generally applied to treat cancer; however, drug tolerance affects its efficacy. Sodium butyrate is an intestinal flora derivative that has general anti-cancer effects in vitro and in vivo via pro-apoptosis effects and can improve prognosis in combination with traditional chemotherapy drugs. The present study aimed to assess the effect of sodium butyrate combined with cisplatin on GC.

Methods: A Cell Counting Kit-8 assay was used to assess the viability of GC cells in vitro. Hoechst 33,258 staining and Annexin V-Phycoerythrin/7-Aminoactinomycin D were used to qualitatively and quantitatively detect apoptosis in GC cells. Intracellular reactive oxygen species (ROS) measurement and a mitochondrial membrane potential (MMP) assay kit were used to qualitatively and quantitatively reflect the function of mitochondria in GC cells. Western blotting was used to verify the above experimental results. A nude mouse xenograft tumor model was used to evaluate the anti-tumor efficacy of sodium and cisplatin butyrate in vivo.

Results: Cisplatin combined with sodium butyrate increased the apoptosis of GC cells. In the nude mouse xenograft tumor model, sodium butyrate in combination with cisplatin markedly inhibited the growth of the tumor more effectively than either single agent. The combination of sodium butyrate and cisplatin increased the intracellular ROS, decreased the MMP, and suppressed the invasion and migration abilities of GC cells. Western blotting verified that the combination of sodium butyrate and cisplatin remarkably enhanced the levels of mitochondrial apoptosis-related pathway proteins.

Conclusion: Sodium butyrate, a histone acetylation inhibitor produced by intestinal flora fermentation, combined with cisplatin enhanced the apoptosis of GC cells through the mitochondrial apoptosis-related pathway, which might be considered as a therapeutic option for GC.

Keywords: sodium butyrate, cisplatin, gastric cancer, apoptosis, mitochondrial pathway

OPEN ACCESS

Edited by:
Marne Carvalho de Vasconcellos, Federal University of Amazonas, Brazil

Reviewed by:
Bibo Tan, Fourth Hospital of Hebei Medical University, China
Consuelo Amantini, University of Camerino, Italy

***Correspondence:**
Weiguo Dong
dongweiguo@whu.edu.cn

Specialty section:
This article was submitted to Pharmacology of Anti-Cancer Drugs, a section of the journal Frontiers in Pharmacology

Received: *11 May 2021*
Accepted: *31 July 2021*
Published: *27 August 2021*

Citation:
Li Y, He P, Liu Y, Qi M and Dong W (2021) Combining Sodium Butyrate With Cisplatin Increases the Apoptosis of Gastric Cancer In Vivo *and* In Vitro *via the Mitochondrial Apoptosis Pathway. Front. Pharmacol. 12:708093. doi: 10.3389/fphar.2021.708093*

INTRODUCTION

Gastric cancer (GC) is one of the most common gastrointestinal malignancies and ranks fifth in the incidence of malignancies worldwide. In 2020, the number of deaths caused by gastric cancer was estimated to exceed 769,000, and its mortality rate ranks only behind lung cancer and liver cancer according to the latest data from GLOBOCAN 2020 (Sung et al., 2021). Although a recent study showed that GC incidence and mortality rates have continued to decline globally (Luo et al., 2017), stomach cancer remains a heavy health burden in China. In 2018, 10.6% of all cases of GC occurred in China, and the 5-year survival rate was quite low, at less than 35% from 2013 to 2015 (Zeng et al., 2018). Currently, the major treatment modalities for GC are combination therapy, radiotherapy, and surgery; however, the fact that 70% of patients with GC are diagnosed as suffering from terminal cancer greatly limits the effectiveness of treatment (Song et al., 2017). Drug resistance to cisplatin and 5-fluorouracil, for example, which are common traditional therapies, has resulted in progressively poor curation outcomes. Therefore, it is necessary to find new natural anticancer drugs with low toxicity and high efficiency to construct new chemotherapy regimen combinations to avoid worsening drug resistance.

Sodium butyrate (NaB), a derivative of butyric acid, is a metabolite produced by the breakdown of fiber in food residues by intestinal microorganisms (Sanna et al., 2019). Sodium butyrate not only regulates intestinal function, provides energy to intestinal epithelial cells, and regulates cell flora but also acts as an anti-inflammatory factor to maintain intestinal homeostasis (Bardhan et al., 2015). In addition, sodium butyrate is a natural histone deacetylase inhibitor (HDACi). HDACis are a new class of oncology chemotherapeutic drugs that have shown enhanced efficacy and reduced toxicity in combination with classical therapies (Guerriero et al., 2017). Scholars have shown experimentally that sodium butyrate can inhibit proliferation and promote apoptosis *in vivo* and *in vitro* of a variety of tumor cells, such as bladder cancer (Wang F. et al., 2020), lung cancer (Xiao et al., 2020), and colorectal cancer (Wang W. et al., 2020; Xi et al., 2021). Sodium butyrate inhibits tumor growth through multiple mechanisms, particularly the mitochondrial apoptosis pathway (Salimi et al., 2017; Qin et al., 2020). Encouragingly, sodium butyrate made tumor cells more sensitive to the anticancer drug, docetaxel (Chen et al., 2020). Previous studies showed that sodium butyrate decreased the focal adhesion kinase (FAK) expression by increasing the death associated protein kinase (DAPK) levels in GC cells (Shin et al., 2012), potentially inducing the cell-cycle inhibitors, cyclin dependent kinase inhibitor 1A (CDKN1A, also known as p21Waf1/Cip1), and cyclin dependent kinase inhibitor 1B (CDKN1B, also known as p27Kip1), as well as the pro-apoptotic genes, *BAX* (encoding BCL2 associated X, apoptosis regulator), *BAK* (encoding BCL2 antagonist/killer), and *BIK* (encoding BCL2 interacting killer) in GC cells, which contributed to apoptosis (Litvak et al., 2000). However, the anti-tumor effect of sodium butyrate in combination with cisplatin in GC and its underlying mechanism remain unknown.

In the present study, GC cells were treated with sodium butyrate and cisplatin separately and in combination. The results showed that sodium butyrate inhibited the proliferation and promoted the apoptosis in GC cells by activating the mitochondrial apoptosis pathway.

MATERIALS AND METHODS

Cell Culture

The China Center for Type Culture Collection (CCTCC) provided the human GC cell lines (HGC-27, SGC-7901, and MGC-803) and the normal cell line (GES-1). The cells were cultured in Dulbecco's modified Eagle's medium (DMEM)/F-12 medium (1:1) (HyClone, Logan, UT, United States) and Roswell Park Memorial Institute (RPMI) 1,640 medium (Gibco, Grand Island, NY, United States) with 10% fetal bovine serum (FBS) (Gibco) and a 1% solution of antibiotics (penicillin at 100 U/ml and streptomycin at 100 g/ml) (Beyotime, Jiangsu, China) at 37°C and 5% CO_2 in a humidified incubator.

Reagents and Antibodies

Sodium butyrate (>99% purity) and cisplatin were obtained from Sigma-Aldrich (St. Louis, MO, United States). Sodium butyrate was dissolved in ultrapure water to prepare a 900 mM stock solution and cisplatin was dissolved in absolute dimethyl sulfoxide (DMSO) to prepare a 4 mg/ml (4 mg cisplatin +1 ml DMSO) stock solution, both of which were stored at −20°C.

Rabbit monoclonal antibodies against B-cell lymphoma 2 (BCL-2), BCL2 associated X (BAX), Cytochrome C (CytC), apoptotic protease activating factor-1 (Apaf-1), apoptosis inducing factor (AIF), proliferating cell nuclear antigen (PCNA), cleaved caspase-3, cleaved caspase-9, matrix metalloproteinase (MMP)-2, MMP-9, survivin, and glyceraldehyde-3-phosphate dehydrogenase (GAPDH) were obtained from Cell Signaling Technology (Danvers, MA, United States). The antibodies are diluted to a working concentration at a ratio of 1:1,000 and stored at 4°C. The secondary antibodies were used at a working concentration of 1:10,000 and were obtained from LI-COR (Lincoln, NE, United States).

Cell Proliferation Assay

The cell proliferation and viability were assessed quantitatively using a Cell Counting Kit-8 (CCK-8, Beyotime, Shanghai, China) *in vitro*. SGC-7901, HGC-27, MGC-803, and GES-1 cells (normal gastric mucosa epithelial cells) were sown in 96-well plates (at 5×10^3 cells/well) and cultured for 24 h. Then, the GC cells were treated initially with different concentrations of sodium butyrate (0, 1, 2, 4, 8, 16, 32, and 64 mM), different concentrations of cisplatin (0, 1, 2, 4, 8, 16, 32, and 64 μg/ml), or a combination of cisplatin (0, 1, 2, 4, 8, 16, 32, and 64 μg/ml) and sodium butyrate (0.5 mM or 0, 1, 2, 4, 8, 16, 32, and 64 mM) for additional 24 h. The next day, we aspirated the supernatant liquid of each well, added 10 μL of CCK-8 solution, and continued the incubation for 2 h. Meanwhile, the control cells were incubated in DMEM/F-12 medium containing 10% CCK-8. Finally, a microplate reader

(Victor3 1,420 Multilabel Counter, Perkin Elmer, Waltham, MA, United States) was used to measure the absorbance of each sample at 450 nm. GraphPad Prism software (GraphPad Inc., La Jolla, CA, United States) was used to calculate the half maximal inhibitory concentration (IC50) and CompuSyn software (CompuSyn Inc., Paramus, NJ, United States), which is based on the Chou-Talalay method, was used to obtain the combination index (CI) and to construct fraction affected (Fa)-CI plots. CI < 1, CI = 1, and CI > 1 represent synergistic, additive, and antagonistic effects, respectively, and the experiment was repeated three times in parallel.

Transwell Invasion Assay

The GC cells were digested using trypsin and 100 μL of the cell suspension (5×10^4 cells) was seeded on the upper chamber of a Transwell insert (Corning Costar Corp, Corning, NY, United States) with 8 μm pores that were precoated with Matrigel (BD Biosciences, San Jose, CA, United States). The next step was to add 600 μL of DMEM/F-12 medium with 15% FBS into the lower chamber and then the insert was incubated overnight in the incubator. The HGC-27 cells were treated with DDP (4 μg/ml), NaB (10 mM), or DDP (4 μg/ml) plus NaB (10 mM). Meanwhile, the SGC-7901 cells were treated with DDP (4 μg/ml), NaB (5 mM), or DDP (4 μg/ml) plus NaB (5 mM). After 24 h of incubation, the Transwell insert was put into a 24-well plate with 600 μL 4% paraformaldehyde to fix the cells for 20 min; then 0.2% crystal violet was used to stain the cells. After washing three times with phosphate-buffered saline (PBS), the Transwell inserts were observed in five random fields for each sample to count the invasive cells under an inverted microscope (BX51; Olympus Corporation, Tokyo, Japan).

Wound-Healing Assay

The cells were seeded into a 6-well plate chamber (5×10^5 cells/well) with fresh medium and incubated for 24 h. The next day, when the cells were spread evenly over the well, a 200 μL pipette tip was used to make a scratch in the cell monolayer. PBS was used to clean floating debris and then the wound was photographed immediately (0 h). The HGC-27 cells on the plates were then cultured in DMEM/F-12 medium with 10% FBS together with DDP (4 μg/ml), NaB (10 mM), or DDP (4 μg/ml) plus NaB (10 mM). Meanwhile, the SGC-7901 cells on the plates were cultured in DMEM/F-12 medium with 10% FBS together with DDP (4 μg/ml), NaB (5 mM), or DDP (4 μg/ml) plus NaB (5 mM). The wounds were photographed at 48 h and the area of wound healing was measured.

Hoechst 33,258 Detection of the Apoptotic Cells

We examined cell apoptosis using a Hoechst 33,258 Staining Kit (Beyotime). HGC-27 cells and SGC-7901 cells in the exponential growth phase were seeded into a 6-well plate (1×10^5 cells/well) and incubated for 24 h. The GC cells were treated with NaB and cisplatin as mentioned in "Transwell Invasion Assay" section.4 and then stained with Hoechst 33,258 according to the manufacturer's instructions. The morphological features of apoptosis, such as chromatin condensation and nuclear fragmentation, were observed using fluorescence microscopy (BX51, Olympus).

Apoptosis Analysis Using Annexin V-PE/7AAD Double Staining

An Annexin V-Phycoerythrin (PE)/7-Aminoactinomycin D (7AAD) kit (MultiSciences, Hangzhou, China) and flow cytometry (FACSCalibur, Becton Dickinson, Franklin Lakes, NJ, United States) were used to quantify the percentage of apoptotic cells. The cells were seeded into a 6-well plate and incubated for 24 h with different treatments and with or without pretreatment with N-acetylcysteine (NAC) or buthionine sulphoximine (BSO) for 2 h. According to the instructions, the adherent cells were collected and washed with PBS and finally co-stained with 5 μL Annexin V-PE and 5 μL 7AAD in binding buffer before the flow cytometry analysis. The cells were divided into four cell populations based on their various fluorescence characteristics: necrotic cells (Annexin V-PE− and 7AAD+), live cells (Annexin V-PE− and 7AAD−), late apoptotic cells (Annexin V-PE+ and 7AAD+), and early apoptotic cells (Annexin V-PE+ and 7AAD−).

Measuring the ROS Levels

A ROS Assay Kit (Beyotime) was used to measure the ROS levels using 2′,7′-dichloro-fluorescein diacetate (DCFH-DA). The cells were seeded into a 24-well plate (1×10^5 cells/well) and then exposed to DDP or NaB at different concentrations, as mentioned in "Transwell Invasion Assay" section, for 24 h. The next day, the cells were incubated with 10 μmol/L DCFH-DA for 20 min at 37°C in the dark. After being washed with PBS three times, coverslips were attached to the glass slides, and the cells were observed under an upright fluorescence microscope (Olympus).

Measuring the Mitochondrial Membrane Potential

The changes to the mitochondrial membrane potential (△Ψm) were assessed using a Mitochondrial Membrane Potential Assay Kit with JC-1 (Beyotime). After the cells were treated, as mentioned in "Transwell Invasion Assay" section, for 24 h, the supernatant was removed and the cells were treated with JC-1 dye for 1 h. Finally, the cells were washed with buffer solution twice before observation under a laser confocal fluorescence microscope (Olympus) or were detected and analyzed using a flow cytometer.

Western Blotting Analysis

After treatment with DDP or NaB, as mentioned in "Transwell Invasion Assay" section, for 24 h, the cell proteins were extracted in RIPA buffer supplemented with phenylmethylsulfonyl fluoride (PMSF) and protease inhibitors (Beyotime). A bicinchoninic acid (BCA) Protein Assay Kit (Beyotime) was then used to determine the protein concentrations according to the manufacturer's instructions. The cellular proteins were separated by 10% SDS-PAGE and transferred to polyvinylidene difluoride (PVDF)

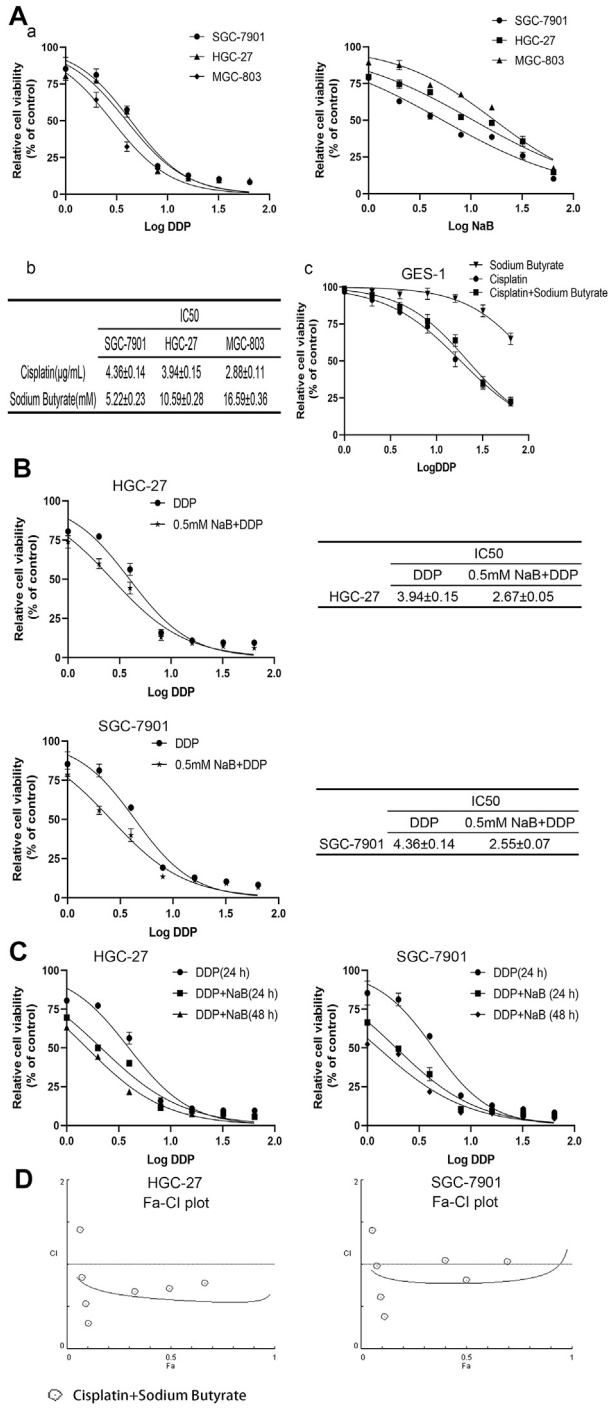

FIGURE 1 | Evaluation of GC cells' growth inhibition induced by cisplatin and/or sodium butyrate by CCK-8 kit. **(A)** (a) GC cells (HGC-27, SGC-7901 and MGC-803) were treated with cisplatin (0, 1, 2, 4, 8, 16, 32, and 64 μg/ml) or sodium butyrate (0, 1, 2, 4, 8, 16, 32, and 64 mM) for 24 h. (b) Cell Counting Kit-8 assays showed that HGC-27 cells and SGC-7901 cells were more sensitive to sodium butyrate. (c) GES-1 cells were treated with the different concentrations of cisplatin or sodium butyrate as described above and a combination of cisplatin and sodium butyrate for 24 h. **(B)** HGC-27 cells and SGC-7901 cells were treated with cisplatin and a combination of cisplatin and sodium butyrate (0.5 mM) for 24 h, respectively. **(C)** HGC-27 cells and

(*Continued*)

TABLE 1 | Specific ways of adding drugs.

Cisplatin (μg/mL)	Sodium butyrate (mM)	Combination (cisplatin + sodium butyrate)
1	1	1 + 1
2	2	2 + 2
4	4	4 + 4
8	8	8 + 8
16	16	16 + 16
32	32	32 + 32
64	64	64 + 64

membranes (Millipore, Billerica, MA, United States). Immediately, the membranes were blocked with 5% non-fat dry milk in Tris-buffered saline-Tween 20 (TBST) for 1 h. Then, the membranes were incubated with primary rabbit antibodies at 4°C overnight. After washing with TBST four times (5 min each time), the membranes were further incubated with secondary antibodies for 2 h at room temperature. The membranes were then washed with TBST four times (5 min each time). The Odyssey infrared imaging system (LI-COR) was used to scan the membranes to determine the immunoreactive protein bands. GAPDH was used as a protein loading control.

Xenograft Tumor Models *In Vivo* and the TUNEL Assay

The Ethics Committee of Renmin Hospital of Wuhan University approved the study protocol and all the animal research procedures were performed according to the institutional ethical standards and/or those of the national research committee and according to the 1964 Helsinki Declaration and its later amendments or comparable ethical standards. The collected SGC-7901 cells were washed in serum-free DMEM, suspended in 100 μL of PBS, and implanted subcutaneously into the dorsal area of male BALB/c nude mice (5 weeks old), purchased from Beijing Life River Experimental Animal Technology Co. Ltd. (Beijing, China). When the tumor volume was approximately 100–150 mm^3, the nude mice were randomly divided into four groups (n = 6 per group), which were treated via intraperitoneal injection with normal saline, DDP (4 mg/kg), NaB (200 mg/kg), or DDP (4 mg/kg) plus NaB (200 mg/kg) every 2 days. The mouse weight and the tumor volume were measured after each treatment time. The tumor volume (TV) was calculated using the following formula: TV (mm^3) = $d^2 \times D/2$, where d and D represent the shortest and longest diameters, respectively. After 15 days, the mice were sacrificed humanely and their tumors were harvested and weighed. A terminal deoxynucleotidyl transferase dUTP nick end labeling (TUNEL) assay was performed using an

FIGURE 1 | SGC-7901 cells were treated with cisplatin and a combination of cisplatin and sodium butyrate for 24 h or 48 h. **(D)** CompuSyn software was used to define the type of drug-combination effect. All the above data are shown as the mean ± SD from an average of three experiments.

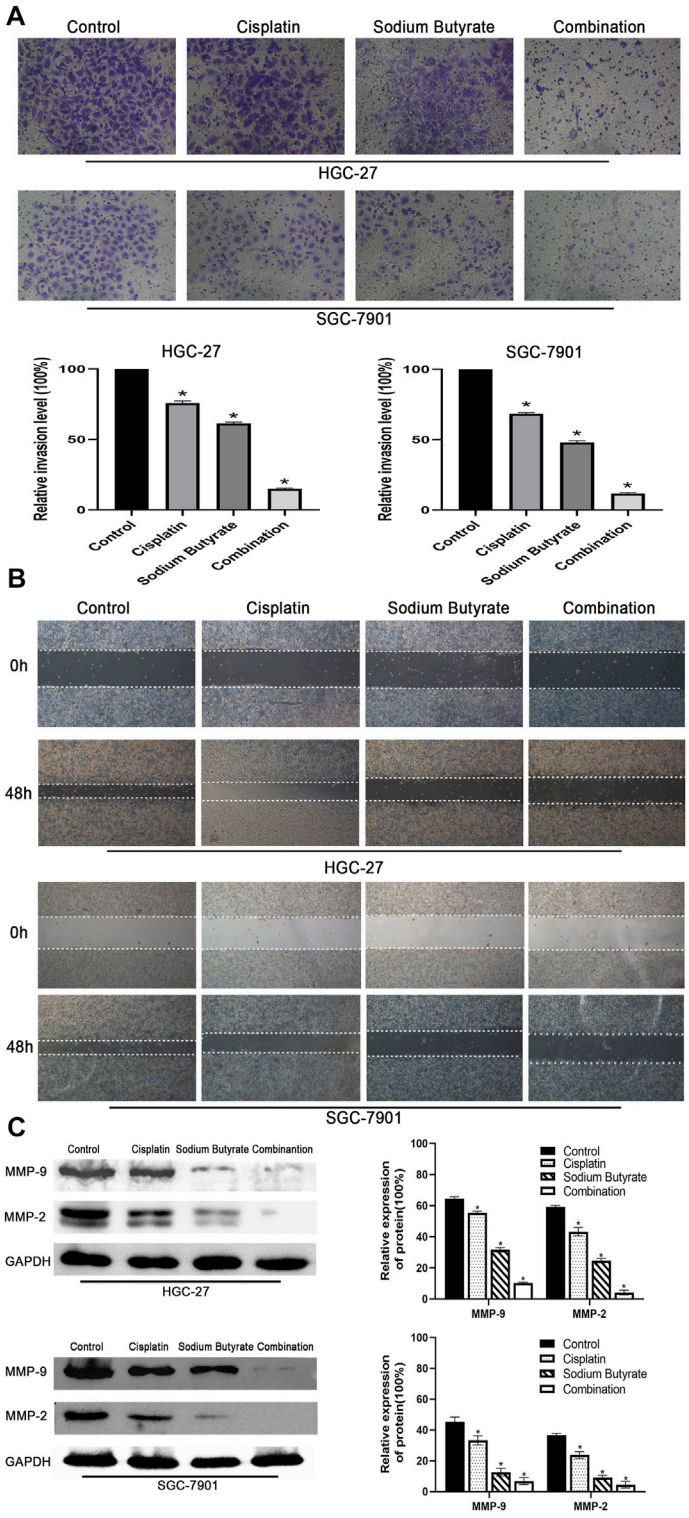

FIGURE 2 | Effects of sodium butyrate and cisplatin on the invasion and migration of GC cells using the Transwell invasion assay and the wound-healing assay. **(A)** Original magnification: ×200. HGC-27 cells were treated with control, 4 μg/ml cisplatin, 10 mM soiudm butyrate, or 4 μg/ml cisplatin +10 mM sodium butyrate; SGC-7901 cells were treated with control, 4 μg/ml cisplatin, 5 mM sodium butyrate, or 4 μg/ml cisplatin +5 mM sodium butyrate. Quantitative analysis of the average invasive cell numbers in each group. *$p < 0.05$ vs the control group. **(B)** Cells were incubated with control, cisplatin, sodium butyrate, or cisplatin + sodium butyrate described in **(A)** above. **(C)** The levels of MMP-9 and MMP-2 were measured using western blotting and quantitative analysis of the proteins was performed. *$p < 0.05$ vs the control group. All the above data are the mean ± SD from an average of three experiments.

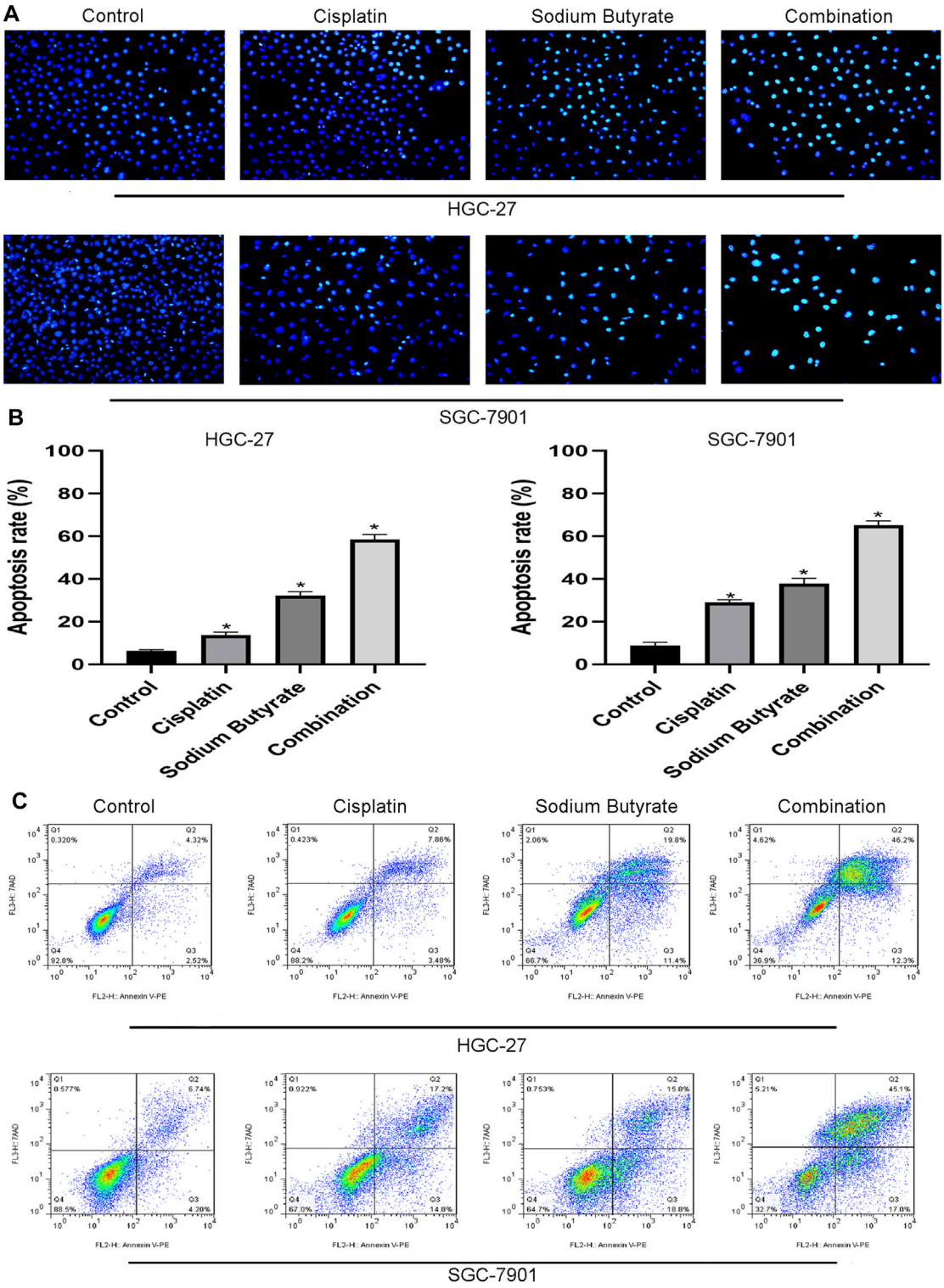

FIGURE 3 | Sodium butyrate combined with cisplatin promotes apoptosis of GC cells. **(A)** Original magnification: ×200. HGC-27 cells were treated with control, 4 μg/ml cisplatin, 10 mM sodium butyrate, or 4 μg/ml cisplatin +10 mM sodium butyrate; SGC-7901 cells were treated with control, 4 μg/ml cisplatin, 5 mM sodium butyrate, or 4 μg/ml cisplatin +5 mM sodium butyrate. **(B)** Quantitative analysis of the apoptosis rate in each group. *$p < 0.05$ vs the control. **(C)** Quantitative flow cytometry measurements of apoptosis in GC cells. All the above data are the mean ± SD from an average of three experiments.

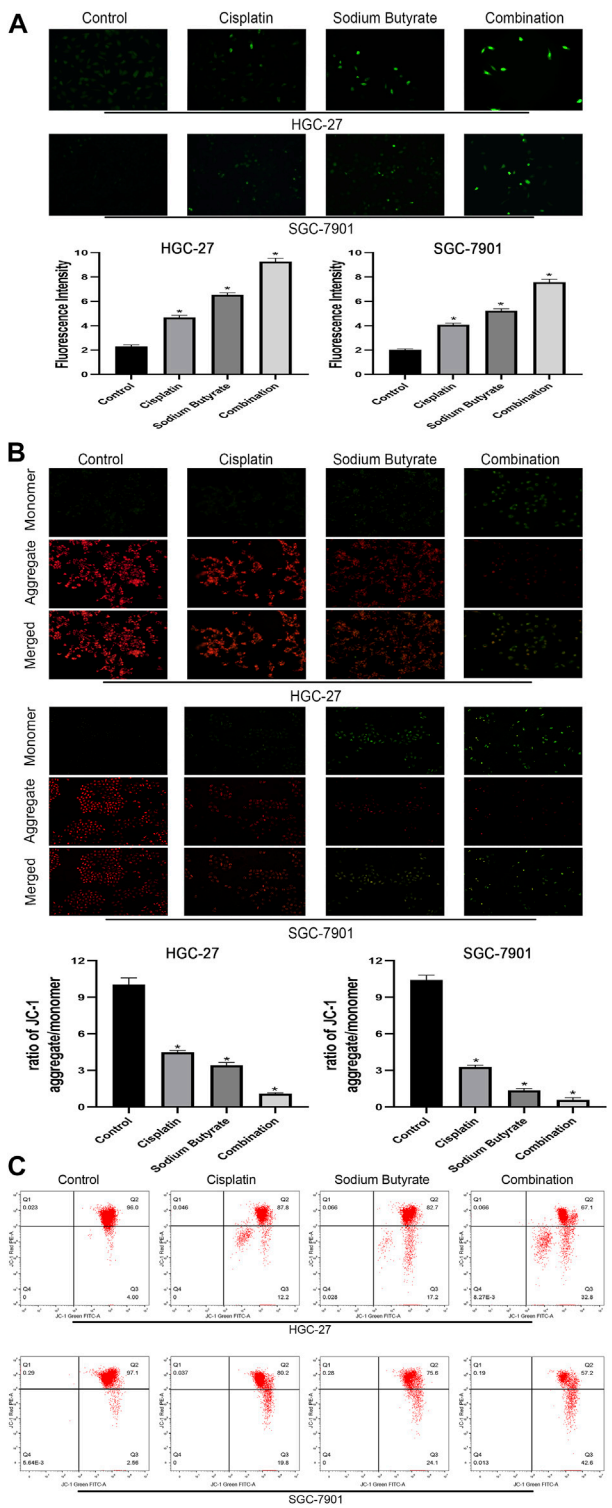

FIGURE 4 | Sodium butyrate combined with cisplatin promotes the accumulation of intracellular ROS and the decreasing trend of the MMP. **(A)** Original magnification: ×200. HGC-27 cells were treated with control, 4 μg/ml cisplatin, 10 mM sodium butyrate, or 4 μg/ml cisplatin +10 mM sodium butyrate; SGC-7901 cells were treated with control, 4 μg/ml cisplatin, 5 mM sodium butyrate, or 4 μg/ml cisplatin +5 mM sodium butyrate. Quantitative

(*Continued*)

apoptosis detection kit (Roche Applied Science, Basel, Switzerland) to detect the apoptotic cells in tumor tissue sections. To measure liver and renal function, we collected mouse blood to detect the activation of alanine aminotransferase (ALT) and aspartate aminotransferase (AST), and blood urea nitrogen (BUN) and serum creatinine (Cr) levels.

Statistical Analysis

SPSS 21.0 software (IBM Corp., Armonk, NY, United States) was used for statistical analysis. The data were expressed as the mean ± SD, and ANOVA was used for comparison between groups. $p < 0.05$ was considered statistically significant.

RESULTS

Sodium Butyrate Combined With Cisplatin Inhibited the Growth of GC Cells

The GC cells and GES-1 cells were exposed to different concentrations of sodium butyrate or cisplatin or both for 24 h. All 3 GC cell lines had different sensitivities to cisplatin and sodium butyrate. There was no significant effect on the viability of 90% of GC cells when the concentration of sodium butyrate was 0.5 mM, and the measured IC50 values are shown in **Figures 1Aa,b**. There was no significant cytotoxicity to GES-1 when the concentration of sodium butyrate was below 32 mM (**Figure 1Ac**). The combination of sodium butyrate with cisplatin decreased the IC50 value of cisplatin and attenuated the cytotoxic effect of cisplatin on the normal cells. Accordingly, we selected SGC-7901 cells and HGC-27 cells, which showed better sensitivities to sodium butyrate to perform the subsequent experiments. The IC50 values of DDP and sodium butyrate in the SGC-7901 cells at 24 h were about 4 μg/ml and 5 mM, respectively. Meanwhile, the IC50 values of DDP and sodium butyrate in the HGC-27 cells at 24 h were about 4 μg/ml and 10 mM. Then, the HGC-27 and SGC-7901 cells were exposed to combinations of cisplatin and sodium butyrate for 24 h or 48 h according to the drug dosing scheme in **Table 1**. **Figure 1C** shows that sodium butyrate combined with cisplatin remarkably inhibited the growth of GC cells to a greater extent than cisplatin alone in a time- and concentration-dependent manner. We generated Fa-CI plots using CompuSyn software, which showed the synergistic effects of the combination of sodium butyrate and cisplatin in inhibiting the viability of GC cells (**Figure 1D**). Using the combination of sodium butyrate (0.5 mM) with cisplatin to treat GC cells caused the IC50 value of cisplatin and sodium butyrate to be significantly lower than that of cisplatin alone (**Figure 1B**).

FIGURE 4 | analysis of ROS in each group. *$p < 0.05$ vs the control group. **((B)** and **(C))** Cells were incubated with control, cisplatin, sodium butyrate, or cisplatin + sodium butyrate described in **(A)** above. MMP was observed via JC-1 staining. Red inflorescence indicates healthy mitochondria; green inflorescence indicates collapsed mitochondrial potential. Quantitative analysis of the MMP in each group. *$p < 0.05$ vs the control group. All the above data are the mean ± SD from an average of three experiments.

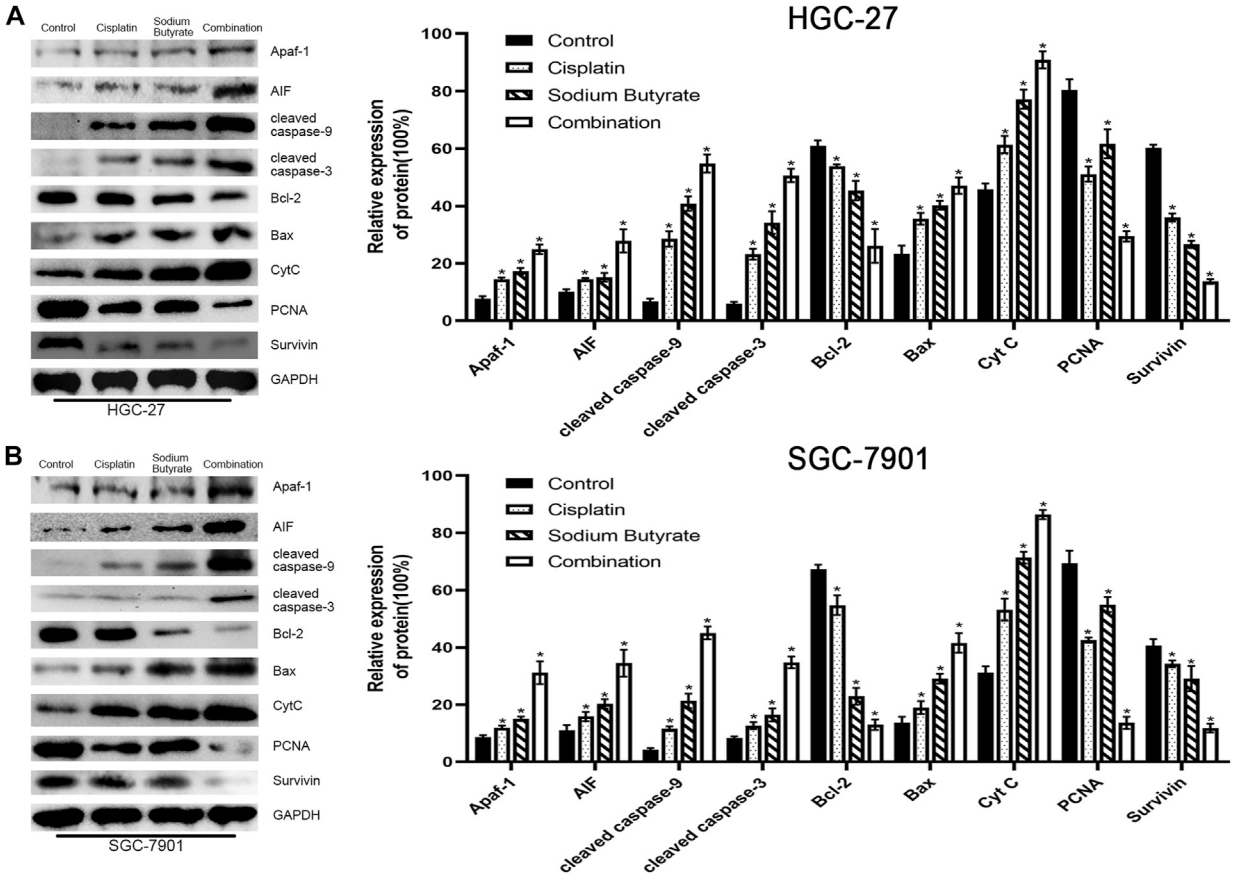

FIGURE 5 | Sodium butyrate combined with cisplatin induces apoptosis through the mitochondrial pathway. **(A)** HGC-27 cells were treated with control, 4 μg/ml cisplatin, 10 mM sodium butyrate, or 4 μg/ml cisplatin +10 mM sodium butyrate, and western blotting was performed to detect the levels of related proteins. *$p < 0.05$ vs the control group. **(B)** SGC-7901 cells were treated with control, 4 μg/ml cisplatin, 5 mM sodium butyrate, or 4 μg/ml cisplatin +5 mM sodium butyrate, and western blotting was performed to detect the levels of related proteins. *$p < 0.05$ vs the control group. All the above data are the mean ± SD from an average of three experiments.

Sodium Butyrate Combined With Cisplatin Inhibited the Migration and Invasion of Gastric Cancer Cells

Wound-healing assays and Transwell invasion assays were used to measure the invasion and migration of GC cells. According to the results shown in **Figures 2A,B**, the cells in the combination treatment group had poorer invasion and migration abilities than the other groups. Meanwhile, western blotting was used to check the levels of MMP-2 and MMP-9 proteins, which showed that the combination group had the lowest levels of MMP-2 and MMP-9 proteins among the groups (**Figure 2C**).

Sodium Butyrate Combined With Cisplatin Promoted Apoptosis in GC Cells

Hoechst 33,258 staining was used to evaluate the nuclei of GC cells exposed to sodium butyrate and/or cisplatin. The normal cell nuclei showed blue fluorescence, while the apoptotic cell nuclei showed bright blue fluorescence with fragmentation and chromatin condensation. The randomly selected fields of view showed that sodium butyrate combined with cisplatin promoted the apoptosis to a greater extent than that in the other groups of GC cells (**Figures 3A,B**). Annexin V-PE/7AAD staining further confirmed that sodium butyrate plus cisplatin promoted apoptosis to a greater extent than did the other treatments (**Figure 3C**).

Sodium Butyrate Combined With Cisplatin Promotes Apoptosis of Gastric Cancer Cells via the Mitochondrial Apoptosis Pathway

To determine whether sodium butyrate combined with cisplatin facilitates the apoptosis of GC cells through the mitochondrial apoptosis pathway, changes in ROS levels and mitochondrial membrane potential ($\Delta\Psi m$) levels were assessed. **Figure 4A** shows that the combination group accumulated more ROS (green fluorescence) than the other groups of GC cells. In **Figures 4B,C**, the fluorescence ratio of the JC-1 polymer of the combined drug group was the lowest among the four groups, indicating a decrease in the $\Delta\Psi m$.

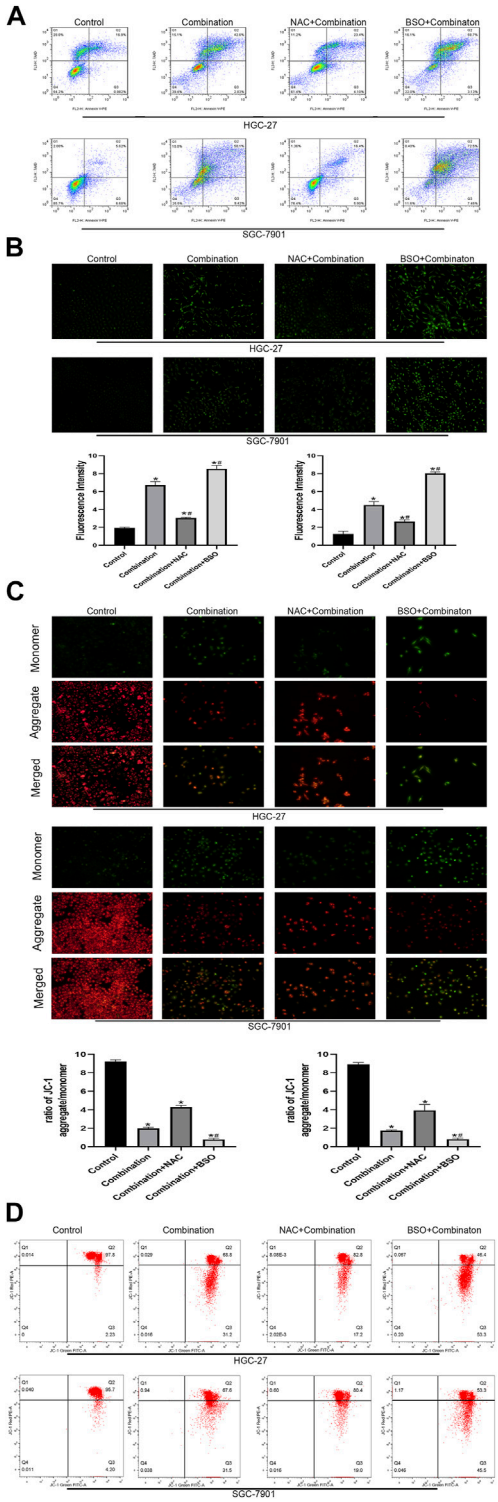

FIGURE 6 | Pretreatment with NAC and BSO respectively influences the apoptosis of GC cells induced by soduim butyrate and cisplatin. **(A)** Quantitative flow cytometry measurements of apoptosis in HGC-27 cells (control, 4 μg/ml cisplatin +10 mM sodium butyrate, NAC pretreated + combination, or BSO pretreated + combination) and SGC-7901 cells (control, 4 μg/ml cisplatin +5 mM sodium butyrate, NAC pretreated + combination, or

(*Continued*)

Western blotting was used to evaluate the levels of mitochondrial apoptosis pathway-related proteins to further validate the relationship between the combination drug treatment and apoptosis promotion via the mitochondrial apoptosis pathway. Western blotting showed that the levels of Apaf-1, Bax, AIF, cleaved-caspase 3, cleaved-caspase 9, and CytC in the combination group were increased, whereas the survivin, PCNA, and Bcl-2 levels were decreased, and the extent of the increase or decrease was higher than that observed using either agent alone and compared with the control (**Figure 5**).

Pretreatment With NAC or BSO Inhibited or Enhanced Apoptosis in GC Cells Promoted by the Combination of Sodium Butyrate and Cisplatin

To further clarify the molecular mechanisms associated with the increased apoptosis via the mitochondrial pathway, a glutathione (GSH) inhibitor (BSO) and promotor (NAC) were used to pretreat the GC cells for 2 h before treatment with the combined drugs. Annexin PE/7AAD staining showed that the number of apoptotic cells was decreased (NAC group) or enhanced (BSO group) (**Figure 6A**). The ROS levels in the combined treatment group were decreased (NAC group) or increased (BSO group) after 2 h of pretreatment (**Figure 6B**). NAC pretreatment reversed the decrease in MMP levels induced by the combined treatment, while BSO pretreatment promoted the decrease in MMP levels induced by the combined treatment (**Figures 6C,D**).

In addition, western blotting showed that NAC pretreatment decreased the levels of mitochondrial apoptosis pathway-related proteins, whereas BSO pretreatment increased their levels (**Figure 7**).

Anti-Tumor Effects of Sodium Butyrate and Cisplatin on GC Cells *In Vivo*

We carried out an *in vivo* study to explore the effects of cisplatin and/or sodium butyrate on the xenograft tumor growth. Compared with the control group, all the treatment groups showed inhibited growth of tumors *in vivo*, with significantly decreased tumor weight and volume; the best effect was achieved in the combination group (**Figures 8A–C**).

FIGURE 6 | BSO pretreated + combination). **(B)** Original magnification: ×200. Cells were incubated with control, combination, NAC pretreatment + combination, or BSO pretreatment + combination described in **(A)** above. Quantitative analysis of ROS in each group. *$p < 0.05$ vs the control group; #$p < 0.05$ vs the combination group. **((C)** and **(D))** Cells were incubated with control, combination, NAC pretreatment + combination, or BSO pretreatment + combination described in **(A)** above. MMP was observed via JC-1 staining. Red inflorescence indicates healthy mitochondria; green inflorescence indicates collapsed mitochondrial potential. Quantitative analysis of MMP in each group. *$p < 0.05$ vs the control group; #$p < 0.05$ vs the combination group. All the above data are the mean ± SD from an average of three experiments.

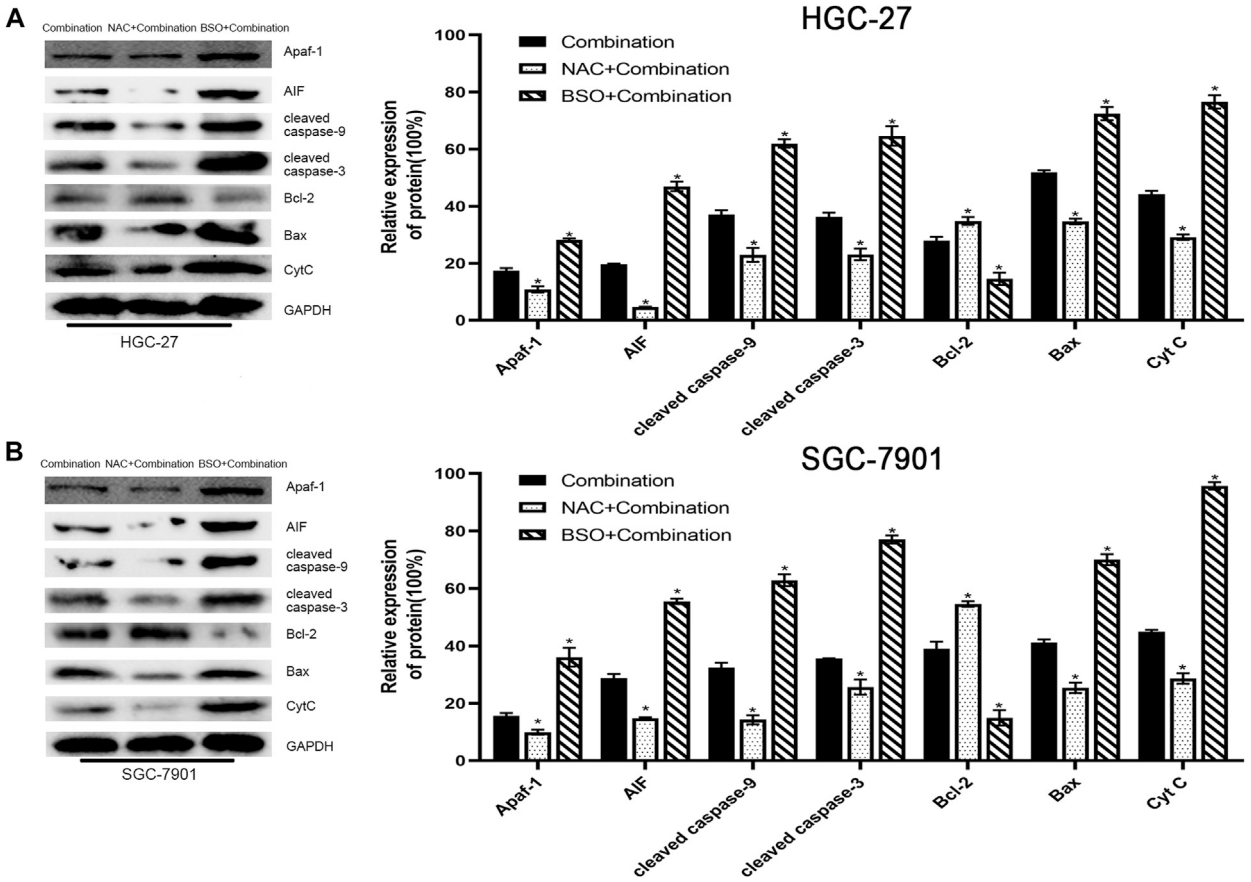

FIGURE 7 | Pretreatment with NAC or BSO, respectively, decreased or increased the levels of mitochondrial apoptosis pathway-related proteins. **(A)** HGC-27 cells were treated with 4 μg/ml cisplatin +10 mM sodium butyrate, NAC pretreatment + combination, or BSO pretreatment + combination and western blotting was performed to detect the levels of related proteins. *$p < 0.05$ vs the combination group. **(B)** SGC-7901 cells were treated with 4 μg/ml cisplatin +5 mM sodium butyrate, NAC pretreatment + combination, or BSO pretreatment + combination and western blotting was performed to detect the levels of related proteins. *$p < 0.05$ vs the combination group. All the above data are the mean ± SD from an average of three experiments.

The TUNEL assay and hematoxylin and eosin (H&E) staining were performed on the tumor tissues isolated from the xenograft mice. In the three treatment groups, the TUNEL staining showed significant cell apoptosis in the tumors and the highest level of cell apoptosis was achieved in the combined treatment group (**Figures 8D,E**). **Table 2** shows the serum BUN, AST, ALT, and Cr levels of blood samples, which assessed liver and kidney dysfunction; there was no visible difference among the four groups for any of these indices ($p > 0.05$).

DISCUSSION

Anti-cancer drugs mainly promote tumor cell apoptosis to exert their effects. There are three main apoptotic pathways: the death receptor pathway, the mitochondrial pathway, and the endoplasmic reticulum stress pathway (Gupta et al., 2009; Lee et al., 2012; Iurlaro and Muñoz-Pinedo, 2016). The mitochondrial pathway, also known as the endogenous pathway, is an evolutionarily highly conserved form of cell death that plays an essential role in the development and homeostasis of multicellular organisms (Roca-Agujetas et al., 2019). The alteration of mitochondrial permeability plays a key role in the mitochondrial apoptotic pathway, which is achieved by the opening of the mitochondrial permeability transition pore (MPTP) (Sileikyte and Forte, 2019). MPTP opening is a central physiological event in maintaining the dynamic homeostasis of mitochondrial health (Barsukova et al., 2011). ROS mainly originate from the mitochondria and, in turn, the mitochondria are the targets of ROS (Venditti and Di Meo, 2020). Short-term, reversible MPTP opening releases a small amount of ROS, which is beneficial to the cell growth; however, continuous, irreversible opening of MPTP causes explosive release of ROS, leading to oxidative stress and damage to the mitochondria and the cells (Bolduc et al., 2019).

ROS are oxidants that promote apoptosis, playing the role of promoter and downstream carrier in the apoptosis process

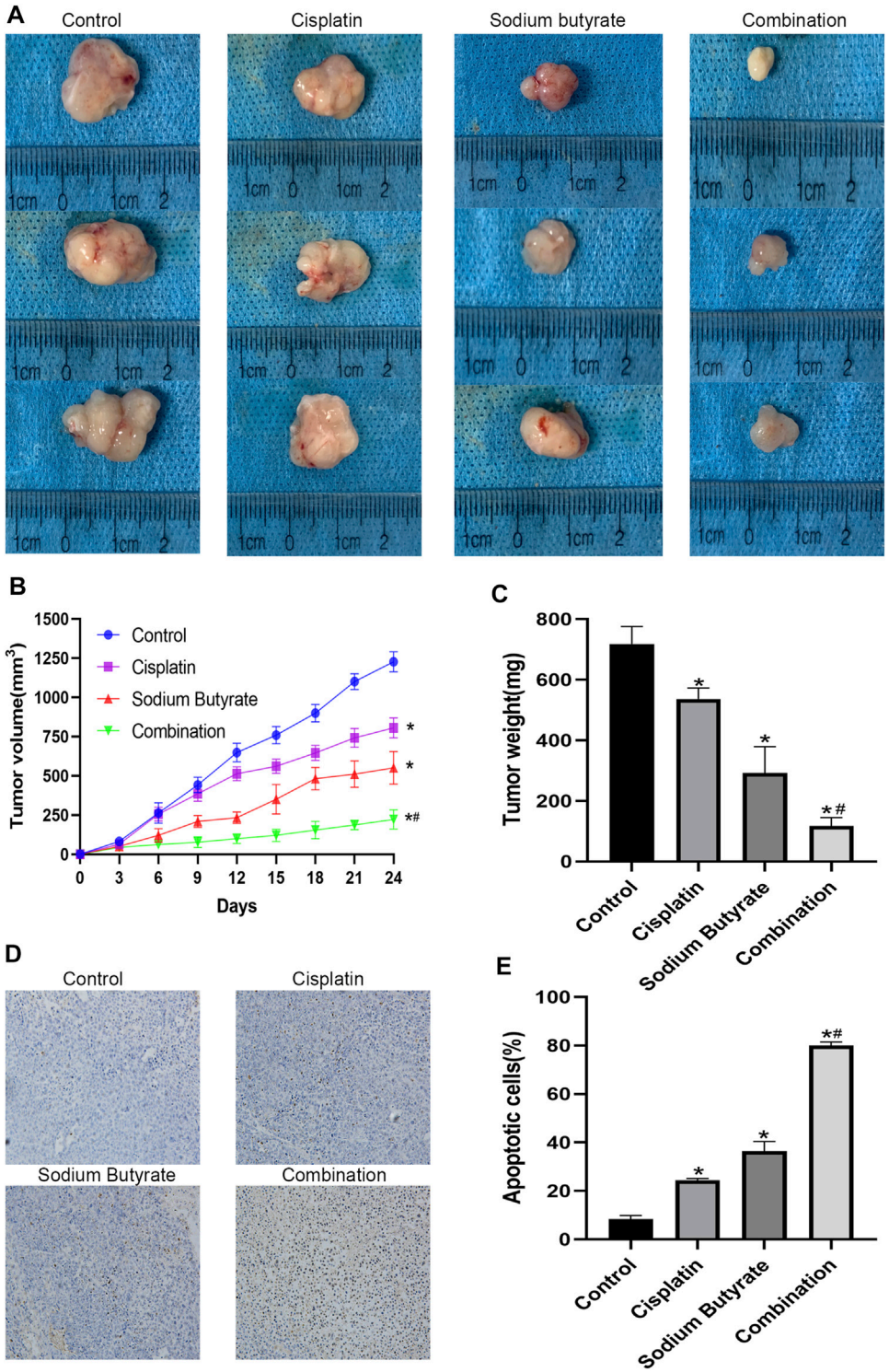

FIGURE 8 | Anti-tumor effects of cisplatin and sodium butyrate *in vivo*. **(A)** Morphology of the subcutaneous implanted tumor. **(B)** Mean tumor volume at each time point. **(C)** The tumor weight obtained at the end of the experiment. **(D)** A TUNEL assay was performed to detect the apoptotic cells in the tumor tissue. **(E)** Quantitative analysis of the apoptosis rate in **(D)**. *$p < 0.05$ vs the control; *#$p < 0.05$ vs cisplatin alone. All the above data are the mean ± SD from an average of three experiments.

TABLE 2 | Effect of sodium butyrate combined with cisplatin or alone on hepatic and renal function.

Group	ALT (U/l)	AST (U/l)	Urea (μmol/l)	Cr (μmol/l)
Control	31.8 ± 2.40	143.3 ± 10.35	8.12 ± 0.44	13.00 ± 1.90
Cisplatin	34.2 ± 2.14	140.8 ± 7.63	8.63 ± 0.84	14.33 ± 1.37
Sodium butyrate	30.8 ± 2.79	146.0 ± 15.24	8.54 ± 0.68	13.67 ± 1.75
Combination	30.5 ± 2.35	142.2 ± 3.19	8.38 ± 0.61	14.17 ± 2.48

Data are presented as the mean ± standard deviation, with n = 6 mice/group. There were no differences in the ALT, AST, urea, and Cr levels among all groups (p > 0.05).

(Kirtonia et al., 2020). Reduced glutathione (GSH) is a key intracellular antioxidant that is important to maintain the proper redox state of sulfhydryl groups in proteins (Sun et al., 2018). The depletion of GSH plays an important role in the proliferation and apoptosis of tumor cells and induces the accumulation of ROS (Lv et al., 2019). As the accumulation of ROS reaches an irreversible point, the mitochondrial membrane oxidative stress is induced, allowing the MPTP to remain open, causing CytC and AIF to be released from the mitochondria into the cytoplasm (Izzo et al., 2016; Baechler et al., 2019). Subsequently, pro-apoptotic factors, such as CytC, interact with the caspase family factor, Apaf-1, and the Bcl-2 protein family are released into the cytoplasm to accelerate the apoptotic process (Burek et al., 2006). In contrast, survivin proteins, as antagonists of the caspase family, inhibit apoptosis (Martínez-García et al., 2018).

The increasing resistance to conventional chemotherapeutic agents, such as docetaxel and cisplatin, and the problem of cytotoxicity have led sodium butyrate, a metabolite produced by the intestinal flora, to be considered as a potential anticancer therapeutic agent (Gentilin et al., 2019; Chen et al., 2020). Intriguingly, a study confirmed that sodium butyrate modulated the gut microbiota beneficially and improved the host immune response in *in vivo* experiments (Ma et al., 2020). As a histone acetylation inhibitor, an increasing number of experiments have demonstrated that sodium butyrate can induce the apoptosis in a variety of cancer cells (Maruyama et al., 2012; Fialova et al., 2016; Mrkvicova et al., 2019; Xiao et al., 2020; Xi et al., 2021). Moreover, there is evidence that sodium butyrate works well in combination with other drugs in many cancers (Fialova et al., 2016; Taylor et al., 2019); however, whether sodium butyrate combined with cisplatin can increase the inhibition of GC cells has not been investigated. Almost all anti-cancer drugs exert their anti-cancer effects by activating the apoptotic pathway to overcome cancer non-surgically, and sodium butyrate is no exception. Sodium butyrate has been proven to induce apoptosis in carcinomas through the mitochondrial apoptotic pathway (Salimi et al., 2017; Qin et al., 2020); therefore, in the current study, we aimed to confirm that sodium butyrate combined with cisplatin promoted apoptosis in GC cells through a mitochondria-mediated signaling pathway.

The results of the present study showed that the combination group remarkably inhibited the growth of GC cells to a greater extent than cisplatin alone, dependent on the duration and concentration of the treatment. Subsequently, we confirmed the synergistic effect of the combination using CompuSyn software. In addition, a significant pro-apoptotic effect of the combined group toward gastric cancer cells was observed using a Hoechst assay and flow cytometry. To explore the pathway responsible for the observed apoptosis, we examined the intracellular ROS levels in the group of cells and found that the ROS levels in the combination group significantly exceeded those in the other three groups. Next, we detected the levels of the fluorescent dye JC-1 in GC cells to show the mitochondrial membrane potential of each group. We found that the accumulation of ROS led to changes in the mitochondrial membrane potential of GC cells, which induced apoptosis. Subsequently, we pretreated the combination group of GC cells with BSO and NAC and found significant differences in the apoptosis rate, ROS levels, and mitochondrial membrane potential levels in GC cells compared with those in the control group (**Figure 6**), which confirmed our hypothesis that the combination treatment induced the apoptosis of GC cells via the mitochondrial apoptosis pathway.

To further demonstrate the role of the mitochondrial pathway in promoting apoptosis in GC cells after the combined drug treatment, we examined the expression levels of relevant proteins in the mitochondrial pathway using western blotting. The results showed that sodium butyrate combined with cisplatin remarkably increased the levels of the pro-apoptotic proteins (Apaf-1, AIF, BAX, CytC, cleaved caspase-3, and cleaved caspase-9) and remarkably decreased the levels of anti-apoptotic proteins (BCL2, PCNA, and survivin). In addition, the increases in mitochondrial apoptosis pathway-related proteins as mentioned above were reversed after pretreatment with NAC or enhanced after pretreatment with BSO (**Figure 7**). Finally, the anti-cancer effects of the combined drugs on GC cells were tested *in vivo*, and the results showed that the combined drug treatment inhibited the proliferation of GC cells and significantly increased the number of apoptotic cells in tumors (**Figure 8**).

In conclusion, our results supported the hypothesis that sodium butyrate combined with cisplatin enhances apoptosis in GC cells through the mitochondrial apoptosis pathway

in vitro and *in vivo*. Thus, sodium butyrate, a histone acetylation inhibitor produced by intestinal flora fermentation, combined with cisplatin could represent a therapeutic option to treat GC.

DATA AVAILABILITY STATEMENT

The raw data supporting the conclusion of this article will be made available by the authors, without undue reservation.

ETHICS STATEMENT

The animal study was reviewed and approved by the Ethics Committee of Renmin Hospital of Wuhan University.

AUTHOR CONTRIBUTIONS

The author contributions are as follows: conceptualization, YBL; data curation, YBL; formal analysis, PZH; investigation, YBL, PZH, and MMQ; methodology, PZH and YHL; project administration, YBL and PZH; supervision, PH; validation, PH and YHL; visualization, YBL and MMQ; Writing—original draft, YBL; Writing—review and editing, WGD.

ACKNOWLEDGMENTS

The authors thank Ying Wang from the Key Laboratory of Hubei Province for Digestive System disease and Qiong Ding from the Central Laboratory of Renmin Hospital of Wuhan University for their laboratory assistance, help, advice, and support.

REFERENCES

Baechler, B. L., Bloemberg, D., and Quadrilatero, J. (2019). Mitophagy Regulates Mitochondrial Network Signaling, Oxidative Stress, and Apoptosis During Myoblast Differentiation. *Autophagy.* 15 (9), 1606–1619. doi:10.1080/15548627.2019.1591672

Bardhan, K., Paschall, A. V., Yang, D., Chen, M. R., Simon, P. S., Bhutia, Y. D., et al. (2015). IFNγ Induces DNA Methylation-Silenced GPR109A Expression via pSTAT1/p300 and H3K18 Acetylation in Colon Cancer. *Cancer Immunol. Res.* 3 (7), 795–805. doi:10.1158/2326-6066.CIR-14-0164

Barsukova, A., Komarov, A., Hajnóczky, G., Bernardi, P., BourdetteandForte, D. M., and Forte, M. (2011). Activation of the Mitochondrial Permeability Transition Pore Modulates Ca2+ Responses to Physiological Stimuli in Adult Neurons. *Eur. J. Neurosci.* 33 (5), 831–842. doi:10.1111/j.1460-9568.2010.07576.x

Bolduc, J. A., Collins, J. A., and Loeser, R. F. (2019). Reactive Oxygen Species, Aging and Articular Cartilage Homeostasis. *Free Radic. Biol. Med.* 132, 73–82. doi:10.1016/j.freeradbiomed.2018.08.038

Burek, M., Maddika, S., Burek, C. J., Daniel, P. T., Schulze-OsthoffandLos, K. M., and Los, M. (2006). Apoptin-Induced Cell Death Is Modulated by Bcl-2 Family Members and Is Apaf-1 Dependent. *Oncogene.* 25 (15), 2213–2222. doi:10.1038/sj.onc.1209258

Chen, M., Jiang, W., Xiao, C., Yang, W., Qin, Q., Mao, A., et al. (2020). Sodium Butyrate Combined With Docetaxel for the Treatment of Lung Adenocarcinoma A549 Cells by Targeting Gli1. *Onco Targets Ther.* Vol. 13, 8861–8875. doi:10.2147/OTT.S252323

Fialova, B., Luzna, P., Gursky, J., Langova, K., KolarandTrtkova, Z. K. S., and Trtkova, K. S. (2016). Epigenetic Modulation of AR Gene Expression in Prostate Cancer DU145 Cells With the Combination of Sodium Butyrate and 5′-Aza-2′-Deoxycytidine. *Oncol. Rep.* 36 (4), 2365–2374. doi:10.3892/or.2016.5000

Gentilin, E., Simoni, E., Candito, M., CazzadorandAstolfi, D. L., and Astolfi, L. (2019). Cisplatin-Induced Ototoxicity: Updates on Molecular Targets. *Trends Mol. Med.* 25 (12), 1123–1132. doi:10.1016/j.molmed.2019.08.002

Guerriero, J. L., Sotayo, A., Ponichtera, H. E., Castrillon, J. A., Pourzia, A. L., Schad, S., et al. (2017). Class IIa HDAC Inhibition Reduces Breast Tumours and Metastases through Anti-Tumour Macrophages. *Nature.* 543 (7645), 428–432. doi:10.1038/nature21409

Gupta, S., Kass, G. E. N., SzegezdiandJoseph, E. B., and Joseph, B. (2009). The Mitochondrial Death Pathway: a Promising Therapeutic Target in Diseases. *J. Cel Mol Med.* 13 (6), 1004–1033. doi:10.1111/j.1582-4934.2009.00697.x

Iurlaro, R., and Muñoz-Pinedo, C. (2016). Cell Death Induced by Endoplasmic Reticulum Stress. *FEBS J.* 283 (14), 2640–2652. doi:10.1111/febs.13598

Izzo, V., Bravo-San Pedro, J. M., Sica, V., KroemerandGalluzzi, G. L., and Galluzzi, L. (2016). Mitochondrial Permeability Transition: New Findings and Persisting Uncertainties. *Trends Cel Biol.* 26 (9), 655–667. doi:10.1016/j.tcb.2016.04.006

Kirtonia, A., Sethi, G., and Garg, M. (2020). The Multifaceted Role of Reactive Oxygen Species in Tumorigenesis. *Cell. Mol. Life Sci.* 77 (22), 4459–4483. doi:10.1007/s00018-020-03536-5

Lee, E.-W., Kim, J.-H., Ahn, Y.-H., Seo, J., Ko, A., Jeong, M., et al. (2012). Ubiquitination and Degradation of the FADD Adaptor Protein Regulate Death Receptor-Mediated Apoptosis and Necroptosis. *Nat. Commun.* 3, 978. doi:10.1038/ncomms1981

Litvak, D. A., Hwang, K. O., EversandTownsend, B. M. C. M., Jr., and Townsend, C. M. (2000). Induction of Apoptosis in Human Gastric Cancer by Sodium Butyrate. *Anticancer Res.* 20 (2A), 779–784.

Luo, G., Zhang, Y., Guo, P., Wang, L., HuangandLi, Y. K., and Li, K. (2017). Global Patterns and Trends in Stomach Cancer Incidence: Age, Period and Birth Cohort Analysis. *Int. J. Cancer.* 141 (7), 1333–1344. doi:10.1002/ijc.30835

Lv, H., Zhen, C., Liu, J., Yang, P., HuandShang, L. P., and Shang, P. (2019). Unraveling the Potential Role of Glutathione in Multiple Forms of Cell Death in Cancer Therapy. *Oxidative Med. Cell Longevity.* 2019, 1–16. doi:10.1155/2019/3150145

Ma, X., Zhou, Z., Zhang, X., Fan, M., Hong, Y., Feng, Y., et al. (2020). Sodium Butyrate Modulates Gut Microbiota and Immune Response in Colorectal Cancer Liver Metastatic Mice. *Cell Biol Toxicol.* 36 (5), 509–515. doi:10.1007/s10565-020-09518-4

Martínez-García, D., Manero-Rupérez, N., Quesada, R., and Korrodi-GregórioandSoto-Cerrato, L. V. (2018). Therapeutic Strategies Involving Survivin Inhibition in Cancer. *Med. Res. Rev.* 39 (3), 887–909. doi:10.1002/med.21547

Maruyama, T., Yamamoto, S., Qiu, J., Ueda, Y., Suzuki, T., Nojima, M., et al. (2012). Apoptosis of Bladder Cancer by Sodium Butyrate and Cisplatin. *J. Infect. Chemother.* 18 (3), 288–295. doi:10.1007/s10156-011-0322-2

Mrkvicova, A., Chmelarova, M., Peterova, E., Havelek, R., Baranova, I., Kazimirova, P., et al. (2019). The Effect of Sodium Butyrate and Cisplatin on Expression of EMT Markers. *PLoS One.* 14 (1), e0210889. doi:10.1371/journal.pone.0210889

Qin, X., Xu, Y., Peng, S., Qian, S., Zhang, X., Shen, S., et al. (2020). Sodium Butyrate Opens Mitochondrial Permeability Transition Pore (MPTP) to Induce a Proton Leak in Induction of Cell Apoptosis. *Biochem. Biophysical Res. Commun.* 527 (3), 611–617. doi:10.1016/j.bbrc.2020.04.133

Roca-Agujetas, V., de Dios, C., Lestón, L., Marí, M., MoralesandColell, A. A., and Colell, A. (2019). Recent Insights into the Mitochondrial Role in Autophagy and its Regulation by Oxidative Stress. *Oxidative Med. Cell Longevity.* 2019, 1–16. doi:10.1155/2019/3809308

Salimi, V., Shahsavari, Z., Safizadeh, B., Hosseini, A., KhademianandTavakoli-Yaraki, N. M., and Tavakoli-Yaraki, M. (2017). Sodium Butyrate Promotes Apoptosis in Breast Cancer Cells Through Reactive Oxygen Species (ROS) Formation and Mitochondrial Impairment. *Lipids Health Dis.* 16 (1), 208. doi:10.1186/s12944-017-0593-4

Sanna, S., van Zuydam, N. R., Mahajan, A., Kurilshikov, A., Vich Vila, A., Võsa, U., et al. (2019). Causal Relationships Among the Gut Microbiome, Short-Chain

Fatty Acids and Metabolic Diseases. *Nat. Genet.* 51 (4), 600–605. doi:10.1038/s41588-019-0350-x

Shin, H., Lee, Y. S., and Lee, Y. C. (2012). Sodium Butyrate-Induced DAPK-Mediated Apoptosis in Human Gastric Cancer Cells. *Oncol. Rep.* 27 (4), 1111–1115. doi:10.3892/or.2011.1585

Sileikyte, J., and Forte, M. (2019). The Mitochondrial Permeability Transition in Mitochondrial Disorders. *Oxid Med. Cel Longev.* 2019, 3403075. doi:10.1155/2019/3403075

Song, Z., Wu, Y., Yang, J., YangandFang, D. X., and Fang, X. (2017). Progress in the Treatment of Advanced Gastric Cancer. *Tumour Biol.* 39 (7), 101042831771462. doi:10.1177/1010428317714626

Sun, Y., Zheng, Y., WangandLiu, C. Y., and Liu, Y. (2018). Glutathione Depletion Induces Ferroptosis, Autophagy, and Premature Cell Senescence in Retinal Pigment Epithelial Cells. *Cell Death Dis.* 9 (7), 753. doi:10.1038/s41419-018-0794-4

Sung, H., Ferlay, J., Siegel, R. L., Laversanne, M., Soerjomataram, I., Jemal, A., et al. (2021). Global Cancer Statistics 2020: GLOBOCAN Estimates of Incidence and Mortality Worldwide for 36 Cancers in 185 Countries. *CA A. Cancer J. Clin.* 71, 209–249. doi:10.3322/caac.21660

Taylor, M. A., Khathayer, F.., and Ray, S. K. (2019). Quercetin and Sodium Butyrate Synergistically Increase Apoptosis in Rat C6 and Human T98G Glioblastoma Cells through Inhibition of Autophagy. *Neurochem. Res.* 44 (7), 1715–1725. doi:10.1007/s11064-019-02802-8

Venditti, P., and Di Meo, S. (2020). The Role of Reactive Oxygen Species in the Life Cycle of the Mitochondrion. *Int. J. Mol. Sci.* 21 (6), 2173. doi:10.3390/ijms21062173

Wang, F., Wu, H., Fan, M., Yu, R., Zhang, Y., Liu, J., et al. (2020a). Sodium Butyrate Inhibits Migration and Induces AMPK-mTOR Pathway-Dependent Autophagy and ROS-Mediated Apoptosis via the miR-139-5p/Bmi-1 Axis in Human Bladder Cancer Cells. *FASEB j.* 34 (3), 4266–4282. doi:10.1096/fj.201902626R

Wang, W., Fang, D., Zhang, H., Xue, J., Wangchuk, D., Du, J., et al. (2020b). Sodium Butyrate Selectively Kills Cancer Cells and Inhibits Migration in Colorectal Cancer by Targeting Thioredoxin-1. *Onco Targets Ther.* Vol. 13, 4691–4704. doi:10.2147/OTT.S235575

Xi, Y., Jing, Z., Wei, W., Chun, Z., Quan, Q., Qing, Z., et al. (2021). Inhibitory Effect of Sodium Butyrate on Colorectal Cancer Cells and Construction of the Related Molecular Network. *BMC Cancer.* 21 (1), 127. doi:10.1186/s12885-021-07845-1

Xiao, X., Xu, Y., and Chen, H. (2020). Sodium Butyrate-activated TRAF6-TXNIP Pathway Affects A549 Cells Proliferation and Migration. *Cancer Med.* 9 (10), 3477–3488. doi:10.1002/cam4.2564

Zeng, H., Chen, W., Zheng, R., Zhang, S., Ji, J. S., Zou, X., et al. (2018). Changing Cancer Survival in China During 2003-15: a Pooled Analysis of 17 Population-Based Cancer Registries. *Lancet Glob. Health.* 6 (5), e555–e567. doi:10.1016/s2214-109x(18)30127-x

Conflict of Interest: The authors declare that the research was conducted in the absence of any commercial or financial relationships that could be construed as a potential conflict of interest.

Publisher's Note: All claims expressed in this article are solely those of the authors and do not necessarily represent those of their affiliated organizations, or those of the publisher, the editors and the reviewers. Any product that may be evaluated in this article, or claim that may be made by its manufacturer, is not guaranteed or endorsed by the publisher.

frontiers in Oncology

REVIEW
published: 23 September 2021
doi: 10.3389/fonc.2021.747718

Anticancer Effects and Mechanisms of OSW-1 Isolated From *Ornithogalum saundersiae*: A Review

Zhixin Zhan, Ziqiang Liu, Jiacheng Lai, Chaochao Zhang, Yong Chen and Haiyan Huang**

Department of Neurosurgery, The First Hospital of Jilin University, Changchun, China

For centuries, cancer has been a lingering dark cloud floating on people's heads. With rapid population growth and aging worldwide, cancer incidence and mortality are growing rapidly. Despite major advances in oncotherapy including surgery, radiation and chemical therapy, as well as immunotherapy and targeted therapy, cancer is expected be the leading cause of premature death in this century. Nowadays, natural compounds with potential anticancer effects have become an indispensable natural treasure for discovering clinically useful agents and made remarkable achievements in cancer chemotherapy. In this regards, OSW-1, which was isolated from the bulbs of Ornithogalum saundersiae in 1992, has exhibited powerful anticancer activities in various cancers. However, after almost three decades, OSW-1 is still far from becoming a real anticancer agent for its anticancer mechanisms remain unclear. Therefore, in this review we summarize the available evidence on the anticancer effects and mechanisms of OSW-1 *in vitro* and *in vivo*, and some insights for researchers who are interested in OSW-1 as a potential anticancer drug. We conclude that OSW-1 is a potential candidate for anticancer drugs and deserves further study.

Keywords: OSW-1, synthesis, anticancer, effect, mechanism, future perspective

OPEN ACCESS

Edited by:
Cecilia Veronica Nunez, National Institute of Amazonian Research (INPA), Brazil

Reviewed by:
Hamed Barabadi, Shahid Beheshti University of Medical Sciences, Iran
Sandeep Kumar Yadav, University of Texas MD Anderson Cancer Center, United States

****Correspondence:***
Yong Chen
chen_yong@jlu.edu.cn
Haiyan Huang
huanghy@jlu.edu.cn

Specialty section:
This article was submitted to Pharmacology of Anti-Cancer Drugs, a section of the journal Frontiers in Oncology

Received: *26 July 2021*
Accepted: *06 September 2021*
Published: *23 September 2021*

Citation:
Zhan Z, Liu Z, Lai J, Zhang C, Chen Y and Huang H (2021) Anticancer Effects and Mechanisms of OSW-1 Isolated From Ornithogalum saundersiae: A Review. Front. Oncol. 11:747718. doi: 10.3389/fonc.2021.747718

INTRODUCTION

Cancer, also known as malignant neoplasm, is a disease caused by abnormal cell growth and proliferation characterized as an uncontrolled cell division with the ability to metastasize. According to the GLOBOCAN 2020 by the International Agency for Research on Cancer, it was estimated that cancer has caused 19.29 million new cases with almost 10.0 million deaths (1). With rapid population growth and aging worldwide, cancer incidence and mortality are rapidly growing, and is expected to surpass cardiovascular disease as the leading cause of premature death in this century (2). Oncotherapy mainly includes surgery, radiation and chemical therapy, as well as immunotherapy and targeted therapy (3). Despite remarkable advances in medical technology, the cure rate and overall survival of cancer are still unsatisfactory in reality. Chemotherapy is the only option in majority of patients with advanced cancer, because surgical and radiation treatments are ineffective and traumatic. However, conventional chemotherapeutic drugs have great limitations. It may attack normal cells due to lack of selectivity to neoplastic cells, induce secondary malignancies during treatment of metastatic cancers, and develop drug resistance and high recurrence after

treatment (4). Therefore, finding new anticancer drugs that are more effective, have multiple targets, and have low toxicity will become the breakthrough of chemotherapy. In this regard, natural compounds have a good potential.

In the 1920s, Berren et al. have begun to study the extracts of plants, marine organisms, and various microorganisms in search of natural anticancer compounds (5). Compared with conventional chemotherapeutic drugs, natural compounds have more diverse structures and excellent anti-tumor activity with low cytotoxicity. Traditional medicinal herbs and plants, which contain valuable bioactive compounds with potential therapeutic effects, have been an important source of several clinically useful anticancer agents; that was developed into standard approaches of tumor chemotherapy available today, such as vincristine for Leukemia, etoposide for small cell lung cancer and paclitaxel for ovarian and breast cancer (6). According to the statistical data released in 2016, from 1940s to the end of 2014, 49% of the 175 anticancer small molecular compounds approved by the US FDA were either natural products or their direct derivatives (7).

Ornithogalum saundersiae is a perennial herb bulbous plant belonging to the genus Ornithogalum of Liliaceae family, which is native to southern Africa and mainly planted in temperate regions of the Eastern Hemisphere. In the 1970s, O. saundersiae was introduced to China from Korea as an ornamental plant. In Chinese folk medicine, O. saundersiae is considered to have anti-inflammatory and antitumor properties, which has been used in therapy for hepatitis and some types of cancers (8). Scientific analyses have revealed that it contains more than 20 kinds of bioactive components, including saponins, polysaccharides, flavonoids, terpenoids, alkaloids, volatile oils and trace elements, and so on. In 1992, Kubo S et al. (9) isolated OSW-1, a steroidal saponins, from the bulbs of O. saundersiae, which has a high cytotoxicity to cancer cells. Its anticancer effect is about 10-100 times that of many chemotherapeutic drugs commonly used in clinic, such as doxorubicin, camptothecin and paclitaxel (10). The sensitivity of normal cells to OSW-1 is significantly lower than that of cancer cells; with the IC50 of OSW-1 is 40–150 folds higher than that observed in malignant cells, demonstrating its relatively high safety (11). However, the selective anticancer mechanism remains largely unclear, which limits further clinical applications. In this review, the anticancer effects of OSW-1 and its underlying mechanisms were summarized, in order to facilitate research to explore potential anticancer targets and prepare for its future clinical application.

Synthesis and Structure Activity Relationship of OSW-1 and Its Derivatives

OSW-1 (C47H68O15), [IUPAC: [(2S,3R,4S,5R)-2-[(2S,3R,4S,5S)-3-acetyloxy-2-[[(3S,8R,9S,10R,13S,14S,16S,17S)-3,17-dihydroxy-10,13-dimethyl-17-[(2S)-6-methyl-3-oxoheptan-2-yl]-1,2,3,4,7,8,9,11,12,14,15,16-dodecahydrocyclopenta[a]phenanthren-16-yl]oxy]-5-hydroxyoxan-4-yl]oxy-4,5-dihydroxyoxan-3-yl] 4-methoxy benzoate], with molecular weight of 873.0 g/mol, is an acylated cholestane glycoside, which was first isolated by Kubo S et al. in 1992 (9). It was also proved by Mimaki Y et al. in 1997 (10), that it has an exceptionally cytostatic activity against various malignant tumor cells. **Figure 1** depicts the chemical structure of OSW-1. For the last three decades, the anticancer mechanisms of OSW-1 have remained unclear due to the extremely low acquisition rate by the traditional extraction methods and the

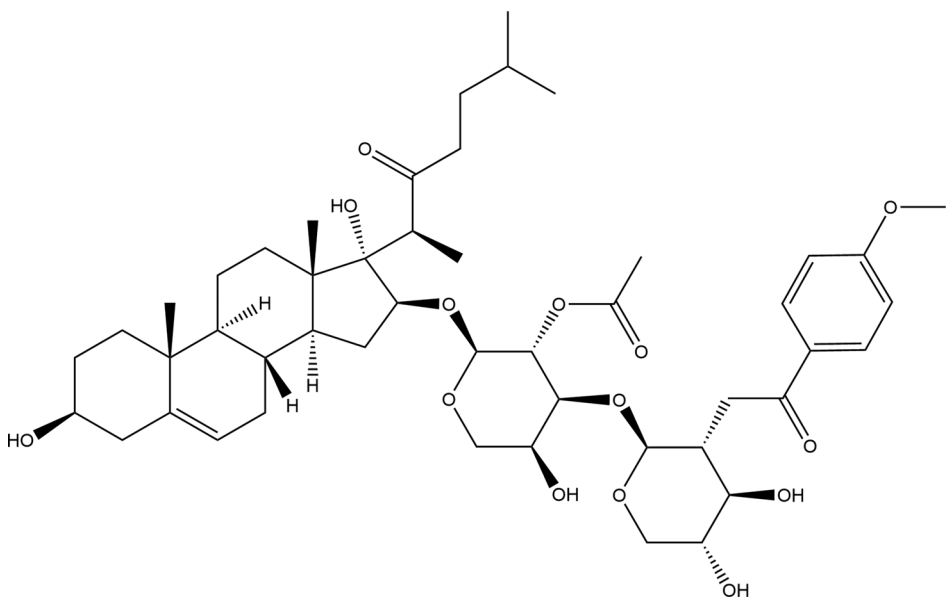

FIGURE 1 | The chemical structure of OSW-1.

relatively difficult chemical synthesis. Therefore, chemical synthesis of OSW-1 has been the subject of research. Recent studies have shown that the synthesis of OSW-1 and its derivatives is gradually improving (12–15).

The structure of OSW-1 can be divided into two parts: the cholestane aglycon and the disaccharide moiety. In 1998, Guo and Fuchs (16) first synthesized the protected aglycon of OSW-1 and confirmed that the anticancer activity of OSW-1 was due to the formation of oxygen cation intermediates between 22 oxygen and 16 β. Ma XQ et al. (17, 18) found that aglycone was an important structural component of OSW-1 to exert the activity by synthesizing a series of glycoside derivatives bearing the disaccharides moiety of OSW-1 and comparing their anticancer activities. In 1999, Deng S et al. (12) first synthesized OSW-1 by coupling of the aglycon with the sugar part from commercially available dehydroisoandrosterone, L-arabinose, and D-xylose, in total 27 steps with the longest linear sequence of 14 steps and with 6% yield. Yu and Jin (19, 20) used the same substrate but adopted a new strategy to synthesize 17 side chains by 1,4-Addition of an acyl anion equivalent to 17 (20)-en-16-one steroids, which greatly simplified the synthesis of OSW-1 into 10 steps with 28% yield. In 2002, Morzycki's group (21) studied the direct glycosylation of the protected aglycone with the disaccharide trichloroimidate and found that the hydroxy-lactone 7 is a valuable intermediate in the synthesis of the highly potent cytostatic OSW-1. In 2005, Shi BF et al. (22) reported an aldol approach to the stereoselective construction of the 16R,17R-dihydroxycholest-22-one structure and provided a convenient route for the synthesis of the 23-oxa-analogue of OSW-1, which has an approximate anticancer activity to OSW-1. In 2008, Tsubuki's group (23) embarked on the synthesis of OSW-1 in which thiophene ring 17 side chains was produced by employing 2,3-Wittig rearrangement reaction from the known 17E (20)-ethylidene-16α-hydroxy steroid. After a series of reactions, the final yield of OSW-1 was 15.6%. In the above synthesis process, the intermediates often need to be separated and purified before the next reaction was carried out, and the reaction conditions were not easily controlled, resulting in difficulties in the large-scale synthesis of OSW-1. To solve this problem, Xue et al. (24) developed a new practical synthetic method to synthesize OSW-1 on a gram scale, with an efficient procedure to prepare the sugar ligands and disaccharides, although the overall yield was just 6.4%. This synthesis is highlighted by the reliable transformations and the simplified workup procedures (25).

In addition, to better understand the SAR of OSW-1, some researchers have focused their work on the synthesis and activity comparison of its derivatives and have achieved some good results (13, 14, 26–29). For example, OSW-1 analogues with different modifications of hydroxyl (3β, 16α, 17β), disaccharide, 17-side chain and parent ABCD ring on OSW-1 can increase or decrease the overall activity. However, none of these studies have further explored the specific action targets of each functional group. In recent years, chemical probe-based approaches were proven powerful in the target identification studies of natural products (30). This may become a strong tool for studying the action targets of OSW-1 in the future.

ANTICANCER EFFECTS OF OSW-1

In Vitro Studies

In 1992, OSW-1 was found to be cytostatic in the U.S. National Cancer Institute 60-cell *in vitro* screen, with a mean IC50 of 0.78 nM and a mean IC100 of 58 nM (31). However, it was not until 1997 when Mimaki et al. (10) discovered that OSW-1 exhibited exceptionally potent cytostatic activities on various malignant tumor cells with little toxicity to normal cells that it began to attract the attention of researchers. Its anticancer effect is about 10-100 times that of doxorubicin, camptothecin and paclitaxel (10). Early studies have mainly focused on the synthesis of its derivatives and anticancer effects (14, 17, 18, 29, 32–34), because of the low field rate. Recently, studies on the anticancer mechanism of OSW-1 *in vitro* have gradually increased with the improvement of total synthetic process (12, 20, 22, 24, 34). OSW-1 has been shown to exhibit anticancer effect on various cancer cells, including ovarian, breast, cervical, colon, leukemia, hepatocellular carcinoma and other cancer cells. **Table 1** tabulates the *in vitro* studies on the efficacy and mechanisms of OSW-1 on different cancer cells (8, 10, 11, 35–43).

As shown in **Table 1**, OSW-1 has a high selective cytotoxicity to cancer cells compared with normal cells. It suggested that OSW-1 is expected to be developed into a new anticancer drug with the potential to specifically kill cancer cells. Although different cancer cells have different sensitivity to the inhibition effect of OSW-1, all of their IC50 values are in the nanomolar concentration range. Furthermore, OSW-1 appears to exert anticancer effects in cancer cells through different mechanisms, since different type of cancers have their unique key action targets. OSW-1 happens to be a natural compound with multiple anticancer targets due to its complex structure, which can regulate various signaling pathways (40, 41) and inhibit the development and progression of cancer cells by arresting cell cycle (38), damaging the structure and function of mitochondria, disrupting the cellular calcium homeostasis, inducing apoptosis (8, 11, 36, 38, 39) and Golgi stress response (37), inhibiting proliferation (35, 42) and metastasis, and repressing the migratory and invasive capabilities *via* EMT (36). Interestingly, necrosis was also detected when cells were treated with a high dose (180 ng/ml), which means OSW-1 may mediate other cell death pathways (8). Overall, OSW-1 exhibits potent anticancer potential against different cancer cells *in vitro*.

In Vivo Studies

Based on some *in vivo* studies, OSW-1 has been proved to be effective in inhibiting tumor growth, such as breast cancer, colon cancer, and leukemia (**Table 2**) (8, 10, 36). In 1997, Mimaki et al. (10) found that OSW-1 was remarkably effective versus mouse P388, with an increased life span of 59% by only one time

TABLE 1 | The cytotoxic effects of OSW-1 against cancer cells in *in vitro* experiments.

References	Cell lines		Efficacy, IC50 (exposure time)	Mechanisms of action
(36)	Human ovarian cancer cell	SKOV-1(monolayer) OVCAR-1(monolayer) OVSAHO(monolayer) OVCAR-8(monolayer) SKOV-3(spheroids) OVCAR-8(spheroids)	4.0 ± 2.7 nM(72h) 2.2 ± 0.85 nM(72h) 1.8 ± 0.61 nM(72h) >1,000 nM(72h) 10 nM(72h) 100 nM(72h)	Anti-proliferation, the targeting of ORP4 is responsible for the anti-proliferative activity of the OSW-1 compound in the absence of exogenously supplied cholesterol
(37)	Human breast cancer cell	MCF-7	3.72 ± 0.78 nM(72h)	Inhibits tumor growth by inducing apoptosis, represses the migratory and invasive capabilities *via* EMT, inhibits tumor growth and metastasis by decreasing the expression of NFATc2
		T47D ZR-75-1 BT474 SKBR3 MDA-MB-231 MDA-MB-453 HCC-1937	5.92 ± 1.21 nM(72h) 10.34 ± 0.07 nM(72h) 6.54 ± 1.14 nM(72h) 6.67 ± 0.13 nM(72h) 5.82 ± 2.35 nM(72h) 8.66 ± 0.19 nM(72h) 11.12 ± 4.42 nM(72h)	
	Human normal mammary epithelial cell	MCF/10A	52.3 ± 8.72 nM(72h)	N/A
(38)	Human cervical cancer cell	HeLa Cells	N/A	Induce mis localization of OSBP, which result in Golgi fragment and TFE3 activation, selectively trigger the apoptotic Golgi stress response *via* ↑CREB3-ARF4 proapoptotic pathway, ↓HSP47 antiapoptotic pathway
(39)	Human promyelocytic leukemia cells	HL-60 Cells	0.061 ± 0.0020nM(72h)	G2/M arrest, DNA fragmentation, caspase 3 activated, induce apoptosis *via* a mitochondria-independent signaling pathway
	Human lung adenocarcinoma cells	A549	0.65 ± 0.018nM(72h)	N/A
(8)	Human colon cancer cell	LoVo SW480	31 ± 2.0 ng/ml(72h) 61 ± 1.0 ng/ml(72h)	inhibition *via* induce intrinsic apoptosis, increased cellular calcium, changed mitochondrial membrane potential, disrupted mitochondrial morphology, release of cytochrome c and the activation of caspase-3
	Human normal colonic mucosal epithelial cells		139 ± 9.0 ng/ml (72h)	N/A
(42)	Human leukemia cells	HL-60 Raj K-562 KBM5, M1	the average IC50 value 0.019 nM(72h)	HL-60: disruption of cellular calcium homeostasis through inhibition of NCX1 and Inducing Apoptosis through a Mitochondrion-mediated Mechanism
	Normal lymphocytes		the average IC50 value 1.64 nM(72h)	N/A
(41)	Human hepatocellular carcinoma cells	Hep3B	N/A	Induce apoptosis and necroptosis, inhibit invasiveness, angiogenesis, cell polarity and cell adhesion of cancer *via* ↓Wnt, ↓MAPK, ↓VEGF, ↑P53 signal pathways
(40)	Human hepatocellular carcinoma cells	Hep3B	N/A	Affect numerous miRNAs that act on specific signaling pathways for proliferation, differentiation, apoptosis, cell adhesion, migration and EMT
(43)	Human colon cancer cell	HCT-116	N/A	Anti-proliferation by targeting OSBP and ORP4L
	Chinese hamster ovary cells human B cell lymphoma	CHO-7 M12 cells		
(44)	Chinese hamster ovary cells Human acute T-lymphocyte leukemia cell	CHO cells FADD and caspase-8-deficient Jurkat T cells	N/A	Induce mitochondrial-mediated apoptosis pathway through caspase-8-dependent cleavage of Bcl-2
(11)	Human leukemia cells	ML-1	0.19 nM(72h)	Damage the structure and function of mitochondrial and induce apoptosis through a calcium-dependent mechanism
		HL-60	0.044nM(72h)	

(Continued)

TABLE 1 | Continued

References	Cell lines		Efficacy, IC50 (exposure time)	Mechanisms of action
	Human lymphoma cell	Raji	0.58nM(72h)	
	Human ovarian cancer cell	SKOV3	0.021nM(72h)	
	Human glioblastoma cell	U87-MG	0.047nM(72h)	
	Human pancreatic cancer cells	AsPC-1	0.0391nM(72h)	
	Nonmalignant cells	normal lymphocytes	1.73nM(72h)	
		ovary fibroblasts	0.83nM(72h)	
		normal brain astrocytes	7.13nM(72h)	
(10)	Human normal pulmonary cell	CCD-19Lu	1.5μg/ml(N/A)	N/A
	Mouse leukemia	P388	0.00013μg/ml(N/A)	
	Adriamycin-rcsistant P388	P388/ADM	0.00077μg/ml(N/A)	
	Camptothecin-resistant P388	P388/CPT	0.00010μg/ml(N/A)	
	Mouse microcarcinoma	FM3A	0.00016μg/ml(N/A)	
	Human pulmonary adenocarcinoma	A549	0.00068μg/ml(N/A)	
	Human pulmonary large cell Carcinoma	Lu-65	0.00020μg/ml(N/A)	
	Human pulmonary large cell Carcinoma	Lu-99	0.00020μg/ml(N/A)	
	Human pulmonary squamous cell	RERF-LC-AI	0.00026μg/ml(N/A)	
	Carcinoma	CCRE-CEM	0.00016μg/ml(N/A)	
	Human leukemia	HL-60	0.00025μg/ml(N/A)	

NA, Not available; ↑, upregulation ; ↓, downregulation.

administration of 0.01 mg kg -1. However, they did not further explore the specific mechanisms behind this effect. For a long time afterwards, the OSW-1 seemed to disappear from the researchers' view. Until recently, Zhang et al. (8) and Ding et al. (36) began to investigate the anticancer effect of OSW-1 *in vivo* and explored the possible mechanism, respectively. To ascertain whether or not OSW-1 was as effective *in vivo*, Zhang et al. (8) adopted heterotopic xenograft tumor model in nude mouse subcutaneously inoculated by LoVo cells, in which OSW-1 was injected intraperitoneally (0.01 mg/kg diluted in PBS in 500 μ, daily) in treated group when tumors became palpable. Compared with the control group, the treated group observed a decrease in tumor size and weight without significant side effects, with fewer Ki-67-positive cells and more apoptotic cells. Interestingly, they also observed a destruction of blood vessels and a reduction in angiogenesis pathologically in the treated group. It suggested that OSW-1 may be involved in reduction in angiogenesis and tumor metastasis.

In 2020, Ding et al. (36) designed a series of experiments to verify the effect of OSW-1 on the tumor growth and metastasis of breast cancer, including three innovative animal models of tumor *in vivo*. They have found the following (1): for xenograft model, OSW-1 can inhibit tumor growth with reduction of tumor size and weight (2); for orthotopic model, fewer metastatic nodules in the lungs and longer survival were observed in treated group, with downregulation of Vimentin and upregulation of E-cadherin, which means OSW-1 can inhibit metastasis mediated by EMT; and (3) for knockdown NFATc2 model, identified NFATc2 may be a pivotal factor for OSW-1-mediated effects on cell death, tumor growth, invasion, and migration.

Overall, OSW-1 has good anticancer properties *in vivo*, and it is worthy of further research in the field of cancer chemotherapy. However, this requires more *in vivo* experiments to prove that OSW-1 can also exert similar anticancer effects in other cancers besides breast and colon cancer. The subsections below will further discuss the anticancer mechanism of OSW-1.

ANTICANCER MECHANISMS OF OSW-1

OSW-1 Inhibits the Proliferation of Cancer Cells

The most fundamental trait of cancer cells is the ability to proliferate and grow without limit. Cancer cells become masters of their own destinies by inducing and sustaining positively acting growth-stimulatory signals, which allow them to enter the proliferation and growth cycles, incessantly (44). Although there is still insufficient knowledge about the precise mechanism controlling the proliferative signals of cancer cells, dysregulation of the cell cycle is considered to be the main contributor to uncontrolled cell proliferation (45). Therefore, cell cycle inhibitors are becoming attractive targets in cancer treatment. It was found that the cell cycle was arrested at the G2/M phase in HL-60 cells following treatment with OSW-1 at concentration of either 0.3 nM or 0.01 μM (38). In addition, Jin et al. (40) examined the potential changes in the gene expression of a hepatocellular carcinoma cell line incubated with OSW-1 *in vitro*, and performed the enrichment analysis of the differentially expressed gene on signaling pathways. The results showed that the cell cycle is ranked first in enrichment score, which mean OSW-1 greatly affects the expression of cell cycle-related genes.

Oxysterol-binding protein (OSBP) and its related proteins (ORPs) constitute a large, evolutionarily conserved family of lipid-binding proteins that mediate signal transduction and lipid

TABLE 2 | The anti-cancer effects of OSW-1 *in vivo* tumor bearing animal models.

References	Animal models		Dose, duration and route of administration	Observations and results	Mechanisms of action
(36)	Human breast cancer cell	MDA-MB-231 xenograft model	0.01 mg/kg diluted in 100 μL PBS, daily, 20 days, ip	Reduction of tumor size and weight, Ki67↓, PCNA↓	Inhibits tumor growth
		MDA-MB-231 orthotopic model	0.01 mg/kg diluted in 100 μL PBS, until the tumors in control group reach 1.0 cm, continue injecting OSW-1 for 1 week, ip	Fewer metastatic nodules in lungs and longer survival, E-cadherin↑ and ↓ Vimentin	Inhibits metastasis mediated by EMT
		knockdown NFATc2 model	0.01 mg/kg diluted in 100 μL PBS, daily, 20 days, ip	Knocking down of NFATc2 using shRNA significantly rescues TNBC cells from OSW-1-mediated effects on cell death, tumor growth, invasion and migration	NFATc2 is involved in OSW-1 inhibition of TNBC progression.
(8)	Human colon cancer cell	LoVo xenograft model	0.01 mg/kg diluted in PBS in 500 μl, daily, 21 days, ip	Reduction of tumor size and weight, no apparent side effects, ki-67↓, no necrotic foci, induce apoptosis	Suppressing colon tumor proliferation without significant side effects through the apoptosis pathway
(10)	Mouse P388 leukemia cell	P388 cell intraperitoneal implantation model	0.01 mg/kg, one time, N/A	Increased life span of 59%	N/A

NA, Not available; ↑, upregulation; ↓, downregulation; i.p., intraperitoneal administration.

transport. It is reported that the OSBP/ORPs family is implicated in cell proliferation and cancer development (46, 47). Therefore, OSBP/ORPs may be potential therapeutic targets in cancer. In 2011, Burgett et al. (42) first identified that OSBPs and ORP4 are high-affinity receptors of OSW-1 and can mediate the anti-proliferative activity of OSW-1 in cancer cells. The activity was also recognized in ovarian cells by Bensen et al. (35). Notably, the cytotoxicity of OSW-1 was consistent with the reduction of the ORP4 expression, but not with the reduction of OSBP expression, suggesting ORP4 is the main anti-proliferative target of OSW-1 (35). Recently, some studies show that OSBP does not have any known role in cellular proliferation (48, 49); while ORP4 participate in the control of human malignant tumor cell proliferation and survival (50, 51). Interestingly, in the absence of extracellular lipids, OSW-1 has enhanced antiproliferative activity and OSBP, but not ORP4, is likely responsible for the striking shift in sensitivity to OSW-1 (35). OSBP is reported to be required for lipid transport by burning off the phosphoinositide phosphatidylinositol 4-phosphate [PI (4)P] between the endoplasmic reticulum (ER) and the Golgi (52), and dysregulation of PI4P metabolism and protein interactions are often associated with tumor progression and a poor prognosis (53). Thus, it is confused whether OSBP or ORP4 take more charge of the antiproliferative activity of OSW-1, or maybe both, which require further investigation.

OSW-1 Induces Apoptosis of Cancer Cells

Apoptosis, a form of programmed cell death that results in the orderly and efficient removal of damaged cells, occurs during development as a homeostatic mechanism to maintain cell populations in tissues, and as a defense mechanism when cells are damaged by harmful stimulations (54, 55). Inappropriate apoptosis is involved in many human diseases, including neurodegenerative diseases, ischemic damage, and autoimmune disorders (56). In cancer, minimal apoptosis results in malignant cells proliferation without limitations (57). The mechanisms of apoptosis can be divided into two main pathways: the intrinsic pathway, which is mediated by the mitochondria; and extrinsic pathway, which is mediated by death receptors, including FasL/FasR and TNF-α/TNFR1 (58). These two apoptotic pathways both involve activation of series of caspases and converge on the same execution pathway, which is initiated by the cleavage of caspase-3, leading to morphological and biochemical cellular alterations that are characteristics of apoptosis (57, 59). The upstream caspase for intrinsic pathway is caspase 9, while that of extrinsic pathway is caspase 8 (57). With the deepening understanding on the regulatory mechanism of apoptosis, drugs that target the deregulated apoptotic pathways to promote apoptosis has become an important strategy for chemotherapy (60).

OSW-1 has been known to effectively induce apoptosis in different cancers. In breast cancer, Ding et al. (36) confirmed that OSW-1 was capable of inducing apoptosis by using Annexin V/PI-labeled flow cytometry and TUNEL assay and discovered that the expression levels of cleaved caspase-3 and cleaved PARP increased in a dose-dependent manner. Furthermore, apoptosis was also observed in other cancer cells including colon cancer (8), leukemia (11, 38, 39, 43), pancreatic cancer (11), and cervical cancer cells (37), though the specific mechanisms were not exactly the same (**Table 1**).

OSW-1 can initiate apoptosis through the intrinsic pathway. In colon cancer, Zhang et al. (8) discovered that OSW-1 damaged the structure and function of mitochondria leading to the release of cytochrome c that caused caspase-3 activation, which was regarded as the classical intrinsic apoptotic pathway. In the two studies by Zhou et al. (43) and Garcia et al. (39), they all suggested that OSW- 1 reduced mitochondrial membrane potential and then induced mitochondria-mediated apoptosis. Notably, the overload of cytoplasmic calcium was found in those studies and regarded to play a key role in cell death. Zhou et al. (11) thought that the damaged mitochondria leading to the calcium imbalance. Garcia et al. (39) hold the view that the

inhibition of NCX1 (sodium-calcium exchanger 1) by OSW-1 was the reason for cytoplasmic calcium to lose homeostasis leading to calcium overload.

Besides the intrinsic pathway, OSW-1 is capable of inducing the extrinsic pathway. Lguchi et al. (38) found that OSW-1 induced apoptosis in HL-60 cells *via* the mitochondria-independent pathway, for no disruption of the mitochondria membrane potential and release of cytochrome C was observed. Zhu et al. (43) showed that OSW-1 induces apoptosis *via* caspase-8-dependent cleavage of Bcl-2 in Chinese hamster ovary cells. Furthermore, Jurkat T cells deficient in caspase-8 or FADD were resistant to apoptosis induced by OSW-1, which suggested that the extrinsic pathway is involved in the OSW-1-induced apoptosis (43). Bcl-2, an anti-apoptotic member of Bcl-2 family, once cleaved, will amplify the apoptotic signal through the mitochondria by altering its membrane permeability to facilitate the release of apoptogenic proteins such as cytochrome C (61).

OSW-1 can also induce apoptosis by Golgi stress-induced mechanism. In 2019, Kimura et al. discovered that OSW-1, as a novel class of selective Golgi stress inducer, can regulate Golgi stress response pathways, in which HSP47 was downregulated and CREB3-ARF4 was upregulated (37). It's reported that the suppression of HSP47 under a Golgi stress condition leads to caspase 2-mediated apoptosis (62). In addition, CREB3-ARF4 mediates pro-apoptotic pathways in response to Golgi stress was also demonstrated by Reiling et al. (63).

In summary, OSW-1 has the ability to promote apoptosis in cancer cells by activating various apoptotic pathways (**Figure 2**).

OSW-1 Induces Golgi Stress Response of Cancer Cells

The classical view of Golgi apparatus is a small membranous organelle involved in protein transport and glycosylation (64). Recent descriptions of Golgi network demonstrate the essential role of Golgi in cellular activities, including mitosis, DNA repair, stress responses, cell death, and cancer development (65, 66). Changes on Golgi trafficking, signaling, and morphology in some malignant cancers were so obvious that the term 'onco-Golgi' has been proposed to describe those particular changes (67). Thus, the Golgi should have a fundamental impact on cancer cell survival and emerge as a new cancer therapeutic target. The Golgi stress response is an autoregulated mechanism for maintaining the homeostasis of Golgi apparatus similar to ER stress response (68) by regulating specific functions and size of various zones of the Golgi apparatus, especially zones related to apoptotic signaling pathway in accordance with cellular demands (69). In short, if the capacity of Golgi function becomes insufficient after various cellular stresses, Golgi will activate the response signaling pathways (70). Normally, Golgi stress response should serve to help alleviate the stress, and only result in cell death if the stress is harmful and irreparable.

Recently, several pathways of the mammalian Golgi stress response have been identified, especially the TFE3, HSP47, and CREB3-ARF4 (71). In 2019, Kimura et al. (37) discovered that OSW-1 preferentially localizes to the Golgi apparatus and activates the major Golgi stress response pathways by inducing mis-localization of OSBP from cytoplasm to the trans-Golgi

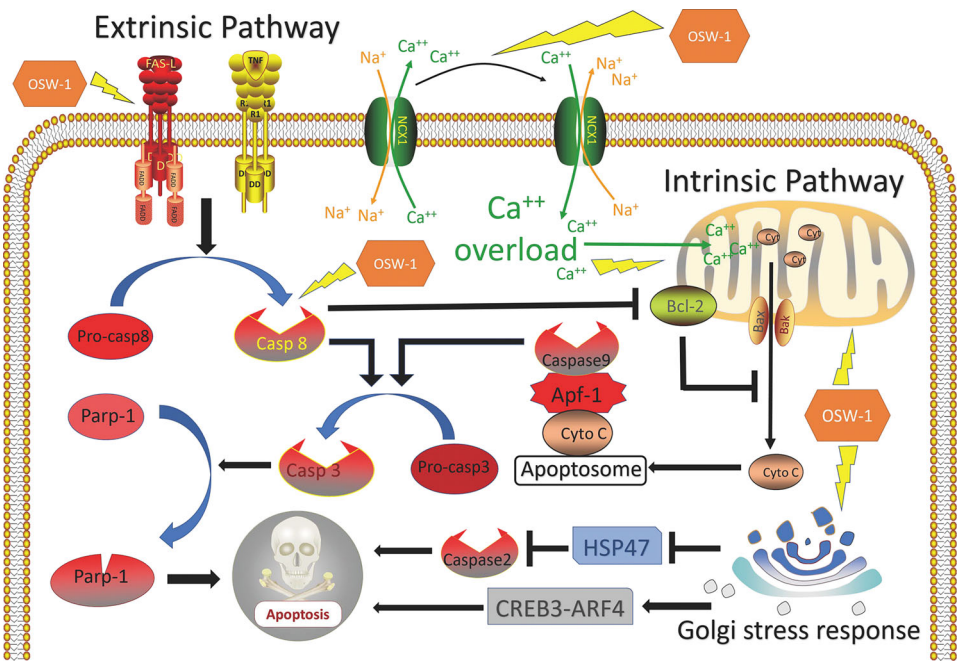

FIGURE 2 | Overview of mechanisms of apoptosis induced by OSW-1 in cancer cells.

network, which lead to the activation of TFE3 and the fragment of Golgi, and then selectively triggering the apoptotic Golgi stress response *via* upregulating CREB3-ARF4 proapoptotic pathway and downregulating HSP47 antiapoptotic pathway. Although OSW-1 induction of the selective Golgi stress response in cancer cells remains to be explored, their study provided the first evidence that link OSW-1-OSBP interactions with cell death induction (37). Overall, OSW-1 can effectively kill cancer cells by inducing Golgi stress response-mediated apoptosis, which provide guidance and reference for clinical development of novel anticancer drugs targeting Golgi apparatus.

OSW-1 Suppresses Migration, Invasion, and Angiogenesis of Cancer Cells

Metastasis is the process by which cancer cells leaves the primary site, travels to distant regions *via* the circulatory system, and establishes a secondary tumor (72). It causes most cancer deaths and involves migration, invasion and angiogenesis, which are broadly regulated by epithelial-mesenchymal transition (EMT) (44). EMT is a biological process in which epithelial cells are converted into cells with mesenchymal phenotype. In cancer, it is also known as epithelial cell plasticity and is associated with tumor initiation, invasion, metastasis, and resistance to therapy (73). It usually begins with the disappearance of epithelial cell polarity and the weakening of intercellular adhesion (74). The loss of epithelial markers, such as cytokeratins and E-cadherin, and the acquisition of mesenchymal markers, such as N-cadherin and vimentin, indicate that the cancer cells gain the ability to migrate and invade. Therefore, blocking EMT of cancer cells will greatly reduce the metastasis rate, thus improving the prognosis of cancer patients.

Triple negative breast cancer (TNBC) is a particularly aggressive subtype of breast cancer and accounts for 15% to 20% of cases (75). It is characterized by a lack of expression of estrogen, progesterone, and human epidermal growth factor 2 receptors and has clinical features that include high invasiveness, high metastatic potential, proneness to relapse, and poor prognosis (76). In 2020, Ding et al. found that the OSW-1 decreased the expressions of NFATc2, and inhibited migration and invasion of TNBC cells *via* blocking the EMT signaling pathways *in vitro* and *in vivo* experiment (36). It was reported that nuclear factor of activated T cells (NFAT) is associated with TGFβ-induced EMT, which could influence proliferation, invasion, migration and angiogenesis of cancer cells (77).

In 2017, Zhang et al. (8) found destruction of blood vessels, reduction of angiogenesis and no metastatic focus in xenograft model with OSW-1 treatment, suggesting that OSW-1 may be involved in angiogenesis and tumor metastasis. The authors did not explore the mechanism behind this phenomenon. It was hypothesized that OSW-1 induce Golgi stress response and lead to the fragment of Golgi apparatus (37), which disrupt the homeostasis of PI4P and PI4P-binding proteins, including GOLPH3 or PITPNC1. However, these proteins are essential to the development of aggressive metastatic and invasive tumor for their ability to induce malignant secretory phenotype conversion leading to the release of proteins that can reshape the extracellular matrix, promote pathological angiogenesis, and enhance cell migration (53). The dysregulation of miRNA and signaling pathways caused by OSW-1 may also contribute to cancer metastasis and angiogenesis as discussed.

Effect of OSW-1 on miRNAs Expression

MicroRNAs (miRNAs) are a major class of small noncoding RNA that consists of approximately 20 nucleotides, which negatively regulate gene expression at the mRNA level, usually silencing genes by binding to the 3′ or 5′-untranslated region (UTR) of their target mRNAs, controlling genes involved in cellular processes, such as inflammation, proliferation, cell-cycle regulation, stress response, differentiation, programed cell death, and migration (78, 79). The cancer-related miRNAs can be divided into two groups: tumor suppressor miRNAs (inhibiting tumor progression by targeting mRNAs that code oncoproteins and repressing the translation of oncogenic mRNAs) and oncogenic miRNAs (promoting tumor progression by promoting metastasis and silencing the tumor suppressor genes) (80). Given that miRNAs play roles in almost all aspects of cancer biology, and dysregulation of miRNAs is common in many cancers, it has been suggested that miRNAs could serve as potential tumor markers for the diagnosis of cancer, and developing new molecules targeting miRNAs expression in cancer represents an attractive strategy for oncotherapy (81, 82).

In 2013, Jin et al. (41) identified differential miRNA expression of Hep3B with OSW-1 treated *in vitro*, and the results showed that OSW-1 regulated many miRNAs, in which miRNA-142, miRNA-299, miRNA-187, miRNA-210, miRNA-125b and miRNA-200c were upregulated, and miRNA-126 was downregulated. Then, authors connected and identified functions of differential miRNAs with unrecognized functions of OSW-1, and drew a conclusion that OSW-1 inhibits cancer by affecting numerous cancer-related miRNAs that acts on specific signaling pathways for proliferation, angiogenesis, apoptosis, cell adhesion, migration, and EMT (41). For instance, miRNA-126, an endothelial cell restricted miRNA, is associated with tumor angiogenesis for its ability to enhance pro-angiogenic actions of VEGF and FGF (83). After OSW-1 treatment, the expression of miRNA-126 decreased significantly (barely detected), which reduced the ability of tumor angiogenesis and led to the inhibition of tumor growth (41). Overall, the effect of OSW-1 on regulating miRNAs deserved further exploring.

Effect of OSW-1 on Various Signaling Pathways

Signaling pathway, also called signal transduction, is a series of enzymatic reaction pathways that can transmit extracellular molecular signals into cells through cytomembrane to exert effects. With the deeper understanding of the molecular basis of neoplastic cell behavior, cancer is considered as a disease with altered signal pathways (84). Currently, signal pathway inhibition by blocking the enzymes and growth factor receptors that are essential for cell proliferation are being explored. Some have achieved remarkable success and are now commonly used as anticancer drugs, such as gefitinib for non-small cell lung cancer (85), imatinib for chronic myeloid leukemia (86) and trastuzumab for breast cancer (87).

Therefore, agents that directly block pathogenic signal pathways by targeting key components to inhibit growth of cancers are a promising therapeutic strategy.

However, all targeting drugs have a common limitation which is the inevitable emergence of drug resistance (88–90). The reason is very simple, cancer cells are not easily killed by blocking one target in a single way, since the signal pathways in them are very complex and cross-talk and usually, when one of the pathways is blocked, another compensatory bypass will be activated (91). In this regard, natural products with potential multiple targets may be a solution (92). In a study of Jin et al. (40), the potential gene expression changes of Hep3B incubated with OSW-1 *in vitro* were examined and results showed that OSW-1 affected the expression of core genes in a number of signaling pathways, including the downregulation of Wnt, MAPK, and VEGF, and upregulation of P53. Wnt signaling pathway is important for its crucial function in development and growth, and has also been tightly associated with cancer for its aberrant activation involved in maintenance of cancer stem cells, metastasis and immune control (93); MAPK signaling pathway represents ubiquitous signal transduction pathways that regulates cell growth, differentiation, proliferation, apoptosis and migration functions, and play a role in tumorigenesis and associated with anticancer drug resistance (94); EGFR is a group of transmembrane proteins with cytoplasmic kinase activity and is frequently mutated and/or overexpressed in human cancers (95), which results in increased cell proliferation, abnormal metabolism, and cell survival through the activation of the downstream signaling pathways, such as MAPK, AKT, and STAT3 (96, 97); P53, a tumor-suppressor gene, is activated by a host of stress stimuli and, in turn, induce cell cycle arrest or apoptosis programs to inhibit cancer (98). Although OSW-1 inhibit cancer cells through regulating above signaling pathways require more rigorous verification, it also provides a new perspective to demonstrate the anticancer mechanisms of OSW-1.

FUTURE PERSPECTIVE

In 1992, OSW-1 was first isolated from O. saundersiae and emerged as a candidate of anticancer drugs for its more powerful anticancer effect than doxorubicin, camptothecin and paclitaxel (9). Currently, many *in vitro* and *in vivo* studies have identified the anticancer effects of OSW-1 in various cancers and explored the potential targets. However, after almost thirty years, the anticancer mechanisms of OSW-1 are still undefined. Although Burgett et al. revealed that OSW-1 exhibits cytotoxicity by targeting OSBP and ORP4L (42), the link between these targeting and apoptosis induction has remained unclear. Furthermore, the OSBP-OSW-1 interaction seem to have more applications in antiviral than anticancer for OSBP is not essential to cell viability (99) but indispensable to virus replication (48, 100). In addition, the OSBPs targeting is hard to explain especially the high selective cytotoxicity of OSW-1. In 2013, Garcia et al. (39) demonstrated that OSW-1 inhibited NCX1 in a fashion similar to the NCX inhibitor KB-R7943, and then disrupted calcium homeostasis of cytoplasm leading to mitochondria-mediated apoptosis. Interestingly, this inhibitory effect of OSW-1 is cancer cell-specific with minimal effect on normal lymphocytes. An earlier study by Harley et al. (101) also found that the NCX inhibitors selectively kill malignant glioma cells but not primary astrocytes. Thus, future studies should concentrate on uncovering the precise key target proteins of OSW-1 to explain the high selective cytotoxicity.

Nowadays, chemical probe-based approaches have emerged as powerful methods for mechanistic studies of natural products by identifying the cellular site of action, the target proteins, and the target cellular pathways. However, studies on the development of chemical probes of OSW-1 for investigation of its biological role are still lacking (30). Recently, network pharmacology approaches for predicting unexplored targets and therapeutic potential are being applied increasingly to find new therapeutic opportunities of natural products (102). These two methods may be beneficial to reveal intracellular localization properties of OSW-1 and discover target proteins leading to the phenotypes of interest. In addition, the surge of "-omics" technologies, including genomics, transcriptomics, epigenomics, proteomics, metabolomics, has enabled us to recognize biological and molecular changes underlying the development and progression of human disease, and multi-omics analyses, which take advantage of these technologies (103, 104), may facilitate the clinical application of OSW-1 in precise treatment of cancer.

Given the low yield from extraction and limited amount present in raw plant materials, it is crucial to find a new way to synthesize OSW-1 in large quantities. Several groups have achieved total synthesis of OSW-1 and a number of its analogues have been synthesized to decipher the SAR (25), but the progress is slow. Comparing total synthesis, exploring derivatives with simplified molecular structure, with a more potent anticancer effects, would be a good strategy taking the complex structure of OSW-1 in consideration. In addition, with the advent of genetic engineering, the mass production of OSW-1 from plants using gene editing is also an option (105).

Notably, the pharmacokinetics of OSW-1, which involves the study of drug movement within the body, including the time course of absorption, distribution, metabolism, and excretion, is a blank of current researches. Moreover, although normal cells are less sensitive to the cytotoxicity of OSW-1, their IC 50 value is in nanomolar range, indicating that OSW-1 is still toxic to them (11). Thus, it is essential to perform vigorous animal toxicology experiments before considering evaluation of clinical application. In fact, toxicity and drug-like properties have become one of the main obstacles for many saponin drugs, including osw-1, to further move to clinical application, despite their extensive research and remarkable anticancer effects (106). However, only a few studies of OSW-1 involve in toxicology *in vivo* experiments (8, 10, 36). It is recommended that more *in vivo* experiments be performed to refine the pharmacokinetics and pharmacology of OSW-1, so that actual metabolites and concentrations are taken into account during *in vitro*

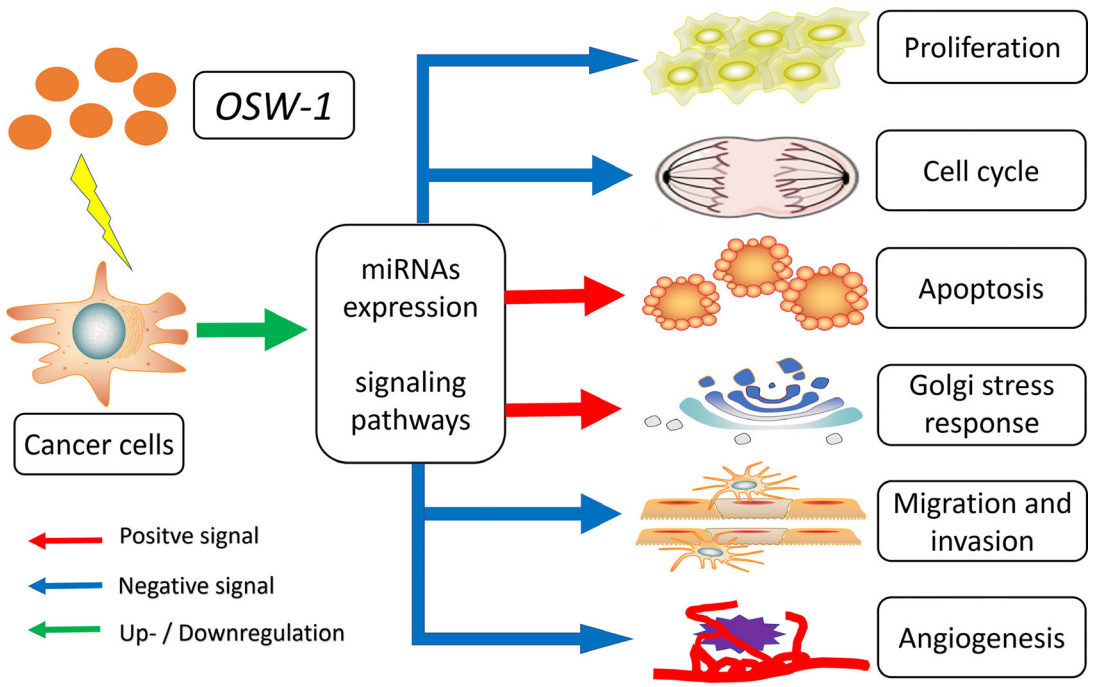

FIGURE 3 | Overview of the anticancer mechanisms of OSW-1 in cancer cells.

experiments to simulate more realistic *in vivo* conditions. In addition, exploring more reasonable combination therapy regimens and more effective drug delivery systems to ensure increased efficacy and decreased toxicity of OSW-1 will also be one of the focuses of future research.

CONCLUSION

It has been almost 30 years since OSW-1, a natural compound with potent anticancer activity, was first discovered in 1992. Currently, an increasing number of preclinical studies have confirmed the role of OSW-1 in anticancer therapies. Summarized in this review are the available evidence on the anticancer effects and mechanisms of OSW-1 *in vitro* and *in vivo*. As mentioned, OSW-1 has been shown to repress cancer progression through inhibiting cell proliferation, arresting cell cycle, inducing apoptosis and Golgi stress response, as well as suppressing migration, invasion and angiogenesis by regulating miRNAs expression and various signaling pathways (**Figure 3**). However, OSW-1 is still far from becoming a real anticancer agent for some issues, including anticancer mechanisms that have not been fully explained, especially the high selective cytotoxicity to cancer cells, the low yield rate from extraction and synthesis, and the need for more vivo experiments to refine pharmacokinetics.

In general, OSW-1 is a potential candidate for anticancer drugs and deserves further study. Since there are still some problems to be solved before it can be used in clinical treatment, this will require the joint efforts of different professional scientists, worldwide.

AUTHOR CONTRIBUTIONS

The manuscript was written by ZZ. The review of literature and data collection were performed by ZL, JL, and CZ. The manuscript was critically reviewed and edited by YC. The project was conceptualized by HH. All authors contributed to the article and approved the submitted version.

FUNDING

This work was supported by Scientific Research Foundation of Jilin province (20180101158JC, 20200201613JC, 20200201388JC, 20190701042GH), Research and Planning Project of the 13th Five-Year Science and Technology Project of Jilin Provincial Department of Education (JJKH20180191KJ) and Interdisciplinary Innovation Project of First Hospital of Jilin University (JDYYJC001).

ACKNOWLEDGMENTS

We would like to thank Editage (www.editage.cn) for English language editing.

REFERENCES

1. Sung H, Ferlay J, Siegel RL, Laversanne M, Soerjomataram I, Jemal A, et al. Global Cancer Statistics 2020: GLOBOCAN Estimates of Incidence and Mortality Worldwide for 36 Cancers in 185 Countries. *CA Cancer J Clin* (2021) 71(3):209–49. doi: 10.3322/caac.21660
2. Bray F, Laversanne M, Weiderpass E, Soerjomataram I. The Ever-Increasing Importance of Cancer as a Leading Cause of Premature Death Worldwide. *Cancer* (2021) 127(16):3029-30. doi: 10.1002/cncr.33587
3. Vanneman M, Dranoff G. Combining Immunotherapy and Targeted Therapies in Cancer Treatment. *Nat Rev Cancer* (2012) 12(4):237–51. doi: 10.1038/nrc3237
4. Yavari B, Mahjub R, Saidijam M, Raigani M, Soleimani M. The Potential Use of Peptides in Cancer Treatment. *Curr Protein Pept Sci* (2018) 19 (8):759–70. doi: 10.2174/1389203719666180111150008
5. Amin AR, Kucuk O, Khuri FR, Shin DM. Perspectives for Cancer Prevention With Natural Compounds. *J Clin Oncol Off J Am Soc Clin Oncol* (2009) 27(16):2712–25. doi: 10.1200/JCO.2008.20.6235
6. Cragg GM, Newman DJ. Plants as a Source of Anti-Cancer Agents. *J ethnopharmacol* (2005) 100(1-2):72–9. doi: 10.1016/j.jep.2005.05.011
7. Newman DJ, Cragg GM. Natural Products as Sources of New Drugs From 1981 to 2014. *J Natural products* (2016) 79(3):629–61. doi: 10.1021/acs.jnatprod.5b01055
8. Zhang Y, Fang F, Fan K, Zhang Y, Zhang J, Guo H, et al. Effective Cytotoxic Activity of OSW-1 on Colon Cancer by Inducing Apoptosis In Vitro and In Vivo. *Oncol Rep* (2017) 37(6):3509–19. doi: 10.3892/or.2017.5582
9. Kubo S MY, Terao M, Sashida Y, Nikaido T, Ohmoto T. Acylated Cholestane Glycosides From the Bulbs of Ornithogalum Saundersiae. *Phytochemistry* (1992) 31:3969–73. doi: 10.1016/S0031-9422(00)97565-4
10. Mimaki Y, Kuroda M, Kameyama A, Sashida Y, Hirano T, Oka K, et al. Cholestane Glycosides With Potent Cytostatic Activities on Various Tumor Cells From Ornithogalum Saundersiae Bulbs. *Bioorg Med Chem Lett* (1997) 7(5):633–6. doi: 10.1016/S0960-894X(97)00071-1
11. Zhou Y, Garcia-Prieto C, Carney DA, Xu RH, Pelicano H, Kang Y, et al. OSW-1: A Natural Compound With Potent Anticancer Activity and a Novel Mechanism of Action. *J Natl Cancer Inst* (2005) 97(23):1781–5. doi: 10.1093/jnci/dji404
12. Deng S, Yu B, Lou Y, Hui Y. First Total Synthesis of an Exceptionally Potent Antitumor Saponin, OSW-1. *J Org Chem* (1999) 64(1):202–8. doi: 10.1021/jo981685c
13. Sakurai K, Takeshita T, Hiraizumi M, Yamada R. Synthesis of OSW-1 Derivatives by Site-Selective Acylation and Their Biological Evaluation. *Org Lett* (2014) 16(24):6318–21. doi: 10.1021/ol503044j
14. Ma X, Yu B, Hui Y, Miao Z, Ding J. Synthesis of OSW-1 Analogues and a Dimer and Their Antitumor Activities. *Bioorg Med Chem Lett* (2001) 11 (16):2153–6. doi: 10.1016/s0960-894x(01)00389-4
15. Zheng D, Zhou L, Guan Y, Chen X, Zhou W, Chen X, et al. Synthesis of Cholestane Glycosides Bearing OSW-1 Disaccharide or its 1–>4-Linked Analogue and Their Antitumor Activities. *Bioorg Med Chem Lett* (2010) 20 (18):5439–42. doi: 10.1016/j.bmcl.2010.07.085
16. Guo CX PLF. The First Synthesis of the Aglycone of the Potent Anti-Tumor Steroidal Saponin OSW-1. *Tetrahedron Lett* (1998) 39(10):1099–102. doi: 10.1016/S0040-4039(97)10814-0
17. Ma X, Yu B, Hui Y, Miao Z, Ding J. Synthesis of Steroidal Glycosides Bearing the Disaccharide Moiety of OSW-1 and Their Antitumor Activities. *Carbohydr Res* (2001) 334(2):159–64. doi: 10.1016/s0008-6215(01)00171-9
18. Ma X, Yu B, Hui Y, Xiao D, Ding J. Synthesis of Glycosides Bearing the Disaccharide of OSW-1 or its 1–>4-Linked Analogue and Their Antitumor Activities. *Carbohydr Res* (2000) 329(3):495–505. doi: 10.1016/s0008-6215(00)00225-1
19. Y u W ZJ. A New Strategy for the Stereoselective Introduction of Steroid Side Chain Viar-Alkoxy Vinyl Cuprates: Total Synthesis of a Highly Potent Antitumor Natural Product OSW-1. *J Am Chem Soc* (2001) 123(14):3369–70. doi: 10.1021/ja004098t
20. Yu W, Jin Z. Total Synthesis of the Anticancer Natural Product OSW-1. *J Am Chem Soc* (2002) 124(23):6576–83. doi: 10.1021/ja012119t
21. Jacek W. Morzycki AW. Synthesis of a Cholestane Glycoside OSW-1 With Potent Cytostatic Activity. *Carbohydr Res* (2002) 337:1269–74. doi: 10.1016/S0008-6215(02)00126-X
22. Shi B, Tang P, Hu X, Liu JO, Yu B. OSW Saponins: Facile Synthesis Toward a New Type of Structures With Potent Antitumor Activities. *J Org Chem* (2005) 70(25):10354–67. doi: 10.1021/jo051536b
23. Tsubuki M MS, Honda T. A New Synthesis of Potent Antitumor Saponin OSW-1 via Wittig Rearrangement. *Tetrahedron Lett* (2008) 49(2):157–61. doi: 10.1016/j.tetlet.2007.11.087
24. Xue J, Liu P, Pan Y, Guo Z. A Total Synthesis of OSW-1. *J Org Chem* (2008) 73(1):157–61. doi: 10.1021/jo7018812
25. Tang Y, Li N, Duan JA, Tao W. Structure, Bioactivity, and Chemical Synthesis of OSW-1 and Other Steroidal Glycosides in the Genus Ornithogalum. *Chem Rev* (2013) 113(7):5480–514. doi: 10.1021/cr300072s
26. Guan YY, Song C, Lei PS. Synthesis of Three OSW-1 Analogs With Maltose Side Chains Bearing Different Protection Groups. *J Asian Nat Prod Res* (2014) 16(1):43–52. doi: 10.1080/10286020.2013.863185
27. Zheng D, Guan Y, Chen X, Xu Y, Chen X, Lei P. Synthesis of Cholestane Saponins as Mimics of OSW-1 and Their Cytotoxic Activities. *Bioorg Med Chem Lett* (2011) 21(11):3257–60. doi: 10.1016/j.bmcl.2011.04.030
28. Maj J, Morzycki JW, Rarova L, Oklest'kova J, Strnad M, Wojtkielewicz A. Synthesis and Biological Activity of 22-Deoxo-23-Oxa Analogues of Saponin OSW-1. *J med Chem* (2011) 54(9):3298–305. doi: 10.1021/jm101648h
29. Morzycki JW, Wojtkielewicz A, Wolczynski S. Synthesis of Analogues of a Potent Antitumor Saponin OSW-1. *Bioorg Med Chem Lett* (2004) 14 (12):3323–6. doi: 10.1016/j.bmcl.2004.03.102
30. Komatsu R, Sakurai K. Development of Chemical Probes for Functional Analysis of Anticancer Saponin OSW-1. *Chem Rec* (2019) 19(12):2362–9. doi: 10.1002/tcr.201900042
31. Boyd MR, Paull KD, Rubinstein LR. *Cytotoxic Anticancer Drugs: Models and Concepts for Drug Discovery and Development*. Amsterdam: Kluwer Academic Publishers (1992) p. 11–34.
32. Deng L, Wu H, Yu B, Jiang M, Wu J. Synthesis of OSW-1 Analogs With Modified Side Chains and Their Antitumor Activities. *Bioorg Med Chem Lett* (2004) 14(11):2781–5. doi: 10.1016/j.bmcl.2004.03.081
33. Morzycki JW, Wojtkielewicz A. Synthesis of a Cholestane Glycoside OSW-1 With Potent Cytostatic Activity. *Carbohydr Res* (2002) 337(14):1269–74. doi: 10.1016/s0008-6215(02)00126-x
34. Yu W, Jin Z. A New Strategy for the Stereoselective Introduction of Steroid Side Chain via Alpha-Alkoxy Vinyl Cuprates: Total Synthesis of a Highly Potent Antitumor Natural Product OSW-1. *J Am Chem Soc* (2001) 123 (14):3369–70. doi: 10.1021/ja004098t
35. Bensen RC, Gunay G, Finneran MC, Jhingan I, Acar H, Burgett AWG. Small Molecule Targeting of Oxysterol-Binding Protein (OSBP)-Related Protein 4 and OSBP Inhibits Ovarian Cancer Cell Proliferation in Monolayer and Spheroid Cell Models. *ACS Pharmacol Transl Sci* (2021) 4(2):744–56. doi: 10.1021/acsptsci.0c00207
36. Ding X, Li Y, Li J, Yin Y. OSW-1 Inhibits Tumor Growth and Metastasis by NFATc2 on Triple-Negative Breast Cancer. *Cancer Med* (2020) 9(15):5558–69. doi: 10.1002/cam4.3196
37. Kimura M, Sasaki K, Fukutani Y, Yoshida H, Ohsawa I, Yohda M, et al. Anticancer Saponin OSW-1 is a Novel Class of Selective Golgi Stress Inducer. *Bioorg Med Chem Lett* (2019) 29(14):1732–6. doi: 10.1016/j.bmcl.2019.05.022
38. Iguchi T, Kuroda M, Naito R, Watanabe T, Matsuo Y, Yokosuka A, et al. Cholestane Glycosides From Ornithogalum Saundersiae Bulbs and the Induction of Apoptosis in HL-60 Cells by OSW-1 Through a Mitochondrial-Independent Signaling Pathway. *J Nat Med* (2019) 73 (1):131–45. doi: 10.1007/s11418-018-1252-4
39. Garcia-Prieto C, Riaz Ahmed KB, Chen Z, Zhou Y, Hammoudi N, Kang Y, et al. Effective Killing of Leukemia Cells by the Natural Product OSW-1 Through Disruption of Cellular Calcium Homeostasis. *J Biol Chem* (2013) 288(5):3240–50. doi: 10.1074/jbc.M112.384776
40. Jin J, Jin X, Qian C, Ruan Y, Jiang H. Signaling Network of OSW-1 Induced Apoptosis and Necroptosis in Hepatocellular Carcinoma. *Mol Med Rep* (2013) 7(5):1646–50. doi: 10.3892/mmr.2013.1366
41. Jin JC, Jin XL, Zhang X, Piao YS, Liu SP. Effect of OSW-1 on microRNA Expression Profiles of Hepatoma Cells and Functions of Novel microRNAs. *Mol Med Rep* (2013) 7(6):1831–7. doi: 10.3892/mmr.2013.1428

42. Burgett AW, Poulsen TB, Wangkanont K, Anderson DR, Kikuchi C, Shimada K, et al. Natural Products Reveal Cancer Cell Dependence on Oxysterol-Binding Proteins. *Nat Chem Biol* (2011) 7(9):639–47. doi: 10.1038/nchembio.625
43. Zhu J, Xiong L, Yu B, Wu J. Apoptosis Induced by a New Member of Saponin Family Is Mediated Through Caspase-8-Dependent Cleavage of Bcl-2. *Mol Pharmacol* (2005) 68(6):1831–8. doi: 10.1124/mol.105.015826
44. Hanahan D, Weinberg RA. Hallmarks of Cancer: The Next Generation. *Cell* (2011) 144(5):646–74. doi: 10.1016/j.cell.2011.02.013
45. Tay KC, Tan LT, Chan CK, Hong SL, Chan KG, Yap WH, et al. Formononetin: A Review of Its Anticancer Potentials and Mechanisms. *Front Pharmacol* (2019) 10:820. doi: 10.3389/fphar.2019.00820
46. Liu H, Huang S. Role of Oxysterol-Binding Protein-Related Proteins in Malignant Human Tumours. *World J Clin cases* (2020) 8(1):1–10. doi: 10.12998/wjcc.v8.i1.1
47. Du X, Turner N, Yang H. The Role of Oxysterol-Binding Protein and its Related Proteins in Cancer. *Semin Cell Dev Biol* (2018) 81:149–53. doi: 10.1016/j.semcdb.2017.07.017
48. Roberts BL, Severance ZC, Bensen RC, Le AT, Kothapalli NR, Nuñez JI, et al. Transient Compound Treatment Induces a Multigenerational Reduction of Oxysterol-Binding Protein (OSBP) Levels and Prophylactic Antiviral Activity. *ACS Chem Biol* (2019) 14(2):276–87. doi: 10.1021/acschembio.8b00984
49. Roberts BL, Severance ZC, Bensen RC, Le-McClain AT, Malinky CA, Mettenbrink EM, et al. Differing Activities of Oxysterol-Binding Protein (OSBP) Targeting Anti-Viral Compounds. *Antiviral Res* (2019) 170:104548. doi: 10.1016/j.antiviral.2019.104548
50. Charman M, Colbourne TR, Pietrangelo A, Kreplak L, Ridgway ND. Oxysterol-Binding Protein (OSBP)-Related Protein 4 (ORP4) Is Essential for Cell Proliferation and Survival. *J Biol Chem* (2014) 289(22):15705–17. doi: 10.1074/jbc.M114.571216
51. Zhong W, Xu M, Li C, Zhu B, Cao X, Li D, et al. ORP4L Extracts and Presents PIP(2) From Plasma Membrane for Plcβ3 Catalysis: Targeting It Eradicates Leukemia Stem Cells. *Cell Rep* (2019) 26(8):2166–77.e9. doi: 10.1016/j.celrep.2019.01.082
52. Antonny B, Bigay J, Mesmin B. The Oxysterol-Binding Protein Cycle: Burning Off Pi(4)P to Transport Cholesterol. *Annu Rev Biochem* (2018) 87:809–37. doi: 10.1146/annurev-biochem-061516-044924
53. Waugh MG. The Great Escape: How Phosphatidylinositol 4-Kinases and PI4P Promote Vesicle Exit From the Golgi (and Drive Cancer). *Biochem J* (2019) 476(16):2321–46. doi: 10.1042/bcj20180622
54. Norbury CJ, Hickson ID. Cellular Responses to DNA Damage. *Annu Rev Pharmacol Toxicol* (2001) 41:367–401. doi: 10.1146/annurev.pharmtox.41.1.367
55. Fuchs Y, Steller H. Programmed Cell Death in Animal Development and Disease. *Cell* (2011) 147(4):742–58. doi: 10.1016/j.cell.2011.10.033
56. Elmore S. Apoptosis: A Review of Programmed Cell Death. *Toxicol Pathol* (2007) 35(4):495–516. doi: 10.1080/01926230701320337
57. Wong RS. Apoptosis in Cancer: From Pathogenesis to Treatment. *J Exp Clin Cancer Res* (2011) 30(1):87. doi: 10.1186/1756-9966-30-87
58. Fulda S, Debatin KM. Extrinsic Versus Intrinsic Apoptosis Pathways in Anticancer Chemotherapy. *Oncogene* (2006) 25(34):4798–811. doi: 10.1038/sj.onc.1209608
59. Igney FH, Krammer PH. Death and Anti-Death: Tumour Resistance to Apoptosis. *Nat Rev Cancer* (2002) 2(4):277–88. doi: 10.1038/nrc776
60. Pistritto G, Trisciuoglio D, Ceci C, Garufi A, D'Orazi G. Apoptosis as Anticancer Mechanism: Function and Dysfunction of its Modulators and Targeted Therapeutic Strategies. *Aging* (2016) 8(4):603–19. doi: 10.18632/aging.100934
61. Degli Esposti M. Mitochondria in Apoptosis: Past, Present and Future. *Biochem Soc Trans* (2004) 32(Pt3):493–5. doi: 10.1042/bst0320493
62. Miyata S, Mizuno T, Koyama Y, Katayama T, Tohyama M. The Endoplasmic Reticulum-Resident Chaperone Heat Shock Protein 47 Protects the Golgi Apparatus From the Effects of O-Glycosylation Inhibition. *PloS One* (2013) 8(7):e69732. doi: 10.1371/journal.pone.0069732
63. Reiling JH, Olive AJ, Sanyal S, Carette JE, Brummelkamp TR, Ploegh HL, et al. A CREB3-ARF4 Signalling Pathway Mediates the Response to Golgi Stress and Susceptibility to Pathogens. *Nat Cell Biol* (2013) 15(12):1473–85. doi: 10.1038/ncb2865
64. Migita T, Inoue S. Implications of the Golgi Apparatus in Prostate Cancer. *Int J Biochem Cell Biol* (2012) 44(11):1872–6. doi: 10.1016/j.biocel.2012.06.004
65. Kulkarni-Gosavi P, Makhoul C, Gleeson PA. Form and Function of the Golgi Apparatus: Scaffolds, Cytoskeleton and Signalling. *FEBS Lett* (2019) 593(17):2289–305. doi: 10.1002/1873-3468.13567
66. Wlodkowic D, Skommer J, McGuinness D, Hillier C, Darzynkiewicz Z. ER-Golgi Network–a Future Target for Anti-Cancer Therapy. *Leukemia Res* (2009) 33(11):1440–7. doi: 10.1016/j.leukres.2009.05.025
67. Petrosyan A. Onco-Golgi: Is Fragmentation a Gate to Cancer Progression? *Biochem Mol Biol J* (2015) 1(1):16. doi: 10.21767/2471-8084.100006
68. Sasaki K, Yoshida H. Organelle Autoregulation—Stress Responses in the ER, Golgi, Mitochondria and Lysosome. *J Biochem* (2015) 157(4):185–95. doi: 10.1093/jb/mvv010%JTheJournalofBiochemistry
69. Sasaki K, Yoshida H. Golgi Stress Response and Organelle Zones. *FEBS Lett* (2019) 593(17):2330–40. doi: 10.1002/1873-3468.13554
70. Machamer CE. The Golgi Complex in Stress and Death. *Front Neurosci* (2015) 9:421. doi: 10.3389/fnins.2015.00421
71. Taniguchi M, Yoshida H. TFE3, HSP47, and CREB3 Pathways of the Mammalian Golgi Stress Response. *Cell struct Funct* (2017) 42(1):27–36. doi: 10.1247/csf.16023
72. Woodhouse EC, Chuaqui RF, Liotta LA. General Mechanisms of Metastasis. *Cancer* (1997) 80:1529–37. doi: 10.1002/(SICI)1097-0142(19971015)80:8+<1529::AID-CNCR2>3.0.CO;2-F
73. Pastushenko I, Blanpain C. EMT Transition States During Tumor Progression and Metastasis. *Trends Cell Biol* (2019) 29(3):212–26. doi: 10.1016/j.tcb.2018.12.001
74. Gurzu S, Silveanu C, Fetyko A, Butiurca V, Kovacs Z, Jung I. Systematic Review of the Old and New Concepts in the Epithelial-Mesenchymal Transition of Colorectal Cancer. *World J Gastroenterol* (2016) 22(30):6764–75. doi: 10.3748/wjg.v22.i30.6764
75. Sporikova Z, Koudelakova V, Trojanec R, Hajduch M. Genetic Markers in Triple-Negative Breast Cancer. *Clin Breast Cancer* (2018) 18(5):e841–e50. doi: 10.1016/j.clbc.2018.07.023
76. Yin L, Duan JJ, Bian XW, Yu SC. Triple-Negative Breast Cancer Molecular Subtyping and Treatment Progress. *Breast Cancer Res BCR* (2020) 22(1):61. doi: 10.1186/s13058-020-01296-5
77. Quang CT, Leboucher S, Passaro D, Fuhrmann L, Nourieh M, Vincent-Salomon A, et al. The Calcineurin/NFAT Pathway Is Activated in Diagnostic Breast Cancer Cases and Is Essential to Survival and Metastasis of Mammary Cancer Cells. *Cell Death Dis* (2015) 6(2):e1658. doi: 10.1038/cddis.2015.14
78. Di Leva G, Garofalo M, Croce CM. MicroRNAs in Cancer. *Annu Rev Pathol* (2014) 9:287–314. doi: 10.1146/annurev-pathol-012513-104715
79. Esquela-Kerscher A, Slack FJ. Oncomirs — microRNAs With a Role in Cancer. *Nat Rev Cancer* (2006) 6(4):259–69. doi: 10.1038/nrc1840
80. Mollaei H, Safaralizadeh R, Rostami Z. MicroRNA Replacement Therapy in Cancer. *J Cell Physiol* (2019) 234(8):12369–84. doi: 10.1002/jcp.28058
81. Rupaimoole R, Slack FJ. MicroRNA Therapeutics: Towards a New Era for the Management of Cancer and Other Diseases. *Nat Rev Drug Discovery* (2017) 16(3):203–22. doi: 10.1038/nrd.2016.246
82. Oliveto S, Mancino M, Manfrini N, Biffo S. Role of microRNAs in Translation Regulation and Cancer. *World J Biol Chem* (2017) 8(1):45–56. doi: 10.4331/wjbc.v8.i1.45
83. Wang S, Aurora AB, Johnson BA, Qi X, McAnally J, Hill JA, et al. The Endothelial-Specific microRNA miR-126 Governs Vascular Integrity and Angiogenesis. *Dev Cell* (2008) 15(2):261–71. doi: 10.1016/j.devcel.2008.07.002
84. Sausville EA, Elsayed Y, Monga M, Kim G. Signal Transduction–Directed Cancer Treatments. *Annu Rev Pharmacol Toxicol* (2003) 43:199–231. doi: 10.1146/annurev.pharmtox.43.100901.135813
85. Sim EH, Yang IA, Wood-Baker R, Bowman RV, Fong KM. Gefitinib for Advanced Non-Small Cell Lung Cancer. *Cochrane Database Syst Rev* (2018) 1(1):Cd006847. doi: 10.1002/14651858.CD006847
86. Deininger M, Buchdunger E, Druker BJ. The Development of Imatinib as a Therapeutic Agent for Chronic Myeloid Leukemia. *Blood* (2005) 105(7):2640–53. doi: 10.1182/blood-2004-08-3097

87. Maximiano S, Magalhães P, Guerreiro MP, Morgado M. Trastuzumab in the Treatment of Breast Cancer. *BioDrugs Clin immunotherapeutics biopharmaceuticals Gene Ther* (2016) 30(2):75–86. doi: 10.1007/s40259-016-0162-9
88. Liu WJ, Du Y, Wen R, Yang M, Xu J. Drug Resistance to Targeted Therapeutic Strategies in Non-Small Cell Lung Cancer. *Pharmacol Ther* (2020) 206:107438. doi: 10.1016/j.pharmthera.2019.107438
89. Konieczkowski DJ, Johannessen CM. Garraway LA. A Convergence-Based Framework for Cancer Drug Resistance. *Cancer Cell* (2018) 33(5):801–15. doi: 10.1016/j.ccell.2018.03.025
90. Groenendijk FH, Bernards R. Drug Resistance to Targeted Therapies: Déjà Vu All Over Again. *Mol Oncol* (2014) 8(6):1067–83. doi: 10.1016/j.molonc.2014.05.004
91. Iqbal J, Sun L, Zaidi M. Complexity in Signal Transduction. *Ann N Y Acad Sci* (2010) 1192:238–44. doi: 10.1111/j.1749-6632.2010.05388.x
92. Yuan R, Hou Y, Sun W, Yu J, Liu X, Niu Y, et al. Natural Products to Prevent Drug Resistance in Cancer Chemotherapy: A Review. *Ann N Y Acad Sci* (2017) 1401(1):19–27. doi: 10.1111/nyas.13387
93. Zhan T, Rindtorff N, Boutros M. Wnt Signaling in Cancer. *Oncogene* (2017) 36(11):1461–73. doi: 10.1038/onc.2016.304
94. Kim EK, Choi EJ. Compromised MAPK Signaling in Human Diseases: An Update. *Arch Toxicol* (2015) 89(6):867–82. doi: 10.1007/s00204-015-1472-2
95. Yarden Y, Pines G. The ERBB Network: At Last, Cancer Therapy Meets Systems Biology. *Nat Rev Cancer* (2012) 12(8):553–63. doi: 10.1038/nrc3309
96. Normanno N, De Luca A, Bianco C, Strizzi L, Mancino M, Maiello MR, et al. Epidermal Growth Factor Receptor (EGFR) Signaling in Cancer. *Gene* (2006) 366(1):2–16. doi: 10.1016/j.gene.2005.10.018
97. Ong CP, Lee WL, Tang YQ, Yap WH. Honokiol: A Review of Its Anticancer Potential and Mechanisms. *Cancers (Basel)* (2019) 12(1):48. doi: 10.3390/cancers12010048
98. Kastenhuber ER, Lowe SW. Putting P53 in Context. *Cell* (2017) 170(6):1062–78. doi: 10.1016/j.cell.2017.08.028
99. Pietrangelo A, Ridgway ND. Bridging the Molecular and Biological Functions of the Oxysterol-Binding Protein Family. *Cell Mol Life Sci* (2018) 75(17):3079–98. doi: 10.1007/s00018-018-2795-y
100. Albulescu L, Strating JR, Thibaut HJ, van der Linden L, Shair MD, Neyts J, et al. Broad-Range Inhibition of Enterovirus Replication by OSW-1, a Natural Compound Targeting OSBP. *Antiviral Res* (2015) 117:110–4. doi: 10.1016/j.antiviral.2015.02.013
101. Harley W, Floyd C, Dunn T, Zhang XD, Chen TY, Hegde M, et al. Dual Inhibition of Sodium-Mediated Proton and Calcium Efflux Triggers Non-Apoptotic Cell Death in Malignant Gliomas. *Brain Res* (2010) 1363:159–69. doi: 10.1016/j.brainres.2010.09.059
102. Kibble M, Saarinen N, Tang J, Wennerberg K, Mäkelä S, Aittokallio T. Network Pharmacology Applications to Map the Unexplored Target Space and Therapeutic Potential of Natural Products. *Natural product Rep* (2015) 32(8):1249–66. doi: 10.1039/c5np00005j
103. Turanli B, Karagoz K, Gulfidan G, Sinha R, Mardinoglu A, Arga KY. A Network-Based Cancer Drug Discovery: From Integrated Multi-Omics Approaches to Precision Medicine. *Curr Pharm design* (2018) 24(32):3778–90. doi: 10.2174/1381612824666181106095959
104. Olivier M, Asmis R, Hawkins GA, Howard TD, Cox LA. The Need for Multi-Omics Biomarker Signatures in Precision Medicine. *Int J Mol Sci* (2019) 20(19):4781. doi: 10.3390/ijms20194781
105. Buyel JF. Plants as Sources of Natural and Recombinant Anti-Cancer Agents. *Biotechnol Adv* (2018) 36(2):506–20. doi: 10.1016/j.biotechadv.2018.02.002
106. Elekofehinti OO, Iwaloye O, Olawale F, Ariyo EO. Saponins in Cancer Treatment: Current Progress and Future Prospects. *Pathophysiology* (2021) 28(2):250–72. doi: 10.3390/pathophysiology28020017

Conflict of Interest: The authors declare that the research was conducted in the absence of any commercial or financial relationships that could be construed as a potential conflict of interest.

Publisher's Note: All claims expressed in this article are solely those of the authors and do not necessarily represent those of their affiliated organizations, or those of the publisher, the editors and the reviewers. Any product that may be evaluated in this article, or claim that may be made by its manufacturer, is not guaranteed or endorsed by the publisher.

frontiers in Pharmacology

ORIGINAL RESEARCH
published: 24 September 2021
doi: 10.3389/fphar.2021.669199

Beneficial Effects of Gracillin From *Rhizoma Paridis* Against Gastric Carcinoma via the Potential TIPE2-Mediated Induction of Endogenous Apoptosis and Inhibition of Migration in BGC823 Cells

Wenming Liu[1†], *Yanting Wang*[1†], *Junjie Chen*[1], *Zhenhe Lin*[1], *Mengjie Lin*[2], *Xiantong Lin*[3*] *and Yanyun Fan*[1*]

[1]*Department of Gastroenterology, Zhongshan Hospital, Xiamen University, Xiamen, China,* [2]*Department of Pathology, Zhongshan Hospital, Xiamen University, Xiamen, China,* [3]*Department of Thoracic and Cardiovascular Surgery, The Third Hospital of Xiamen, Xiamen, China*

Tumor necrosis factor-α inducible protein-8 (TIPE2), initially recognized as a negative immune regulator, exerts an important role in suppressing the progression of numerous cancers. In our previous investigation, we found that TIPE2 expression displayed a decrease or absence in gastric tumor tissue, and the overexpression of TIPE2 suppressed the growth of gastric cancer tumors and cells, demonstrating that TIPE2 could be a potential medicinal target for gastric cancer treatment. However, it's seldomly reported that several medicinal agents or candidates targeted TIPE2 for treating diseases, including gastric cancer. To identify the candidate targeting TIPE2 to fight against gastric cancer, several extractions from traditional natural medicinal plants with anti-tumor functions were employed to screen the active compounds according to bioassay-guided isolation. Interestingly, gracillin, a component from the ethyl acetate extraction of *Rhizoma Paridis*, was identified to induce the expression of TIPE2 and inhibit the cell proliferation in gastric cancer BGC-823 cells. Furthermore, the underlying mechanisms that restrain gastric cancer were evaluated by clone formation, EdU staining, flow cytometry, and other assays. Meanwhile, the role of TIPE2 in the anti-tumor effect of gracillin was elucidated via the use of siTIPE2 RNA. It was determined that gracillin could fight against gastric cancer cells by inhibiting the cell proliferation participated by the PI3K/AKT pathway and cell cycle arrest, suppressing the EMT pathway-regulating cell migration, and inducing bcl2-associated mitochondrial apoptosis. Additionally, TIPE2 maybe contribute to the benefits of gracillin. These results of the present study are an important step toward the medicinal development of gracillin, and are also of use in understanding the effect of TIPE2 as a potential tumor target.

Keywords: TIPE2, gracillin, rhizoma paridis, gastric carcinoma, BGC-823

OPEN ACCESS

Edited by:
Marne Carvalho De Vasconcellos, Federal University of Amazonas, Brazil

Reviewed by:
Qiang Wang, Nanjing Drum Tower Hospital, China
XiuJuan Qu, The First Affiliated Hospital of China Medical University, China

***Correspondence:**
Yanyun Fan
trudy1@163.com
Xiantong Lin
lindylam@163.com

[†]*The authors contributed equally*

Specialty section:
This article was submitted to Pharmacology of Anti-Cancer Drugs, a section of the journal Frontiers in Pharmacology

Received: *18 February 2021*
Accepted: *03 September 2021*
Published: *24 September 2021*

Citation:
Liu W, Wang Y, Chen J, Lin Z, Lin M, Lin X and Fan Y (2021) Beneficial Effects of Gracillin From Rhizoma Paridis *Against Gastric Carcinoma via the Potential TIPE2-Mediated Induction of Endogenous Apoptosis and Inhibition of Migration in BGC823 Cells. Front. Pharmacol. 12:669199. doi: 10.3389/fphar.2021.669199*

INTRODUCTION

Gastric cancer has become the fourth most common incidence and the second most common cause of death globally, as such is a serious threat to human health and happiness (Rui et al., 2019; Elizabeth et al., 2020; Tony et al., 2020; Yoshiki, 2020; Hyuna et al., 2021). Therapeutic strategies for treating gastric cancer have been challenged by the complex and controversial causes of gastric cancer development (Antonia and Wagner, 2016; Helge and Reidar, 2018; Camilla and Giuseppe, 2020; Nalinie et al., 2020). For several decades, chemotherapy has remained one of the most commonly used therapies following surgical treatment to fight against gastric cancer. However, the traditional chemotherapeutical agents, such as 5-fluorouracil, cyclophosphamide, and other broad-spectrum anti-tumor agents, presented serious toxic side effects, such as weight loss, hair loss, and anorexia, during the treatment of gastric cancer. This has been attributed to their lack of selectivity for healthy and tumor cells (Mary et al., 2020; Yong et al., 2021). To improve the selectivity of chemotherapeutical agents, drugs targeting proteins specifically expressed in tumor tissue or selectively-mediated tumor have aroused great interest, and a few target drugs have also been effectively developed to treat liver cancer, lung cancer, and gastric cancer in the clinic (G Schinzari et al., 2014).

Tumor necrosis factor-α inducible protein-8 (TNFAIP8L2, also called TIPE2) is a negative immune mediator that was discovered in 2008 (Eric et al., 2008; Honghong et al., 2008). The emerging evidence shows that TIPE2 could inhibit gastric carcinoma growth and metastasis (Qian et al., 2015; Jie et al., 2016; Ganesan et al., 2018). Our previous research suggested that TIPE2 is missing or has low expression in gastric carcinoma but not in normal gastric mucosa (Wenming et al., 2018; Zhenhe et al., 2018). Furthermore, the overexpression of TIPE2 could suppress the proliferation and migration of gastric cancer BGC823 cells. These data demonstrate that TIPE2 could be a novel potential therapeutic target for gastric cancer treatment. However, candidates targeting TIPE2 to restrain gastric carcinoma are as yet seldom reported. Therefore, exploring TIPE2's mediator would be an important and significant strategy in the development of new anti-tumor medicine for gastric cancer.

Natural products, especially those found in various traditional medicine systems such as Traditional Chinese Medicine (TCM), have served as folk medicinal agents to regulate immune, inflammation, metabolism, and other physiologies for thousands of years (Daniel et al., 2012; Tai et al., 2019). The medicine of natural products was wildly applied to relieve all kinds of diseases including cancer (Amit and Vikas, 2019; Min et al., 2019; Tohid et al., 2019; Xuanmei et al., 2019). Excitingly, Lianhuaqingwen, (TCM) formula consisting of multiple natural herbs such as fructus forsythiae, Lonicera japonica Thunb, and Houttuynia cordata Thunb have also contributed to controlling the 2019 novel SARS-CoV-2 global pandemic (Li et al., 2020; Ming et al., 2021). These natural products had crucial roles in maintaining individual's health and defeating disease, in both history and present. However, its complicated ingredients with numerous different yet remarkably similar structural molecules hindered the modern clinical application. In the last hundred years, these pure and simple pharmaceutical agents are slipping into the mainstream of clinical drugs, rather than natural product mixtures (Emma and Margaret, 2019). Fortunately, the majority of these pure medicinal compounds were sourced or derived from natural product components. From 1981 to 2014, 65% of all single pharmaceutical agents approved by the American Food and Drug Administration (FDA) came from natural product components and their derivatives. Furthermore, 75% of the anti-tumor agents came from natural products and their derivatives (David and Gordon, 2016). In the future, natural products will remain a valuable source of novel medicine agents, and identifying potential lead molecules from natural product mixtures is still an important strategy of drug discovery.

In this study, we aimed to identify a potential TIPE2 candidate for restraining gastric carcinoma from a traditional natural herb, and to clarify the mechanism by which the candidate suppresses gastric carcinoma via TIPE2. The present research started with screening active compounds for inhibiting the proliferation of gastric cancer cell BGC-823 and regulating TIPE2 protein expression from the fractions of four medicinal plants *Curcuma longa L., Tripterygium Wilfordii, Rhizoma Paridis,* and *Reynoutria japonica Houtt*. Following screening the active fractions from the medicinal plant extracts and identifying the potential candidate from the active fractions via bioassay-guided isolation, a TIPE2 mediator named gracillin from *Rhizoma Paridis* was discovered to have potential in suppressing gastric cancer cell proliferation. Furthermore, we assessed the mechanism by which gracillin suppressed gastric carcinoma, and found that gracillin could induce cellular apoptosis and inhibit migration via TIPE2-mediated endogenous apoptosis and EMT pathway in BGC-823. The results provided a theoretical basis for developing drugs to treat gastric cancer by targeting TIPE2.

MATERIALS AND METHODS

Preparation of Medicinal Plants Extraction and the Identification of Active Compounds

The medicinal plants *Curcuma longa L., Tripterygium Wilfordii, Rhizoma Paridis*, and *Reynoutria japonica Houtt* were purchased from the Traditional Chinese Medicine Trade Center of Bozhou in Anhui Province, China. These plants were first crushed into a coarse powder and soaked for 2 h in six volumes of 60% ethanol (volume/weight) to extract by reflux. The extraction solution was filtered, and the residue was subjected to this process two more times. The filtered solutions were merged and concentrated to obtain the total extraction using rotary evaporation (EYELA, Japan). The total extraction was suspended in water and extracted with petroleum ether, chloroform, and ethyl acetate (Sinopharm, Beijing, China) to obtain the fractions of PE, C, and EA. After a bio-activities test, the active fractions were separated using preparative high-performance liquid chromatography with a flow phase of 40–55% acetonitrile (Merck, Germany) and the active compounds were identified by mass spectroscopy.

Cell Culture

Human gastric tumor BGC-823 cells (Chinese Academy of Medical Sciences, Shanghai, China) were cultured in an RPMI-1640 medium (Hyclone, Utah, United States) containing 10% FBS (Gibco, Waltham, United States) and 1% bi-antibiotic of penicillin and streptomycin (Hyclone, Utah, United States) in an atmosphere of 5% CO_2 and 37°C (Thermofisher, MA, United States). Before the bio-assays of agents were performed, BGC-823 cells were seeded into the preassigned culture plates and administrated with the different plant extractions or gracillin for a corresponding time. Then the cells were harvested and the detection was carried out according to standard protocol.

MTT Assay

Cell proliferation was evaluated using an MTT assay. Briefly, BGC-823 cells were seeded into a 96-well plate at a density of 10,000 cells/well and cultured for 12 h. Then the seeded cells were administrated with plant extractions or gracillin and cultured for 24/48 h. An MTT solution with 5 mg/ml (Solarbio, Beijing, China) was added to the well and incubated for another 3 h. After incubation, the medium was removed, the cells were washed twice with PBS, and 100 μL DMSO (Solarbio, Beijing, China) was added to each well to dissolving the formazan. Finally, the absorbance was read at 490 nm using a microplate reader (Thermofisher, MA, United States) and the proliferation ratio was calculated as follows:

Western Blot

BGC-823 cells were seeded into a 6-well plate with 60% confluence and maintained in a CO_2 incubator for 12 h. Then the seeded cells were administrated with different doses of gracillin for another 12 h. The treated cells were harvested, lysed in a RIPA buffer (Solarbio, Beijing, China) on ice with a vortex of once per 5 min for 30 min, and centrifuged at 12,000 rpm and 4°C. The supernatants were collected, the total protein concentration was evaluated by BCA assay kit (Thermofisher, MA, United States), and boiled using dry baths (Yiheng, Hangzhou, China) to denature the protein. A sample of 20 μg of prepared protein was subjected to 8–12% SDS-PAGE to separate the total protein and then transferred to a PVDF membrane (Millipore, MA, United States). The transferred PVDF membrane was immersed in 5% defatted milk at room temperature for 1 h to block, incubated overnight at 4°C with the primary antibodies of TIPE2, AKT, p-AKT, CDK1, p-CDK1, cyclin B1, p21, E-cadherin, N-cadherin, vimentin, cleaved PARP, bcl2, cleaved caspase3, and cleaved caspase9 (CST, United States), then incubated with a secondary antibody (Proteinteck, Wuhan, China) at room temperature for 1 h. Finally, ECL chemiluminescent solution was added to the PVDF membranes (Pierce, United States) for imaging.

EdU Staining

The cell proliferation was evaluated using EdU staining. Briefly, BGC-823 cells and BGC823/TIPE2$^{-/-}$ cells were seeded into a 12-well plate with 30% confluence and maintained in a CO_2 incubator for 12 h. Then the seeded cells were administrated with 5 μM gracillin and cultured. Later, the cells were added with EdU solution to stain for 2 h, washed with PBS, and imaged with a microscope (Olympus, Japan).

Colony Formation

The cell proliferation was also assessed using colony formation. Briefly, BGC-823 cells and BGC823/TIPE2$^{-/-}$ cells were seeded into a 12-well plate with 5,000 cells per well and maintained in a CO_2 incubator for 12 h. Then the seeded cells were administrated with 5 μM gracillin and cultured for 7 days. Later, the cells were washed with PBS and fixed with 4% paraformaldehyde and then stained with gimsa solution for 30 min and imaged.

Cell Cycle Distribution Analysis

BGC-823 cells and BGC823/TIPE2$^{-/-}$ cells were seeded into a 6-well plate with 50% confluence and maintained in a normal medium for 12 h, then replaced with an FBS-free medium to culture for another 12 h. After starvation culture, the cells were treated with 3 μM gracillin for 24 h. Then the treated cells were collected, fixed with pre-cooled 70% ethanol overnight at 4°C, and stained with 5 μg/ml propidium iodide (Solarbio, Beijing, China) at room temperature for 20 min. Finally, the stained cells were detected using the flow cytometer (Beckman, United States).

Scratch Assay

The cell migration was assessed using a scratch assay. Briefly, BGC-823 cells and BGC823/TIPE2$^{-/-}$ cells were seeded into a 6-well plate with 60% confluence and cultured for 12 h. Then the seeded cells were scratched with a white pipette tip to form a cell-free area and administrated with 3 μM gracillin for 48 h. The cell-free area was imaged and its width was quantified using Image J software.

Flow Cytometer for Cell Apoptosis

The cell apoptosis was examined by dual-staining with FITC-Annexin V and PI. Briefly, BGC-823 cells and BGC823/TIPE2$^{-/-}$ cells were seeded into a 6-well plate with 60% confluence and cultured for 12 h. Then the seeded cells were administrated with 3 μM gracillin for 24 h. The cells were digested with a 0.25% trypsin solution and transferred to a 1.5 ml EP tube, then suspended in 500 μL binding buffer, and dyed with 5 μLAnnexin V-FITC and 5 μL PI according to the manufacturer's manual of FITC-Annexin apoptosis detection kit (BD, United States). The stained cells were detected using a flow cytometer (Beckman, United States).

Animal Experiment

Male nude mice aged 6 weeks were purchased from the Xiamen University Laboratory Animal Center. The mice were raised in pathogen-free conditions with 12 h light/12 h dark cycles for a week, then randomly divided into two groups, the control group and the gracillin administration group, and subcutaneously inoculated with BGC-823 gastric cancer cells of 2×10^6 cells per mice. The inoculated mice were maintained for another week, then injected with gracillin or normal saline once every other day for 21 days. During this period, the tumor size and body weight were measured once every 3 days. On the 21st day, the mice were sacrificed and their tumors were collected for immunohistochemistry and western blotting test.

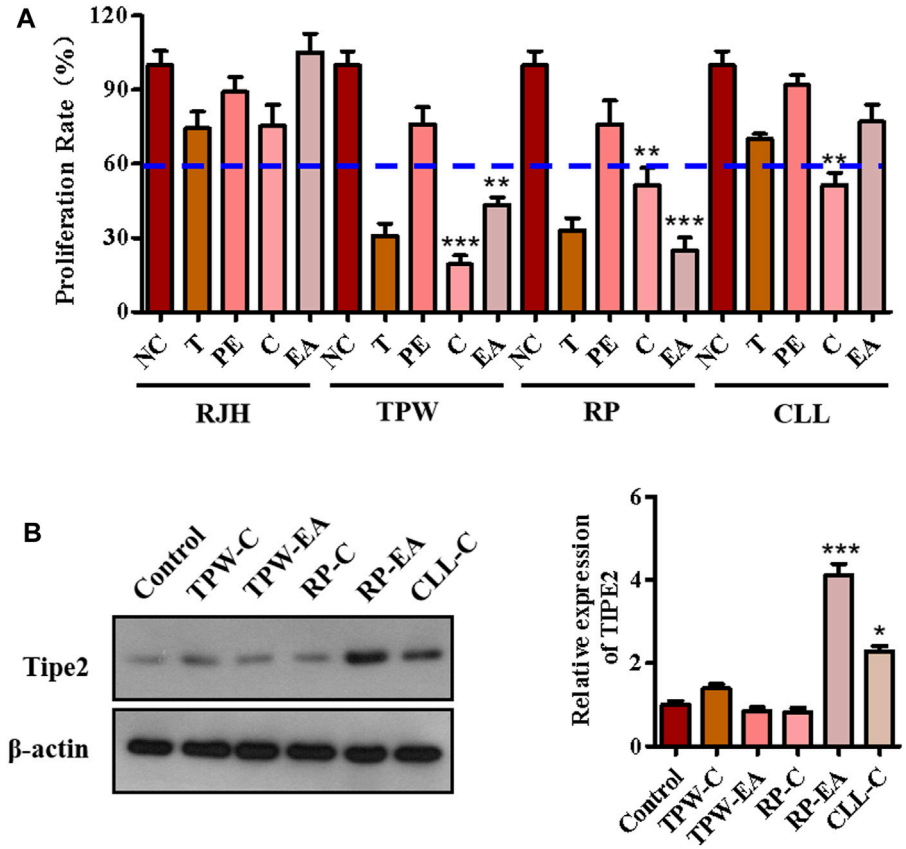

FIGURE 1 | The components analysis of active fractions from medicinal plants. **(A)** The effect of medicinal plants on cell proliferation in BGC823 cells. 50 μg/ml extractions of the plants were used to treat BGC823 cells for 48 h. **(B)** The effects of active fractions on the expression of TIPE2. 50 μg/ml active fractions were used to treat the BGC823 cells for 12 h. The values in the histogram are displayed as mean ± SD; $0.01 < p < 0.05$ (*) represents a significant difference, and $p < 0.001$ (***) represents an extremely significant difference to the normal control.

Hematoxylin and Eosin Staining and Immunohistochemistry Staining

Tumor tissue specimens were fixed in 4% paraformaldehyde for 1 h, then soaked in wax and sectioned. The sections were firstly dewaxed via incubation at 60°C for 1 h, soaked twice in xylene for 5 min, then in 100, 100, 95, 80% alcohol for 1 min each. In HE staining, the dewaxed sections were stained with hematoxylin for 6 min and eosin for 2 min, then washed with distilled water, dehydrated with gradient alcohol (95, 95, 100, and 100%) for 1 min each, vitrified with xylene twice, and sealed with neutral gum. In IHC staining, the dewaxed sections were immersed in a citrate buffer, washed with 0.01 M PBS, and cooled for antigen repair. Then the sections were incubated with the primary antibody ki67 overnight and a secondary antibody for 1 h. Finally, the specimens were stained with hematoxylin, dehydrated, vitrified, and sealed.

Statistical Analysis

Statistical analysis was carried out using SPSS software. The data were displayed as mean± (SEM). One-way ANOVA was employed to compare the differences between groups. $p < 0.05$ was considered statistically significant.

RESULTS

The Main Components Analysis of Active Fractions From Natural Plants

The anti-proliferation effect of fractions from four traditional natural plants, *Reynoutria japonica Houtt (RJH), Tripterygium Wilfordii (TPW), Rhizoma Paridis (RP),* and *Curcuma longa L. (CLL),* were first examined by MTT assay to screen active factions. As shown in **Figure 1A**, five fractions (chloroform extraction and ethyl acetate extraction from *Tripterygium Wilfordii and Rhizoma Paridis* (TPW-C, TPW-EA, RP-C, and RP-EA) and chloroform extraction from *Curcuma longa L.*(CLL-C)) showed a proliferation inhibitory ratio of more than 40% compared with the control group (**Figure 1A**). In these active fractions, RP-EA exhibited an evident induction of TIPE2 protein expression in comparison with the control group (**Figure 1B**), implying that some active compounds with the potential to induce TIPE2 expression and inhibit gastric tumor cell proliferation could exist in ethyl acetate extraction from *Rhizoma Paridis*. To identify the active compounds, high-performance liquid chromatography (HPLC) and mass spectroscopy were employed to separate and characterize the

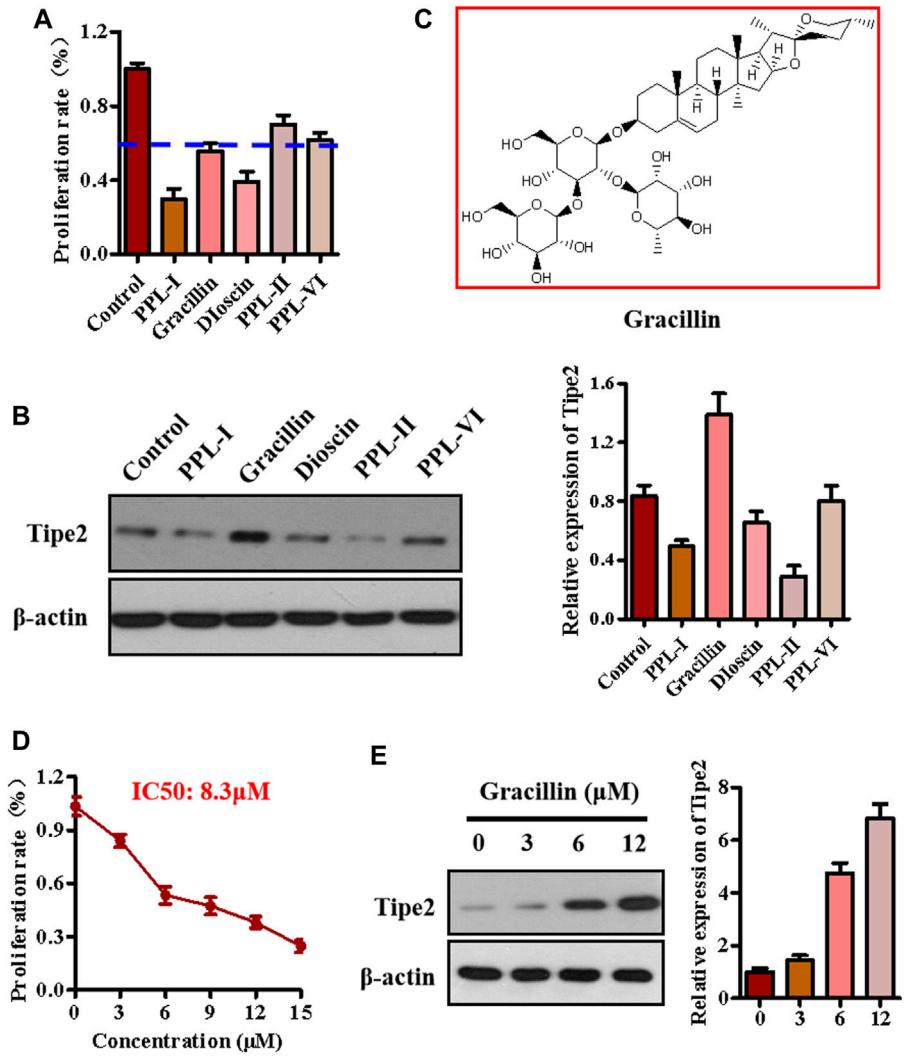

FIGURE 2 | The effect of gracillin on TIPE2 expression and cell proliferation in BGC-823 cells. **(A)** The effect of five active compounds on cell proliferation. 5 μM active compounds were used to treat the BGC823 cells for 48 h. **(B)** The effect of five active compounds on TIPE2 expression. 5 μM active compounds were used to treat the BGC823 cells for 12 h. **(C)** The structure of gracillin. **(D)** The effect of gracillin at different concentrations on cell proliferation. The different concentrations of gracillin with 3, 6, 9, 12, 15 μM were used to treat the BGC823 cells for 12 h. **(E)** The effect of gracillin with the indicated concentrations for 12 h on TIPE2 expression. The values of the histogram are displayed as mean ± SD.

main components of RP-EA extraction. Five obvious peaks detected by HPLC chromatography were identified as polyphyllin II (PPL-II), dioscin, gracillin, polyphyllin I (PPL-I), and polyphyllin VI (PPL-VI) using mass spectroscopy (**Supplementary Figures S1–S6**).

Identifying Gracillin as a Tumor Necrosis Factor-α Inducible Protein-8 Inducer With Potential Suppressing Cell Proliferation in Gastric Cancer BGC823 Cells

The above experiments identified five main components from the chloroform extraction of *Rhizoma Paridis*. We next screened the active compound with the highest potential for regulating TIPE2 and gastric carcinoma from these main components via MTT and immunoblotting. MTT assay showed that polyphyllin I, gracillin, and dioscin exhibited lower cellular proliferation ratio (lower than 60 versus 100% of the control group, **Figure 2A**), meanwhile, immunoblotting indicated that gracillin had an obvious induction of TIPE2 expression in BGC823 cells (**Figure 2B**), demonstrating that gracillin could be a TIPE2 inducer suppressing gastric tumor cell proliferation. The structure of gracillin was shown in **Figure 2C**. In addition, gracillin concentration-dependently inhibited the gastric tumor BGC823 cell proliferation with IC50 value of 8.3 μM in the range of 0–15 μM (**Figure 2D**) and gastric tumor SGC7901 cell proliferation with IC50 value of 8.9 μM in the range of 0–15 Mm (**Supplementary Figure S7**). TIPE2 expression tests also showed that gracillin exhibited a

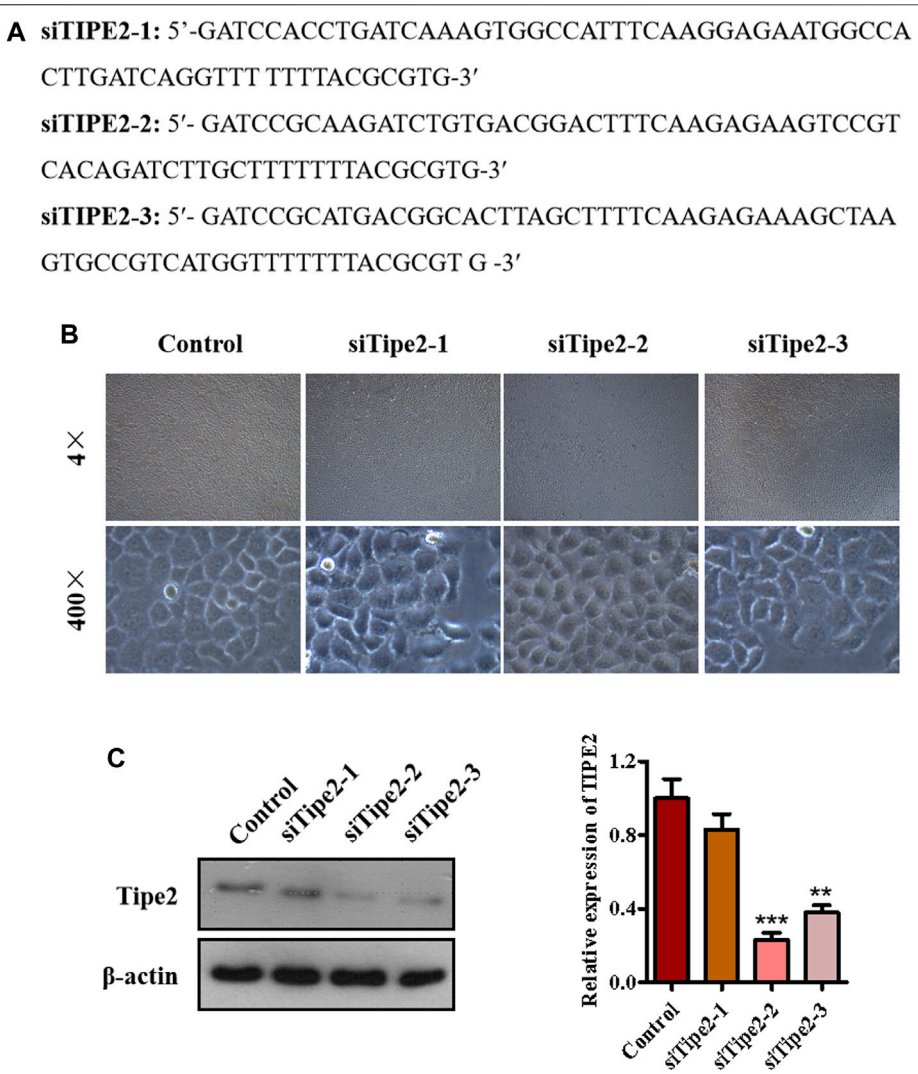

FIGURE 3 | The establishment of TIPE2-silence cell line BGC823/TIPE2−/−. **(A)** The sequence of siTIPE2 RNA. **(B)** The effect of siTIPE2 RNA on BGC-823 cells. **(C)** The effect of siTIPE2 RNA on TIPE2 expression. The values of the histogram are displayed as mean ± SD, $0.001 < p < 0.01$ (**) represented for very significant difference and $p < 0.001$ (***) represents an extremely significant difference to the normal control.

concentration-dependent TIPE2 induction in 3, 6, and 12 μM (**Figure 2E** and **Supplementary Figure S10**).

Establishment of Tumor Necrosis Factor-α Inducible Protein-8-Silence Cell Line BGC823/Tumor Necrosis Factor-α Inducible Protein-8$^{-/-}$

To explore the role of TIPE2 in gracillin suppression of gastric tumors, we synthesized three fragments of TIPE2 siRNA sequence, which were respectively siTIPE2-1, siTIPE2-2, and siTIPE2-3 (**Figure 3A**). The fragments were transfected into BGC823 gastric tumor cells and **Figure 3B** shows the BGC823 and BGC823/TIPE2$^{-/-}$ cellular images of TIPE2 siRNAs transfection for 36 h. The transfection efficiency was evaluated by immunoblotting. As displayed in **Figure 3C**, siTIPE2-2 and siTIPE2-3 inhibited the expression of TIPE2 in BGC823. Furthermore, siTIPE2-2 was more efficient compared with siTIPE2-3. Therefore, we choose siTIPE2-2 as a tool for suppressing TIPE2 expression to illustrate the role of TIPE2 in gracillin suppression of gastric tumors.

Effects of Gracillin on Cellular Proliferation via Tumor Necrosis Factor-α Inducible Protein-8 in BGC823 Cells

To confirm whether TIPE2 participated in gracillin inhibition of gastric tumor cellular growth, the BGC823 and BGC823/TIPE2$^{-/-}$ cellular viability in the administration of gracillin (5 μM) were first examined using MTT assay. As seen in

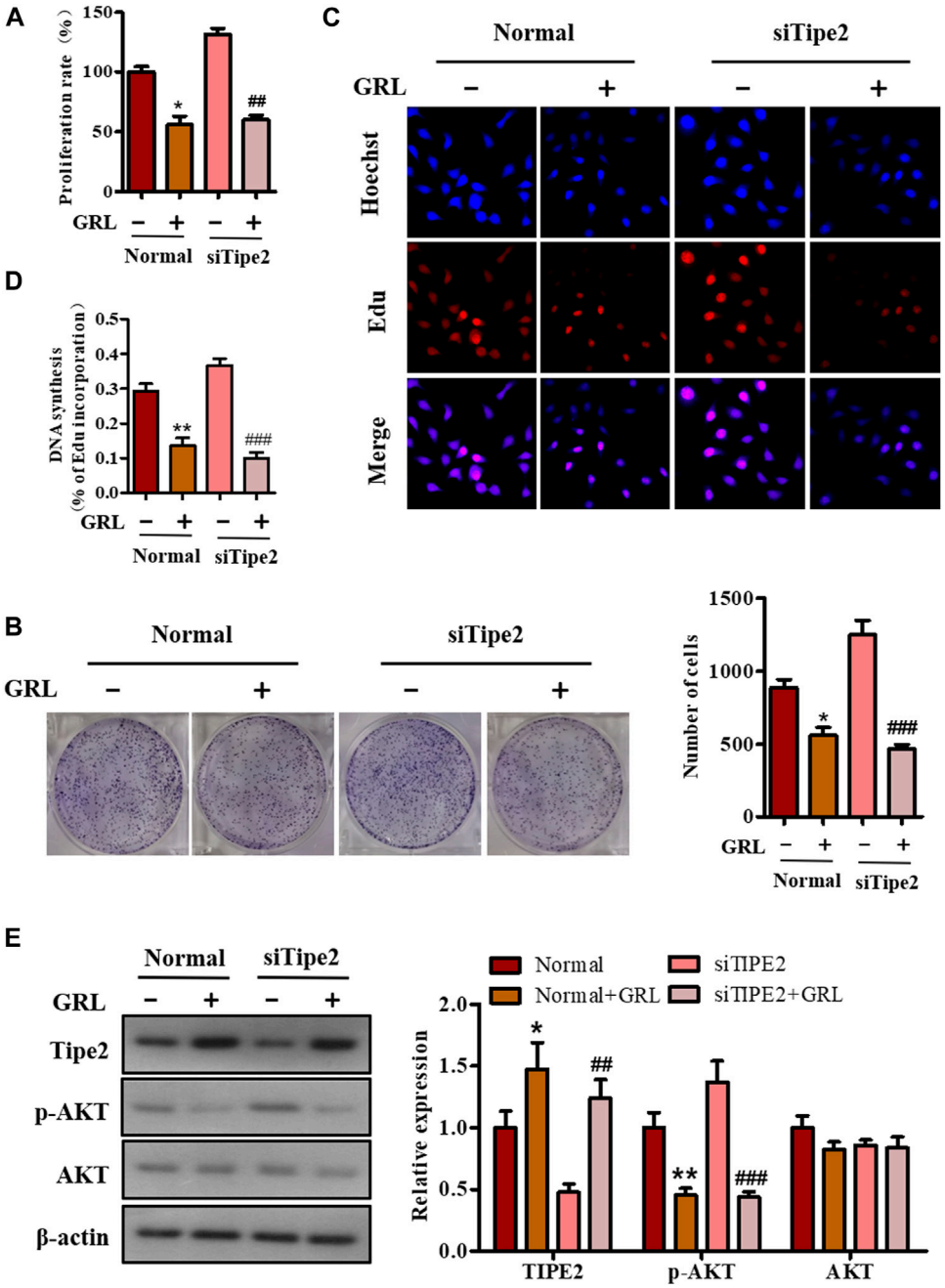

FIGURE 4 | The role of TIPE2 in cell proliferation mediated by gracillin in BGC823 cells. **(A)** MTT assay for cell proliferation by TIPE2 and gracillin. 5 μM gracillin was used to treat the BGC823 cells and TIPE2 siRNA BGC823 cells for 48 h. **(B)** Colony formation for cell proliferation by TIPE2 and gracillin. 5 μM gracillin was used to treat the BGC823 cells and TIPE2 siRNA BGC823 cells for 7 days. **(C)** EdU staining for cell proliferation by TIPE2 and gracillin. 5 μM gracillin was used to treat the BGC823 cells and TIPE2 siRNA BGC823 cells for 12 h. **(D)** The quantitative analysis for EdU staining. **(E)** Western blot for the expression of TIPE2, AKT, and p-AKT. The values of the histogram are displayed as mean ± SD. $0.01 < p < 0.05$ (*) represents a significant difference and $0.001 < p < 0.01$ (**) represents a very significant difference to the normal control; $0.001 < p < 0.01$ ($^{\#\#}$) represents a very significant difference and $p < 0.001$ ($^{\#\#\#}$) represents an extremely significant difference to the TIPE2 siRNA control.

Figure 4A, 5 μM of gracillin inhibited cell proliferation from 131.6 to 60.0% in BGC823/TIPE2$^{-/-}$ cells, and from 100 to 56.0% in BGC823 cells, demonstrating that the proliferation inhibitory ratio of gracillin with siTIPE2 RNA treatment is higher than that without siTIPE2 RNA treatment (54.4 vs 44.0%) in BGC823 cells. Plate clone formation assay showed that the cellular clone number in BGC823/TIPE2$^{-/-}$ cells subjected to gracillin decreased to 466 from 1,247 in the control group, and in

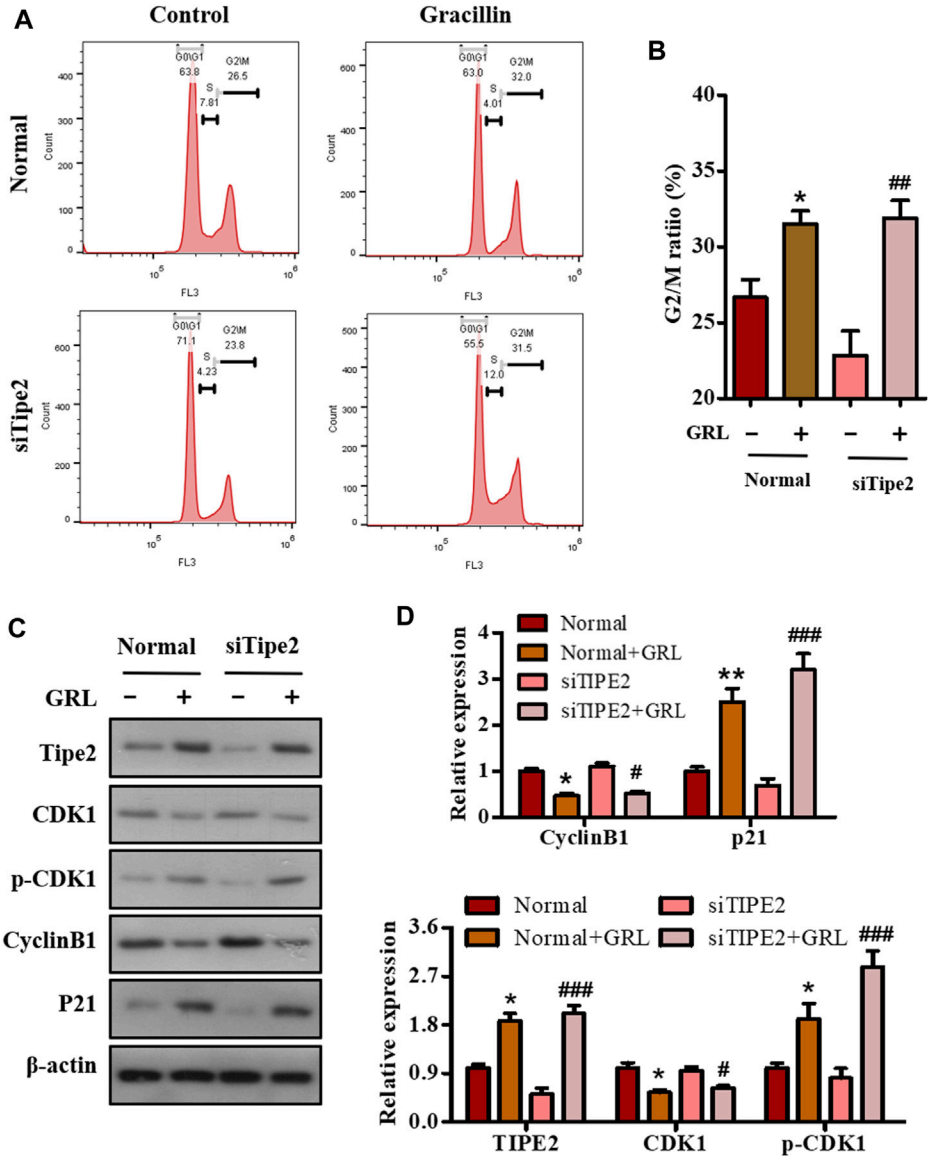

FIGURE 5 | The role of TIPE2 in the cell cycle distribution mediated by gracillin in BGC823 cells. **(A)** Flow cytometry for cell cycle distribution by TIPE2 and gracillin. BGC823 cells and TIPE2 siRNA BGC823 cells were maintained with FBS-free medium for 36 h, then treated with 3 μM gracillin for another 24 h. **(B)** The quantitative analysis of cell cycle distribution by TIPE2 and gracillin. **(C)** Western blot for the expression of TIPE2, CDK1, p-CKD1, cyclin B1, and p21. **(D)** The quantitative analysis of protein expression. The values of the histogram were displayed as mean ± SD. $0.01 < p < 0.05$ (*) represents a significant difference and $0.001 < p < 0.01$ (**) represents a very significant difference to the normal control; $0.01 < p < 0.05$ ($^{\#}$) represents a significant difference, $0.001 < p < 0.01$ ($^{\#\#}$) represents a very significant difference and $p < 0.001$ ($^{\#\#\#}$) represents an extremely significant difference to the TIPE2 siRNA control.

BGC823 cells subjected to gracillin decreased to 557 from 885 (**Figure 4B**), indicating that gracillin more markedly suppressed the cellular clone formation in BGC823/TIPE2$^{-/-}$ cells compared with that in BGC823 cell. EdU-incorporation data revealed the consistent effect that the proportion of incorporated EdU with gracillin treatment presented a more obvious reduction in BGC823/TIPE2$^{-/-}$ cells compared with BGC823 cells (**Figures 4C,D**). Collectively, these results suggested that TIPE2 may participate in gracillin inhibition of cell proliferation in BGC823.

PI3K/AKT is an important signaling pathway involved with cell proliferation and phosphorylation of AKT is an essential molecular event in the process of PI3K/AKT activation. To further confirm whether gracillin inhibited gastric tumor cell proliferation via TIPE2, we conducted western blot assay to detect the AKT phosphorylation in the supplement of gracillin and siTIPE2 RNA in BGC823 cells. The data showed that gracillin more evidently promoted the induction of TIPE2 in BGC823/TIPE2$^{-/-}$ than in BGC823,

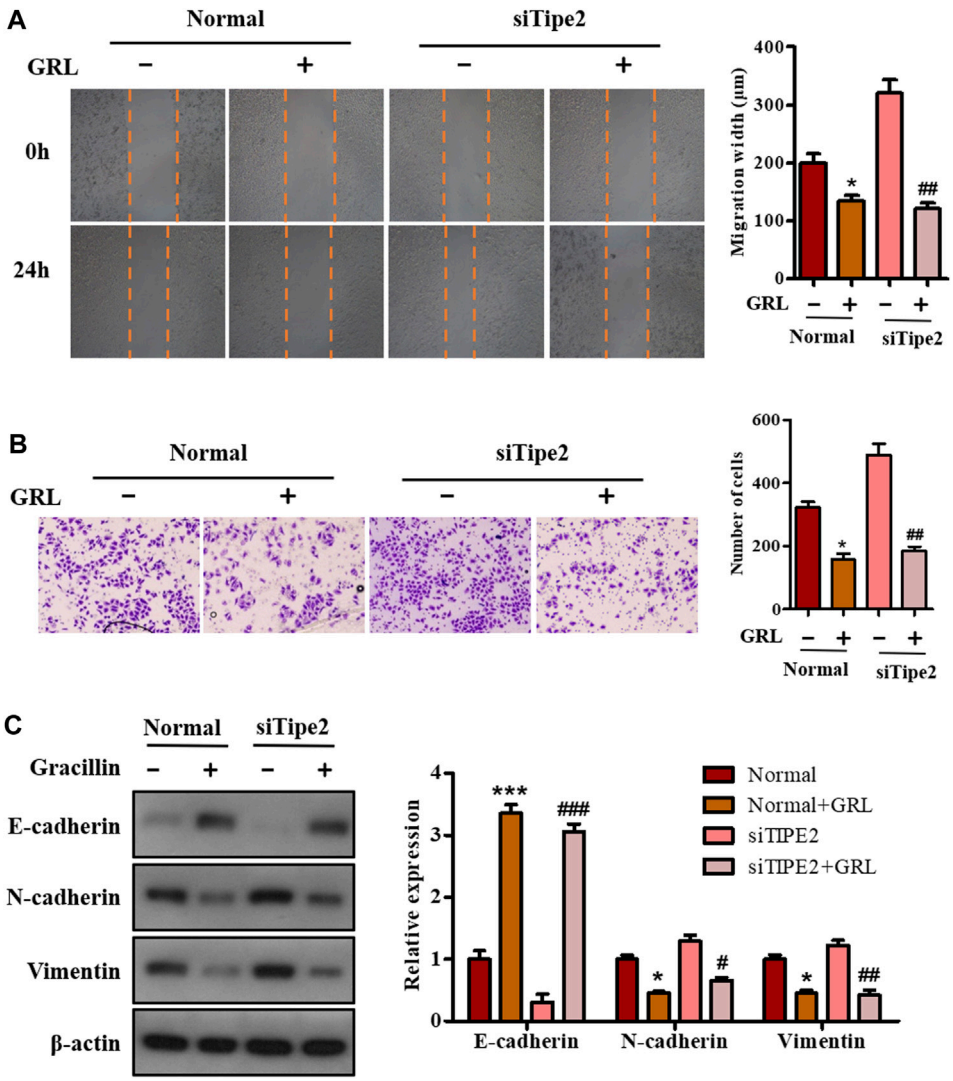

FIGURE 6 | The role of TIPE2 in the cell migration mediated by gracillin in BGC823 cells. **(A)** Scratch assay for cell migration by TIPE2 and gracillin. BGC823 cells and TIPE2 siRNA BGC823 cells were treated with 3 μM gracillin for 24 h. **(B)** Transwell assay for cell migration by TIPE2 and gracillin. **(C)** Western blot for the expression of E-cadherin, N-cadherin, and vimentin. $0.01 < p < 0.05$ (*) represents a significant difference and $p < 0.001$ (***) represents an extremely significant difference to the normal control; $0.01 < p < 0.05$ ($^{\#}$) represents a significant difference, $0.001 < p < 0.01$ ($^{\#\#}$) represents a very significant difference and $p < 0.001$ ($^{\#\#\#}$) represents an extremely significant difference to the TIPE2 siRNA control.

meanwhile, the inhibition effect of AKT phosphorylation by gracillin is stronger in BGC823/TIPE2$^{-/-}$ than that in BGC823 (**Figure 4E**). Thus, TIPE2 maybe contribute to the anti-proliferation effect by gracillin.

Effects of Gracillin on Cell Cycle Arrest via Tumor Necrosis Factor-α Inducible Protein-8 in BGC823 Cells

Deregulation of the cell cycle results in the unlimited proliferation of tumor cells including gastric carcinoma cell BGC823, and controlling the deregulated cell cycle would be a crucial strategy to fight against tumors. To evaluate the association of the cell cycle with cell proliferation mediated by gracillin, BGC823/TIPE2$^{-/-}$ and BGC823 cells with or without gracillin were stained by PI, and the cell cycle distribution was analyzed using flow cytometry. The histogram from flow analysis indicated that gracillin induced the increase of G2/M phase ratio in BGC823 cells, meanwhile, the induction of the G2/M phase ratio by gracilllin was more evident in BGC823/TIPE2$^{-/-}$ cells (**Figures 5A,B**). Moreover, the expression of G2/M phase-associated proteins CDK1, p-CDK1, cyclin B1, and p21 in the supplement of gracillin were detected by western blot. The band graph revealed that gracillin induced the upregulation of TIPE2, p-CDK1, and p21 and downregulation of CDK1 and cyclin B1 in BGC823 cells, meanwhile, these change trends of protein expressions mediated by gracillin were more evident in BGC823/TIPE2$^{-/-}$ cells (**Figures 5C,D**). These results

demonstrated that TIPE2 maybe contribute to the cell cycle G2/M arrest effect induced by gracillin in BGC823 cells, which was consistent with our previous report that TIPE2 blocks the cell cycle G2/M phase (Zhenhe et al., 2018).

Effects of Gracillin on Cellular Migration via Tumor Necrosis Factor-α Inducible Protein-8 in BGC823 Cells

To investigate the effect of gracillin on gastric cell migration and the role of TIPE2 in this effect, scratch-wound assay and transwell assay were performed in BGC823/TIPE2$^{-/-}$ and BGC823 cells. As seen in **Figure 6A**, the migration width of BGC823 cells in the supplement of gracillin for 24 h decreased by 32.2% (from 199 to 135 μm), and BGC823/TIPE2$^{-/-}$ cells displayed a higher fall of migration width of 62.2% (from 320 to 121 μm) induced by gracillin. The data from the transwell assay also revealed that gracillin inhibited the cell migration, which displayed a fall of cell migrations from 321 to 157 in BGC823 cells, while a larger decrease was observed in BGC823/TIPE2$^{-/-}$ cell. Additionally, the expression of EMT pathway-related proteins was detected by western blot to study the molecular mechanism by which TIPE2 mediates cell migration in gracillin. **Figure 6C** shows that gracillin induced the upregulation of E-cadherin and downregulation of N-cadherin and vimentin in BGC823 cells, and these trends maintain a similar level in BGC823/TIPE2$^{-/-}$ cells. Taken together, these results demonstrate that gracillin could inhibit the cell migration via the EMT pathway in BGC823 cells and TIPE2 maybe contribute to the inhibitory effect of gracillin.

Effects of Gracillin on Cellular Apoptosis via Tumor Necrosis Factor-α Inducible Protein-8 in BGC823 Cells

Sustained proliferation and resistance to cell apoptosis are two major hallmarks of cancer. The above-mentioned data have shown that gracillin could fight against gastric cancer via TIPE2-regulation of cell proliferation. We performed flow cytometry, enzyme activity tests, and western blot assay to study the apoptotic effect of gracillin via TIPE2 in BGC823 cells. Scatter diagrams flow cytometry showed that the apoptosis ratio of BGC823 cells supplied with gracillin increased from 3.11 to 32.24% while BGC823/TIPE2$^{-/-}$ cells displayed a similar change trend (**Figures 7A,B**). Enzyme activity tests (**Figure 7C**) revealed that gracillin induced the enzyme activities of caspase three and nine in BGC823 cells and BGC823/TIPE2$^{-/-}$ cells, and that caspase9 activity displayed a more obvious induction in BGC823/TIPE2$^{-/-}$ cells than that in BGC823 cells. Western blot (**Figure 7D**) showed that gracillin induced the cleavage of PARP, caspase3, and caspase9, and the inhibition of bcl-2 expression in BGC823 cells, furthermore, the regulation by gracillin in BGC823/TIPE2$^{-/-}$ cells were more statistically significant. These results demonstrate that TIPE2 maybe contribute to the pro-apoptosis effect of gracillin in BGC823 cells.

Effects of Gracillin on Gastric Tumor and Tumor Necrosis Factor-α Inducible Protein-8 Expression *in vivo*

To determine the anti-tumor effect of gracillin *in vivo*, a xenograft tumor model of nude mice bearing BGC823 cells was established and gracillin was administrated. As seen in **Figure 8A**, the tumor size of mice treated with gracillin began to fall compared to that of mice in the control group from the 12th day and reached a great significant difference at the end of the 21st day ($^{**}p < 0.01$ compared to the control group). The curve of body weight showed that the mice that received gracillin had no statistical change of body weight compared with that in the control group. The tumor images and weight on the 21st day of gracillin administration revealed that gracillin suppressed the tumor size and tumor weight ($^{**}p < 0.01$ compared to the control group, **Figure 8C**). The immunohistochemistry test revealed that gracillin greatly inhibited the expression of Ki67 in the mice tumor tissue ($^{***}p < 0.001$ compared to the control group, **Figures 8D–F**). Additionally, western blot data (**Figures 8G,H**) showed that gracillin induced the cleavage of PARP and expression of TIPE2, and inhibited the phosphorylation of AKT and expression of bcl-2 in the tumor tissue of mice. Together, these results demonstrated that gracillin could inhibit tumors via TIPE2-mediation of proliferation and apoptosis.

DISCUSSION

Gastric cancer has been a serious threat to human life and health for several decades, which has promoted the identification of new therapeutic targets and the development of novel therapeutic agents for gastric cancer. TIPE2 protein was first identified only a few years ago, and since then a great deal of evidence has indicated that TIPE2 plays a crucial role in suppressing gastric cancer. Like other cancer cells, gastric cancer cells are characterized by sustained proliferative signaling, evasion of growth suppressors, activate invasion and metastasis, resistance to cell death, and so on (Douglas and Robert, 2011). The expression of TIPE2 could control these defects of gastric cancer cells. It had been verified that TIPE2 could suppress cell growth and proliferation by inducing the inhibition of the AKT and ERK1/2 pathways and promoting the p27-associated signal cascade in gastric cancer cells (Qian et al., 2015). Biochemical molecular analysis revealed that TIPE2 could reduce the activation of RAC1 and MMP9 by binding to RAC1, thereby suppressing gastric cancer cell metastasis (Xuelei et al., 2013). Also, TIPE2 is reported to elicit cell apoptosis by activating caspase three and caspase 9, inducing the cleavage of PARP, and inhibiting bcl-2 expression in BGC-823 gastric cancer cells. This information demonstrates that TIPE2 could be a novel and extremely potent gastric cancer target that suppresses gastric cancer through mediating multiple molecular pathways in patients with gastric tumors. However, it has not been well reported that several medicinal agents could regulate TIPE2 to fight against diseases such as gastric cancer. Therefore, the

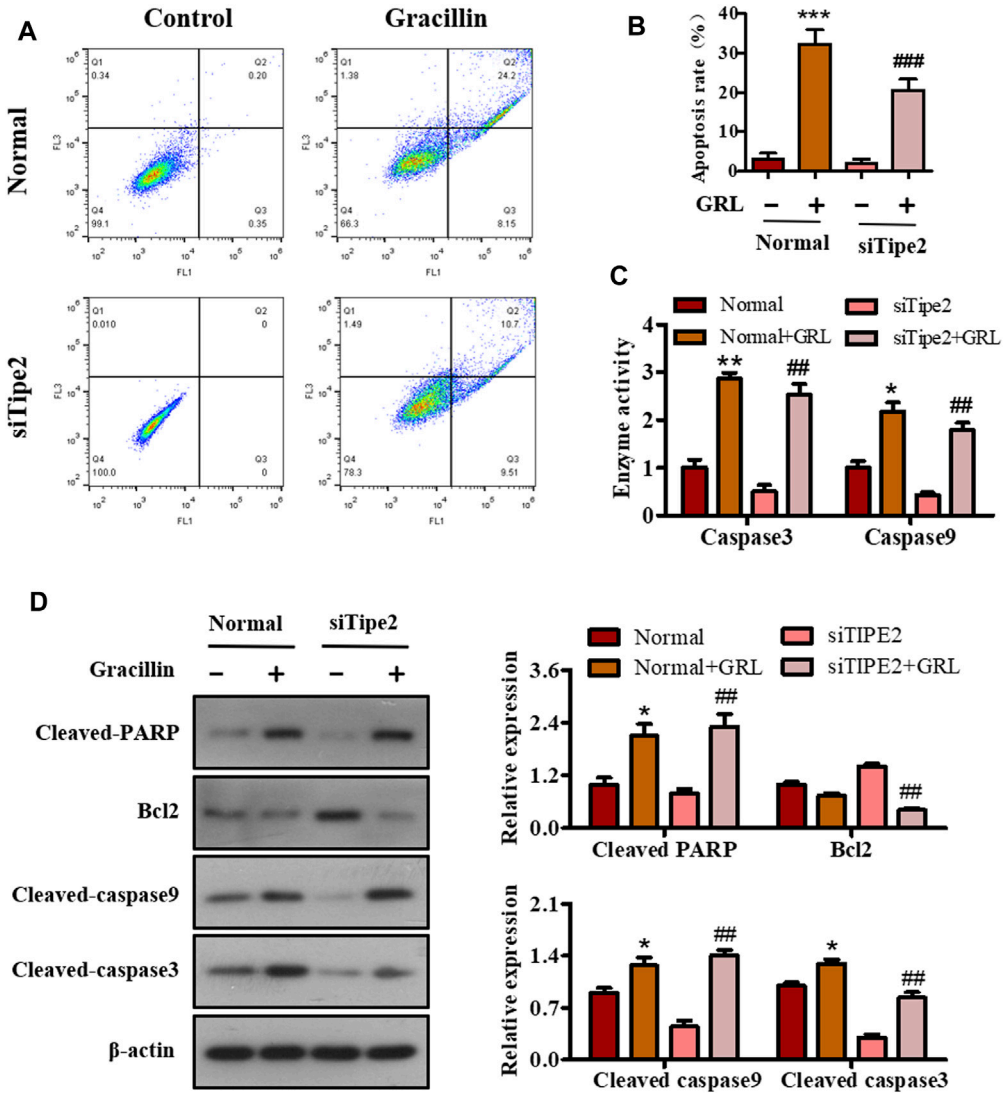

FIGURE 7 | The role of TIPE2 in the cell apoptosis mediated by gracillin in BGC823 cells. **(A)** Flow cytometer for cell apoptosis by TIPE2 and gracillin. BGC823 cells and TIPE2 siRNA BGC823 cells were treated with 3 μM gracillin for 24 h. **(B)** The quantitative analysis of cell apoptosis. **(C)** Elisa assay for the enzyme activities of caspase three and caspase 9. **(D)** Western blot for the expression of cleaved PARP, bcl2, cleaved caspase 9, and cleaved caspase 3. $0.01 < p < 0.05$ (*) represents a significant difference, $0.001 < p < 0.001$ (**) represents a very significant difference and $p < 0.001$ (***) represents an extremely significant difference to the normal control; $0.01 < p < 0.05$ ($^{\#}$) represents a significant difference, $0.001 < p < 0.01$ ($^{\#\#}$) represents a very significant difference and $p < 0.001$ ($^{\#\#\#}$) represents an extremely significant difference to the TIPE2 siRNA control.

development of a TIPE2 regulator that suppresses gastric cancer and clarifying its function would be encouraging for the clinical treatment of gastric cancer and is urgently needed.

Natural products are generally complex multi-ingredient systems and contain a great deal of different and remarkably similar structural compounds that have contributed to the majority of modern medicinal agents. However, these natural compounds were seldom reported to mediate TIPE2 and explore its medicinal value. In the present study, we employed four traditional natural plants with anti-tumor effects, respectively *Curcuma longa L., Tripterygium Wilfordii, Rhizoma Paridis,* and *Reynoutria japonica Houtt*, to screen the TIPE2 regulator fighting against gastric cancer in BGC823 cells, and found that the ethyl acetate extraction of *Rhizoma Paridis* exerted the induction of TIPE2 expression and inhibition of cellular proliferation. *Rhizoma Paridis* is a plant that generally grows in southwest China, and has been widely applied to prevent and treat chronic diseases including cancer as a traditional Chinese medicine with heat-clearing and detoxifying properties. Its numerous active ingredients have also been reported to exert multiple anti-cancer effects, eg. pennogenyl saponins for inhibiting the growth of hepatoma, dioscin for suppressing osteosarcoma via inducing cell cycle arrest and apoptosis, and polyphyllin II for relieving bladder cancer migration. However, the underlying anti-

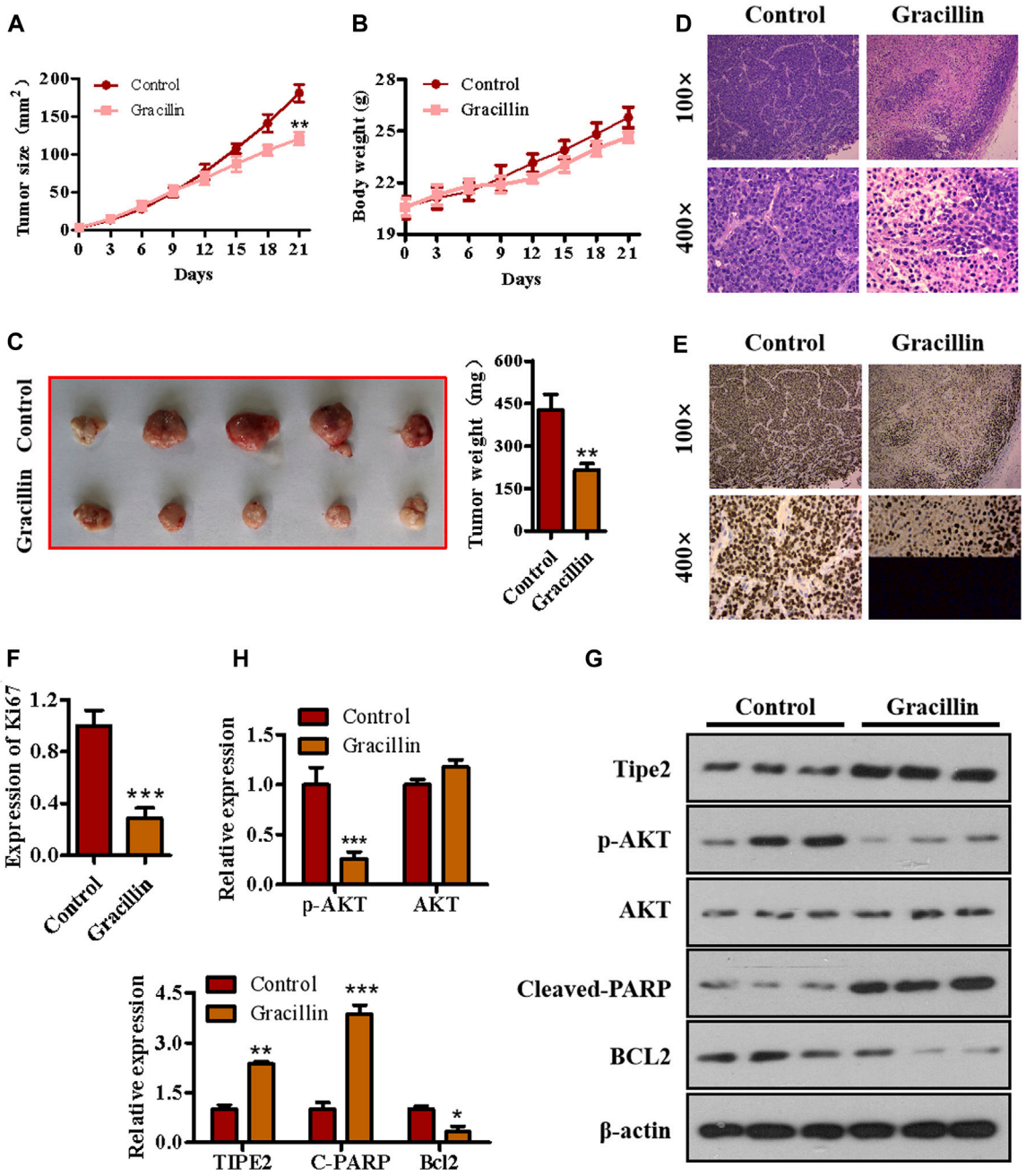

FIGURE 8 | The effect of gracillin on gastric tumor and TIPE2 expression *in vivo*. **(A)** The growth curve of tumors. **(B)** The curve of body weight. **(C)** The tumor images. **(D)** HE stain for tumor pathology. **(E)** IHC assay for ki67 expression in tumors. **(F)** The quantitative analysis of ki67 expression. **(G)** Western blot for the expression of TIPE2, p-AKT, AKT, cleaved PARP, and bcl2 in tumor tissue. **(H)** The quantitative analysis of protein expression as detected by western blot. $0.01 < p < 0.05$ (*) represents a significant difference, $0.001 < p < 0.001$ (**) represents a very significant difference and $p < 0.001$ (***) represents an extremely significant difference to the normal control.

cancer mechanism of these active ingredients from *Rhizoma Paridis* remains unclear. In this context, we analyzed the active compounds based on bioassay-guided isolation combining with the reported ingredient information of *Rhizoma Paridis* and evaluated the underlying target and mechanism of the active compound fighting against gastric cancer. We identified gracillin as a TIPE2 inducer from *Rhizoma Paridis* and elucidated the potential mechanism by which gracillin alleviates gastric carcinoma via TIPE2-mediated inhibition of proliferation, induction of endogenous apoptosis, and suppression of migration (**Figure 9**). Our findings laid a theoretical understanding of the underlying mechanism and function of

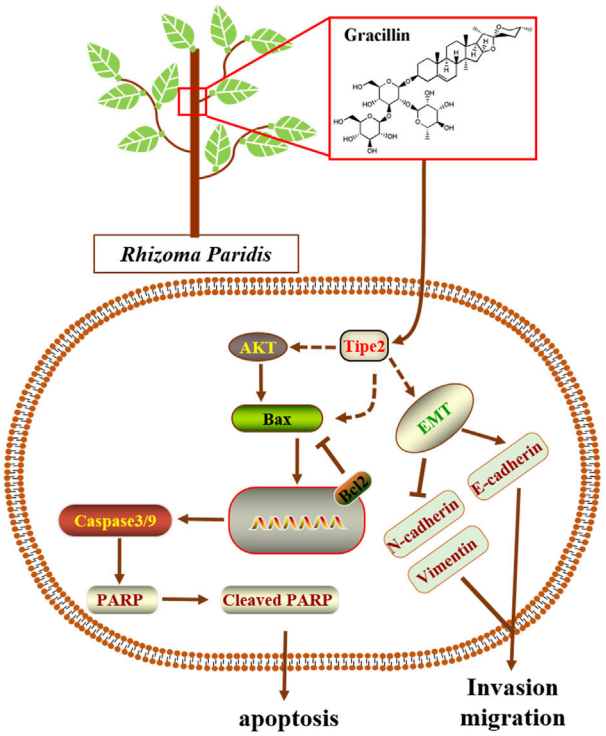

FIGURE 9 | Scheme summarizing the mechanism of gracillin suppress gastric cancer via TIPE2.

Rhizoma Paridis and provided an important insight for the modern medicinal development of *Rhizoma Paridis*.

Sustained proliferation is considered as a primary characteristic of malignant tumor cells differing from the restricted proliferation of normal cells. AKT, also named protein kinase B (PKB), is an important part of the PI3K/AKT/mTOR pathway and its phosphorylation is a sign of the pathway activation which exerts a vital effect on cell proliferation, including of malignant cells. Our previous findings revealed that TIPE2 expression was negatively associated with gastric cell proliferation, and that it could suppress cell proliferation by reducing phosphorylation of AKT. In the present study, we found that gracillin inhibited AKT phosphorylation and cell proliferation in gastric cancer BGC-823 cells, and in the absence of TIPE2, gracillin exhibited a more obvious induction of TIPE2 expression and inhibition of AKT phosphorylation, demonstrating that gracillin maybe inhibit the gastric cancer cells via TIPE2-mediated AKT phosphorylation. Additionally, cell cycle progression on the rails is recognized to be crucial to maintaining normal cell proliferation, and its dysfunction and un-limitation contribute to the development of malignant tumor cells. Our previous data revealed that TIPE2 overexpression could cause G2/M phase cell cycle arrest and regulate the expression of CDK1, phosphorylated CDK1, cyclin B1, and p21, and in the present study, gracillin also displayed a similar effect on cell cycle with TIPE2 overexpression. Together, these results confirmed that gracillin could inhibit gastric cancer cell proliferation via AKT phosphorylation and cell cycle distribution, which may be associated with TIPE2 expression.

Tumor metastasis is a typical and fatal symptom of advanced cancer, which contributes to approximately 90% of cancer-related deaths. During the process of tumor metastasis, malignant tumor cells begin to migrate via the epithelial-mesenchymal transition process (EMT), spread to the patient's organs, and finally threaten the patient's life. The EMT process is usually characterized by high expression of N-cadherin and vimentin and low expression of E-cadherin. Recent evidence has revealed that TIPE2 could suppress the migration of tumor cells by promoting the induction of E-cadherin expression and inhibition of N-cadherin and vimentin expression. Our present data show that gracillin suppresses the migration of gastric cancer BGC-823 cells, and that TIPE2 partly participated in this effect. Furthermore, gracillin induced the expression of E-cadherin and inhibited the expression of N-cadherin and vimentin, and cells treated with TIPE2 siRNA displayed a more obvious regulation effect of gracillin on E-cadherin and vimentin expression. These results reveal that gracillin possesses the potential to suppress tumor cell migration via the EMT process in BGC-823 cells, which may be associated with TIPE2 expression.

Additionally, cell apoptosis is recognized as a process of programmed cell death that maintains physiological homeostasis by clearing away the dysfunctional and valueless cells. However, the resistance to apoptosis is a classic characteristic of malignant tumor development. Hence, reducing the resistance to apoptosis would be an important strategy for fighting tumors. Bcl2, an antiapoptotic protein found in mitochondria, plays an important role in determining the occurrence of apoptosis and regulating tumor progression. Several previous reports revealed that TIPE2 could inhibit the expression of bcl2 and suppress mitochondrial apoptosis as a tumor suppressor in gastric cancer cells and other tumor cells. This information implied that the effects of gracillin fighting against gastric cancer were also associated with TIPE2-mediation of mitochondrial apoptosis. We investigated this issue and confirmed that gracillin could promote cell apoptosis and suppress the expression of bcl2, and that the effect of gracillin was statistically more significant in the absence of TIPE2. These results demonstrated that TIPE2-mediation of mitochondrial apoptosis may also be a way that gracillin suppresses gastric cancer. Of course, the role of mitochondria needs to be elucidated in future research, to better understand the pro-apoptotic effect of gracillin.

Overall, the present study has identified gracillin as a TIPE2 inducer that can fight against gastric carcinoma, which was extracted from the medicinal plant *Rhizoma Paridis* following bioassay-guided isolation. Furthermore, we elucidated the mechanism of gracillin's benefits against gastric carcinoma: that gracillin inhibits cell proliferation involving the PI3K/AKT pathway and cell cycle arrest, suppresses the EMT pathway to regulate cell migration, and induces bcl2-associated mitochondrial apoptosis. Moreover, we confirmed the role of TIPE2 in these effects. These findings regarding the benefits and mechanism of gracillin isolated from *Rhizoma Paridis* will be beneficial to the modern medicinal development of *Rhizoma*

Paridis and gracillin, and it is also interesting to understand the role of TIPE2 in gastric carcinoma. Of course, several issues regarding how gracillin regulates TIPE2 and the more precise mechanism of TIPE2 in gastric carcinoma remain obscure. Our laboratory will continue to explore these issues, and some of this work is already underway.

DATA AVAILABILITY STATEMENT

The raw data supporting the conclusions of this article will be made available by the authors, without undue reservation.

ETHICS STATEMENT

The animal study was reviewed and approved by The Animal Care and Use Committee of Xiamen University.

AUTHOR CONTRIBUTIONS

Conceptualization, YF, XL, and WL; Methodology and Investigation, WL, YW, JC, ZL, and ML; Writing, YF, XL, and WL.

FUNDING

The present study was supported by the Medical Health Science and Technology Project of Xiamen (3502Z20194020) and the Health Science Foundation of Fujian Youth Program (2019-2-49).

SUPPLEMENTARY MATERIAL

The Supplementary Material for this article can be found online at: https://www.frontiersin.org/articles/10.3389/fphar.2021.669199/full#supplementary-material

REFERENCES

Amit, K., and Vikas, J. (2019). Natural Products as Multidrug Resistance Modulators in Cancer. *Eur. J. Med. Chem.* 176, 268–291. doi:10.1016/j.ejmech.2019.05.027

Antonia, D., and Wagner, A. D. (2016). Advanced Gastric Cancer: Current Treatment Landscape and Future Perspectives. *World J. Gastroenterol.* 22 (8), 2403–2414. doi:10.3748/wjg.v22.i8.2403

Camilla, M., and Giuseppe, L. (2020). Cancer Statistics: a Comparison between World Health Organization (WHO) and Global Burden of Disease (GBD). *Eur. J. Public Health* 30 (5), 1026–1027. doi:10.1093/eurpub/ckz216

Daniel, A. A., Sylvia, U., and Ute, R. (2012). A Historical Overview of Natural Products in Drug Discovery. *Metabolites* 2 (2), 303–336. doi:10.3390/metabo2020303

David, J. N., and Gordon, M. C. (2016). Natural Products as Sources of New Drugs from 1981 to 2014. *J. Nat. Prod.* 79 (3), 629–661. doi:10.1021/acs.jnatprod.5b01055

Douglas, H., and Robert, A. W. (2011). Hallmarks of Cancer: the Next Generation. *Cell* 144 (5), 646–674. doi:10.1016/j.cell.2011.02.013

Elizabeth, C. S., Magnus, N., Heike, I. G., van Grieken, N. C., and Florian, L. (2020). Gastric Cancer. *Lancet* 396 (10251), 635–648. doi:10.1016/S0140-6736(20)31288-5

Emma, K. D., and Margaret, A. B. (2019). Natural Product Derived Privileged Scaffolds in Drug Discovery. *Curr. Opin. Chem. Biol.* 52, 1–8. doi:10.1016/j.cbpa.2018.12.007

Eric, C. F., Nicolas, B., and Michael, J. L. (2008). A Different TIPE of Immune Homeostasis. *Cell* 133 (3), 401–402. doi:10.1016/j.cell.2008.04.017

Ganesan, P., Kishore, B., Javadi, M., Devivasha, B., Bano, S., Frank, A., et al. (2018). Novel Tumor Necrosis Factor-α Induced Protein Eight (TNFAIP8/TIPE) Family: Functions and Downstream Targets Involved in Cancer Progression. *Cancer Lett.* 432, 260–271. doi:10.1016/j.canlet.2018.06.017

Helge, L. W., and Reidar, F. (2018). Types of Gastric Carcinomas. *Int. J. Mol. Sci.* 19 (12), 4109. doi:10.3390/ijms19124109

Honghong, S., Shunyou, G., Ruaidhri, J. C., Anja, H., Li, L., Jing, S., et al. (2008). TIPE2, a Negative Regulator of Innate and Adaptive Immunity that Maintains Immune Homeostasis. *Cell* 133 (3), 415–426. doi:10.1016/j.cell.2008.03.026

Jie, W., Haitao, Z., Chun, X., Hong, X., Xiumin, Z., Yufeng, X., et al. (2016). TIPE2 Functions as a Metastasis Suppressor via Negatively Regulating β-catenin through Activating GSK3β in Gastric Cancer. *Int. J. Oncol.* 48 (1), 199–206. doi:10.3892/ijo.2015.3224

Li, R., Hou, Y., Huang, J., Pan, W., Ma, Q., Shi, Y., et al. (2020). Lianhuaqingwen Exerts Anti-viral and Anti-inflammatory Activity against Novel Coronavirus (SARS-CoV-2). *Pharmacol. Res.* 156, 104761. doi:10.1016/j.phrs.2020.104761

Mary, O., Gregory, M., Barbara, R., and Anthony, O. (2020). Gastrointestinal Side Effects of Cancer Treatments. *Ther. Adv. Chronic Dis.* 11, 2040622320970354. doi:10.1177/2040622320970354

Min, Yuen. T., Dana, E. R., and Philip, K. (2019). Treatment of Advanced Prostate Cancer. *Annu. Rev. Med.* 70, 479–499. doi:10.1146/annurev-med-051517-011947

Ming, L., Ya, G., Yuan, Y., Kelu, Y., Shuzhen, S., Jinhui, T., et al. (2021). Efficacy and Safety of Herbal Medicine (Lianhuaqingwen) for Treating COVID-19: A Systematic Review and Meta-Analysis. *Integr. Med. Res.* 10 (1), 100644. doi:10.1016/j.imr.2020.100644

Nalinie, J-H., Kai, K. S., and Khurum, K. (2020). Challenges in the Treatment of Gastric Cancer in the Older Patient. *Cancer Treat. Rev.* 85, 101980. doi:10.1016/j.ctrv.2020.101980

Qian, Z., Min, Z., Tianyi, D., Chengjun, Z., Yanping, P., Xiangyu, Z., et al. (2015). Tumor Necrosis Factor-α-Induced Protein-8 Like-2 (TIPE2) Upregulates P27 to Decrease Gastric Cancer Cell Proliferation. *J. Cell Biochem.* 116 (6), 1121–1129. doi:10.1002/jcb.25068

Rui, -M. F., Yi, -N. Z., Su, -M. C., and Rui, -H. X. (2019). Current Cancer Situation in China: Good or Bad News from the 2018 Global Cancer Statistics? *Cancer Commun. (Lond).* 39 (1), 22. doi:10.1186/s40880-019-0368-6

Schinzari, G., Cassano, A., Orlandi, A., Basso, M., and Barone, C. (2014). Targeted Therapy in Advanced Gastric Carcinoma: the Future Is Beginning. *Curr. Med. Chem.* 21 (8), 1026–1038. doi:10.2174/09298673216661311290124054

Sung, H., Ferlay, J., Siegel, R. L., Laversanne, M., Soerjomataram, I., Jemal, A., et al. (2021). Global Cancer Statistics 2020: GLOBOCAN Estimates of Incidence and Mortality Worldwide for 36 Cancers in 185 Countries. *CA A. Cancer J. Clin.* 71, 209–249. doi:10.3322/caac.21660

Tai, R., Zhirong, T., Jingbo, P., Ying, G., Yao, C., Honghao, Z., et al. (2019). The Pharmacogenetics of Natural Products: A Pharmacokinetic and Pharmacodynamic Perspective. *Pharmacol. Res.* 146, 104283. doi:10.1016/j.phrs.2019.104283

Tohid, H., Saeid, G., and Leila, K. (2019). Curcumin and Gastric Cancer: a Review on Mechanisms of Action. *J. Gastrointest. Cancer* 50 (2), 185–192. doi:10.1007/s12029-018-00186-6

Tony, N., Robert, J. K., Scott, M. L., Katherine, V. F-G., Suzanne, B., Melinda, G. H., et al. (2020). Clinical Evolution of Epithelial-Mesenchymal Transition in Human Carcinomas. *Cancer Res.* 80 (2), 304–318. doi:10.1158/0008-5472.CAN-18-3539

Wenming, L., Yanyun, F., Ying, S., Zhenhe, L., Xiaoxiao, H., Wei, H., et al. (2018). Knockdown of TIPE2 Increases the Proliferation in Lipopolysaccharide-Stimulated Gastric Cancer Cells. *BMC Cancer* 18 (1), 857. doi:10.1186/s12885-018-4761-3

Xuanmei, H., Zhijie, Y., Qing, X., Zikang, Z., Hua, Z., and Junying, M. (2019). Natural Products for Treating Colorectal Cancer: A Mechanistic Review. *Biomed. Pharmacother.* 117, 109142. doi:10.1016/j.biopha.2019.109142

Xuelei, C., Li, Z., Yongyu, S., Yue, S., Shen, D., Chun, G., et al. (2013). Human Tumor Necrosis Factor (TNF)-alpha-induced Protein 8-like 2 Suppresses Hepatocellular Carcinoma Metastasis through Inhibiting Rac1. *Mol. Cancer* 12 (1), 149. doi:10.1186/1476-4598-12-149

Yong, Q. L., Xiao, L. W., Dan, H. H., and Cheng, Y-X. (2021). Protection against Chemotherapy- and Radiotherapy-Induced Side Effects: A Review Based on the Mechanisms and Therapeutic Opportunities of Phytochemicals. *Phytomedicine* 80, 153402. doi:10.1016/j.phymed.2020.153402

Yoshiki, M. (2020). Gastric-type Mucinous Carcinoma of the Cervix and its Precursors - Historical Overview. *Histopathology* 76 (1), 102–111. doi:10.1111/his.13993

Zhenhe, L., Wenming, L., Chuanxing, X., Yanyun, F., Guohong, Z., and Zhongquan, Q. (2018). TIPE2 Inhibits GC via Regulation of Cell Proliferation, Apoptosis and Inflammation. *Oncol. Rep.* 40 (3), 1307–1316. doi:10.3892/or.2018.6576

Conflict of Interest: The authors declare that the research was conducted in the absence of any commercial or financial relationships that could be construed as a potential conflict of interest.

Publisher's Note: All claims expressed in this article are solely those of the authors and do not necessarily represent those of their affiliated organizations, or those of the publisher, the editors, and the reviewers. Any product that may be evaluated in this article, or claim that may be made by its manufacturer, is not guaranteed or endorsed by the publisher.

frontiers in Oncology

REVIEW
published: 04 October 2021
doi: 10.3389/fonc.2021.710061

Targeting the Tumor Extracellular Matrix by the Natural Molecule 4-Methylumbelliferone: A Complementary and Alternative Cancer Therapeutic Strategy

Daiana L. Vitale[1,2], *Antonella Icardi*[1,2], *Paolo Rosales*[1,2], *Fiorella M. Spinelli*[1,3], *Ina Sevic*[1,2] *and Laura D. Alaniz*[1,2]*

[1] Laboratorio de Microambiente Tumoral, Centro de Investigaciones Básicas y Aplicadas (CIBA), Universidad Nacional del Noroeste de la Provincia de Buenos Aires, Junin, Argentina, [2] Centro de Investigaciones y Transferencia del Noroeste de la Provincia de Buenos Aires (CITNOBA), Universidad Nacional del Noroeste de la Provincia de Buenos Aires (UNNOBA), Universidad Nacional de San Antonio de Areco (UNSAdA), Consejo Nacional de Investigaciones Científicas y Técnicas (CONICET), Pergamino, Argentina, [3] Centre de Recherche en Cancérologie et Immunologie Nantes Angers (CRCINA), Inserm, Centre National de la Recherche Scientifique (CNRS), Université de Nantes, Nantes, France

OPEN ACCESS

Edited by:
Raquel Montenegro, Federal University of Ceara, Brazil

Reviewed by:
Rob McKallip, Mercer University, United States
Hedwich Fardau Kuipers, University of Calgary, Canada
Matias A. Pibuel, Universidad de Buenos Aires, Argentina

***Correspondence:**
Laura D. Alaniz
ldalaniz@comunidad.unnoba.edu.ar

Specialty section:
This article was submitted to Pharmacology of Anti-Cancer Drugs, a section of the journal Frontiers in Oncology

Received: *15 May 2021*
Accepted: *10 September 2021*
Published: *04 October 2021*

Citation:
Vitale DL, Icardi A, Rosales P, Spinelli FM, Sevic I and Alaniz LD (2021) Targeting the Tumor Extracellular Matrix by the Natural Molecule 4-Methylumbelliferone: A Complementary and Alternative Cancer Therapeutic Strategy. Front. Oncol. 11:710061. doi: 10.3389/fonc.2021.710061

In antineoplastic therapy, one of the challenges is to adjust the treatment to the needs of each patient and reduce the toxicity caused by conventional antitumor strategies. It has been demonstrated that natural products with antitumoral properties are less toxic than chemotherapy and radiotherapy. Also, using already developed drugs allows developing substantially less costly methods for the discovery of new treatments than traditional drug development. Candidate molecules proposed for drug repositioning include 4-methylumbelliferone (4-MU), an orally available dietetic product, derivative of coumarin and mainly found in the plant family Umbelliferae or Apiaceae. 4-MU specifically inhibits the synthesis of glycosaminoglycan hyaluronan (HA), which is its main mechanism of action. This agent reduces the availability of HA substrates and inhibits the activity of different HA synthases. However, an effect independent of HA synthesis has also been observed. 4-MU acts as an inhibitor of tumor growth in different types of cancer. Particularly, 4-MU acts on the proliferation, migration and invasion abilities of tumor cells and inhibits the progression of cancer stem cells and the development of drug resistance. In addition, the effect of 4-MU impacts not only on tumor cells, but also on other components of the tumor microenvironment. Specifically, 4-MU can potentially act on immune, fibroblast and endothelial cells, and pro-tumor processes such as angiogenesis. Most of these effects are consistent with the altered functions of HA during tumor progression and can be interrupted by the action of 4-MU. While the potential advantage of 4-MU as an adjunct in cancer therapy could improve therapeutic efficacy and reduce toxicities of other antitumoral agents, the greatest challenge is the lack of scientific evidence to support its approval. Therefore, crucial human clinical studies have yet to be done to respond to this need. Here, we discuss and review the possible applications of 4-MU as an adjunct in

conventional antineoplastic therapies, to achieve greater therapeutic success. We also describe the main proposed mechanisms of action that promote an increase in the efficacy of conventional antineoplastic strategies in different types of cancer and prospects that promote 4-MU repositioning and application in cancer therapy.

Keywords: 4-methylumbelliferone, hyaluronan, extracellular matrix, cancer, antitumoral action

1 INTRODUCTION

Natural products derived from plants have been extensively used for thousands of years. However, to guarantee their correct application and safety, their benefits should be thoroughly investigated through both basic and clinical studies. Although the World Health Organization (WHO) has established the operational guide to use and conduct clinical studies of these products, rules and regulations depend on the region or country. Several products that contain active principles from plant extracts are already included in the health system, but their percentages in the prescription depend on the authorization by entities such as the European Medicines Agency (EMA) or the Food and Drug Administration (FDA). For example, in an analysis made of prescriptions dispensed from community pharmacies in the USA between 1959 and 1980, 25% were products derived from plants (1). Among these herbal-derived products are coumarins, whose name originated from the fact that they were first found in the seed of the tree *Dipteryx odorata* of the family *Fabaceae*, commonly known as "cumaru" or "kumaru" in Central and South America (2). Coumarin derivatives are currently extracted from many plants across continents and are found in high levels in fruits, roots, stems and leaves (3). It has been described that coumarin and its derivatives have diverse biological effects, acting as anti-inflammatory (4), anticoagulant (5), antiviral (6), fungicidal (7) and antitumor agents (8). Chemically, they are benzo-α-pyrones (IUPAC nomenclature: 2H-chromen-2-one), which consist of a benzene ring joined to a pyrone ring. Among coumarin derivatives is 4-methylumbelliferone (4-MU), considered to belong to the group of simple coumarins (9). 4-MU is hydroxylated in position seven, known as umbelliferone, and methylated in position four (IUPAC nomenclature: 7-hydroxy-4-methylcoumarin), and also known by the international nonproprietary or generic name: hymecromone. The information provided in the National Center for Advancing Translational Sciences (NCATS) Inxight portal Drugs indicates that this substance is approved in Europe and Asia to treat biliary spasm and is used orally as a choleretic and antispasmodic drug and as a standard for the fluorometric determination of enzyme activity (https://drugs.ncats.io/).

Umbelliferones are widely distributed among the plant families *Rutaceae*, *Umbelliferae* (celery, anise) and *Asteraceae* (chamomile) (1). However, since these compounds are not easily extracted from plants, they are synthesized using the "Pechmann" condensation reaction of resorcinol and formyl acetic acid (10). Our interest in these molecules lies on their mechanism of action. In particular, 4-MU is able to inhibit hyaluronan (HA) synthesis since the active glucuronidation of 4-MU depletes the cellular UDP-glucuronic acid (UDP-GlcUA) pool necessary for HA synthesis. It has also been determined that 4-MU downregulates the mRNA levels of HA synthases (HAS) (11). Since HA is an important extracellular glycosaminoglycan, able to modulate tumor behavior (12), 4-MU can be considered as a drug with antitumor action. In addition, some reports have demonstrated that its therapeutic action in pathological conditions relies on more than just its effects on HA synthesis (13, 14). However, it is still necessary to deepen the knowledge on this mechanism of action. As mentioned, 4-MU depletes the UDP-GlcUA pool, whose synthesis is dependent on glucose metabolism, thus affecting the cellular energetic state (15). Besides, several metabolic routes that use UDP-GlcUA, such as conjugation reaction, which allows inactivation of other metabolites, could be affected.

Thus, in this review, we discuss the tumor process that might be modulated by 4-MU, focusing on the type of tumor as well as on its action on different tumor-associated cells besides the tumor cell itself.

2 PHARMACOLOGICAL ASPECTS

2.1 4-MU Metabolism

4-MU metabolism gives rise to a limited number of metabolites however the metabolites that are produced depend on the species (3). Specifically, 4-MU is metabolized mainly by glucuronyltransferases to a glucuronide conjugate in phase II reactions, transforming it into 4-methylumbelliferone-beta-D-glucuronide (4-MUG) (16). 4-MU, like other coumarins, is insoluble in water, and since it is not a polar molecule, it can cross the lipidic intestinal barrier easily, allowing its complete absorption when orally administered, finally binding to plasma protein, which allows it to adequately reach the tissues (3). It has a short half-life and low bioavailability and is excreted primarily in urine (17). Besides, the methyl group in position four offers 4-MU several advantages over the other derived molecules, such as lower toxicity, since it prevents its metabolism to the mutagenic 3,4-coumarin epoxide by the action of liver cytochrome P450 enzymes (18), and lower anticoagulant effect compared to dicoumarol or warfarin. Thus, products containing 4-MU are available in the USA and Europe as dietary supplements (Heparvit®, Heparmed®, DetoxPro®). Besides, a clinical trial in the USA in patients with chronic hepatitis B and C (ClinicalTrials.gov identifier NCT00225537) has also demonstrated that 4-MU is safe, reaching phase II of the study in 2007, although complete results are not published yet. The dose ranges used in humans are between

8 and 7000 mg/day (19), being several times higher than the acceptable daily intake in food and cosmetic products, which is 0.06 mg/kg/day (20). However, no mutagenic or genotoxic effects have been observed (21). This makes it an interesting compound to consider for use in several diseases and propose its repositioning in cancer, since positive responses have been observed even in advanced stages of this disease (22).

Based on studies in rats, which are poor models to compare with humans for this particular type of metabolism, the FDA classified coumarins as toxic compounds (9). However, as compared with their hepatotoxicity in rats and mice (23), studies carried out in humans have shown little evidence of liver dysfunction (3). Moreover, as compared with other coumarin derivatives, 4-MU has been safely used in liver therapy as a choleretic and spasmolytic, improving liver detoxification systems through increased bile production (24). In humans, 4-MU is consumed at a dose of 1500 to 2200 mg/day as a choleretic, and, in several cancer models in mice, it has shown antitumor activity in doses of 1000 to 3000 mg/kg, being the maximal tolerated dose 2300 to 7200 mg/kg (3). Thus, taking into account this pharmacological aspect of 4-MU, it is possible to suggest that, in combination with other cancer chemotherapeutic drugs, these doses could be lower without loss of their effectiveness, providing additive or synergistic effects, as will be discussed below.

2.2 Differential Pharmacological Effects of 4-MU

Regarding the undesirable pharmacological effects of 4-MU, García-Vilas et al. observed that it could show a potent antiangiogenic effect by inducing the inhibition of HA synthesis and that since HA is a normal constituent of the extracellular matrix (ECM) in several tissues in humans, its longtime use might cause systemic damage (25). In the context of cancer, it would be considered that 4-MU should be used at similar time and in combination with a chemotherapy protocol. Therefore, tissues that have active HA synthesis could be affected during chemotherapy treatment. Besides, due to the current difficulty of deliver the drug in a tumor-specific manner, the time schedule during cancer treatment must be carefully studied in human patients. In an atherosclerosis mouse model, Nagy et al. found that 4-MU alters the normal vascular endothelial glycocalyx, favoring its progression (26). This also suggests that this compound could induce side-effects like cardiovascular alterations, and therefore the correct dose and treatment time should be analyzed in different contexts to reduce potential adverse effects. However, experiments at our lab support the hypothesis that, in a context where HA is overproduced, 4-MU could have therapeutic effect. In hepatocellular cell lines with different levels of HA production, we observed that significant antiproliferative or apoptotic effects were detected only in cells with high HA levels (27). In fact, 4-MU treatment has been found to be beneficial for pathologies with high level or dysregulated synthesis of HA like endometriosis (28), where the adherence of menstrual CD44-expressing endometrial cells to mesothelial cells *via* binding to HA is involved in endometriotic lesions, or autoimmune diseases, such as rheumatoid arthritis, type 1 Diabetes or multiple sclerosis, where the chronic inflammation state is associated with abnormal deposition of HA in the synovial compartment, pancreatic islets and spaces between myelinated axons, respectively (29).

In the next section, we will discuss the antitumor effects of 4-MU in different types of cancers, which is the focus of this review.

3 ANTITUMORAL EFFECTS OF 4-MU TREATMENT IN DIFFERENT TYPES OF CANCER

In several human cancers, HA concentration is increased (30, 31) and it is well known that a HA-rich stroma has an active role in the tumor microenvironment, promoting tumor development, angiogenesis, metastasis (32, 33), and drug resistance (34), and even acting as an immune-regulatory factor (35). Therefore, targeting HA synthesis by 4-MU represents a specific therapeutic approach to control HA levels in the cancer cell stroma. Several reports have shown that 4-MU inhibits the proliferation, migration, and invasion of multiple cancer types, both *in vitro* and *in vivo*, by a mechanism dependent on the inhibition of HA synthesis (**Table 1**), which will be the mechanism mainly discussed, although independent mechanisms will also be reviewed.

3.1 Colorectal Carcinoma

Colorectal cancer (CRC), one of the most observed types of tumor worldwide, presents treatment limitations due to the necessity of surgical treatment and the high rates of metastasis and mortality (68). For this reason, it is one of the main targets of the investigation about alternative therapies that seek to control tumor spread and reduce mortality. In this sense, several scientific reports have demonstrated the specific role of 4-MU in CRC. In colon cancer cells, Heffler et al. *showed that the inhibition of* the inhibition of HAS and HA decreases tumor growth and increase apoptosis in a dose-dependent manner (69). Similarly, in the HCT-8 cell line, Wang et al. showed that 4-MU can effectively reduce 2D and 3D proliferation as well as cell motility and that this effect could be reversed by addition of exogenous HA, indicating that the reduction of HA production in cancer cells could inhibit tumor growth and metastasis (70). In another metastatic CRC cell line, SW620, Heffler et al. also found that *in vitro* treatment with 4-MU significantly reduced cell viability (69). Besides, based on the fact that HA and focal adhesion kinase (FAK) signaling are associated with the promotion of tumorigenesis, these authors observed that 4-MU could act synergistically during FAK inhibition (69). Also, in CT26 CRC cells, Malvicini et al. observed that 4-MU significantly reduced HA synthesis without affecting their viability and that, in an *in vivo* mouse model, the reduction of HA by 4-MU treatment reduced tumor interstitial pressure without affecting tumor growth (36). However, in this model, the authors also found that 75% of mice treated with 4-MU in combination with

TABLE 1 | Effect of 4-MU treatment in different types of tumors.

Tumor	Effect of 4-MU treatment (*in vitro* and/or *in vivo*)	References
Colon carcinoma	*Higher expression of antiangiogenic factors* *Higher migration rates of cytotoxic T lymphocytes* *Reduction of tumor interstitial pressure*	(36)
Pancreatic cancer	*Suppressed cell proliferation, migration and invasion* *Increased apoptosis* *Alterations in intercellular spaces* *Decreased liver metastasis* *Potentiated effect of gemcitabine and 5-fluoruracil* *Enhanced cytotoxic effect of T lymphocytes*	(37–42)
Prostate cancer	*Inhibited proliferation, motility and invasion* *Higher apoptosis* *Decreased tumor growth and microvessel formation*	(43, 44)
Ovarian cancer	*Inhibition of cell migration, proliferation and invasion* *Decreased tumor growth*	(45–47)
Breast cancer	*Inhibition of the proliferation of human breast carcinoma cells* *Decreased cell motility, invasion and proliferation* *Decreased incidence of metastasis and growth of CSC in the bone*	(48–51)
Hepatocellular carcinoma	*Inhibition of cancer stem cell properties* *Reduction of liver fibrosis and impairment of tumor growth by reduction of proangiogenic factors*	(27, 52, 53)
Bone-derived cancer	*Osteosarcoma:* *Inhibition of cell proliferation, migration and invasion.* *Reduced lung metastasis* *Chondrosarcoma:* *Suppression of cell proliferation, migration and invasion* *Inhibition of local tumor growth* *Fibrosarcoma:* *Positive effect on the sensitivity of cells to radiotherapy*	(54–57)
Melanoma	*Inhibition of cell adhesion and locomotion* *Suppression of liver metastasis* *Positive effect on the sensitivity of cells to vemurafenib*	(58–60)
Chronic myeloid leukemia	*Induction of apoptosis in vitro and in vivo* *Reduced tumor growth* *Sensitization of CML cells to doxorubicin and vincristine*	(61–64)
Glioblastoma	*Decreased cell migration and proliferation* *Induction of apoptosis* *Sensitization of glioblastoma cells to temozolomide*	(65–67)

cyclophosphamide and IL-12 showed tumor regression (36). This triple combination induced the production of antiangiogenic factors and increased the migration of cytotoxic T lymphocytes in tumors, showing that tumor microenvironment remodeling and reduction of HA synthesis increase the efficacy of anticancer immunotherapies combined with chemotherapy agents (36).

These reports indicate that, in CRC models, 4-MU exerts its action by inhibiting HA synthesis, but the impact of this inhibition could be associated or not with the modulation of tumor cell survival, suggesting that it affects both tumor cells and the tumor microenvironment.

3.2 Pancreatic Cancer

Pancreatic ductal adenocarcinoma (PDAC) is the most malignant of all solid cancers because of the difficulties in early diagnosis and the poor response to chemotherapy (37). PDAC has an abundant volume of stroma composed of large amounts of HA (30, 71). It has been demonstrated that, in this type of cancer, 4-MU inhibits HA synthesis, thus affecting tumor cell behavior (38). In pancreatic cancer cells, Nagase et al. first determined that 4-MU suppressed cell proliferation and invasion and increased apoptosis by inhibiting HA production (37). Then, in an *in vivo* mouse model of PDAC, these authors found that 4-MU treatment suppressed HA accumulation in pancreatic tumor tissue and improved survival rate (37). To better understand tumor microenvironment interactions, Cheng et al. studied this inhibition in PDAC Panc-1 cells co-cultured with stromal fibroblasts (39). Specifically, they. found that 4-MU inhibited the enhanced migration of PDAC cells in response to tumor-stromal interactions with fibroblasts (39). In addition, Nakazawa et al. showed that 4-MU inhibited HA synthesis and the formation of the pericellular HA coat in KP1-NL pancreatic cells and decreased liver metastases *in vivo* (40). In another human pancreatic cancer cell-bearing mouse model, Yoshida et al. observed a decrease in tumor volume and a significant reduction of the intratumoral HA amount (41). Besides, histological analysis by electron microscopy revealed that 4-MU altered the intercellular space, causing it to become less cohesive and more permissive to drug delivery, indicating that this could be a promising combination with chemotherapy agents, improving their effects (41). In fact, several reports have indicated the potential role of 4-MU as a co-adjuvant during the chemotherapeutic treatment of this cancer. In this

regards, Nagase et al. found that *in vivo* co-administration of 4-MU and the chemotherapeutic drug gemcitabine to tumor-inoculated mice decreased the size of primary and metastatic tumors more than gemcitabine alone (37). By combining 5-fluorouracil with 4-MU treatment in an *in vivo* pancreatic cancer model, Yoshida et al. found similar results, where 4-MU potentiated the effects of 5-fluorouracil by sensitizing tumor cells to its cytotoxic action (42). Also, the role of 4-MU as a modulator of immunotherapy strategy during PDAC has been recently determined. Suto et al., for example, have recently shown that 4-MU inhibited PDAC cell proliferation and HA synthesis in four different PDAC cell lines, and enhanced γδ T-cell-rich peripheral blood mononuclear cell-mediated cytotoxicity against pancreatic cells (72). These authors found the same results *in vivo*, where 4-MU reduced intratumor HA deposition and promoted infiltration of transferred γδ T-cells into tumor tissue, and consequently suppressed tumor growth (72). These data indicate that 4-MU inhibits HA synthesis and reduces the amount of HA in the ECM of prostate cancer, thus affecting tumor cell behavior and its response to chemo- or immunotherapy.

3.3 Prostate Cancer

Some researchers have proposed that, in prostate cancer, 4-MU acts as a regulator of HA synthesis and angiogenesis. Lokeshwar et al., for example, studied the effects of 4-MU on different prostate cancer cell lines and demonstrated that 4-MU inhibited proliferation, motility, and invasion and increased apoptosis (43, 44). Besides, in a mouse model of prostate cancer, these authors observed that oral administration of 4-MU significantly decreased transgenic adenocarcinoma and PC3-ML tumor growth without organ toxicity or changes in serum chemistry or body weight. They also found that tumors from 4-MU–treated animals showed reduced microvessel density and downregulated HA receptors, Akt signaling and β-catenin activation (43, 44). Although not many reports have evaluated 4-MU as a modulator of prostate cancer behavior, these studies, together with other studies analyzing the effect of 4-MU in other types of tumors, reinforce the inhibitory role of 4-MU in prostate cancer growth with an anti-angiogenic potential. Therefore, these data open up new avenues of investigation of the effect of this natural molecule on pancreatic cancer and its possible therapeutic applications.

3.4 Ovarian Cancer

Ovarian cancer is one of the most frequent gynecological pathologies in adult women. It has a high mortality rate since it metastasizes early and quickly, presenting high resistance to chemotherapy (45, 73). Importantly, high levels of HA have been detected in histological samples from tumor and metastatic lesions derived from patients with epithelial ovarian cancers with worse prognostics, suggesting that this molecule could be considered a therapeutic target (46). Thus, many studies are currently assessing the ability of natural products as 4-MU to induce ovarian cancer cell death and complement the antitumor treatment. One of the first studies performed for Kultti et al. showed in SKOV-3 ovarian cancer cells determined that 4-MU inhibits HA synthesis and produces large quantities of 4-MU-glucuronide *in vitro*, depleting the cellular UDP-GlcUA source (11). The inhibitory effect of 4-MU has also been observed in the down-regulation of HAS3 expression (11). In addition, Anttila et al. found that the reduction of the HA-pericellular coat was related to the inhibition of cell migration, proliferation and invasion (46). Extending the studies on ovarian cancer, Tamura et al. demonstrated the effect of 4-MU on HRA human ovarian serous adenocarcinoma cells, using *in vitro* assays and an *in vivo* rat peritoneal carcinoma model (47). These authors found that 4-MU inhibited ovarian cancer cell proliferation in a dose-dependent manner *in vitro*, but also found non-inhibitory effects of 4-MU on cell invasion and migration (47). In their *in vivo* experiments they found that 4-MU administration inhibited the growth of peritoneal tumors and significantly prolonged rat survival (47). Recently, An et al. have determined the molecular mechanisms associated with the inhibitory effect of 4-MU on ES2 and OV90 epithelial ovarian cancer cells (45). Specifically, they observed a decrease in cell proliferation and cell arrest in the G2/M phase of the cell cycle, which defines lower cell division rates. They also found that 4-MU interfered with calcium homeostasis, induced endoplasmic reticulum stress, inhibited AKT and S6 phosphorylation, and increased MAPK phosphorylation (45).

Certain ovarian cell carcinomas show a spherule-like mucoid stroma with a hollow acellular space. Despite the absence of stromal cells, both the mucoid stroma and hollow spheroids contain abundant ECM, mainly composed of HA, which plays a crucial role in the formation of those structures and in tumor progression. In this sense, Kato et al. determined that after 4-MU treatment of HAC-2 ovarian cancer cells, HA synthesis was inhibited and consequently, the spherule-like accumulation of HA and hollow spheroids were not observed (74). These authors determined that the inhibition of HA synthesis was associated with the reduction of cell growth (74).

All these reports indicate that tumor-derived HA is essential for the regulation of cell growth, migration and invasion ability of ovarian clear cell carcinoma. Thus, the inhibition of HA synthesis could be a potential adjunctive therapy, avoiding the interaction of this molecule with its receptors, like CD44, and in turn blocking the signaling that allows tumor dissemination in this type of cancer. However, it has been observed that 4-MU effect could also be independent of the modulation of HA expression, affecting other tumor signals besides HA-CD44, a fact that also supports its therapeutic use.

3.5 Breast Cancer

Breast cancer is one of the most frequently diagnosed cancers in women and is considered to have a high phenotypic diversity, which heavily influences the progression and outcome of the treatment. In this sense, three receptors are frequently analyzed for the correct treatment decision: the estrogen receptor (ER), the progesterone receptor (PR) and the human epidermal growth factor receptor 2 (HER2) (75). Some reports have shown that 4-MU treatment leads to changes in the proliferative phenotype of ER^- and ER^+ cells (48, 75). Karalis et al., for example, found that 4-MU treatment led to a reduction in cell proliferation in both cell types, which, in ER+ cells, was more pronounced after 2 days,

and in ER- cells much faster on the first day of treatment (48). This quicker reaction of ER- cells to lower concentrations of 4-MU than ER+ cells could indicate a stronger susceptibility of these cells to low 4-MU concentrations showed that 4-MU inhibits proliferation of human breast carcinoma cells in different cell lines, like T-47D ($ER^+PR^+HER2^-$) and MDA-MB-231 ($ER^-PR^-HER2^-$) cells (48). Additionally, these authors showed that low levels of HA and glucose in the tumor microenvironment could increase the sensitivity of breast cancer cells to 4-MU treatment and thus inhibit cell proliferation more strongly (48).

In breast cancer cell lines with highly invasive character, such as MDA-MB-231 cells. Urakawa et al. demonstrated that 4-MU suppresses HA synthesis and accumulation probably due to the suppression of HAS2 expression, which could in turn lead to lower cell motility, invasion and proliferation (49). By using 4-MU to inhibit HA synthesis in breast cancer cells, Brett et al. suggested that a decrease in pericellular matrix formation is correlated with decreased invasiveness, and proposed that a reduction in HA synthesis could inhibit the formation of the pericellular matrix and provide a good strategy for inhibition of metastatic progression (50). Also, Kultti et al. showed that 4-MU inhibits migration of the non-invasive MCF-7 ($ER^+PR^+HER2^-$) breast cancer cells and that the growth of these cells is sensitive to 4-MU, being almost completely blocked by high concentrations of the drug (11). These authors also showed that 4-MU inhibits HA by reduction of the cellular HAS substrate UDP-GlcUA and that in MCF-7 cells this reduction was dose-sensitive, with less pronounced response at higher doses, while MDA-MB-361 ($ER^+PR^-HER2^+$) cells lost most of their UDP-GlcUA at higher doses of 4-MU (11).

To form metastasis, metastatic tumor cells usually move into a specific organ. In particular, breast cancer preferentially metastasizes to the bone and lungs. Okuda et al. showed that cancer stem cells (CSCs) from a metastatic breast tumor show considerably higher tumorigenic and metastatic capability than CSCs from a low-metastatic tumor and indicate that HAS2 is essential to provide CSCs with a metastatic phenotype (51). These authors proposed that 4-MU, due to the specific inhibition of HA by affecting HAS2 activity, can considerably suppress the incidence of metastasis and growth of CSCs in the bone (51).

Thus, the above-mentioned reports indicate that 4-MU could be beneficial to treat breast cancer, although the sensitivity of tumor cells and the response to this drug will depend on the hormonal receptor status. Interestingly, this opens a line of investigation that could associate ECM remodeling by 4-MU with the signal mediated by progestogens in breast cancer. On the other hand, it is important to highlight that, due to its ability to modulate the phenotype of CSCs, 4-MU has a great therapeutic potential and could help to control tumor resistance.

3.6 Hepatocellular Carcinoma

Hepatocellular carcinoma (HCC) is a tumor that frequently occurs in the inflammatory microenvironment, usually as a reaction process that arises in response to chronic injuries, like chronic hepatitis C and B virus infection or alcohol abuse (76). Regardless of the etiology, in chronic liver disease, the ECM components, like HA and collagen, deposit in the liver, depending on the level of fibrosis progression. For this reason, the level of HA could be used as a biomarker to assess the stage of liver fibrosis (77). In high-HA-producing murine Hepa129 cells and in medium-HA-producing human Hep3B cells, Piccioni et al. showed that 4-MU inhibited proliferation and induced apoptosis (78). Contrarily, in human low-HA-producing Huh7 cells, these authors observed partial resistance to 4-MU treatment (78). These results show that the mechanism of 4-MU action in HCC is highly dependent on HA levels (78). It has also been demonstrated that 4-MU, by inhibiting HA, could reduce liver fibrosis and diminish tumor growth by reduction of proangiogenic factors, like VEGF and CXCL12, and also by reduction of IL-6 production in the liver tumor microenvironment (27). Some reports have shown that 4-MU inhibits the properties of CSCs by the inhibition of HA, accompanied by a reduction of CSC markers, like transmembrane glycoproteins CD44 and CD133, as well as CD90 and EpCAM cells, indicating a possible mechanism which involves HA in cell-to-cell and cell-to-matrix interactions (52, 53). In contrast to these reports, Mikami et al. showed that systemic inhibition of HA synthesis by oral 4-MU administration promotes the development of tumor in mice with liver tumors induced by administration of thioacetamide (TAA) (79). A possible explanation for this opposite result could be associated with the HCC model used by the authors. The administration of TAA induces DNA damage by increasing the levels of reactive oxygen species (ROS) and affecting the oxidative status of the liver microenvironment. Thus, HA inhibition at early stages could be affecting the documented protective action of HA during oxidative damage (80). At this time, 4-MU administration would be detrimental, perpetuating the damage of TAA and accelerating its carcinogenic action.

These results suggest that 4-MU administration could have a positive impact on the treatment of HCC by affecting angiogenic factors as well as hepatic CSCs. However, as commented in section 2.2, further preclinical studies will be required to adjust the moment of its application and the length of its use according to the tumor stage to avoid systemic alterations. On the other hand, analysis of the data about the interaction of 4-MU with other drugs are also necessary to determine whether they could affect its antitumoral action in HCC.

3.7 Bone-Derived Tumors

Osteosarcoma (OS), the most common primary bone tumor, is responsible for considerable morbidity and mortality due to its high rates of pulmonary metastasis. Although the prognosis of OS patients has improved dramatically with the introduction of chemotherapy, cases with metastases or an unresectable tumor still have a poor prognosis (54). Several researchers have suggested the involvement of a HA-rich ECM in the tumorigenicity of OS cells, and proposed that suppression of this HA-rich ECM leads to inhibition of malignant cell behavior (81–83). Arai et al. demonstrated that 4-MU reduces the formation of functional cell-associated matrices in OS cells and inhibits cell proliferation, migration, and invasion, resulting in the reduction of tumorigenicity and lung metastasis (54). These

authors further studied 4-MU treatment in *in vivo* models of OS and found that, although it showed only a mild inhibitory effect on the growth of the primary tumor, it markedly inhibited the development of lung metastasis (54).

4-MU treatment has also shown antitumor effects on low-grade chondrosarcoma, which is the second most common primary malignant bone tumor and a tumor generally considered resistant to conventional chemo- and radiotherapy (84). This type of tumor is characterized by the formation of a HA-rich ECM which has been proposed to be associated with drug resistance (85). Hamada et al. determined that, in chondrosarcoma cells, inhibition of HA synthesis by 4-MU suppressed cell proliferation, migration, and invasiveness, and that, *in vivo*, daily administration of 4-MU markedly inhibited local tumor growth and significantly suppressed the amount of HA in tumoral tissue (55).

Regarding fibrosarcoma, another of the most common bone-derived tumors, some reports have also shown a positive effect of 4-MU treatment on the sensitivity of cells to radiotherapy (56, 57, 86, 87). In primary solid tumors, external radiotherapy is generally effective and non-invasive and improves local control in the target region. However, although radiotherapy is an effective adjuvant treatment, metastasis and radiation resistance are associated with poor prognosis in patients (88). Saga et al. have shown that 4-MU administration in combination with exposure to 2-Gy ionizing radiation reduced HA production, cell invasion and the metastatic potential of fibrosarcoma cells *in vitro* (86), suggesting that 4-MU could be a radio-sensitizing molecule. Besides, in a later study, these same authors determined that the radio-sensitizing effect of 4-MU was not completely associated with its inhibitory effect on HA synthesis and that 4-MU improved the radiosensitivity of fibrosarcoma cells by suppressing inflammation (56). Specifically, they revealed that 4-MU increased the sensitivity of fibrosarcoma cells to X-ray radiation by inhibiting the production of the pro-inflammatory cytokines IL-1β, IL-6 (87), IL-1α, IL-36γ and IL-37 (56). Recently, the authors demonstrated that the radio-sensitizing effects of 4-MU are intrinsically related to the suppression of antioxidant activity through previously discovered anti-inflammatory effects (57).

Even more, in a model of metastatic breast cancer, Urakawa et al. determined that 4-MU suppressed metastatic lesions of bone *in vivo* and inhibited the expansion of osteolytic lesions and intraosseous tumor growth in breast cancer xenograft models by inhibiting HA accumulation in tumor tissues (49).

These results suggest that, in bone-derived tumors, 4-MU could be a beneficial adjuvant during radiotherapy by inducing radio-sensitization of tumor cells as a consequence of HA synthesis inhibition as well as by an independent mechanism associated with the modulation of inflammatory and oxidative factors.

3.8 Melanoma

Melanoma is one of the three main types of skin cancer, being the most serious form. The prognosis of melanoma has historically been poor, with a median survival of less than 12 months, which can be ascribed to the aggressive nature of the disease and low response rates to conventional chemotherapy (89). In recent years, although major therapeutic advances have been made, resistance to these new therapies has also emerged (90). Thus, new treatment modalities are needed to improve the outcome, and 4-MU is one of the candidate molecules for use in new therapeutic strategies. In this sense, different studies have evaluated the potential role of 4-MU as a modulator of melanoma progression.

Kudo et al. demonstrated that 4-MU inhibits the formation of cell surface HA by B16F-10 melanoma cells and its release into the culture medium. These authors also showed that 4-MU had no significant cytotoxic effects on cell growth, but inhibited the adhesion and locomotion abilities of melanoma cells in a dose-dependent manner (58). Since adhesion and locomotion are involved in the early stages of metastasis, these results suggest that HA-rich matrices adjacent to melanoma cells provide a suitable environment for metastasis. In line with these findings, Yoshihara et al. evaluated the role of 4-MU in melanoma metastasis *in vivo*, by pre-treating melanoma cells with 4-MU before mouse inoculation, showing both decreased cell surface HA formation and suppression of metastasis after injection (59). These authors also demonstrated that oral administration of 4-MU to mice decreased liver HA content, which also contributed to a suppressed liver metastasis (59). Thus, in agreement with the data published by Kudo et al. (58), both cell surface HA of melanoma cells and recipient liver HA can promote liver metastasis of melanoma *in vivo* (59), strongly supporting 4-MU as a potential anti-metastatic agent in a highly malignant tumor as melanoma.

Another interesting study that reinforces the anti-invasive role of 4-MU was carried out by Edward et al. These authors showed that 4-MU inhibited tumor cell growth and the activation of stromal HA synthesis by melanoma cell-derived factors (91). Specifically, they demonstrated that 4-MU caused a dose-dependent growth inhibition of fibroblast and melanoma cells. The inhibition of cell growth was more pronounced when fibroblasts were stimulated with C8161 melanoma cell-conditioned medium (91). In addition, 4-MU reduced the level of HA in fibroblast-contracted collagen lattices, and inhibited both the growth of melanoma cells and invasion into the lattices (91). These results allow concluding that 4-MU has an anti-proliferative effect on the melanoma microenvironment, not only suppressing HA synthesis, but also inhibiting the induction of stromal HA accumulation and the proliferation of fibroblasts and melanoma cells.

Based on its growth-inhibitory activities against melanoma cells, Abildgaard et al. have recently proposed 4-MU as a new drug candidate for melanoma treatment and combination with chemotherapy (60). These authors showed that 4-MU affected cellular metabolism through inhibition of glycolysis and increased ROS production, suggesting the involvement of oxidative stress in the cellular response (60).

3.9 Glioblastoma

Glioblastoma (GBM) represents the most malignant and deadly brain tumor in adults (92). Despite invasive treatment strategies, involving a triad of surgery, radiation and chemotherapy,

patients inevitably relapse due to resistance and invasion within the brain parenchyma and succumb within 15 months post-diagnosis (92). It is noteworthy that the ECM of malignant gliomas, like GBM, contains higher amounts of HA than normal brain tissue, indicating that HA could be instrumental for tumor adhesion and invasion (93, 94). It has been proposed that the aggressiveness of GBM depends on the co-expression of HAS and hyaluronidases (95). In this sense, based on the fact that 4-MU is a small molecule able to cross the blood brain barrier (96), Pibuel et al. proposed its use as an interesting therapeutic strategy to complement GBM treatment (65). These authors demonstrated that, in the GL26 murine GBM cell line, 4-MU diminished HA synthesis while increasing apoptosis and decreasing cell proliferation and migration (66). Yan et al. found that alterations in HA metabolism, by silencing HAS3 or by treating with 4-MU, inhibited glioma cell proliferation by affecting the autophagy flux (67). Although these new results are encouraging, more investigations are needed to understand the action and mechanism of 4-MU in GBM cells.

3.10 Chronic Myeloid Leukemias

Leukemia is the general name for cancer that involves blood-forming cells. Among them, Chronic myeloid leukemia (CML) is a type of cancer where the myeloid lineage is affected and comprises a group of myeloproliferative neoplasms. In 2020, approximately 15% of new cancer cases diagnosed in adults in the USA were leukemias (97). Most patients have typical cytogenetic alterations, the Philadelphia chromosome (Ph1), and the BCR/ABL rearrangement, the latter of which produces an abnormal tyrosine kinase and allows the specific treatment with inhibitors of this kinase. However, a group of patients can be Ph1-negative and have worse prognosis and shorter survival than Ph1-positive patients. This group thus needs special attention to find a successful therapy. Although there are different well-established therapeutic strategies to control CML progression (98), some studies have analyzed the potential role of 4-MU in CML. Ban et al. demonstrated that 4-MU is able to induce apoptosis in K562 CML cells by activating the intrinsic apoptosis pathway (61). These authors found that treatment with 4-MU leads to apoptosis in K562 cells through poly (-ADP-ribose) polymerase (PARP) cleavage and alteration of the mitochondrial membrane potential (61). Interestingly, they also observed that the addition of exogenous soluble HA protects K562 cells from 4-MU-induced apoptosis (61), which suggests that the pro-apoptotic effect of 4-MU demonstrated on CML cells is directly related to the inhibition of HA synthesis. In line with this study, the same research group later demonstrated the molecular mechanism by which 4-MU promotes apoptosis in CML cells (62). They showed that 4-MU treatment induced caspase-dependent apoptosis characterized by diminished HA synthesis, in correlation with increased phosphorylation of p38 and PARP cleavage (62). These authors also showed the pro-apoptotic effect of 4-MU *in vivo*, where treatment of tumor-bearing mice with 4-MU significantly reduced tumor growth through the induction of apoptosis (62). These results, together with those of other studies, determine the role of 4-MU as a molecule that favors the response of CML to chemotherapy (63, 64) and suggest that 4-MU is an excellent candidate for use in combination with conventional therapeutic strategies.

4 EFFECTS OF 4-MU ON SPECIFIC COMPONENTS OF THE TUMOR MICROENVIRONMENT

Thanks to the numerous advances in the understanding of tumor biology and cancer progression, it is well known that the microenvironment where a tumor resides and develops is just as important and critical for its growth as tumor cells themselves. Therefore, it has been proposed that the modulation of the tumor microenvironment (TME) is particularly important to improve tumor response to cancer therapies (99). The TME is composed of non-cellular and cellular components. For decades, the specific role of non-cellular components of this microenvironment has been studied, focusing on the ECM components which can modulate tumor behavior. Even more, several functions of the different cell types associated with the tumor, such as immune cells, endothelial cells and mesenchymal stem cells, have been demonstrated. The modulation of the TME caused by 4-MU treatment is summarized in **Figure 1**.

4.1 Effects of 4-MU on Tumor-Associated Cells

4.1.1 Tumor-Associated Fibroblasts

The cellular components of the TME include not only tumor cells themselves, but also cancer-associated fibroblasts (100, 101). Some authors have described that the interactions between tumor cells and associated stromal fibroblasts stimulate the synthesis of HA, which, as already mentioned, is present in large amounts in several types of tumor (102, 103). Recently, Cheng et al. showed that co-cultivation of PDAC cells and stromal fibroblasts increased HA production, resulting in a marked increase in the migration of PDAC cells (39).

Other authors have also shown that increased levels of HA in the tumor stroma are associated with poor prognosis (31, 104). In this sense, Urakawa et al. analyzed the effect of 4-MU on tumor stromal cells, particularly in a murine fibroblast cell line, and showed that 4-MU decreased HA levels, cell growth and motility of fibroblasts (49). Also, in a murine bone metastasis model of breast cancer, these authors showed that 4-MU administration decreased the accumulation of HA around both tumor and stromal cells, being well marked in the regions adjacent to bone which correspond to the stroma, where fibroblasts are generally abundant (49). In line with these results, Edward et al. showed that 4-MU inhibited fibroblast growth and reduced HA levels in fibroblast-contracted collagen lattices, which in turn inhibited both the growth and invasion by melanoma cell culture in this condition (91), indicating that the remodeling of the tumor stroma affects tumor development and metastatic capacity.

4.1.2 Macrophages

Macrophages (MØ) are the main infiltrating immune cells of the TME. They differentiate from monocytes of systemic circulation

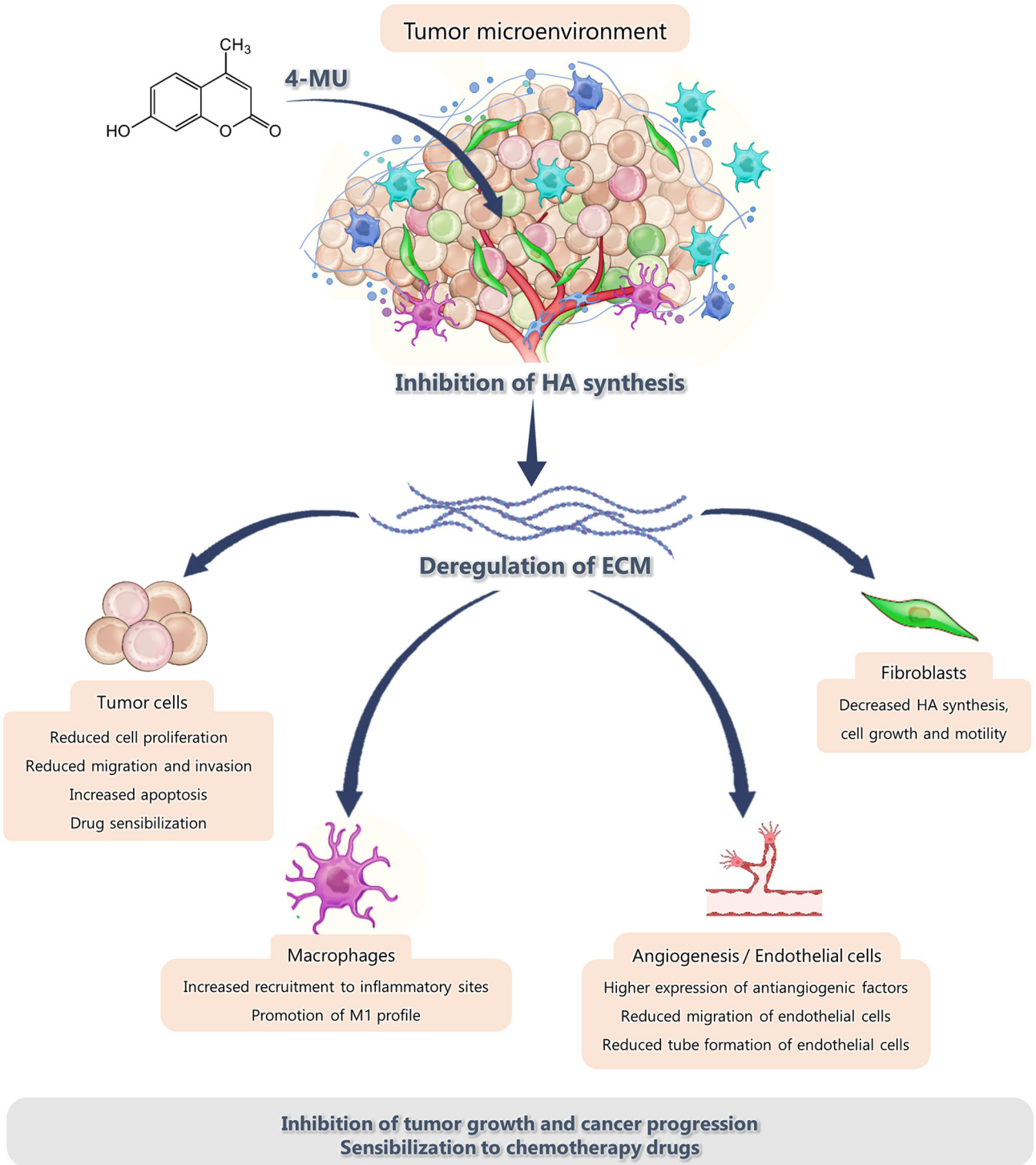

FIGURE 1 | Effect of 4-MU treatment on the components of the tumor microenvironment.

in response to different stimuli from the environment and can exhibit two phenotypic profiles, M1 and M2. Despite these cells present high plasticity, MØ classically can be identified as M1 cells, that actively express HLA-DR and CD197 and have intrinsic phagocytosis capacity. Contrary, M2 cells express high levels of CD163, CD209, CD206 and CCL2 with anti-inflammatory functions (105). Specially, tumor-associated macrophages (TAMs) can be considered as M2-like phenotype

due to anti-inflammatory cytokines of the TME. They can induce angiogenesis and lymphangiogenesis, by the release of growth factors like VEGF, FGF, PDGF and TGF-β and matrix-remodeling proteases. Moreover, they can suppress adaptive and innate immune responses by the release of anti-inflammatory factors like IL-10, TGF-β, and PD1L (106). Therefore, TAMs promote the growth and spread of tumor cells and reduce patient's survival. Because of this, TAMs have been proposed as therapeutic targets for cancer therapy. Additionally, HA from the tumor ECM can modulate MØ adhesion, migration and activation through its surface receptors, depending on the size of the molecule. It is well known that low-molecular-weight HA stimulates the expression of inflammatory cytokines and chemokines and growth factors (107). The interaction between receptors such as CD44 and TLR and HA fragments induces the expression of inflammatory mediators in murine and human macrophages (108, 109) and can act as a danger signal by promoting antigen-specific T-cell response (110). On the other hand, high-molecular-weight HA has anti-inflammatory and antiproliferative properties, like regulatory T-cell activation (111, 112). At our lab, in a breast cancer model, we have previously demonstrated that high-molecular-weight HA promotes MØ pro-angiogenic capabilities (113). For this reason, HA-inhibitors like 4-MU could be a promising therapy. However, the effect of 4-MU on immune cells in the context of cancer is poorly studied. In an atherosclerosis *in vivo* model, Nagy et al. showed that 4-MU oral administration in mice led to a significant increase in MØ recruitment in atherosclerotic lesions, promoting an inflammatory response and the development of the disease (26). In addition, Rodríguez et al. demonstrated that long-term 4-MU oral administration in mice with hepatocarcinoma caused, in MØ, an increase in the secretion of pro-inflammatory cytokines, IL-1β and TNF-α, and a decrease in anti-inflammatory cytokines, IL-10 and TGF-β, indicating the polarization of these cells towards an M1 profile in tumor and non-tumor regions. These examples demonstrate that 4-MU action over immune cells is context-dependent.

4.1.3 Endothelial Cells

Endothelial cells are involved in angiogenesis, i.e. the formation of new blood vessels by sprouting from preexisting vessels. In tumors, this process is essential as it allows their growth and dissemination. Although this process is targeted by different therapeutic drugs approved for use in cancer, development of resistance has been observed. Thus, since 4-MU can affect endothelial cell behavior, it could be a good strategy to maximize anti-angiogenic therapy (114). Garcia-Vilas et al. have shown evidence of action of 4-MU over endothelial cells. These authors observed that 4-MU inhibited cell growth, was able to generate new vessels without affecting the migration capacity, and enhanced the expression of metalloproteinases (25). Finally, by using different angiogenesis models *in vivo*, they observed that 4-MU led to a significant reduction of this process (25). In an HCC model, Piccioni et al. found evidence of 4-MU effect on endothelial cells in the TME (27). They observed that 4MU-treated mice showed significantly diminished systemic levels of VEGF and expression of the specific vascular marker CD31. They also found that 4-MU was able to inhibit endothelial cell migration and tube formation, demonstrating that 4-MU has an anti-angiogenic activity in HCC (27). Similar results have been observed in a model of prostate cancer (44). However, since little is known about the direct action of 4-MU over endothelial cells in cancer, this topic should be further explored.

4.2 Effects of 4-MU Treatment on the Non-Cellular TME

The ECM is the non-cellular component of the TME. During embryonic development and organ homeostasis, the composition of the ECM is tightly regulated. However, in diseases such as cancer, it is usually deregulated and disorganized, and undergoes extensive remodeling, acting as a key player driving disease progression (76, 115). In this sense, extremely high interstitial fluid pressures and a dense ECM combine to limit the delivery and distribution of therapeutic agents in solid tumors (116). In addition, high concentrations of HA cause an expansion of the ECM, which contributes to increased tumor interstitial pressure, which retards the delivery and distribution of drugs from the vessels into the tumor (117–120). Therefore, strategies to remove HA or block its synthesis may improve drug delivery into solid tumors. In this sense, several studies have shown that the inhibition of HA synthesis by enzymatic agents, like PEGylated recombinant hyaluronidase (PEGPH20), normalize interstitial fluid pressure and re-expand the microvasculature, improving the delivery, distribution and accumulation of drugs in tumors (117–119). Regarding this, Dufort et al. showed that the systemic treatment of mice with PEGPH20 reduced the extracellular levels of HA and interstitial pressure, thus removing a significant barrier for drug delivery in PDAC (117). Other authors also showed that the treatment with PEGH20 *in vivo* reduces HA content, induces the re-expansion of the microvasculature, and consequently improves gemcitabine and DOX uptake in murine PDAC (118, 119). This example demonstrates the potential of targeting the ECM/stroma and modulating the mechanical properties of the surrounding microenvironment, as an anti-PDAC therapy.

Unfortunately, recent research has shown that the promising results obtained for PEGH20 in a phase I/II clinical trial in PDAC (121) did not translate into the subsequent phase III study HALO 301 (122) and further development of this drug was stopped. This highlights the importance of looking for other strategies that allow blocking HA synthesis. In this context, the use of 4-MU may be a promising strategy. An interesting research has shown that 4-MU significantly reduced the amount of tumor HA, leading to a significant decrease in tumor interstitial pressure and achieving improved tumor perfusion in murine colorectal carcinoma (36). Similarly, as described above, in a model of pancreas tumor, 4-MU was able to remodel the ECM-generated interstitial gap within the tumor cell by inhibiting HA production (72).

However, it is likely that 4-MU can also affect the synthesis and organization of other ECM components, such as other non-cellular components of the TME. In this regards, Keller et al.

found that 4-MU reduced both versican and fibronectin in trabecular meshwork cells of the eye (123). Even more, Andreichenko et al. confirmed that 4-MU inhibits ECM deposition by directly affecting the production not only of HA, but also of Col1a, a major form of collagens contributing to ECM remodeling in liver fibrosis (124). It was observed that other glycosaminoglycans, such as chondroitin and heparin sulfates, were sensitive to 4-MU treatment in epidermal keratinocyte cultures. In this sense, a 4-MU concentration-dependent decrease was found in the production of these glycosaminoglycans, although the effect was greater on HA In epidermal keratinocyte cultures, Rilla et al. observed that other glycosaminoglycans, such as chondroitin and heparin sulfates, were sensitive to 4-MU treatment. They found that the production of these glycosaminoglycans decreased in a 4-MU concentration-dependent manner, although the effect was greater on HA (125). In addition, an effect of 4-MU on matrix metalloproteinases (MMPs), a family of proteolytic enzymes that degrade many ECM components and play an important role in tissue degradation and remodeling under various physiological and pathological conditions, has been observed. Nakamura et al. reported that, in human skin fibroblasts, 4-MU induces MMP2 activation (126). Surprisingly, in pathological conditions, 4-MU shows a differential effect. Nakamura et al. reported that, in a human lymphoma cell line as well as in other cultured human carcinoma cells, 4-MU inhibited MMP9, an inhibition that could not be mimicked by treatment of the cells with hyaluronidase (127). These studies show that 4-MU may target ECM components other than HA. Even more, as described above, in a model of fibrosarcoma cells, 4-MU was able to remodel the surrounding TME by inhibiting the production of pro-inflammatory cytokines, altering other non-cellular components of the TME, different from the ECM (56, 87).

Although many reports have highlighted the importance of 4-MU in inhibiting HA synthesis, it could also be affecting the synthesis of other ECM components like proteoglycans and have biological effects on soluble tumoral factors. In fact, further studies about its effect on other non-cellular components of the TME, their interaction, and their role in cancer pathogenesis will be necessary. For example, it will be interesting to investigate the impact of 4-MU modulation over different ECM components and the mechanical properties of the surrounding TME.

5 4-MU TREATMENT AS A NEW STRATEGY OF CO-ADJUVANT DRUG ON CONVENTIONAL ANTINEOPLASTIC THERAPIES

One of the most important challenges of antineoplastic therapies is to adjust the treatment to the needs of each patient and reduce the toxicity caused by conventional antitumoral strategies. Several scientific studies have reported the key role of the pericellular HA-rich ECM as a biological barrier in the TME. Among the processes controlled by this natural barrier are the modulation of immune effectors (35, 113), the inhibition of diffusion of chemotherapeutic drugs (128) and the difficult uptake of DNA transgene complexes in gene therapy (129). Furthermore, previous studies from our laboratory and other authors have shown that ECM components play important roles in acquired resistance to anticancer drugs (34, 130, 131). Therefore, the development of novel cancer treatments that target HA by altering the ECM represents a pioneering approach to the treatment of several cancers.

According to the evidence collected so far, 4-MU represents one of the candidate molecules for drug repositioning in cancer therapy. While the potential advantage of 4-MU as an adjunct in cancer therapy could improve therapeutic efficacy and reduce toxicities, the greatest challenge is the lack of strong scientific evidence to support its approval. Therefore, crucial human clinical studies have yet to be performed to respond to this need. Nevertheless, numerous scientific reports in the early stages of research have studied the role of 4-MU as a co-adjuvant of conventional antineoplastic treatments. Since it has been previously demonstrated that 4-MU mediates the inhibition of HA synthesis and pericellular HA matrix formation, this molecule would increase the efficacy of anticancer treatments.

In a study of alternative therapies applicable to pancreatic cancer, Nakazawa et al. showed that pre-treatment of KP1-NL cells with 4-MU increased the anticancer effect of gemcitabine (40). Particularly, these authors showed that pancreatic cancer cells are enclosed by HA-rich coats, and that 4-MU treatment inhibited the formation of HA pericellular coat, which promoted the perfusion and uptake of gemcitabine (41). These results were also confirmed in an *in vivo* murine model, where co-administration of 4-MU and gemcitabine to tumor-bearing mice reduced the size of the primary and metastatic tumors (40). These data suggest that the combination of 4-MU and gemcitabine is effective against human pancreatic cancer cells and tumor progression *in vivo*. Regarding the possible use of 4-MU as a modulator of chemotherapy in pancreatic cancer, Yoshida et al. found a similar effect in combination with 5-fluorouracil (5-FU) (42). These authors showed that 4-MU administration changed the antitumor efficacy of 5-FU, enhancing its cytotoxicity *in vitro* and *in vivo* and that combined treatments of 5-FU and 4-MU inhibited cell proliferation and enhanced the intracellular concentration of 5-FU *in vitro* (42). In the *in vivo* model, the authors found that mouse tumors treated with 5-FU and 4-MU decreased in size and animal survival was prolonged, in addition to a decrease in the cohesiveness of the intercellular space, which favored 5-FU perfusion and activity (42).

These findings are consistent with a recent study showing that chemotherapy with carboplatin (CBP) induces HA synthesis, which can contribute to chemoresistance by regulating ABC transporter expression in ovarian cancer (132). Specifically, this study determined that, in combination with CBP, 4-MU treatment significantly decreased ovarian cancer cell survival and increased apoptosis compared to CBP alone (132). In addition, this combined treatment reduced the expression of cancer stem cell markers such as ALDH1 and ABCG2 (132). Furthermore, 4-MU inhibits the invasion ability of chemoresistant primary cells *in vivo*, demonstrating that HA inhibition is a promising new strategy to

overcome chemoresistance and improve ovarian cancer survival (132).

The effect of 4-MU as a promoter of chemotherapeutic treatment has also been determined in other types of tumors such as glioblastoma, the most frequent primary tumor of the central nervous system (133). In this work, the potential antitumor effect of 4-MU was tested in combination with temozolomide on GL26 glioblastoma cells. As expected, 4-MU decreased HA synthesis, but also diminished cell proliferation and induced apoptosis while reducing cell migration and the activity of MMPs. Besides, 4-MU sensitized GL26 cells to the effect of temozolomide and showed selective toxicity in tumor cells without exhibiting neurotoxic effects, highlighting its potential usefulness to improve glioblastoma treatment (66).

Another antineoplastic strategy mainly used for cancer treatment is radiotherapy. In this regards, 4-MU has been proposed as a positive modulator of radiotherapy response in fibrosarcoma. Saga et al. reported that co-administration of 4-MU enhanced the lethality of X-ray irradiation in HT1080 human fibrosarcoma cells and decreased their invasiveness (86). After that, the authors continued investigating the molecular bases of their discovery and found that co-administration of 4-MU suppressed the activation of IL-6 and IL-8 after X-ray irradiation (86). Similar results have been observed for the upstream signaling component IL-1 (87). These results indicate that the radiosensitivity of fibrosarcoma cells is improved by suppressing inflammation through the administration of 4-MU.

Consistent results have also been found when evaluating 4-MU as a co-adjuvant of antineoplastic therapies against melanoma and CML. In the case of melanoma, one of the therapeutic strategies is based on the inhibition of the BRAF oncogene, since the most prevalent BRAF mutation in melanoma is directly associated with cellular metabolic reprogramming by the Warburg effect (134, 135). Therefore, treatment with BRAF inhibitors reverses the Warburg effect and stimulates mitochondrial activity, which favors disease control (136, 137). In this regards, Abildgaard et al. demonstrated that 4-MU potentiates the antitumor effect of the BRAF inhibitor vemurafenib (60). Particularly, they found that the combination of 4-MU and vemurafenib was more effective in reducing viability of ED-013 and ED-196 melanoma cells than vemurafenib treatment alone, inducing cell cycle arrest in G1 phase. These authors also found that 4-MU plus vemurafenib treatment increased the cellular production of ROS (60).

Similarly, different studies have proposed 4-MU as a candidate molecule for co-adjuvant treatments for CML. Uchakina et al. showed that 4-MU sensitizes K562 cells to doxorubicin treatment, by inhibiting HA synthesis and increasing apoptosis rates through p38 activation and PARP cleavage (63). Lompardía et al. found similar results when combining 4-MU treatment with the chemotherapeutic agent vincristine on K562 and K562 vincristine-resistant cells (Kv562) (64). These authors revealed that 4-MU decreased tumor cell proliferation and sensitized Kv562 resistant cells to vincristine effect and determined that 4-MU effect was related to the inhibition of P-glycoprotein and the induction of senescence (64). These results support the potential use of 4-MU for combination of therapies in cancer and may encourage preclinical validation and clinical testing of such treatment strategies.

6 4-MU REPURPOSED FROM A DIETARY COMPONENT TO AN ANTICANCER DRUG: POTENTIALS FOR ITS REPOSITIONING

By definition, "drug repositioning" is a method that can help the conventional drug discovery process by using existing drugs for treatment of a different disease instead of their original indication (138). During the COVID-19 pandemic, it has been shown that this reasoning about the reuse of drugs is an effective and fast way to provide a treatment solution in a short time (139). The integration of bioinformatics data tools or "Big Data" (-omic data, sequencing DNA/RNA, molecular modeling, tumor biobanks, clinical trials, etc.) and experimental data offers the possibility to identify how feasible drugs are to be reused (138). 4-MU, originally identified as a hepatoprotective component, could be considered for this purpose and be now used as an antitumoral drug. The results described in this review suggest that this drug could be a good option to improve efficacy and reduce toxicity of current cancer treatment.

7 CONCLUSIONS AND PERSPECTIVES

The mechanisms of action of 4-MU are not yet known in detail. However, different results suggest that some of these mechanisms may be independent of HA synthesis inhibition. In this sense, over the last years, some authors have described HA-independent effects for 4-MU toxicity (13, 75). For example, in trabecular meshwork cells of the eye, Keller et al. found that 4-MU reduced the ECM components versican and fibronectin, and that the addition of exogenous HA failed to reverse the effects of 4-MU (123). Since versican and fibronectin can affect tumor progression and development (140), it is likely that 4-MU can also affect the synthesis and organization of other ECM components to mediate its effects in tumor cells. However, more studies are required to corroborate this hypothesis. Together, these reports reinforce that 4-MU may have different anti-tumor mechanisms depending on the type of cancer. However, toxicological, pharmacokinetic and pharmacodynamic aspects that determine the treatment regimen (way of administration, doses that impact on its bioavailability, time of interval between them and schedule) should be extensively reviewed in preclinical studies. An important study performed by Kuipers et al. in an EAE mouse model determined that, to observe a systemic decrease in HA levels, 4-MU should be administered for 7 days or more and that longer use does not completely reduce HA levels (141). Besides, they observed that, after oral administration, 4-MU is rapidly metabolized to 4-MUG and in

minor proportion to 4-MUS and, since there is a low bioavailability of 4-MU, high doses are required to reach a considerable percentage at systemic level (141). Thus, its metabolites and bioavailability are important points to be considered in the use of 4-MU without risk of toxic effect. In fact, Nagy et al. showed that 4-MUG is a bioactive metabolite that can be hydrolyzed into 4-MU and that 4-MUG also had effects similar to those of 4-MU *in vivo* (142), suggesting that studies using 4-MU should rethink the concept of its bioavailability.

All these reports suggest the feasibility of using 4-MU in cancer treatment. However, deepening the knowledge of its mechanisms of action and other pharmacological aspects will allow its application in clinical trials and its consideration as a therapeutic option, in combination or not, in current oncology treatments.

AUTHOR CONTRIBUTIONS

DV contributed to the design of the review and combination of subtopics. DV, AI, PR, FS, IS, and LA each wrote the subtopic of the review. LA contributed to the conception and design of the review. DV, IS, and LA contributed to the final manuscript revision. All authors contributed to the article and approved the submitted version.

FUNDING

UNNOBA, SIB 0561/2019, UNNOBA (to LA and IS), PICTO UNNOBA 2019-00011 (to LA).

REFERENCES

1. Newman DJ, Cragg GM. Natural Products as Sources of New Drugs Over the Nearly Four Decades From 01/1981 to 09/2019. *J Natural Products* (2020) 83:770–803. doi: 10.1021/acs.jnatprod.9b01285
2. Jang DS, Park EJ, Hawthorne ME, Vigo JS, Graham JG, Cabieses F, et al. Potential Cancer Chemopreventive Constituents of the Seeds of Dipteryx Odorata (Tonka Bean). *J Nat Prod* (2003) 66(5):583–7. doi: 10.1021/np020522n
3. Lacy A. Studies on Coumarins and Coumarin-Related Compounds to Determine Their Therapeutic Role in the Treatment of Cancer. *Curr Pharm Des* (2005) 10(30):3797–811. doi: 10.2174/1381612043382693
4. Arshad A, Osman H, Bagley MC, Lam CK, Mohamad S, Zahariluddin ASM. Synthesis and Antimicrobial Properties of Some New Thiazolyl Coumarin Derivatives. *Eur J Med Chem* (2011) 46(9):3788–94. doi: 10.1016/j.ejmech.2011.05.044
5. Abdelhafez OM, Amin KM, Batran RZ, Maher TJ, Nada SA, Sethumadhavan S. Synthesis, Anticoagulant and PIVKA-II Induced by New 4-Hydroxycoumarin Derivatives. *Bioorg Med Chem* (2010) 18 (10):3371–8. doi: 10.1016/j.bmc.2010.04.009
6. Xia Y, Yang ZY, Xia P, Hackl T, Hamel E, Mauger A, et al. Antitumor Agents. 211. Fluorinated 2-Phenyl-4-Quinolone Derivatives as Antimitotic Antitumor Agents. *J Med Chem* (2001) 44(23):3932–6. doi: 10.1021/jm0101085.
7. Sunthitikawinsakul A, Kongkathip N, Kongkathip B, Phonnakhu S, Daly JW, Spande TF, et al. Coumarins and Carbazoles From Clausena Excavata Exhibited Antimycobacterial and Antifungal Activities. *Planta Med* (2003) 69(2):155–7. doi: 10.1055/s-2003-37716.
8. Bhattacharyya SS, Paul S, Mandal SK, Banerjee A, Boujedaini N, Khuda-Bukhsh AR. A Synthetic Coumarin (4-Methyl-7 Hydroxy Coumarin) has Anti-Cancer Potentials Against DMBA-Induced Skin Cancer in Mice. *Eur J Pharmacol* (2009) 614(1–3):128–36. doi: 10.1016/j.ejphar.2009.04.015.
9. Fylaktakidou K, Hadjipavlou-Litina D, Litinas K, Nicolaides D. Natural and Synthetic Coumarin Derivatives With Anti-Inflammatory / Antioxidant Activities. *Curr Pharm Des* (2005) 10(30):3813–33. doi: 10.2174/1381612043382710.
10. Mazimba O. Umbelliferone: Sources, Chemistry and Bioactivities Review. *Bull Fac Pharmacy Cairo Univ* (2017) 55(2):223–32. doi: 10.1016/j.bfopcu.2017.05.001
11. Kultti A, Pasonen-Seppänen S, Jauhiainen M, Rilla KJ, Kärnä R, Pyöriä E, et al. 4-Methylumbelliferone Inhibits Hyaluronan Synthesis by Depletion of Cellular UDP-Glucuronic Acid and Downregulation of Hyaluronan Synthase 2 and 3. *Exp Cell Res* (2009) 315(11):1914–23. doi: 10.1016/j.yexcr.2009.03.002
12. Spinelli FM, Vitale DL, Sevic I, Alaniz L. Hyaluronan in the Tumor Microenvironment. *Adv Exp Med Biol* (2020) 1245:67–83. doi: 10.1007/978-3-030-40146-7_3
13. Ishizuka S, Askew EB, Ishizuka N, Knudson CB, Knudson W. 4-Methylumbelliferone Diminishes Catabolically Activated Articular Chondrocytes and Cartilage Explants *via* a Mechanism Independent of Hyaluronan Inhibition. *J Biol Chem* (2016) 291(23):12087–104. doi: 10.1074/jbc.M115.709683
14. Rodríguez MM, Onorato A, Cantero MJ, Domínguez L, Bayo J, Fiore E, et al. 4-Methylumbelliferone-Mediated Polarization of M1 Macrophages Correlate With Decreased Hepatocellular Carcinoma Aggressiveness in Mice. *Sci Rep* (2021) 11(1):6310. doi: 10.1038/s41598-021-85491-0
15. Bhagavan NV, Ha C-E. Chapter 14 - Carbohydrate Metabolism II: Gluconeogenesis, Glycogen Synthesis and Breakdown, and Alternative Pathways. In: E Second, Editor. *Bhagavan N V, Ha C-EBT-E of MB*. San Diego: Academic Press (2015). p. 205–25.
16. Egan D, O'kennedy R, Moran E, Cox D, Prosser E, Thornes RD. The Pharmacology, Metabolism, Analysis, and Applications of Coumarin and Coumarin-Related Compounds. *Drug Metab Rev* (1990) 22(5):503–29. doi: 10.3109/03602539008991449
17. Ritschel WA, Hoffmann KA. Pilot Study on Bioavailability of Coumarin and 7-Hydroxycoumarin Upon Peroral Administration of Coumarin in a Sustained-Release Dosage Form. *J Clin Pharmacol* (1981) 21(7):294–300. doi: 10.1002/j.1552-4604.1981.tb01770.x
18. Vassallo JD, Hicks SM, Born SL, Daston GP. Roles for Epoxidation and Detoxification of Coumarin in Determining Species Differences in Clara Cell Toxicity. *Toxicol Sci* (2004) 82(1):26–33. doi: 10.1093/toxsci/kfh237
19. Marshall ME, Mohler JL, Edmonds K, Williams B, Butler K, Ryles M, et al. An Updated Review of the Clinical Development of Coumarin (1,2-Benzopyrone) and 7-Hydroxycoumarin. *J Cancer Res Clin Oncol* (1994) 120(1 Supplement):S39–42. doi: 10.1007/BF01377124
20. Pelkonen O, Raunio H, Rautio A, Pasanen M LM. Coumarins: Biology, Applications and Mode of Action. (1997). https://oehha.ca.gov/media/downloads/crnr/coumarinhid.pdf (Accesed May 10, 2021)
21. Lake BG. Coumarin Metabolism, Toxicity and Carcinogenicity: Relevance for Human Risk Assessment. *Food Chem Toxicol* (1999) 37:423–53. doi: 10.1016/S0278-6915(99)00010-1
22. Menezes JCJMDS, Diederich M. Translational Role of Natural Coumarins and Their Derivatives as Anticancer Agents. *Future Med Chem* (2019) 11 (9):1057–82. doi: 10.4155/fmc-2018-0375
23. Lake BG, Evans JG, Chapuis F, Walters DG, Price RJ. Studies on the Disposition, Metabolism and Hepatotoxicity of Coumarin in the Rat and Syrian Hamster. *Food Chem Toxicol* (2002) 40(6):809–23. doi: 10.1016/S0278-6915(02)00036-4
24. Krawzak HW, Heistermann HP, Andrejewski K, Hohlbach G. Postprandial Bile-Duct Kinetics Under the Influence of 4-Methylumbelliferone (Hymecromone). *Int J Clin Pharmacol Ther* (1995) 33(10):569–72.
25. García-Vilas JA, Quesada AR, Medina MÁ. 4-Methylumbelliferone Inhibits Angiogenesis *In Vitro* and *In Vivo*. *J Agric Food Chem* (2013) 61(17):4063–71. doi: 10.1021/jf303062h
26. Nagy N, Freudenberger T, Melchior-Becker A, Röck K, Ter Braak M, Jastrow H, et al. Inhibition of Hyaluronan Synthesis Accelerates Murine Atherosclerosis: Novel Insights Into the Role of Hyaluronan Synthesis.

Circulation (2010) 122(22):2313–22. doi: 10.1161/CIRCULATIONAHA.110.972653
27. Piccioni F, Fiore E, Bayo J, Atorrasagasti C, Peixoto E, Rizzo M, et al. 4-Methylumbelliferone Inhibits Hepatocellular Carcinoma Growth by Decreasing IL-6 Production and Angiogenesis. *Glycobiology* (2015) 25 (8):825–35. doi: 10.1093/glycob/cwv023
28. Olivares CN, Alaniz LD, Menger MD, Barañao RI, Laschke MW, Meresman GF. Inhibition of Hyaluronic Acid Synthesis Suppresses Angiogenesis in Developing Endometriotic Lesions. *PloS One* (2016) 11(3):e0152302. doi: 10.1371/journal.pone.0152302
29. Nagy N, Kuipers HF, Frymoyer AR, Ishak HD, Bollyky JB, Wight TN, et al. 4-Methylumbelliferone Treatment and Hyaluronan Inhibition as a Therapeutic Strategy in Inflammation, Autoimmunity, and Cancer. *Front Immunol* (2015) 6(MAR):1–11. doi: 10.3389/fimmu.2015.00123
30. Theocharis AD, Tsara ME, Papageorgacopoulou N, Karavias DD, Theocharis DA. Pancreatic Carcinoma Is Characterized by Elevated Content of Hyaluronan and Chondroitin Sulfate With Altered Disaccharide Composition. *Biochim Biophys Acta - Mol Basis Dis* (2000) 1502(2):201–6. doi: 10.1016/S0925-4439(00)00051-X
31. Lipponen P, Aaltomaa S, Tammi R, Tammi M, Ågren U, Kosma VM. High Stromal Hyaluronan Level is Associated With Poor Differentiation and Metastasis in Prostate Cancer. *Eur J Cancer* (2001) 37(7):849–56. doi: 10.1016/S0959-8049(00)00448-2
32. Sironen RK, Tammi M, Tammi R, Auvinen PK, Anttila M, Kosma VM. Hyaluronan in Human Malignancies. *Exp Cell Res* (2011) 17(4):383–91. doi: 10.1016/j.yexcr.2010.11.017
33. Toole BP. Hyaluronan-CD44 Interactions in Cancer: Paradoxes and Possibilities. *Clin Cancer Res* (2009) 15(24):7462–68. doi: 10.1158/1078-0432.CCR-09-0479
34. Vitale DL, Spinelli FM, Del Dago D, Icardi A, Demarchi G, Caon I, et al. Co-Treatment of Tumor Cells With Hyaluronan Plus Doxorubicin Affects Endothelial Cell Behavior Independently of VEGF Expression. *Oncotarget* (2018) 9(93):36585–602. doi: 10.18632/oncotarget.26379
35. McBride WH, Bard JBL. Hyaluronidase-Sensitive Halos Around Adherent Cells: Their Role in Blocking Lymphocyte-Mediated Cytolysis. *J Exp Med* (1979) 149(2):507–15. doi: 10.1084/jem.149.2.507
36. Malvicini M, Fiore E, Ghiaccio V, Piccioni F, Rizzo M, Olmedo Bonadeo L, et al. Tumor Microenvironment Remodeling by 4-Methylumbelliferone Boosts the Antitumor Effect of Combined Immunotherapy in Murine Colorectal Carcinoma. *Mol Ther* (2015) 23(9):1444–55. doi: 10.1038/mt.2015.112
37. Nagase H, Kudo D, Suto A, Yoshida E, Suto S, Negishi M, et al. 4-Methylumbelliferone Suppresses Hyaluronan Synthesis and Tumor Progression in SCID Mice Intra-Abdominally Inoculated With Pancreatic Cancer Cells. *Pancreas* (2017) 46(2):190–7. doi: 10.1097/MPA.0000000000000741
38. Sato N, Cheng XB, Kohi S, Koga A, Hirata K. Targeting Hyaluronan for the Treatment of Pancreatic Ductal Adenocarcinoma. *Acta Pharm Sin B* (2016) 6(2):101–5. doi: 10.1016/j.apsb.2016.01.002
39. Cheng XB, Sato N, Kohi S, Koga A, Hirata K. 4-Methylumbelliferone Inhibits Enhanced Hyaluronan Synthesis and Cell Migration in Pancreatic Cancer Cells in Response to Tumor-Stromal Interactions. *Oncol Lett* (2018) 15(5):6297–301. doi: 10.3892/ol.2018.8147
40. Nakazawa H, Yoshihara S, Kudo D, Morohashi H, Kakizaki I, Kon A, et al. 4-Methylumbelliferone, a Hyaluronan Synthase Suppressor, Enhances the Anticancer Activity of Gemcitabine in Human Pancreatic Cancer Cells. *Cancer Chemother Pharmacol* (2006) 57(2):165–70. doi: 10.1007/s00280-005-0016-5
41. Yoshida E, Kudo D, Nagase H, Shimoda H, Suto S, Negishi M, et al. Antitumor Effects of the Hyaluronan Inhibitor 4-Methylumbelliferone on Pancreatic Cancer. *Oncol Lett* (2016) 12(4):2337–44. doi: 10.3892/ol.2016.4930
42. Yoshida E, Kudo D, Nagase H, Suto A, Shimoda H, Suto S, et al. 4-Methylumbelliferone Decreases the Hyaluronan-Rich Extracellular Matrix and Increases the Effectiveness of 5-Fluorouracil. *Anticancer Res* (2018) 38 (10):5799–804. doi: 10.21873/anticanres.12919
43. Lokeshwar VB, Lopez LE, Munoz D, Chi A, Shirodkar SP, Lokeshwar SD, et al. Antitumor Activity of Hyaluronic Acid Synthesis Inhibitor 4-Methylumbelliferone in Prostate Cancer Cells. *Cancer Res* (2010) 70 (7):2613–23. doi: 10.1158/0008-5472.CAN-09-3185
44. Yates TJ, Lopez LE, Lokeshwar SD, Ortiz N, Kallifatidis G, Jordan A, et al. Dietary Supplement 4-Methylumbelliferone: An Effective Chemopreventive and Therapeutic Agent for Prostate Cancer. *J Natl Cancer Inst* (2015) 107 (7):1–10. doi: 10.1093/jnci/djv085
45. An G, Park S, Lee M, Lim W, Song G. Antiproliferative Effect of 4-Methylumbelliferone in Epithelial Ovarian Cancer Cells Is Mediated by Disruption of Intracellular Homeostasis and Regulation of PI3K/AKT and Mapk Signaling. *Pharmaceutics* (2020) 12(7):1–14. doi: 10.3390/pharmaceutics12070640
46. Anttila MA, Tammi RH, Tammi MI, Syrjänen KJ, Saarikoski SV, Kosma VM. High Levels of Stromal Hyaluronan Predict Poor Disease Outcome in Epithelial Ovarian Cancer. *Cancer Res* (2000) 60(1).
47. Tamura R, Yokoyama Y, Yoshida H, Imaizumi T, Mizunuma H. 4-Methylumbelliferone Inhibits Ovarian Cancer Growth by Suppressing Thymidine Phosphorylase Expression. *J Ovarian Res* (2014) 7(1):1–8. doi: 10.1186/s13048-014-0094-2
48. Wang R, Zhou W, Wang J, Liu Y, Chen Y, Jiang S, et al. Role of Hyaluronan and Glucose on 4-Methylumbelliferoneinhibited Cell Proliferation in Breast Carcinoma Cells. *Anticancer Res* (2015) 35(9):4799–806.
49. Urakawa H, Nishida Y, Wasa J, Arai E, Zhuo L, Kimata K, et al. Inhibition of Hyaluronan Synthesis in Breast Cancer Cells by 4-Methylumbelliferone Suppresses Tumorigenicity *In Vitro* and Metastatic Lesions of Bone *In Vivo*. *Int J Cancer* (2012) 130(2):454–66. doi: 10.1002/ijc.26014
50. Brett M-E, Bomberger HE, Doak GR, Price MA, McCarthy JB, Wood DK. *In Vitro* Elucidation of the Role of Pericellular Matrix in Metastatic Extravasation and Invasion of Breast Carcinoma Cells. *Integr Biol* (2018) 10(4):242–52. doi: 10.1039/C7IB00173H
51. Okuda H, Kobayashi A, Xia B, Watabe M, Pai SK, Hirota S, et al. Hyaluronan Synthase HAS2 Promotes Tumor Progression in Bone by Stimulating the Interaction of Breast Cancer Stem-Like Cells With Macrophages and Stromal Cells. *Cancer Res* (2012) 72(1):537–47. doi: 10.1158/0008-5472.CAN-11-1678
52. Sukowati CHC, Anfuso B, Fiore E, Ie SI, Raseni A, Vascotto F, et al. Hyaluronic Acid Inhibition by 4-Methylumbelliferone Reduces the Expression of Cancer Stem Cells Markers During Hepatocarcinogenesis. *Sci Rep* (2019) 9(1):1–11. doi: 10.1038/s41598-019-40436-6
53. Rodríguez MM, Fiore E, Bayo J, Atorrasagasti C, García M, Onorato A, et al. 4Mu Decreases CD47 Expression on Hepatic Cancer Stem Cells and Primes a Potent Antitumor T Cell Response Induced by Interleukin-12. *Mol Ther* (2018) 26(12):2738–50. doi: 10.1016/j.ymthe.2018.09.012
54. Arai E, Nishida Y, Wasa J, Urakawa H, Zhuo L, Kimata K, et al. Inhibition of Hyaluronan Retention by 4-Methylumbelliferone Suppresses Osteosarcoma Cells *In Vitro* and Lung Metastasis *In Vivo*. *Br J Cancer* (2011) 105 (12):1839–49. doi: 10.1038/bjc.2011.459
55. Hamada S, Nishida Y, Zhuo L, Shinomura T, Ikuta K, Arai E, et al. Suppression of Hyaluronan Synthesis Attenuates the Tumorigenicity of Low-Grade Chondrosarcoma. *J Orthop Res* (2018) 36(6):1573–80. doi: 10.1002/jor.23794
56. Hasegawa K, Saga R, Takahashi R, Fukui R, Chiba M, Okumura K, et al. 4-Methylumbelliferone Inhibits Clonogenic Potency by Suppressing High Molecular Weight-Hyaluronan in Fibrosarcoma Cells. *Oncol Lett* (2020) 19(4):2801–8. doi: 10.3892/ol.2020.11370
57. Saga R, Matsuya Y, Takahashi R, Hasegawa K, Date H, Hosokawa Y. 4-Methylumbelliferone Administration Enhances Radiosensitivity of Human Fibrosarcoma by Intercellular Communication. *Sci Rep* (2021) 11(1):8258. doi: 10.1038/s41598-021-87850-3
58. Kudo D, Kon A, Yoshihara S, Kakizaki I, Sasaki M, Endo M, et al. Effect of a Hyaluronan Synthase Suppressor, 4-Methylumbelliferone, on B16F-10 Melanoma Cell Adhesion and Locomotion. *Biochem Biophys Res Commun* (2004) 321(4):783–7. doi: 10.1016/j.bbrc.2004.07.041
59. Yoshihara S, Kon A, Kudo D, Nakazawa H, Kakizaki I, Sasaki M, et al. A Hyaluronan Synthase Suppressor, 4-Methylumbelliferone, Inhibits Liver Metastasis of Melanoma Cells. (2005) 579(12):2722–6.. doi: 10.1016/j.febslet.2005.03.079
60. Abildgaard C, Rizza S, Christiansen H, Schmidt S, Dahl C, Abdul-Al A, et al. Screening of Metabolic Modulators Identifies New Strategies to Target Metabolic Reprogramming in Melanoma. *Sci Rep* (2021) 11(1):4390. doi: 10.1038/s41598-021-83796-8

61. Ban H, Uchakina O, McKallip RJ. Hyaluronic Acid Inhibitor 4-Methylumbelliferone Activates the Intrinsic Apoptosis Pathway in K562 Chronic Myelogenous Leukemia Cells. *Anticancer Res* (2015) 35(10).
62. Uchakina ON, Ban H, McKallip RJ. Targeting Hyaluronic Acid Production for the Treatment of Leukemia: Treatment With 4-Methylumbelliferone Leads to Induction of MAPK-Mediated Apoptosis in K562 Leukemia. *Leuk Res* (2013) 37(10):1294–301. doi: 10.1016/j.leukres.2013.07.009
63. Uchakina ON, Ban H, Hostetler BJ, McKallip RJ. Inhibition of Hyaluronic Acid Formation Sensitizes Chronic Myelogenous Leukemia to Treatment With Doxorubicin. *Glycobiology* (2016) 26(11):1171–9. doi: 10.1093/glycob/cww064
64. Lompardía SL, Papademetrio DL, Mascaró M, Del Carmen Álvarez EM, Hajos SE. Human Leukemic Cell Lines Synthesize Hyaluronan to Avoid Senescence and Resist Chemotherapy. *Glycobiology* (2013) 23(12):1463–76. doi: 10.1093/glycob/cwt074
65. Pibuel MA, Poodts D, Díaz M, Hajos SE, Lompardía SL. The Scrambled Story Between Hyaluronan and Glioblastoma. *J Biol Chem* (2021) 296:100549. doi: 10.1016/j.jbc.2021.100549.
66. Pibuel MA, Díaz M, Molinari Y, Poodts D, Silvestroff L, Lompardía SL, et al. 4-Methylumbelliferone as a Potent and Selective Antitumor Drug on a Glioblastoma Model. *Glycobiology* (2021) 31(1):29–43. doi: 10.1093/glycob/cwaa046
67. Yan T, Chen X, Zhan H, Yao P, Wang N, Yang H, et al. Interfering With Hyaluronic Acid Metabolism Suppresses Glioma Cell Proliferation by Regulating Autophagy. *Cell Death Dis* (2021) 12(5):486. doi: 10.1038/s41419-021-03747-z
68. Winawer SJ, Fletcher RH, Miller L, Godlee F, Stolar MH, Mulrow CD, et al. Colorectal Cancer Screening: Clinical Guidelines and Rationale. *Gastroenterology* (1997) 112(2):594–642. doi: 10.1053/gast.1997.v112.agast970594
69. Heffler M, M. Golubovskaya V, Conroy J, Liu S, Wang D, G. Cance W, et al. FAK and HAS Inhibition Synergistically Decrease Colon Cancer Cell Viability and Affect Expression of Critical Genes. *Anticancer Agents Med Chem* (2013) 13(4):584–94. doi: 10.2174/1871520611313040008
70. Wang TP, Pan YR, Fu CY, Chang HY. Down-Regulation of UDP-Glucose Dehydrogenase Affects Glycosaminoglycans Synthesis and Motility in HCT-8 Colorectal Carcinoma Cells. *Exp Cell Res* (2010) 316(17):2893–902. doi: 10.1016/j.yexcr.2010.07.017
71. Fries H, Elsässer HP, Mahlbacher V, Kern HF, Neumann K. Localisation of Hyaluronate (HA) in Primary Tumors and Nude Mouse Xenografts of Human Pancreatic Carcinomas Using a Biotinylated HA-Binding Protein. *Virchows Arch* (1994) 424(1):7–12. doi: 10.1007/BF00197386
72. Suto A, Kudo D, Yoshida E, Nagase H, Suto S, Mimura J, et al. Increase of Tumor Infiltrating γδ T-Cells in Pancreatic Ductal Adenocarcinoma Through Remodeling of the Extracellular Matrix by a Hyaluronan Synthesis Suppressor, 4-Methylumbelliferone. *Pancreas* (2019) 48(2):292–8. doi: 10.1097/MPA.0000000000001211
73. National Cancer Insitute. *Cancer Stat Facts: Cancer of Any Site*. National Cancer Institute. Available at: https://seer.cancer.gov/statfacts/html/all.html (Accesed May 10, 2021).
74. Kato N, Shibata K, Uchigasaki S, Kurose A. Relation Between Hyaluronan Synthesis and Cell Morphology in Ovarian Clear Cell Carcinomas. *Pathol Int* (2016) 66(4):218–23. doi: 10.1111/pin.12405
75. Karalis TT, Heldin P, Vynios DH, Neill T, Buraschi S, Iozzo RV, et al. Tumor-Suppressive Functions of 4-MU on Breast Cancer Cells of Different ER Status: Regulation of Hyaluronan/HAS2/CD44 and Specific Matrix Effectors. *Matrix Biol* (2019) 78–79(2017):118–38. doi: 10.1016/j.matbio.2018.04.007
76. Sevic I, Spinelli FM, Cantero MJ, Reszegi A, Kovalszky I, Garcia MG, et al. The Role of the Tumor Microenvironment in the Development and Progression of Hepatocellular Carcinoma. *In: Hepatocell Carcinoma Codon Publications* (2019) p:29–45. doi: 10.15586/hepatocellularcarcinoma.2019.ch2
77. Loomba R, Adams LA. Advances in non-Invasive Assessment of Hepatic Fibrosis. *Gut* (2020) 69(7):1343–52. doi: 10.1136/gutjnl-2018-317593
78. Piccioni F, Malvicini M, Garcia MG, Rodriguez A, Atorrasagasti C, Kippes N, et al. Antitumor Effects of Hyaluronic Acid Inhibitor 4-Methylumbelliferone in an Orthotopic Hepatocellular Carcinoma Model in Mice. *Glycobiology* (2012) 22(3):400–10. doi: 10.1093/glycob/cwr158
79. Mikami K, Endo T, Sawada N, Igarashi G, Kimura M, Sakuraba H, et al. Inhibition of Systemic Hyaluronan Synthesis Exacerbates Murine Hepatic Carcinogenesis. *In Vivo (Brooklyn)* (2018) 32(2):273–8. doi: 10.21873/invivo.11234
80. Takasugi M, Firsanov D, Tombline G, Ning H, Ablaeva J, Seluanov A, et al. Naked Mole-Rat Very-High-Molecular-Mass Hyaluronan Exhibits Superior Cytoprotective Properties. *Nat Commun* (2020) 11(1):2376. doi: 10.1038/s41467-020-16050-w
81. Nishida Y, Knudson W, Knudson CB, Ishiguro N. Antisense Inhibition of Hyaluronan Synthase-2 in Human Osteosarcoma Cells Inhibits Hyaluronan Retention and Tumorigenicity. *Exp Cell Res* (2005) 307(1):194–203. doi: 10.1016/j.yexcr.2005.03.026
82. Suzuki Y, Nishida Y, Naruse T, Gemba T, Ishiguro N. Pericellular Matrix Formation Alters the Efficiency of Intracellular Uptake of Oligonucleotides in Osteosarcoma Cells. *J Surg Res* (2009) 152(1):148–56. doi: 10.1016/j.jss.2008.02.037
83. Hosono K, Nishida Y, Knudson W, Knudson CB, Naruse T, Suzuki Y, et al. Hyaluronan Oligosaccharides Inhibit Tumorigenicity of Osteosarcoma Cell Lines MG-63 and LM-8 *In Vitro* and *In Vivo via* Perturbation of Hyaluronan-Rich Pericellular Matrix of the Cells. *Am J Pathol* (2007) 171(1):274–86. doi: 10.2353/ajpath.2007.060828
84. Gelderblom H, Hogendoorn PCW, Dijkstra SD, van Rijswijk CS, Krol AD, Taminiau AHM, et al. The Clinical Approach Towards Chondrosarcoma. *Oncologist* (2008) 13(3):320–9. doi: 10.1634/theoncologist.2007-0237
85. Van oosterwijk JG, Herpers B, Meijer D, Briaire-de bruijn IH, Cleton-jansen AM, Gelderblom H, et al. Restoration of Chemosensitivity for Doxorubicin and Cisplatin in Chondrosarcoma *In Vitro*: BCL-2 Family Members Cause Chemoresistance. *Ann Oncol* (2012) 23(6):1617–26. doi: 10.1093/annonc/mdr512
86. Saga R, Monzen S, Chiba M, Yoshino H, Nakamura T, Hosokawa Y. Anti-Tumor and Anti-Invasion Effects of a Combination of 4-Methylumbelliferone and Ionizing Radiation in Human Fibrosarcoma Cells. *Oncol Lett* (2017) 13(1):410–6. doi: 10.3892/ol.2016.5385
87. Saga R, Hasegawa K, Murata K, Chiba M, Nakamura T, Okumura K, et al. Regulation of Radiosensitivity by 4-Methylumbelliferone *via* the Suppression of Interleukin-1 in Fibrosarcoma Cells. *Oncol Lett* (2019) 17(3):3555–61. doi: 10.3892/ol.2019.9990
88. Zagars GK, Ballo MT, Pisters PWT, Pollock RE, Patel SR, Benjamin RS, et al. Prognostic Factors for Patients With Localized Soft-Tissue Sarcoma Treated With Conservation Surgery and Radiation Therapy: An Analysis of 1225 Patients. *Cancer* (2003) 97(10):2530–43. doi: 10.1002/cncr.11365
89. Eggermont AMM, Spatz A, Robert C. Seminar Cutaneous Melanoma. *Lancet* (2014) 383(9919):816–27. doi: 10.1016/S0140-6736(13)60802-8
90. Bai X, Flaherty KT. Targeted and Immunotherapies in BRAF Mutant Melanoma: Where We Stand and What to Expect. *Br J Dermatol* (2020) 185(2):253–62. doi: 10.1111/bjd.19394
91. Edward M, Quinn JA, Pasonen-Seppänen SM, McCann BA, Tammi RH. 4-Methylumbelliferone Inhibits Tumour Cell Growth and the Activation of Stromal Hyaluronan Synthesis by Melanoma Cell-Derived Factors. *Br J Dermatol* (2010) 162(6):1224–32. doi: 10.1111/j.1365-2133.2010.09699.x
92. André-Grégoire G, Gavard J. Spitting Out the Demons: Extracellular Vesicles in Glioblastoma. *Cell Adhesion Migration* (2017) 11(2):164–72. doi: 10.1080/19336918.2016.1247145.
93. Wiranowska M, Ladd S, Moscinski LC, Hill B, Haller E, Mikecz K, et al. Modulation of Hyaluronan Production by CD44 Positive Glioma Cells. *Int J Cancer* (2010) 127(3):532–42. doi: 10.1002/ijc.25085
94. Kim Y, Kumar S. CD44-Mediated Adhesion to Hyaluronic Acid Contributes to Mechanosensing and Invasive Motility. *Mol Cancer Res* (2014) 12(10):1416–29. doi: 10.1158/1541-7786.MCR-13-0629
95. Enegd B, King JAJ, Stylli S, Paradiso L, Kaye AH, Novak U, et al. Overexpression of Hyaluronan Synthase-2 Reduces the Tumorigenic Potential of Glioma Cells Lacking Hyaluronidase Activity. *Neurosurgery* (2002) 50(6):1311–8. doi: 10.1227/00006123-200206000-00023
96. Mueller AM, Yoon BH, Sadiq SA. Inhibition of Hyaluronan Synthesis Protects Against Central Nervous System (CNS) Autoimmunity and Increases CXCL12 Expression in the Inflamed CNS. *J Biol Chem* (2014) 289(33):22888–99. doi: 10.1074/jbc.M114.559583
97. Institute NNC. Cancer Facts & Figures 2020. *CA Cancer J Clin* (2020). Available at: https://www.cancer.org/research/cancer-facts-statistics/all-cancer-facts-figures/cancer-facts-figures-2020.html (Accesed May 10, 2021).

98. Jabbour E, Kantarjian H. Chronic Myeloid Leukemia: 2018 Update on Diagnosis, Therapy and Monitoring. *Am J Hematol* (2018) 93(3):442–59. doi: 10.1002/ajh.25011
99. Jain RK. Normalizing Tumor Microenvironment to Treat Cancer: Bench to Bedside to Biomarkers. In: Journal of Clinical Oncology. *Am Soc Clin Oncol* (2013) 31(17):2205–18. doi: 10.1200/JCO.2012.46.3653
100. Casey T, Bond J, Tighe S, Hunter T, Lintault L, Patel O, et al. Molecular Signatures Suggest a Major Role for Stromal Cells in Development of Invasive Breast Cancer. *Breast Cancer Res Treat* (2009) 114(1):47–62. doi: 10.1007/s10549-008-9982-8
101. Naba A, Clauser KR, Hoersch S, Liu H, Carr SA, Hynes RO. The Matrisome: *In Silico* Definition and *In Vivo* Characterization by Proteomics of Normal and Tumor Extracellular Matrices. *Mol Cell Proteomics* (2012) 11(4): M111.014647. doi: 10.1074/mcp.M111.014647
102. Knudson W, Biswas C, Toole BP. Interactions Between Human Tumor Cells and Fibroblasts Stimulate Hyaluronate Synthesis. *Proc Natl Acad Sci USA* (1984) 81(21):6767–71. doi: 10.1073/pnas.81.21.6767
103. Asplund T, Versnel MA, Laurent TC, Heldin P. Human Mesothelioma Cells Produce Factors That Stimulate the Production of Hyaluronan by Mesothelial Cells and Fibroblasts. *Cancer Res* (1993) 53(2).
104. Pirinen R, Tammi R, Tammi M, Hirvikoski P, Parkkinen JJ, Johansson R, et al. Prognostic Value of Hyaluronan Expression in Non-Small-Cell Lung Cancer: Increased Stromal Expression Indicates Unfavorable Outcome in Patients With Adenocarcinoma. *Int J Cancer* (2001) 95(1):12–7. doi: 10.1002/1097-0215(20010120)95:1<12::AID-IJC1002>3.0.CO;2-E
105. Liu J, Geng X, Hou J, Wu G. New Insights Into M1/M2 Macrophages: Key Modulators in Cancer Progression. *Cancer Cell Int* (2021) 21(1):389. doi: 10.1186/s12935-021-02089-2.
106. Bingle L, Brown NJ, Lewis CE. The Role of Tumour-Associated Macrophages in Tumour Progression: Implications for New Anticancer Therapies. *J Pathol* (2002) 196(3):254–65. doi: 10.1002/path.1027
107. McKee CM, Penno MB, Cowman M, Burdick MD, Strieter RM, Bao C, et al. Hyaluronan (HA) Fragments Induce Chemokine Gene Expression in Alveolar Macrophages: The Role of HA Size and CD44. *J Clin Invest* (1996) 98(10):2403–13. doi: 10.1172/JCI119054
108. Noble PW, Lake FR, Henson PM, Riches DWH. Hyaluronate Activation of CD44 Induces Insulin-Like Growth Factor-1 Expression by a Tumor Necrosis Factor-α-Dependent Mechanism in Murine Macrophages. *J Clin Invest* (1993) 91(6):2368–77. doi: 10.1172/JCI116469
109. Yamawaki H, Hirohata S, Miyoshi T, Takahashi K, Ogawa H, Shinohata R, et al. Hyaluronan Receptors Involved in Cytokine Induction in Monocytes. *Glycobiology* (2009) 19(1):83–92. doi: 10.1093/glycob/cwn109
110. Scheibner KA, Lutz MA, Boodoo S, Fenton MJ, Powell JD, Horton MR. Hyaluronan Fragments Act as an Endogenous Danger Signal by Engaging Tlr2. *J Immunol* (2006) 177(2):1272–81. doi: 10.4049/jimmunol.177.2.1272
111. Jiang D, Liang J, Noble PW. Hyaluronan as an Immune Regulator in Human Diseases. *Physiol Rev* (2011) 91(1):221–64. doi: 10.1152/physrev.00052.2009
112. Bollyky PL, Lord JD, Masewicz SA, Evanko SP, Buckner JH, Wight TN, et al. Cutting Edge: High Molecular Weight Hyaluronan Promotes the Suppressive Effects of CD4 + CD25 + Regulatory T Cells. *J Immunol* (2007) 179(2):744–7. doi: 10.4049/jimmunol.179.2.744
113. Spinelli FM, Vitale DL, Icardi A, Caon I, Brandone A, Giannoni P, et al. Hyaluronan Preconditioning of Monocytes/Macrophages Affects Their Angiogenic Behavior and Regulation of TSG-6 Expression in a Tumor Type-Specific Manner. *FEBS J* (2019) 286(17):3433–49. doi: 10.1111/febs.14871
114. Itatani Y, Kawada K, Yamamoto T, Sakai Y. Resistance to Anti-Angiogenic Therapy in Cancer-Alterations to Anti-VEGF Pathway. *Int J Mol Sci* (2018) 19(4):1232. doi: 10.3390/ijms19041232
115. Karamanos NK, Theocharis AD, Piperigkou Z, Manou D, Passi A, Skandalis SS, et al. A Guide to the Composition and Functions of the Extracellular Matrix. *FEBS J* (2021). doi: 10.1111/febs.15776
116. Provenzano PP, Hingorani SR. Hyaluronan, Fluid Pressure, and Stromal Resistance in Pancreas Cancer. *Br J Cancer Br J Cancer* (2013) 108:1–8. doi: 10.1038/bjc.2012.569
117. Dufort CC, DelGiorno KE, Carlson MA, Osgood RJ, Zhao C, Huang Z, et al. Interstitial Pressure in Pancreatic Ductal Adenocarcinoma Is Dominated by a Gel-Fluid Phase. *Biophys J* (2016) 110(9):2106–19. doi: 10.1016/j.bpj.2016.03.040
118. Jacobetz MA, Chan DS, Neesse A, Bapiro TE, Cook N, Frese KK, et al. Hyaluronan Impairs Vascular Funct0ion and Drug Delivery in a Mouse Model of Pancreatic Cancer. *Gut* (2013) 62(1):112–20. doi: 10.1136/gutjnl-2012-302529
119. Provenzano PP, Cuevas C, Chang AE, Goel VK, Von Hoff DD, Hingorani SR. Enzymatic Targeting of the Stroma Ablates Physical Barriers to Treatment of Pancreatic Ductal Adenocarcinoma. *Cancer Cell* (2012) 21 (3):418–29. doi: 10.1016/j.ccr.2012.01.007
120. Ariffin AB, Forde PF, Jahangeer S, Soden DM, Hinchion J. Releasing Pressure in Tumors: What do We Know So Far and Where Do We Go From Here a Review. *Cancer Res Am Assoc Cancer Res Inc* (2014) 74:2655–62. doi: 10.1158/0008-5472.CAN-13-3696
121. Infante JR, Korn RL, Rosen LS, Lorusso P, Dychter SS, Zhu J, et al. Phase 1 Trials of PEGylated Recombinant Human Hyaluronidase PH20 in Patients With Advanced Solid Tumours. *Br J Cancer* (2018) 118(2):153–61. doi: 10.1038/bjc.2017.327
122. Hakim N, Patel R, Devoe C, Saif MW. Why HALO 301 Failed and Implications for Treatment of Pancreatic Cancer. *Pancreas – Open J* (2019) 3(1):e1–4. doi: 10.17140/POJ-3-e010
123. Keller KE, Sun YY, Vranka JA, Hayashi L, Acott TS. Inhibition of Hyaluronan Synthesis Reduces Versican and Fibronectin Levels in Trabecular Meshwork Cells. *PloS One* (2012) 7(11):48523. doi: 10.1371/journal.pone.0048523
124. Andreichenko IN, Tsitrina AA, Fokin AV, Gabdulkhakova AI, Maltsev DI, Perelman GS, et al. 4-Methylumbelliferone Prevents Liver Fibrosis by Affecting Hyaluronan Deposition, FSTL1 Expression and Cell Localization. *Int J Mol Sci* (2019) 20(24):6301. doi: 10.3390/ijms20246301
125. Rilla K, Pasonen-Seppänen S, Rieppo J, Tammi M, Tammi R. The Hyaluronan Synthesis Inhibitor 4-Methylumbelliferone Prevents Keratinocyte Activation and Epidermal Hyperproliferation Induced by Epidermal Growth. *J Invest Dermatol* (2004) 123(4):708–14. doi: 10.1111/j.0022-202X.2004.23409.x
126. Nakamura T, Ishikawa T, Nanashima N, Miura T, Nozaka H, Nakaoka R, et al. 4-Methylumbelliferone Induces the Expression of Membrane Type 1-Matrix Metalloproteinase in Cultured Human Skin Fibroblasts. *Biochem Biophys Res Commun* (2002) 298(5):646–50. doi: 10.1016/S0006-291X(02)02516-0
127. Nakamura R, Kuwabara H, Yoneda M, Yoshihara S, Ishikawa T, Miura T, et al. Suppression of Matrix Metalloproteinase-9 by 4-Methylumbelliferone. *Cell Biol Int* (2007) 31(9):1022–6. doi: 10.1016/j.cellbi.2007.03.016
128. Hobarth K, Maier U, Marberger M. Topical Chemoprophylaxis of Superficial Bladder Cancer With Mitomycin C and Adjuvant Hyaluronidase. *Eur Urol* (1992) 21(3):206–10. doi: 10.1159/000474839
129. Ruponen M, Honkakoski P, Tammi M, Urtti A. Cell-Surface Glycosaminoglycans Inhibit Cation-Mediated Gene Transfer. *J Gene Med* (2004) 6(4):405–14. doi: 10.1002/jgm.522
130. Vitale DL, Caon I, Parnigoni A, Sevic I, Spinelli FM, Icardi A, et al. Initial Identification of UDP-Glucose Dehydrogenase as a Prognostic Marker in Breast Cancer Patients, Which Facilitates Epirubicin Resistance and Regulates Hyaluronan Synthesis in MDA-MB-231 Cells. *Biomolecules* (2021) 11(2):1–31. doi: 10.3390/biom11020246
131. Miyamoto H, Murakami T, Tsuchida K, Sugino H, Miyake H, Tashiro S. Tumor-Stroma Interaction of Human Pancreatic Cancer: Acquired Resistance to Anticancer Drugs and Proliferation Regulation Is Dependent on Extracellular Matrix Proteins. *Pancreas* (2004) 28(1):38–44. doi: 10.1097/00006676-200401000-00006
132. Lokman NA, Price ZK, Hawkins EK, Macpherson AM, Oehler MK, Ricciardelli C. 4-Methylumbelliferone Inhibits Cancer Stem Cell Activation and Overcomes Chemoresistance in Ovarian Cancer. *Cancers (Basel)* (2019) 11(8):1187. doi: 10.3390/cancers11081187
133. Wirsching H-G, Galanis E. Chapter 23 – Glioblastoma. *Handbook of Clinical Neurology* (2016) 134:381–97. doi: 10.1016/B978-0-12-802997-8.00023-2.
134. Hall A, Meyle KD, Lange MK, Klima M, Sanderhoff M, Dahl C, et al. Dysfunctional Oxidative Phosphorylation Makes Malignant Melanoma Cells Addicted to Glycolysis Driven by the V600EBRAF Oncogene. *Oncotarget* (2013) 4(4):584–99. doi: 10.18632/oncotarget.965
135. Haq R, Fisher DE, Widlund HR. Molecular Pathways: BRAF Induces Bioenergetic Adaptation by Attenuating Oxidative Phosphorylation. *Clin Cancer Res* (2014) 20(9):2257–63. doi: 10.1158/1078-0432.CCR-13-0898

136. Haq R, Shoag J, Andreu-Perez P, Yokoyama S, Edelman H, Rowe GC, et al. Oncogenic BRAF Regulates Oxidative Metabolism *via* PGC1α and MITF. *Cancer Cell* (2013) 23(3):302–15. doi: 10.1016/j.ccr.2013.02.003
137. Vazquez F, Lim JH, Chim H, Bhalla K, Girnun G, Pierce K, et al. Pgc1α Expression Defines a Subset of Human Melanoma Tumors With Increased Mitochondrial Capacity and Resistance to Oxidative Stress. *Cancer Cell* (2013) 23(3):287–301. doi: 10.1016/j.ccr.2012.11.020
138. Sleire L, Førde-Tislevoll HE, Netland IA, Leiss L, Skeie BS, Enger PØ. Drug Repurposing in Cancer. *Pharmacol Res* (2017) 124:74–91. doi: 10.1016/j.phrs.2017.07.013
139. Singh TU, Parida S, Lingaraju MC, Kesavan M, Kumar D, Singh RK. Drug Repurposing Approach to Fight COVID-19. *Pharmacol Rep* (2020) 72 (6):1479–508. doi: 10.1007/s43440-020-00155-6
140. Kobayashi N, Miyoshi S, Mikami T, Koyama H, Kitazawa M, Takeoka M, et al. Hyaluronan Deficiency in Tumor Stroma Impairs Macrophage Trafficking and Tumor Neovascularization. *Cancer Res* (2010) 70 (18):7073–83. doi: 10.1158/0008-5472.CAN-09-4687
141. Kuipers HF, Nagy N, Ruppert SM, Sunkari VG, Marshall PL, Gebe JA, et al. The Pharmacokinetics and Dosing of Oral 4-Methylumbelliferone for Inhibition of Hyaluronan Synthesis in Mice. *Clin Exp Immunol* (2016) 185 (3):372–81. doi: 10.1111/cei.12815
142. Nagy N, Gurevich I, Kuipers HF, Ruppert SM, Marshall PL, Xie BJ, et al. 4-Methylumbelliferyl Glucuronide Contributes to Hyaluronan Synthesis Inhibition. *J Biol Chem* (2019) 294(19):7864–77. doi: 10.1074/jbc.RA118.006166

Conflict of Interest: The authors declare that the research was conducted in the absence of any commercial or financial relationships that could be construed as a potential conflict of interest.

Publisher's Note: All claims expressed in this article are solely those of the authors and do not necessarily represent those of their affiliated organizations, or those of the publisher, the editors and the reviewers. Any product that may be evaluated in this article, or claim that may be made by its manufacturer, is not guaranteed or endorsed by the publisher.

frontiers in Pharmacology

REVIEW
published: 20 October 2021
doi: 10.3389/fphar.2021.710304

Polyphenols as Antitumor Agents Targeting Key Players in Cancer-Driving Signaling Pathways

Manuel Humberto Cháirez-Ramírez[1], *Karen Griselda de la Cruz-López*[1,2] *and Alejandro García-Carrancá*[1]*

[1]Unidad de Investigación Biomédica en Cáncer, Instituto de Investigaciones Biomédicas, Universidad Nacional Autónoma de México and Instituto Nacional de Cancerología, Secretaría de Salud, Mexico City, Mexico, [2]Programa de Doctorado en Ciencias Biomédicas, Instituto de Investigaciones Biomédicas, Universidad Nacional Autónoma de México, Mexico City, Mexico

Polyphenols constitute an important group of natural products that are traditionally associated with a wide range of bioactivities. These are usually found in low concentrations in natural products and are now available in nutraceuticals or dietary supplements. A group of polyphenols that include apigenin, quercetin, curcumin, resveratrol, EGCG, and kaempferol have been shown to regulate signaling pathways that are central for cancer development, progression, and metastasis. Here, we describe novel mechanistic insights on the effect of this group of polyphenols on key elements of the signaling pathways impacting cancer. We describe the protein modifications induced by these polyphenols and their effect on the central elements of several signaling pathways including PI3K, Akt, mTOR, RAS, and MAPK and particularly those affecting the tumor suppressor p53 protein. Modifications of p53 induced by these polyphenols regulate p53 gene expression and protein levels and posttranslational modifications such as phosphorylation, acetylation, and ubiquitination that influence stability, subcellular location, activation of new transcriptional targets, and the role of p53 in response to DNA damage, apoptosis control, cell- cycle regulation, senescence, and cell fate. Thus, deep understanding of the effects that polyphenols have on these key players in cancer-driving signaling pathways will certainly lead to better designed targeted therapies, with less toxicity for cancer treatment. The scope of this review centers on the regulation of key elements of cancer signaling pathways by the most studied polyphenols and highlights the importance of a profound understanding of these regulations in order to improve cancer treatment and control with natural products.

Keywords: polyphenols, signaling pathways, cancer, MAPK, PI3K-AKT pathway, p53, RAS

OPEN ACCESS

Edited by:
Cecilia Veronica Nunez, National Institute of Amazonian Research (INPA), Brazil

Reviewed by:
Sonam Mittal, Medical College of Wisconsin, United States
Ivana Samarzija, Rudjer Boskovic Institute, Croatia
Xia Guo, West China Second University Hospital, China

***Correspondence:**
Alejandro García-Carrancá
carranca@iibiomedicas.unam.mx

Specialty section:
This article was submitted to Pharmacology of Anti-Cancer Drugs, a section of the journal Frontiers in Pharmacology

Received: *15 May 2021*
Accepted: *15 September 2021*
Published: *20 October 2021*

Citation:
Cháirez-Ramírez MH, de la Cruz-López KG and García-Carrancá A (2021) Polyphenols as Antitumor Agents Targeting Key Players in Cancer-Driving Signaling Pathways. Front. Pharmacol. 12:710304. doi: 10.3389/fphar.2021.710304

INTRODUCTION

Cancer represents the second cause of death attributable to noncommunicable diseases, after only cardiovascular diseases. Despite the fact that the cancer death rate has been reduced in the last 30 years by about 31%, related to the fact that healthier lifestyle habits improve health status, it continues to be a major concern for public health systems worldwide (Sung et al., 2021). At present, there are numerous treatments for cancer, including surgery, chemotherapy, hormonal therapy, radiation, immune therapy, targeted treatments, nanotechnology, and RNA therapeutics (microRNA and RNAi). Chemotherapeutics have been predominant for systemic cancer

treatment; the majority of these are acting to cause DNA damage in order to kill or to inhibit cells from an accelerated rate of division. Chemotherapeutics are administered as single doses or short therapies at the maximal tolerable dose, followed by a treatment-free time that must be observed to allow for the recovery of normal cells (Nurgali et al., 2018). Despite the benefits of chemotherapy, it gives rise to adverse effects including hematological toxicity, alterations of gastrointestinal activity, alopecia, alterations of neurological activity, anaphylaxis, hepatotoxicity, and nephrotoxicity. The adverse effects of systemic chemotherapy are often severe and reduce the quality of life of patients. Although many adverse effects can be prevented with adequate prophylaxis, the toxicity of some agents cannot be controlled; therefore, a dose reduction becomes the only alternative. In this regard, plant-derived natural compounds such as polyphenols may arise as ideal alternatives for single or concomitant therapies for cancer treatment with more effectiveness, safety, and less toxicity.

Plant-derived natural compounds have been used for the prevention and treatment of many diseases. Plants produce a wide range of secondary metabolites that confer on them great adaptability to act as antimicrobial agents, as growth enhancers, in resistance to water stress, as sun screeners, and as an aid to repel predators (Weng et al., 2012). Secondary metabolites include polyphenols with nearly 10,000 known members, composed of several aromatic rings and multiple hydroxyl groups in their structure, with moderate water solubility and considerable antioxidant capacity (Brglez Mojzer et al., 2016). Individuals obtain approximately 1 g/day of polyphenols from their diet; however, this varies according to socioeconomic factors, gender, and the region of the world where people live. More than 800 polyphenols have been identified in food sources, including cereals, cocoa, coffee, tea, wine, and berries (Pérez-Jiménez et al., 2010). Despite the advances in drug discovery and development during the last decades, herbal medicine continues to be used as primary therapy in many developing countries (nearly 4 billion persons) (Ekor, 2014). Regular consumption of polyphenols has been related to beneficial health effects, including regulation of the intestinal microbiota and antiaging effects (Shimizu et al., 2019), a risk reduction of atherosclerosis (Nie et al., 2019), a decrease in the risk of colorectal cancer development (Bahrami et al., 2019), and the modulation of antioxidant enzymes through Nrf2 regulation (Lee et al., 2018). One of the major challenges for the therapeutic use of polyphenols is their low oral bioavailability. The absorption, transportation, bioavailability, and bioactivity of polyphenols are of interest in terms of their use and as new drug candidates. After oral administration, polyphenols pass through the gastrointestinal tract (GI) with absorption in the stomach and small intestine, and some are biotransformed by gut microbiota or by those absorbed during the early stages of digestion by hepatic phase I/II metabolism, prior to reaching the systemic circulation, which may affect bioavailability and bioactivity. Results of importance consider all of these processes and how they will affect the pharmacokinetics and pharmacodynamics of polyphenols. However, accessibility, economic importance, beneficial health effects, and the safety of polyphenols compared to synthetic drugs (Karimi et al., 2015) make them perfect candidates to explore possible therapeutic effects for preventing or treating different types of cancer due to the capacity of polyphenols to modulate multiple signaling pathways such as MAPK and PI3K/Akt and the key proteins involved in cancer development, such as p53 and RAS, rendering a promising expectation regarding these compounds. The present review aimed at focusing on the chemistry, bioavailability, and bioactivities of polyphenols in the key elements involved in cancer development and progression.

POLYPHENOLS: THEIR CHEMISTRY AND THEIR IMPORTANCE IN HUMAN HEALTH

Relevant Members of the Polyphenol Family

Polyphenols are classified as derivatives of shikimic acid/phenylpropanoids (derived from tyrosine and phenylalanine) and polyketide (lacking functional groups related to nitrogen) pathways. For shikimic acid derivatives, phenylpropanoid units serve as the basis for multiple types of polyphenols, such as cinnamic (C6–C3), benzoic acids (C6–C1), flavonoids (C6–C3–C6), proanthocyanidins [(C6–C3–C6)n], stilbenoids (C6–C2–C6), and lignins [(C6–C3)n] (**Figure 1**) (Pereira et al., 2009; Cirkovic-Velickovic and Stanic-Vucinic, 2018).

Phenolic Acids

Phenolic acids are the simplest phenolic compounds, formed of only one phenolic ring with multiple hydroxy or methoxy groups attached to their backbone. Hydroxycinnamic acids are aromatic carboxylic acids with unsaturation in the side chain (commonly of *trans*-configuration) and are more abundant than hydroxybenzoic acids. Cinnamic acids work as phytohormones, which are important components of lignin and the precursors of chalcones, flavonoids, anthocyanins, and stilbenes (El-Seedi et al., 2012). Hydroxycinnamic acids are considered potent antitumor agents due to the presence of α, β-unsaturation, acting as Michael acceptors (De et al., 2011). Relevant hydroxycinnamic acids include caffeic, ferulic, p-coumaric, and sinapic acids, and the most representative hydroxybenzoic acids include gallic, vanillic, syringic, protocatechuic, and p-hydroxybenzoic acids. Phenolic acids can be found in vegetable-derived foods including cereals, legumes, soybeans, coffee, tea, rosemary, thyme, apples, various berries, plums, cherries, and citrus fruits (Clifford and Scalbert, 2000; El-Seedi et al., 2012). Different health effects have been related to phenolic acids. Chlorogenic acid has exhibited its anticancer potential by inducing differentiation through an increase of KHSRP, p53, and p21, a decrease of poor differentiation-related genes *c-Myc* and *CD44*, and downregulation of oncogenic miRNA-17 family members in cancer cell lines (Huang et al., 2019). Other mechanisms involve epigenetic regulation; gallic acid inhibits DNMT1 activity through the negative regulation of p-Akt, reducing the nuclear import and stability of DNMT1. Potential epigenetic targets include *CCNE2*, *CCND3*, *CDKN1A*, and *CCNB1* genes,

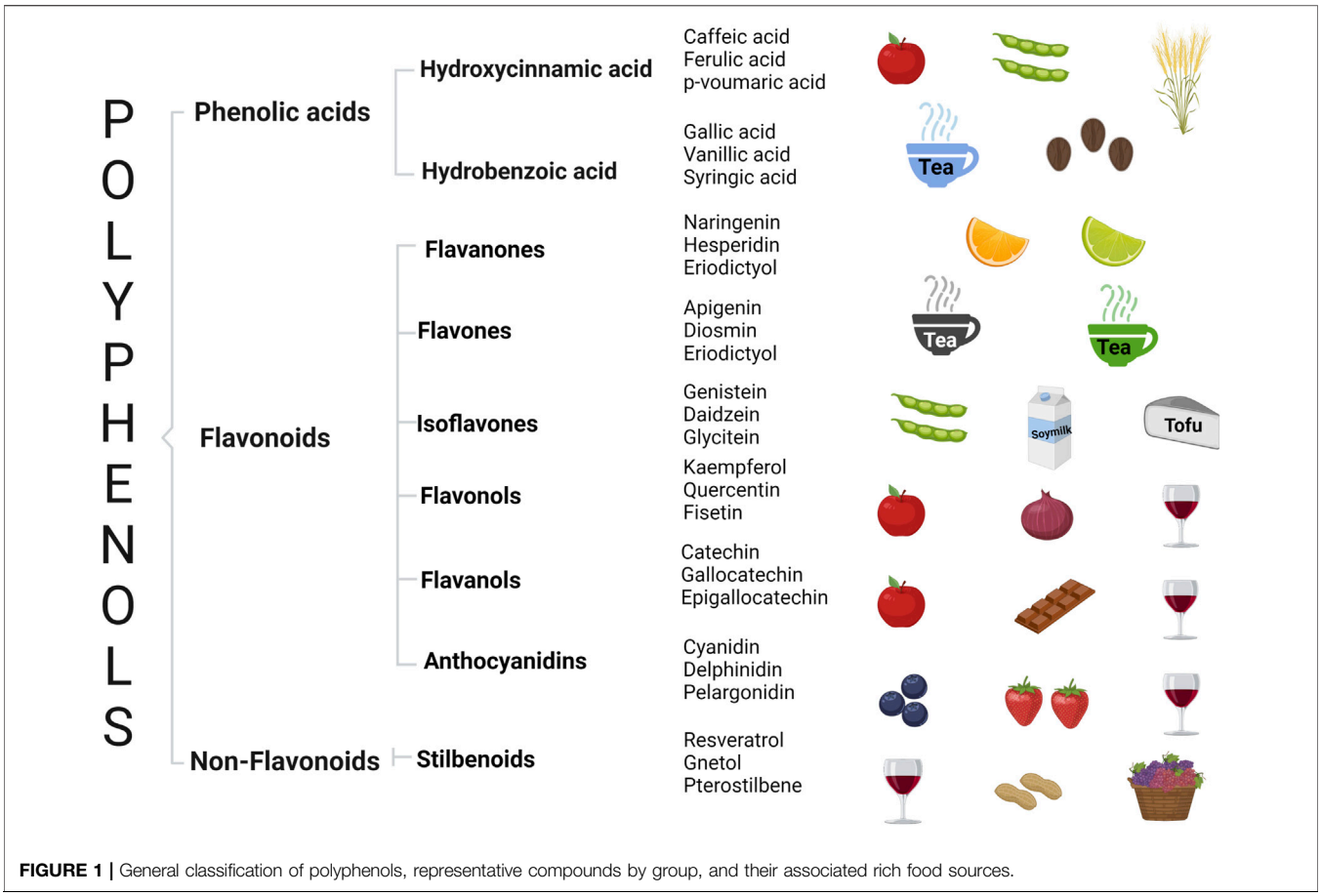

FIGURE 1 | General classification of polyphenols, representative compounds by group, and their associated rich food sources.

which play important roles in the GADD45 signaling pathway (Weng et al., 2018).

Flavonoids

Flavonoids are ubiquitous compounds in plants that are responsible for the fragrance, color, and flavor of fruits, seeds, and flowers, with important roles in pollination and protecting plants from ultraviolet (UV) light and acting as detoxifying agents and as signaling molecules, and they may play important roles in cold and heat acclimation (Koes et al., 1994; Panche et al., 2016). There are nearly 6,000 flavonoid-related compounds, including their derivatives flavanones, flavones, isoflavones, flavanols, flavonols, and anthocyanidins. Benzo-γ-pyrone is the basic chemical structure of flavonoids characterized by the presence of 15 carbon atoms as the base skeleton, organized in the form C6–C3–C6 (A+C–B) (two benzenic rings A and B) and linked by a unit of three carbons that may or not form a third-ring structure (pyran ring C). Flavonoids can occur as aglycones and as hydroxylated, methylated, and glycosylated derivatives and have great relevance for the sensory quality of citrus fruits. For example, flavonoids such as naringerin and neohesperidin are responsible for bitterness (Wang et al., 2017). Regular consumers of tea may have intakes of over 1,000 mg/day; however, normal diets only provide between 20 and 200 mg/day (Birt and Jeffery, 2013), and a regular dietary intake of flavonoids (500 mg/day) has been related to a diminished mortality risk (Bondonno et al., 2019).

Flavanones

The chemical structure is based on two benzene rings, A–B (the flavan core), bound by a dihydropyrone ring C, chirality at C3 of the C ring, and the absence of double-bound at the C2–C3 position, with 100 glycosides and 350 aglycones as known members (Barreca et al., 2017). The principal flavanones comprise naringenin, hesperidin, eriodictyol, taxifolin, didymin, and eriocitrin, regularly found in citric fruits and juices such as oranges, mandarins, and lemon (Khan et al., 2014; Barreca et al., 2017). The beneficial health effects related to the consumption of citric fruits have been linked to flavanones such as naringenin through modulation of the PI3K/Akt pathway and the nuclear translocation of the Nrf2 transcription factor, promoting the expression of HO-1 (heme oxygenase-1) and improving antioxidant defense (Zhang et al., 2017).

Flavones

Chemical characteristics of these flavonoids include a double bond between C3 and C4, a keto group at C4, and no substitution in C3. Flavones have a characteristic yellow color or can be colorless; they act as primary pigments in white flowers, as copigments in combination with anthocyanidins in blue

flowers, and as plant-signaling molecules. Relevant flavones include apigenin, diosmin, chrysin, tangeretin, luteolin, 7,8-dihydroxyflavone, and 6-hydroxiflavone. Flavones are found in plants employed for preparing infusions such as chamomile and parsley. Apigenin glycosides are abundant in traditional teas (black, green, and oolong), while luteolin glycosides are found in rooibos tea (Hostetler et al., 2017; Seleem et al., 2017). Important bioactivities have been related to flavones; apigenin has demonstrated health benefits including the inhibition of cell proliferation, apoptosis induction, the prevention of stem-cell migration through the upregulation of p21 and p27, and the downregulation of NF-κB and PI3K/Akt pathways (Erdogan et al., 2016). Luteolin inhibits MCF-7 cell proliferation and cell-cycle arrest and activates apoptosis through the regulation of IGF-1-dependent IGF-1R and p-Akt without disruption of ERK1/2 phosphorylation (Sabzichi et al., 2014).

Isoflavones

Isoflavones differ from flavones because of the phenyl group located in C3 instead of in C2 in the pyran ring, and some of their derivatives can form a D ring (e.g., rotenoid) (Marais et al., 2006). Isoflavones represent the most abundant flavonoids in soybeans, in soy-derived products (tofu, soymilk, soybean flour) (Jung et al., 2000; Preedy, 2013; Terahara, 2015), and in green and mung beans. In humans, isoflavones may act as phytoestrogens because of their similarity to 17-β-estradiol (Křížová et al., 2019). Isoflavones may be found as conjugated forms with acetyl, malonyl glycosides (e.g., genistin, daidzin, and glycitin), or aglycones (e.g., genistein, daidzein, and glycitein) (Zaheer and Humayoun Akhtar, 2017). Isoflavones may regulate cancer-related signaling pathways. Genistein and daidzein treatment of ovarian cancer cells inhibits invasion and cell migration in a dose-dependent manner through the downregulation of FAK and the PI3K/Akt/GSK signaling pathway and modulates p21 and cyclin D1 expression, related to the presence of ERβ (Chan et al., 2018).

Flavonols

Constituted of a 3-hydroxyflavone backbone, flavonols entertain an unsaturation between C2 and C3, an OH^- at C3, and a carbonyl group at C4, and along with flavones and anthocyanidins, they act as copigments to strengthen the color of flowers (Bueno et al., 2012). Flavonols are usually found as β-*O*-glycoside conjugates to facilitate storage in vacuoles (glucose being the most common conjugate) (Aherne and O'Brien, 2002). Flavonol-rich dietary sources include fresh capers, dried parsley, elderberry juice, rocket lettuce, red onions, fresh cranberries, fresh figs, apples, red wine, and tea (Di Matteo et al., 2007; Kozłowska and Szostak-Wegierek, 2014; Haytowitz et al., 2018). The principal flavonols include kaempferol, quercetin, fisetin, isorhamnetin, and myricetin, and their consumption has been related to a broad spectrum of health benefits. Different mechanisms are involved in the anticancer effects of flavonoids. Quercetin-3-*O*-glucoside inhibits cell growth, arrests the cell cycle in phase S, induces apoptosis through caspase-3 activation, and inhibits topoisomerase II activity in human hepatic-cancer cells (Sudan and Rupasinghe, 2014). Other mechanisms include apoptosis induction through modification of the BAX/Bcl-2 ratio and evoking paclitaxel chemosensitization by the downregulation of MDR-1 (associated with paclitaxel resistance) in myricetin-treated ovarian cells (Zheng et al., 2017).

Flavanols

Flavanols (also known as flavan-3-ols or catechins) have a pyran ring with an OH^- at C3, the B ring is bound to C2, and there is a lack of a double bond between C2 and C3 (allowing for two chiral centers). Flavan-3-ols are found either in free form or as gallic acid esters in different food sources such as apples, black tea, green tea, dark chocolate, and red wine (Rothwell et al., 2013). Relevant flavanols include the following: (+)-catechin; (+)-gallocatechin; (−)-epicatechin; (−)-epigallocatechin; (−)-epicatechin 3-gallate; (−)-epigallocatechin 3-gallate; theaflavin; theaflavin 3-gallate; theaflavin 3′-gallate; theaflavin 3,3′-digallate; and thearubigins (Haytowitz et al., 2018). Several health benefits have been related to flavanols. Lung cancer cells treated with (−)-epigallocatechin 3-gallate decreased the cell migration induced by human neutrophil elastase and induced α-1 antitrypsin through PI3K-pathway regulation (Xiaokaiti et al., 2015).

Proanthocyanidins

Proanthocyanidins (condensed tannins) are linked by C–C (sometimes by C–O–C) bonds, varying in the degree of polymerization (Rue et al., 2018). According to interflavan linkages, proanthocyanidins are classified as type A or type B. Type A lacks interflavan linkage but possesses another bond between the OH- from A ring and the C2 of C ring (C2–O–C7 or C2–O–C5) and type B with bonds between the C4 of B ring and either C6 or C8 of C ring (C4–C6 or C4–C8) (Rauf et al., 2019). Proanthocyanidins, which are composed of catechin or epicatechin subunits, are known as procyanidins; if they are composed of epigallocatechin subunits, they are called prodelphinidins. Proanthocyanidins confer astringency and bitterness and are regularly found in natural sources such as the fruits/seeds/peels of *Vitus vinifera*, *Punica granatum*, and *Theobroma cacao*, the leaves of *Fructus crataegi* and *Eucalyptus* spp., the flowers of *Rosa rugosa* and *Nymphaea tetragona*, and the roots/stems of *Rheum palmatum* and *Ipomoea batatas* (Yang et al., 2018). Procyanidins along with flavones possess high antioxidant activity (Lv et al., 2015); catechin-related compounds are the most powerful flavonoids against reactive oxygen species (ROS), with a broad spectrum of health benefits. Grape proanthocyanidins have been associated with a decrease of UVB-induced photocarcinogenesis in SKH-1 mice through the regulation of immunosuppression by decreasing the expression of IL-10 and increasing that of IL-12 (Katiyar et al., 2017). Proanthocyanidins also inhibit cell proliferation by means of the modulation of miRNA expression (Wang et al., 2019).

Anthocyanidins

Anthocyanidins are composed of ring A linked to ring C, which is bound in C3 to ring B, with no carbonyl group in C4 and two unsaturations in ring B at the O–C2 and C3–C4 positions.

Anthocyanidins are salt derivatives from the flavylium cation with a positive charge in the oxygen atom. Their color is pH-dependent, with red predominating under acidic conditions, whereas blue predominates under alkaline conditions (Laleh et al., 2005). Anthocyanidins can be found as aglycones, but when they are conjugated into a glycoside, they are known as anthocyanins (Khoo et al., 2017). Anthocyanidins act as naturally occurring pigments found in the flowers and fruits of many plants that confer red, pink, blue, or violet shades (Kumar and Pandey, 2013) and that occur in the outer cell layer of many edible products including blueberries, strawberries, raspberries, red wine, and red onion. The most representative anthocyanidins are cyanidin, delphinidin, pelargonidin, peonidin, malvidin, and petunidin (Castañeda-Ovando et al., 2009; Rothwell et al., 2013; Haytowitz et al., 2018). Many anthocyanidin-rich plants have been employed in traditional folk medicine and their effects have been extensively studied. A phase 0 clinical trial showed that an anthocyanin-rich raspberry lozenge administered to patients with oral squamous cell carcinomas (OSCC) for 14 days caused a reduction in the expression of prosurvival genes *AURKA*, *BIRC5,* and *EGFR*, and downregulation of proinflammatory genes *NFKB1*, *PTGS1*, and *PTGS2* (Knobloch et al., 2016).

Stilbenoids

Stilbenoids are nonflavonoid polyphenols derived from the phenylpropanoid pathway, in the form of hydroxylated derivatives of stilbene backbone C6–C2–C6 (two aromatic rings linked by a methylene bridge), with two possible planar configurations (*cis* or *trans*). Stilbenoids are usually found as aglycones, glycosidic/methoxyl conjugates, or oligomeric units (viniferins). Stilbenoids act as phytoalexins and 1,000 of these compounds have been identified to date (Xiao et al., 2008; Mekinić et al., 2016). Stilbenoid-rich sources include the plants of the Gnetaceae, Pinaceae, Cyperaceae, Fabaceae, and Dipterocarpaceae families; however, their content is <10% of that found in the Vitaceae family, and the richest sources of stilbenoids are wine, berries, and grape juice (Niesen et al., 2013; El Khawand et al., 2018). Resveratrol represents by far the most important compounds of its kind, followed by gnetol, piceid, astringin, pterostilbene, piceatannol, viniferins, etc. The bioactivities of stilbenoids include anticancer effects. Pterostilbene has shown upregulation of PTEN in prostate cancer cells and xenografts through the reduction of levels of oncogenic miR-17, miR-20a, and miR-106b (Dhar et al., 2015), thus highlighting the potential health effects of stilbenoids in terms of their being promising candidates as novel therapeutic agents.

Absorption and Metabolism of Polyphenols

There are several considerations for the development of new drugs, including bioaccessibility and bioavailability. Bioaccessibility is the fraction released from the food matrix into the intestinal milieu, rendering the drug bioavailable (Dima et al., 2020), whereas bioavailability is the extent of the drug absorbed that reaches the systemic circulation, with the drug becoming available at the site of action (Chow, 2014).

Ingested polyphenols are subjected to biotransformation in the GI tract by either digestive enzymes or the gut microbiota and may impact their bioactivities. The majority of polyphenols are released in the stomach (65%) and small intestine (10%) (Bouayed et al., 2011). The main sites of polyphenol absorption include the intestine and the colon (5–10% of the ingested polyphenols), whereas unabsorbed polyphenolics accumulate at mM concentrations in the large intestine, where the gut microbiota will exert biotransformation (Cardona et al., 2013) because complex polyphenols cannot be absorbed without modifications (Deprez et al., 2001). The gut microbiota involved in the biotransformation of polyphenols includes *Eubacterium* spp., *Clostridium* spp., *Bifidobacterium* spp., and *Lactobacillus* spp. (Marín et al., 2015). Biotransformed polyphenols are absorbed through the intestinal wall, transported to the liver where hepatic enzymes will break down (phase I metabolism) or conjugate (phase II metabolism) polyphenolics, and then they are distributed to target organs or eliminated in urine. The biotransformation of polyphenols may limit biological effects, and this may explain the discrepancy between *in vitro* and *in vivo* effects. For example, although many metabolites of anthocyanins can be found in urine, parent compounds are not detectable, possibly due to full metabolization (Agulló et al., 2020).

Another example is curcumin, which has low bioavailability and poor absorption, and the majority of the ingested curcumin is detected in the form of phase II metabolism-derived products, whereas the parent compound is scarcely detectable in the organism (Liu et al., 2016; Tsuda, 2018). The gut microbiota plays a significant role in the metabolism of curcumin, especially *Escherichia coli*, which converts curcumin into tetrahydrocurcumin (Hassaninasab et al., 2011). Biotransformation is not always linked to the loss of bioactivity; the oxidative metabolites of curcumin possess important biological effects (Edwards et al., 2017). However, like the majority of polyphenols, after passing through the GI, 90% of curcumin is excreted (Metzler et al., 2013); this is significant in that 10% of the ingested curcumin is responsible for its biological effects. The low bioavailability and complex metabolism of polyphenols render it difficult to present recommendations concerning their daily intake. The high variability of results of *in vivo* experiments and clinical trials is attributed to the poor absorption and metabolism of polyphenols; however, their safety and the ease of obtaining make them ideal candidates for the treatment of many diseases.

Anticancer Activities of Polyphenols Against the Foremost Malignant Tumors

Cancer constitutes an important public health concern worldwide with 19.3 million new cases and 10 million deaths in 2020. Principal cancer types include lung, colorectal, stomach, liver, breast, esophagus, prostate, and cervix uteri (Sung et al., 2021). Cancer development is closely related to unhealthy nutritional habits; the low consumption of fruits and vegetables (<800 g/day) has been related to an increase of 30–50% in the incidence of colorectal cancer (Vargas and Thompson, 2012; Aune et al., 2017). Plant-derived compounds are widely utilized by

individuals due to their cost accessibility, the belief in better effectiveness compared to medical prescription drugs, and the trend toward the use of products of natural origin. The contribution of plant-derived natural compounds to the pharmaceutical field is extensive; important examples include aescin, morphine, paclitaxel, and vincristine and, in the most recent two decades, more than 30% of US Food and Drug Administration (FDA)-approved drugs are derived from natural compounds (Li F. et al., 2019).

Polyphenols may act as antioxidants through two main mechanisms as follows: first, phenolic groups accept an electron to form relatively stable phenoxyl radicals, preventing oxidative damage in cellular components. Second, OH^- groups act as hydrogen donors and interact directly with reactive nitrogen species (RNS) and ROS (Leopoldini et al., 2011), which could explain their preventive role in oxidative damage.

Polyphenols provide protection from cancer risk factors, including tobacco, alcohol, unhealthy diets, sedentarism, and even those related to carcinogenic infections caused by pathogens such as the hepatitis B/C virus (HBV; HCV), the Epstein-Barr virus, and the human papillomavirus (HPV).

Nicotine represents the most toxic factor of tobacco, may lead to excessive cell proliferation through an increase in oxidative stress, and also has been related to an improvement of the invasiveness of lung and breast cancer cells (Bose et al., 2005; Dasgupta et al., 2009). Resveratrol prevents nicotine-induced cell proliferation through the MAPK signaling pathway by means of the downregulation of p-ERK in pancreatic cells (Chowdhury et al., 2018a). Alcohol consumption has been related to the development of colorectal cancer (Nishihara et al., 2014). Epigallocatechin 3-gallate (EGCG) inhibits ERK and activates JNK, thus fostering apoptotic cell death by the release of cytochrome c in human colon cancer cells (Cerezo-Guisado et al., 2015). Healthy food habits improve the health status of persons. The kaempferol present in apples and onions suppresses the expression of MMP-9 (related to metastasis progression) *via* the inactivation of the MAPK/AP-1 pathway in breast cancer cells (Li et al., 2015). HCV promotes the proteasomal degradation of pRb through the E6 ubiquitin-dependent mechanism, thus interfering with cell-cycle regulation and the response to cellular DNA damage. Treatment with theaflavins prevents the entry of HCV into hepatocytes but does not prevent viral replication (Chowdhury et al., 2018b); however, it represents a promising preventive approach for future malignancy induced by HCV infection. High-risk HPV represents other infectious agents of relevance for the development of malignant tumors; they account for approximately 25% of cases of HNSCC (HPV-16), and virtually all cervical cancers are caused by high-risk HPV (16 and 18). The combination of TriCurin polyphenols (curcumin, epicatechin 3-gallate, and resveratrol) reduces mRNA and the protein levels of E6 and E7, leading to the accumulation of p53 and pRb, thus decreasing tumor weight and cell proliferation by 86.3 and 19.9%, respectively (Piao et al., 2017). The effects of TriCurin on HNSCC appear promising, considering that this cancer is the sixth most prevalent malignancy worldwide (Shield et al., 2017).

Despite the fact that the bioactivities of polyphenols can often be limited by bioavailability, the detoxification metabolism, and the individual variability index, their wide range of health benefits is not limited to a single type of cancer or to a single mechanism of action. Therefore, polyphenols represent promising therapeutic agents for different cancers.

ACTIVITIES OF POLYPHENOLS IN RELEVANT CANCER-DRIVING SIGNALING PATHWAYS

p53 Tumor Suppressor

p53 Overview

p53 represents the most important human tumor suppressor and a central element for cell-cycle control and apoptosis. p53 is composed of 393 amino acid (aa) residues and includes the following six domains: two N-terminus transactivation domains (TAD, including TAD1 and TAD2); a proline-rich domain (PRD); a central DNA-binding domain (DBD); a tetramerization domain (TD); and a C-terminus regulatory domain (CRD) (a rich-lysine region). The acidic nature of TAD (~20%) contributes to the efficacy of the transactivation (Raj and Attardi, 2017). TAD are important for interaction with regulators including Mdm2 and MdmX and for the recruitment of chromatin modifiers CBP/p300, the latter prompting chromatin opening and p53 stabilization through the acetylation of CRD, preventing its ubiquitination (Raj and Attardi, 2017). The DBD contains six "hotspots" where the most frequent mutations occur in cancer. While R248Q and R273H disrupt p53/DNA binding, others produce local (R248Q; R273H) and global (R175H; R282W) conformational distortions (Brosh and Rotter, 2009; Baugh et al., 2018). TD facilitates p53 tetramerization, contains a nuclear export signal hidden in a tetrameric form that allows for nuclear accumulation, also influences the strength and conformation of DNA/p53 complexes, and is important for protein-protein interactions (CK2, PKC, and RelA bind to p53 through TD) (Chène, 2001; Gencel-Augusto and Lozano, 2020). CRD is required for the binding of promoters and structural changes in DBD (Laptenko et al., 2015) and undergoes extensive posttranslational modifications (PTM) on Lys residues.

p53 is under strict regulation because of its role as a central hub in the signal transduction of many cellular processes. In fact, while p53-null mice can live, those lacking Mdm2 and those that are incapable of regulating p53 die (Jones et al., 1995). The p53 half-life accounts for from 5 to 20 min in nearly all cell types, but after stress signals, senescence, or DNA damage, its stability is increased (Giaccia and Kastan, 1998). Negative regulators of p53 include Mdm2 and MdmX. Mdm2 promotes Lys ubiquitination at the C-terminus, targeting p53 for proteasomal degradation and abolishing the acetylation essential for the p53-mediated stress response (Tang et al., 2008). MdmX regulates p53 by direct interaction with TAD independent of E3-ubiquitin ligase activity (Raj and Attardi, 2017); however, MdmX can associate with Mdm2, enhancing its E3-ligase activity (Badciong and Haas, 2002). Recently, it has

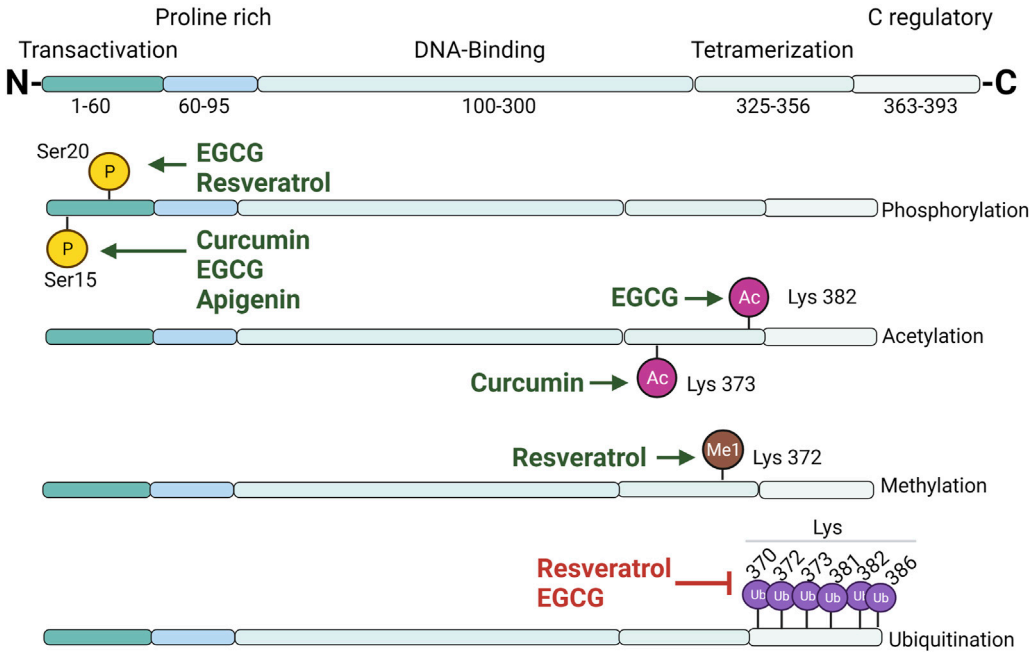

FIGURE 2 | Overview of p53 domain structure and posttranslational modifications induced by polyphenols. Principal sites where polyphenols induce p53 posttranslational modifications (phosphorylation, acetylation, methylation, or ubiquitination) are plotted. TAD, transactivation domain; PRD, proline-rich domain; DBD, DNA-binding domain; TD, tetramerization domain; CRD, C-terminal regulatory domain.

been demonstrated that MdmX inhibits the p53/DNA-binding function in association with CK1α (Wei et al., 2016). All of these control mechanisms highlight the importance of p53 regulation, which renders it an important therapeutic target due to its central role in cell fate control.

Polyphenols and Their Regulation on p53

p53 control is carried out by a variety of mechanisms, and the regulatory activities of polyphenols on p53 are widely reported in the literature. p53 undergoes extensive PTM (**Figure 2**), including phosphorylation, acetylation, ubiquitination, and methylation, which influence its stability, localization, and function; in addition, polyphenols may influence the posttranslational status of p53. It was recently described that curcumin promotes hyperphosphorylation in Ser15, thus promoting the expression of proapoptotic *Bex* genes in neuroblastoma cells (Sidhar and Giri, 2017). However, curcumin may also impair p53 folding into the required conformation for its phosphorylation, which affects its tumor-suppression function (Moos et al., 2004). Curcumin may alter p53/p300 interaction through p53 acetylation (Lys373), leading to the transcription of *BAX*, *PUMA*, and *Noxa*, thus enabling p53-mediated apoptosis in breast cancer cells (Sen et al., 2011). p53/p300 Interaction is important, considering that the genotoxic stress-related transcriptional activity of p53 is regulated by its interaction with its transcriptional coactivator p300. Nrf2 plays a protective role against oxidative stress in mammals by the regulation of antioxidant and detoxifying enzyme transcription (Saha et al., 2020). Dalton's lymphoma has low levels of Nrf2; treatment with curcumin restores Nrf2 messenger RNA (mRNA) levels and enhances the binding of the protein Nrf2 to ARE and the NF-2E consensus sequence, thus increasing the levels of endogenous antioxidants and enhancing the general antioxidant status. Interestingly, curcumin increased p53 mRNA and protein levels, and this increase was related to the stabilization of Nrf2 expression (Das and Vinayak, 2015). Nrf2 induces the expression of the antioxidant enzyme NQO1 that, aside from its primary function, forms a complex with p53, leading to its stabilization in curcumin-treated cervical cancer cells (Patiño-Morales et al., 2020).

Several anticancer effects have been linked to treatment with resveratrol. Resveratrol induces phosphorylation in Ser20, promoting p53 stabilization, thus leading to the activation of target genes and the induction of apoptosis (Hernandez-Valencia et al., 2018). Polyphenols may contribute to p53 stabilization through the prevention of Mdm2-mediated ubiquitination or by the modulation of deubiquitinating enzymes. Ubiquitination plays an important role in p53 degradation and localization. USP10 (a cytosolic deubiquitinating enzyme) with an affinity for p53 reverses Mdm2-mediated ubiquitination, cytoplasmatic degradation, and nuclear export and impacts the transcriptional activity of p53 (Sun and Dai, 2014). Resveratrol binds to G3BP1 and interrupts the G3BP1/USP10 interaction, releasing USP10 and promoting its deubiquitinating activity, increasing p53-mediated apoptosis in melanoma (Oi et al., 2015). Without the disruption of the p53/USP10 complex by G3BP1, p53-deubiquitination results were affected, leading to its proteasomal degradation.

SET7/9 methyltransferases regulate p53 through monomethylation in Lys372, resulting in protein stabilization and activation. Resveratrol treatment in colon cancer cells induces p53 methylation, leading to *BAX* and *PUMA* gene expression. The absence of SET7/9 abolishes p53 proapoptotic effects; hence, their presence appears to be essential for cell death (Liu L. D. et al., 2019).

Flavonols possess important regulatory activities on p53. Quercetin upregulates p53 mRNA and protein levels as well as increases caspase 3/7 activity in mesothelioma (Lee et al., 2015). Combined treatments of curcumin and quercetin augment phosphorylation and acetylation levels in lung carcinogenesis with the downregulation of Bcl2 and the upregulation of p21 and *BAX*, leading to apoptosis (Zhang and Zhang, 2018). An important premise with respect to polyphenols relies on their apparent affinity for inducing regulatory effects in cancer cells, but not in normal cells. Quercetin induces cytotoxic effects in leukemic and breast cancer cells but did not affect normal cells through direct quercetin/DNA interaction, thus increasing p53 and p-p53 levels, leading to the induction of apoptosis and cell-cycle arrest in the S phase. Quercetin reduced tumors, improved lifespan, and had no adverse effects in mice (Srivastava et al., 2016). A combination of quercetin with the chemotherapeutic MG132 (a specific 26S proteasome inhibitor) appears promising. This combination demonstrated a synergistic effect, extending the half-life of p53 from 74 to 184 min, stabilizing p53 through Ser15 phosphorylation, and preventing ubiquitination in HepG2 cells (Tanigawa et al., 2008).

Kaempferol, which is another important flavonol, also exhibits relevant bioactivities in p53 in cancer. Kaempferol treatment of human cancer cell lines containing mutant p53 led to apoptotic cell death with an increase of cleaved PARP and caspase (3, 7, 9) levels, the release of cytochrome c, and DNA fragmentation (Lee et al., 2014). In another study, human colon cancer cell lines (HCT116, HCT15, and SW480) were treated with kaempferol; molecular markers cleaved PARP and caspase-3 increased after treatment. The proapoptotic effects of kaempferol may be exerted through the regulation of different pathways; the expression of p53, p21, and p-p38 was upregulated, whereas p-JNK and p-ERK were attenuated. Interestingly, the proapoptotic effects of kaempferol were related to an increase in the intracellular ROS level (Choi et al., 2018).

Catechins, present in many tea-derived products, also possess important regulatory activities. EGCG promotes p53 accumulation, increases transcriptional activity through phosphorylation on Ser15 and Ser20, and prevents p53/Mdm2 interaction, increasing the half-life from 40 to 90 min in lung cancer (Jin et al., 2013). EGCG increases p53 acetylation in Lys382, enhancing its stabilization and DNA binding, increases p21 expression, downregulates HDAC-4, -5, and -6, and stimulates apoptotic induction in lung cancer cells (Oya et al., 2017). Relevant mechanisms of EGCG regulation on p53 include direct interaction between p53 and p53. EGCG binds to the N-terminal domain of p53 (aa involved in this interaction include W23 and W25, F54, G52, and T55) and shields p53 TAD, which is the Mdm2 interaction site (involving p53 residues F19, L22, T23, L26, G58, E68, V75, and C77), thus inhibiting Mdm2-mediated ubiquitination (Nagata et al., 2014; Karakostis et al., 2016; Zhao et al., 2021).

Flavones have also been linked to bioactivities against important types of cancer. Apigenin modulates the balance between prosurvival and proapoptotic pathways by the activation of p53, the repression of STAT-3, and decreased ROS levels in lymphoma cells (Granato et al., 2017). Apigenin enhances the response to Cisplatin-induced apoptosis by disruption of the p53/Mdm2 interaction and favors MAPK-mediated p53 Ser15 phosphorylation, protecting it from proteasomal degradation (Liu et al., 2017). The combination of apigenin with TRAIL has been related to apoptotic effects on non-small-cell lung cancer (NSCLC) in a p53-dependent manner. This combination revealed a synergistic effect by increasing the mRNA levels of DR4, DR5, and protein p53. TRAIL interaction with DR4/5 leads to the formation of the death-inducing signaling complex (DISC), with the subsequent binding of caspase-8, which activates the caspase cascade. The use of the p53 inhibitor (PFT-α) abolished the effect of the combined treatment; hence, these effects showed to be p53-dependent. Proapoptotic effects on lung cancer cells were related to the upregulation of BAX and Bad and to a prominent reduction of Bcl-2 and Bcl-xL levels (Chen et al., 2016).

As discussed so far, polyphenols appear to possess promising activities in p53 regulation through different mechanisms; however, several studies must be performed to elucidate the fully implicated mechanisms and consequences of polyphenol treatments in p53 regulation for the development of new, efficient, and safe cancer therapies.

MAPK Pathway

MAPK Overview

MAPK belong to serine/threonine kinases central to one of the principal signaling cascades involved in the control of cell growth, differentiation, survival, and cell death. MAPK signaling is activated in response to intra- and extracellular signals; these signals activate transmembrane glycoproteins of the tyrosine kinase receptor type, leading to the regulation of target genes. MAPK signaling cascades are composed of three main players as follows: the stress-activated protein kinase c-Jun NH2-terminal kinase (JNK), the stress-activated protein kinase 2 (SAPK2, p38), and the extracellular signal-regulated protein kinases (ERK1/2, p44/p42). JNK and p38 are activated by cytokines, hypoxia, genotoxicity, and oxidative stress; ERK is activated by mitogens and cytokines, principally by means of the activation of RAS family members (Rodríguez-Berriguete et al., 2012).

The dysregulation of MAPK can lead to cell transformation; the RAS–Raf–MEK–ERK axis is altered in 40% of human cancers, principally in RAS (30%) (Santarpia et al., 2012). RAS represents a family of GTPases composed of 150 G-proteins (HRAS, KRAS, and NRAS) and represents the first actors in the MAPK/ERK phosphorylation cascade (Johnson and Chen, 2012). Activation of RAS will result in ERK phosphorylation and activation; therefore, ERK translocates to the nucleus and promotes the activation of transcription factors such as c-Fos and c-Jun (Eblen, 2018).

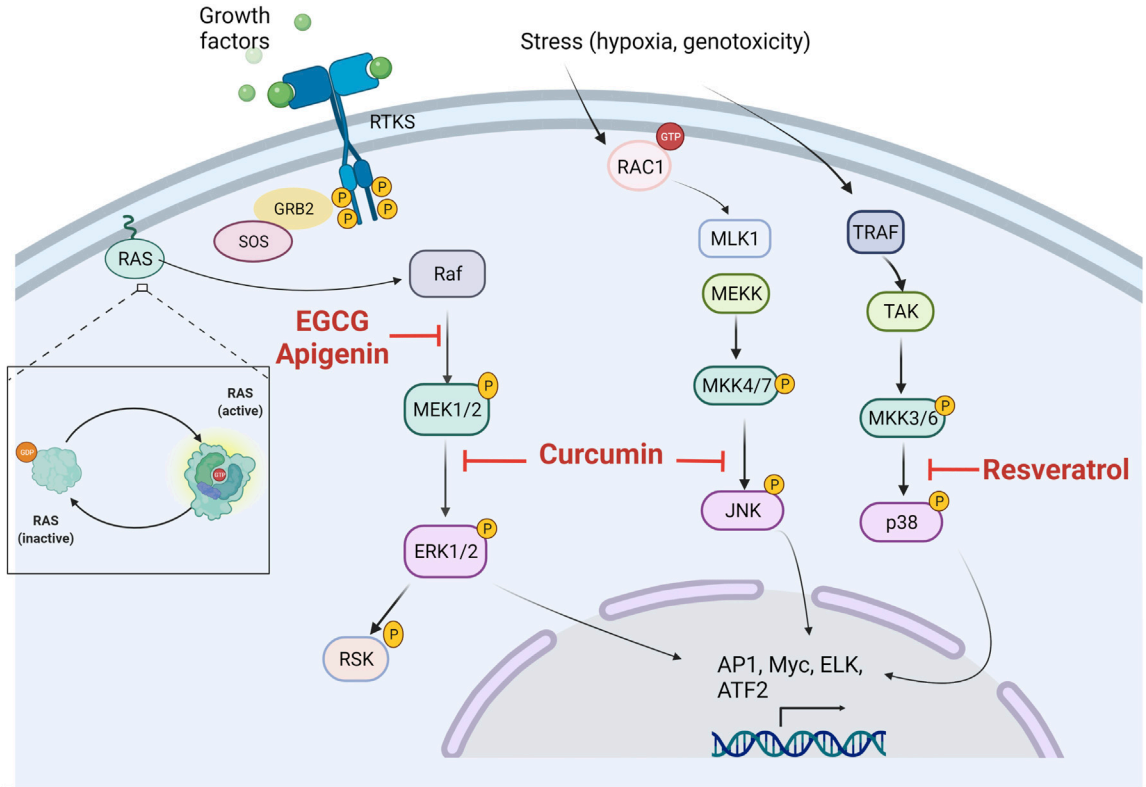

FIGURE 3 | Potential sites of inhibitory actions of polyphenols in MAPK signaling pathways. ERK, extracellular signal-related kinases; JNK, c-Jun amino-terminal kinases; p38, p38 mitogen-activated protein kinase.

JNK and p38 are known as stress-activated protein kinases. JNK translocates from the cytosol to the nuclei and evokes c-Jun activation through Ser63 and Ser73 phosphorylation, changing the expression patterns of BAX and Bcl-2 (Zhou et al., 2015). The role of JNK in cancer development is found in its multiple targets that are implicated in many cell-regulation mechanisms, such as STAT1/3, c-Jun, c-Myc, FOXO4, Bcl-2, ATF2, Smad2/3, PPARγ1, and RXRα (Dou et al., 2019). Multiple JNK-activated targets render JNK an important objective for targeted cancer therapies.

The p38 MAPK family comprises four isoforms expressed by different genes. Isoform p38α is ubiquitously expressed in all tissues, whereas isoforms β, γ, and δ are tissue-specific. Isoforms of p38 MAPK engage in redundant activities; however, the absence of p38α is lethal (Gerits et al., 2007). As many as 200–300 substrates are phosphorylated by p38 MAPK, including kinases involved in gene regulation, such as MSK1/2 (implicated in the regulation of transcription factors NF-κB p65 and STAT1/3), cytoplasmatic substrates such as cyclin D1, CDK inhibitors, Bcl-2 family proteins, and nuclear substrates including p53 (Cuadrado and Nebreda, 2010). Several interesting activities have been related to p38α, including, but not limited to, the suppression of ERK and JNK signaling by neutralizing RAS transformation, leading to senescence and cell-cycle arrest (Wang et al., 2002; Hui et al., 2007) and to the neutralization of tumorigenesis in lung, breast, colon, and liver through ROS production in response to oncogene activation, leading to the induction of p38-dependent apoptosis (Dolado et al., 2007). However, its role in tumor neutralization is only exerted at early stages; once the tumor is established, p38 promotes tumor growth and metastasis (Igea and Nebreda, 2015; Vidula et al., 2017).

The vast number of pathways regulated by MAPK make them ideal candidates for targeted therapies, and polyphenols may emerge as a promising alternative for the regulation of key players of MAPK pathways.

Polyphenols and Their Regulation on MAPK

The bioactivities exerted by natural phenolic compounds rely on their different regulation mechanisms, which strongly contribute to their anticancer activities. Polyphenols have been associated with promising regulatory activities in MAPK pathways (**Figure 3**).

Curcumin as one of the most promising anticancer agents has exhibited different regulation mechanisms in MAPK. Curcumin treatment in Ishikawa cells (endometrial carcinoma) induces apoptosis, cell-cycle arrest in phase S, and the downregulation of ERK and Jun mRNA, as well as the reduction of the p-ERK-2/c-Jun pathway. Interestingly, curcumin reduced cell invasion by the downregulation of p-ERK/c-Jun and diminishing AP-1 synthesis, thus decreasing MMP2/9 transcription (Zhang et al., 2019). The effects of curcumin on MAPK pathways are not only

limited to *in vitro* results. Curcumin treatment in the xenograft prostate cancer model demonstrated a reduction in tumor development. In this study, the mechanism involved in prostate cancer reduction by curcumin was related to a reduction of p-JNK, and curcumin was also effective for p-c-Jun reduction, leading to a decrease in Bcl-2 and Bcl-xL mRNA levels (Zhao W. et al., 2018). Stilbenoids have also revealed relevant activities for MAPK inhibition in different cancers. Resveratrol was effective in increasing p-p38 levels, leading to a decrease of Bcl-2 and an increase in Bad expression, as well as acting as a potent tumor growth inhibitor. The involvement of p38 was assessed using its inhibitor SB203580, which abolished the protective effects of the resveratrol treatment (Yuan et al., 2016). Urologic cancers represent a major concern. Resveratrol treatment reduces cell proliferation and the metastatic potential of renal-cancer cells. Resveratrol regulates ERK1/2 signaling pathways, specifically by altering the expression of ERK1/2, p-ERK1/2, E-cadherin, MMP-2, and MMP-9 (Zhao Y. et al., 2018). The apigenin treatment of melanoma-cancer cells A375 and C8161 promoted growth arrest through the downregulation of p-ERK1/2, p-Akt, and p-mTOR (Zhao et al., 2017). Tea polyphenols may act as potent anticancer agents alone or in combination with another chemotherapy. EGCG has demonstrated synergy with Sunitinib in cancer cell lines; both compounds decreased cell viability and suppressed the ERK pathway (Zhou et al., 2016). Kaempferol and quercetin stand as two of the most promising flavonols for cancer treatment. Quercetin possesses activities against colon cancer with mutant-type *KRAS* through JNK-pathway regulation; such activity results are very promising since *KRAS* is considered undruggable. In this study, quercetin selectively inhibited Akt and activated the p-JNK/c-Jun axis, leading to caspase-3 activation and subsequent apoptosis (Yang et al., 2019). In fact, flavonols can act as chemosensitizers. Kaempferol treatment overcomes resistance to 5-FU in resistant colon cancer cells. Concomitant treatment led to an increase in apoptosis, cell-cycle arrest, and modulated the protein expression of the JAK/STAT3, MAPK (ERK, p38), PI3K/Akt, and NF-κB involved in the progression and development of colorectal cancer (Riahi-Chebbi et al., 2019). All of these regulatory activities on MAPK pathways highlight the pharmacological importance that polyphenols may possess for the treatment of cancer by inhibiting these pathways; however, more research is necessary to fully elucidate the mechanisms involved.

PI3K/Akt Pathway

PI3K/Akt/mTORC1 Pathway

The phosphatidylinositol 3-kinase (PI3K)/protein kinase B (Akt) and the mammalian target of rapamycin (mTOR) are signaling pathways that regulate survival and growth processes (Hemmings and Restuccia, 2012). These pathways are activated through several cellular stimuli and control essential cellular functions such as proliferation, transcription, translation, survival, and growth (Liu R. et al., 2020).

There are three classes of PI3K isoforms. Class I PI3K are heterodimer lipid kinases composed of the p110 catalytic subunit and the p85 regulatory subunit. Akt, also known as protein kinase B (due to its similarity with PKA and PKC) is a serine protein kinase, activated by growth factors in a PI3K-dependent manner (Hemmings and Restuccia, 2012). PI3K phosphorylates the inositol ring of the membrane phospholipid, phosphatidylinositol-4,5-biphosphate (PI-4,5-P2), to generate phosphatidylinositol-3,4,5-trisphosphate (PIP3) on the cytoplasmic side of the cellular membrane (Rathinaswamy and Burke, 2019). PIP3 recruits a subset of pleckstrin homology (PH) domain-containing proteins, such as the same protein kinase Akt and the constitutively active phosphoinositide-dependent kinase 1 (PDK1). In turn, PDK1 phosphorylates Akt into T308 (Ding et al., 2010); however, maximal activation of Akt requires its additional phosphorylation in S473 located at the carboxyl-terminus site, mediated by mTORC2 (Ikenoue et al., 2008).

mTOR is one of the downstream signaling targets of PI3K/Akt, which regulates several cellular processes, such as cell growth, motility, survival, and metabolism (Saxton and Sabatini, 2017). mTOR exists in two protein complexes, that is, mTORC1 and mTORC2, of which mTORC1 is directly inhibited by Rapamycin, a macrolide and antifungal compound; however, mTORC2 is insensitive to rapamycin (Saxton and Sabatini, 2017). mTORC1 controls cell growth and proliferation mainly by promoting transcription, translation, ribosome biogenesis, and autophagic regulation. On the other hand, mTORC2 regulates proliferation and survival primarily by phosphorylating several members of the AGC family of protein kinases (Fu and Hall, 2020).

Akt inhibits the tuberous sclerosis complex (TSC) that limits mTORC1 signaling. The TSC complex is composed of the following three subunits: TSC1 (Harmatin), TSC2 (Tuberin), and TBC1D7. Akt phosphorylates TSC2 in five residues (S939, S981, S1130, S1132, and T1462), leading to its inactivation. The TSC complex is a negative regulator of the small GTPase Rheb (RAS homolog enriched in brain) (Takahashi et al., 2003) *via* the stimulation of GTP hydrolysis. On the other hand, Rheb-GTP is translocated into the lysosomal membrane, where it directly interacts with the catalytic domain of mTOR, promoting its activation (Dibble and Manning, 2013; Kim and Guan, 2019).

PI3K/Akt/mTOR pathways are one of the main prosurvival pathways that are activated in human cancers (Noorolyai et al., 2019). The PI3K/Akt/mTOR pathway is found deregulated in cancer, which is characterized by an overexpression/hyperactivation of its effector proteins and alterations in the genes that encode those proteins (Revathidevi and Munirajan, 2019).

Polyphenols and PI3K/Akt/mTOR in Cancer

The PI3K/Akt/mTOR pathway has been considered a major drug target due to its frequent hyperactivation in cancer (Liu Z. et al., 2020; Pevzner et al., 2021). Plant-derived natural compounds are one of the most reliable resources for cancer therapy. Several polyphenols, such as resveratrol, curcumin, apigenin, epigallocatechin 3-gallate, and quercetin, target numerous signaling pathways to exert tumor inhibitory and antiproliferative effects. One of these pathways is PI3K/Akt/mTOR (**Figure 4**).

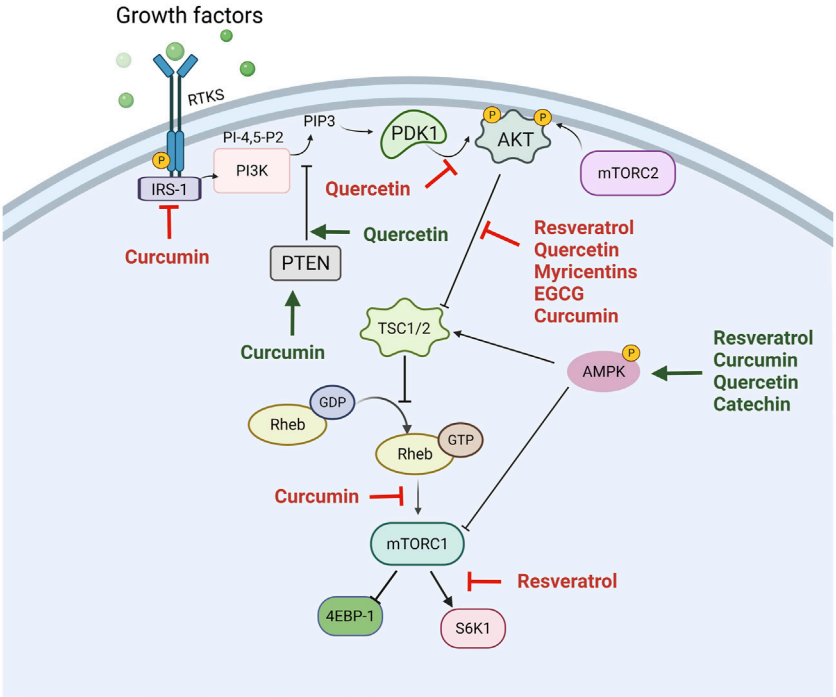

FIGURE 4 | The inhibition of the PI3K/Akt/mTOR pathway by polyphenols in cancer. The phosphoinositide 3-kinase-AKT-mammalian target of rapamycin (PI3K/Akt/mTOR) pathway is hyperactivated in several cancers and is important in terms of tumor cell growth and survival. Activation of RTK, such as insulin-like growth factor-1 receptor (IGFR), by growth factors such as insulin, can initiate activation of intracellular pathways. Akt is phosphorylated downstream of PI3K with various effects, including the activation of mTOR. mTOR phosphorylates p70S6K and 4E-binding protein 1 (4EBP-1), which then leads to an increased translation of mRNA and cell growth. Polyphenols act by inhibiting this pathway by means of decreasing the phosphorylation of several protein kinases that are part of this signaling pathway. The green arrows indicate the activation of the pathway, while the red arrows indicate the inhibition of the pathway using different polyphenols.

Hyperactivation of Akt signaling is frequent in several cancers, which maintains a high oxidative state in a tumor microenvironment that is necessary for tumor adaptation. Antioxidants are proposed to exhibit anticancer roles by interfering with the tumor microenvironment. Resveratrol is a natural antioxidant and affects cellular oxidative stress and mitochondrial membrane potential by interfering with the PI3K/Akt signaling pathway in SCLC H446 cell lines (Li et al., 2020). In another study conducted by Jiao and collaborators (2015), resveratrol inhibited invasive behaviors *in vitro and in vivo* by PI3K/Akt/NF-κB suppression and the inhibition of MMP-2 secretion in glioblastoma (Jiao et al., 2015). An alternative antioxidant ubiquitously found in dietary sources with potential health-promising effects is quercetin, a bioactive flavonoid that has been identified as having antioxidant and anticancer effects. Many reports showed that quercetin possesses anticancer activities *via* Akt inhibition. Recently, it was found that quercetin attenuates cell survival, inflammation, and angiogenesis by modulating Akt signaling in lymphoma-bearing mice (Maurya and Vinayak, 2017).

The PI3K/Akt/mTOR is known to be involved in drug resistance (Liu R. et al., 2020). In agreement with this, resveratrol prevents resistance to Adriamycin by decreasing the expression of multidrug resistance protein (MRP1) through PI3K/Akt/Nrf2 in acute myeloid leukemia (Li Y. et al., 2019). Earlier researchers observed that green tea polyphenols such as EGCG act as a chemosensitizer, leading to minimizing chemoresistance and enhancing the chemosensitivity of tumor cells. EGCG and theaflavin (TF) synergistically inhibited the growth of HeLa cells through PI3K/Akt inhibition (Chakrabarty et al., 2019). TF or EGCG reduced the expression of both p85 (the regulatory subunit of PI3K) and phosphorylated Akt (Ser473), and interestingly, the reduction of protein expression was observed in a much higher amount in the case of the combination of these doses of polyphenols. This synergistic activity might be due to stronger microtubule depolymerization by the simultaneous binding of TF and EGCG to a different site on tubulin. This stronger microtubule depolymerization results in a higher G2/M arrest of the cell cycle and more drastic mitochondrial damage and synergistic augmentation of apoptosis (Chakrabarty et al., 2019).

Resveratrol possesses antitumor activity when used alone or in combination. Bian et al. examined that the coadministration of resveratrol and rapamycin significantly reduced the phosphorylation of Akt and p70S6K compared to treatment with rapamycin alone. This coadministration ablates mTOR function and prevents Akt activation, which overcomes the feedback activation of Akt and improves the antitumor effects (Bian et al., 2020). In an investigation, it was shown that combining the grape polyphenol resveratrol, quercetin, and

catechin at equimolar concentrations inhibits mTOR signaling by means of a dual mechanism of PI3K/Akt and AMPK regulation and potentiates breast cancer to anti-EGFR therapy with Gefitinib, suggesting that this mixture may have synergistic effects against cancer (Castillo-Pichardo and Dharmawardhane, 2012).

PTEN is a tumor suppressor often deleted or mutated in a variety of cancers at a high frequency (Codrich et al., 2021; Zhang et al., 2021). It acts as a phosphatase that specifically catalyzes the dephosphorylation of the 3-phosphate of the inositol ring in phosphatidylinositol (3,4,5)-trisphosphate (PIP3), leading to the biphosphate product PIP2. The dephosphorylation of PIP3 results in the inactivation of the PI3K/Akt signaling pathway, because PIP3 is critical for the activation of Akt.

Resveratrol possesses anticancer activity through upregulating the bone morphogenetic protein 7 (BMP7) in order to inactivate the PI3K/Akt signaling pathway through partly suppressing the phosphorylation of PTEN in colorectal cancer. On the other hand, curcumin inhibits the proliferation of glioblastoma, and this effect is associated with the inhibition of both Akt and mTOR phosphorylation by promoting PTEN and p53 expression (Wang et al., 2020).

Accumulating evidence indicates that the PI3K/Akt/mTORC1 pathway is a negative regulator of autophagy (Yu et al., 2015). Autophagy is a process of the digestion of long-lived proteins and the damage of organelles and superfluously unwanted materials (Tavakol et al., 2019). According to the latter, it was demonstrated that resveratrol induces autophagic and apoptotic cell death through decreasing the phosphorylation of Akt in Ser473 and increasing the protein levels of phosphorylated AMPKα in Thr172. Resveratrol simultaneously enhanced the protein level of autophagy-associated proteins and the mRNA expression of the autophagic genes *Atg5, Atg12, Beclin-1,* and *LC3-II* in Cisplatin-resistant human oral cancer CAR cells (Chang et al., 2017). Interestingly, curcumin also induced autophagy and apoptosis in gastric cancer cells by activating p53 and the inhibition of the PI3K pathway (Fu et al., 2018).

Curcumin is a potent anticancer agent for the treatment of leukemia. A study by Zhou et al. in 2021 concluded that curcumin had stronger cytotoxic activity against acute myeloid leukemia cells compared with three other types of phytochemicals (epigallocatechin 3-gallate, genistein, and resveratrol). Mechanistically, curcumin treatment suppressed Akt activation, leading to cell-cycle arrest and apoptosis (Zhou et al., 2021).

mTORC1 functions as a downstream effector for PI3K/Akt, resulting in mTORC1 hyperactivation in a high percentage of human cancers (Saxton and Sabatini, 2017). Curcumin repressed mTORC1 signaling by two mechanisms involving the loss of IRS-1/Akt/PRAS40/Raptor/mTOR signaling and the activation of AMPK (Kaur and Moreau, 2021). These authors demonstrated that curcumin decreases the abundance of IRS-1 protein and inhibits the p-Akt (Ser473). Therefore, this led to a decrease in the phosphorylation of PRAS40 (Thr246), a negative regulator of mTORC1 (Kaur and Moreau, 2021).

On the other hand, in head-and-neck cancers, curcumin reduced the expression of phospholipase D1 (PLD1), the enzyme that catalyzes the production of phosphatidic acid (Borges et al., 2020). PLD1 binds to mTOR and displaces the mTOR-interacting protein (DEPTOR), an mTOR endogenous inhibitor, which results in mTORC1 activation and stabilization. In this manner, curcumin downregulates the PI3K/Akt/mTOR pathway and finally induces an arrest in the G2 phase of the cell cycle and induces cell death by apoptosis (Borges et al., 2020).

The PI3K/Akt pathway plays an important role in cancer progression, related to cell survival, growth, angiogenesis, and metastasis (Liu Z. et al., 2020; Lu et al., 2020). An important process in the progression of metastasis comprises vasculogenic mimicry (VM), the *de novo* formation of perfusable and vessel-like networks by aggressive tumor cells without endothelial cells. Several genes, such as vascular endothelial cadherin (*VE-cadherin*), participate in the formation of VM (Delgado-Bellido et al., 2017). Curcumin inhibits the VM of HCC cells by downregulating the Akt pathway (Chiablaem et al., 2014). Recently, it was shown that EGCG reduced p-Akt and Akt expression and reduced the ability of the VM of PC-3 cells. EGCG inhibited the nuclear localization of twist, followed by the downregulation of *VE-cadherin* expression, which in turn impaired the Akt pathway (Yeo et al., 2020). On the other hand, EGCG suppresses invasion and migration by preventing the cadherin switch and decreasing the expression level of TCF8/ZEB1, β-catenin, and vimentin in pancreatic cancer. Mechanistically, EGCG inhibited the Akt pathways in a time-dependent manner by suppressing IGFR phosphorylation and inducing Akt degradation (Wei et al., 2019). It has been reported that quercetin suppresses the mobility of breast cancer by the inhibition of glycolysis through the Akt-mTOR pathway and the activation of autophagy (Jia et al., 2018). Recently, it was shown that flavonoids quercetin and myricetin suppressed the HGF and TGF-α induced migration of HuH7 cells due to the attenuation of the PIK3/Akt pathway (Yamada et al., 2020).

RAS Oncogene

RAS Overview

RAS proteins are eukaryotic small GTPases that cycle back and forth between the GDP-bound inactive state and the GTP-bound active state. RAS-GTP leads to the activation of various signaling pathways, such as MAPK, PI3K, and RAL-GEF, promoting a variety of crucial cellular processes including cell proliferation, differentiation, and survival in response to extracellular stimuli. RAS family members are encoded by three highly homologous genes that encode four highly homologous proteins: HRAS, NRAS, KRAS4A, and KRAS4B (the results of alternative splicing at the C-terminus) (Weiss, 2020).

RAS signaling responds to many extracellular stimuli, such as soluble growth factors. Growth factor binding to cell-surface receptors creates intracellular docking sites for adaptor molecules and signal-relay proteins that recruit and activate guanine nucleotide-exchange factors (GEF). GEF displace guanine nucleotides from RAS and permit passive biding to GTP, which is abundant in the cytosol. On the other hand, RAS proteins are negatively regulated by GTPase-activating proteins (GAP), which markedly stimulate intrinsic GTPase activity by stabilizing a high energy-transition state that occurs

during the RAS-GTP hydrolysis reaction (Fernández-Medarde et al., 2021).

Human cancers frequently express mutant RAS proteins, termed "oncogenic RAS." RAS oncogene mutations are those that result in a persistent GTP-bound, active state. The most common oncogenic RAS mutation comprises the substitution of a single amino acid at positions 12, 13, or 61, which induces a constitutively active RAS phenotype (Muñoz-Maldonado et al., 2019).

KRAS is the most frequently mutated RAS family member that can potentiate tumor-promoting activity. These *KRAS* alterations have been identified in 25% of all cancers, such as blood, breast, colorectal, gynecological, lung, prostate, and pancreatic cancer, in which some cancers, pancreatic cancer (90%), colorectal cancer (52%), and lung adenocarcinoma (32%) have extremely high mutation rates (Mustachio et al., 2021).

RAS Oncogene and Polyphenols

The RAS oncogene is particularly difficult to target with specific therapeutics. These RAS-mutated cancers respond poorly to standard chemotherapy; thus, targeted approaches need to be found (Sheffels and Kortum, 2021). Significant efficacy has been demonstrated in the treatment of tumors with various polyphenols, in particular the majority of polyphenols that entertain specificity toward tumor cells that express mutated *KRAS* and not so in normal cells.

Several flavonoids were tested on *HRAS*-transformed cells. Of these, apigenin, kaempferol, and genistein were able to reverse the transformed phenotypes, affecting cellular proliferation, morphological change, and colony formation in soft agar. The antitumor effect of resveratrol on oncogenic RAS was explored using a WR-21 cell line derived from a submandibular salivary adenocarcinoma. These WR-21 cells express an activated human *HRAS* transgene (mutated Asp12) RAS protein, as well as p53. This established that resveratrol inhibited cell proliferation and induced cell death by apoptosis, through p53 without direct modulation of the expression of both mRNA and the protein of mutant *HRAS* (Young et al., 2005).

Manna et al. examined the *in vivo* antitumor efficiency of black tea polyphenols such as theaflavin, EGCG, and ECG in lung cancer. Treatment with these polyphenols inhibited benzo(a) pyrene-induced lung carcinogenesis in mice; moreover, it significantly reduced the expression of proliferation-associated genes such as *HRAS*, *c-Myc*, and *cyclin D1* compared to the B(a)P-treated lung lesions (Manna et al., 2009).

It was shown that polyphenols such as curcumin and resveratrol, on being supplemented in a diet, can prevent the formation and growth of tumors by downregulating *KRAS* expression (Limtrakul et al., 2001; Saud et al., 2014). EGCG inhibited cell proliferation induced by oncogenic RAS in intestinal epithelial cells and blocked cell-cycle transition at the G1 phase *via* inhibition of *cyclin D1* expression, and EGCG exhibited a stronger inhibitory effect on cell proliferation in transformed cells than on nontransformed cells (Peng et al., 2006). The latter demonstrated the potential of the natural compound EGCG as effective adjuvant therapy for colon tumors bearing RAS mutations.

An *in vivo* investigation was conducted by Saud and collaborators (2014) to evaluate the preventive and antitumor effect of resveratrol using a genetically engineered mouse model for colorectal cancer that has a conditional knock-out of both copies of APC combined with a latent activated gain-of-function in the *KRASG12D* mutation specifically in the distal colon. The finding demonstrated that resveratrol orally administered at human equivalent doses (210 mg/day) prevented initial tumor formation and retarded the growth of established tumors. Resveratrol suppressed the expression of *KRAS* both *in vitro* and *in vivo* and induced the expression of miR-96, a microRNA (miRNA) previously shown to regulate *KRAS* translation. These data indicate that resveratrol can prevent the formation and growth of colorectal tumors by downregulating *KRAS* expression (Saud et al., 2014).

Oncogenic RAS has been shown to sensitize colon cancer cells to treatment with quercetin; moreover, this quercetin preferentially reduces the half-time life of the oncogenic RAS protein vs. the wild-type RAS (Psahoulia et al., 2007). Epicatechin-rich cocoa polyphenol extract inhibits the growth of human premalignant and malignant *KRAS*-activated pancreatic ductal adenocarcinoma. This finding demonstrated that both the extract and epicatechin alone reduced the GTP-bound active RAS protein level without having any effect on total protein. Moreover, they showed that this extract decreased PI3K/Akt and MAPK signaling by inhibiting *KRAS* activity (Siddique et al., 2012).

Clinical Trials of Polyphenols With High Potential of Cancer Health Benefits

In recent times, polyphenols have gained importance as possible therapeutic agents, significantly increasing their use in clinical trials to explore potential health benefits in different cancers. Despite the abundance of studies in which curcumin, EGCG, resveratrol, quercetin, apigenin, and kaempferol have demonstrated excellent anticancer properties, the majority of these studies were performed in preclinical models. The bioactivities of polyphenols must also be investigated in humans because it cannot be assumed that the experimental results in cellular/animal models can be extrapolated to humans, principally due to differences in genetics and metabolism. The majority of these studies imply the exploration of pharmacokinetics, pharmacodynamics, safety, and the mechanisms by which these compounds reveal their effects. Currently, according to the US National Library of Medicine, 386,104 research studies can be consulted that have been conducted in all 50 US states and in 219 countries to date (August 2021), and 71, 39, 17, 14, 1, and 0 clinical trials related to different cancers using the polyphenols curcumin, EGCG, resveratrol, quercetin, apigenin, and kaempferol are available, with relevant studies listed in **Table 1**.

For quercetin, apigenin, and kaempferol, scarce evidence has been published to date in the literature on cancer clinical trials. An extensive search in the database clinicaltrials.gov resulted in only four completed studies of quercetin, and only two of these are reported in the literature. In the case of apigenin, the sole

TABLE 1 | Clinical trials of polyphenols-of-importance for cancer treatment.

Polyphenolic compound	Cancer type	Clinical trial Phase	*n*	Dose and trial length	Adverse and/or toxic effects	Effect	Endpoints	References
Curcumin	Precancerous lesions of the urinary bladder, Bowen's disease, uterine cervical intraepithelial neoplasia, oral leukoplakia, and intestinal metaplasia	I	25	0.5–8.0 g/day; oral administration for 3 months	No	Improved histological status of 7 out of 25 patients with high risk or precancerous lesions at all applied doses	No dose-dependent effect was observed since histological studies showed improvement at nearly all doses The recommended dose for a phase II clinical trial is 6–8 g/day	Chen et al. (2001)
	Multiple myeloma	I	15	3.0-4-0 g/day oral administration, combined with immune-modulatory drugs (IMD) or proteasome inhibitors (PI) for 1–3 months	Yes, two patients developed diarrhea	Decreased paraprotein and plasmacytosis levels by 38 and 59%, respectively	Curcumin, when used in a combination regimen in multiple myeloma patients, has comparable progression-free survival without the adverse effects of steroid-based combination therapies. Curcumin may be a viable alternative to corticosteroids in combination with an IMD or PI	Ramakrishna et al. (2020)
	Metastatic breast cancer	II	150	Paclitaxel 80 mg/m^2 and intravenous curcumin 300 mg/week for 12 weeks	No, curcumin may decrease fatigue in the paclitaxel-treated patients	Tumor reduction by 50.7% in curcumin treatment compared with 33.3% placebo	Paclitaxel-curcumin combination therapy showed superiority over paclitaxel monotherapy in patients with advanced or metastatic breast cancer	Saghatelyan et al. (2020)
	Pancreatic cancer	II	25	8 g/day orally administered curcumin for over 1 year	No	Curcumin showed poor oral bioavailability. Two patients showed relevant clinical activity: one patient showed stable disease for more than 1.5 years; patient showed brief but consistent tumor regression (73%) accompanied by increased levels of serum cytokines (IL6, IL8, IL10, and IL1) in the range of 4-35-fold. Curcumin reduced the expression of NF-κB, COX-2, and pSTAT3 in mononuclear blood cells from patients	Oral curcumin is well tolerated and, despite its limited intestinal absorption, had a stable plasmatic level for 4 weeks, and had biological activity in some patients with pancreatic cancer	Dhillon et al. (2008)
	Pancreatic cancer	I/II	21	8 g/day of orally administered curcumin combined with Gemcitabine at 1,000 mg/m^2 on days 1 and 8 plus 60 mg/m^2 of S-1 every 3 weeks	Yes, two patients developed grade 1 diarrhea	Seventeen patients (81%) died during the study period. Median survival time of 161 days and 19% of 1-year survival rate. Patients reported an improvement in cancer or in chemotherapy-related symptoms (e.g., fatigue, pain, and constipation) after the initiation of curcumin intake. Among 18 evaluable patients, no patient experienced a partial or complete response, and five patients (28%) demonstrated stable disease according to RECIST	Curcumin treatment in combination with chemotherapy showed interesting outcomes concerning its tolerability and fewer side effects and even after 6 months of intake had no significant toxicity	Kanai et al. (2011)
	Metastatic colorectal cancer	IIa	28	2 g/days orally administered curcumin plus standard chemotherapy of folinic acid/5-Fluorouracil/Oxaliplatin (FOLFOX) every 2 weeks for 12 cycles	Yes, 10 events of low-grade diarrhea	Patients treated with curcumin plus FOLFOX had fewer negative changes in functional, symptom, and global health scores after trial than FOLFOX. Decreased plasma levels of CXCL1 by 1.7-fold for curcumin plus FOLFOX in comparison with FOLFOX alone	Curcumin resulted in safe and tolerable adjunct to FOLFOX chemotherapy in patients with metastatic colorectal cancer	Howells et al. (2019)
EGCG	Bladder cancer	II	31	800–1,200 mg/day of orally administered EGCG for 14–28 days prior to surgery	Yes, 4 patients developed headache with dose-dependent relation	Nearly, all tumor and normal tissue levels of ECG, EGC, and EC are zero; none of the catechins showed a trend toward differences in tissue. A dose-dependent correlation of catechins was found in plasma and urine. Possible chemoprotective activity by reduction of tumor biomarkers PCNA and clusterin	Demonstration of EGCG levels in plasma, urine, and bladder tissue and the establishment of a dose-response relationship, as did modulation of tissue biomarkers of proliferation and apoptosis. The pharmacodynamics and favorable bioactivity warrant further clinical studies of EGCG in bladder cancer prevention	Gee et al. (2017)

(Continued on following page)

TABLE 1 | (*Continued*) Clinical trials of polyphenols-of-importance for cancer treatment.

Polyphenolic compound	Cancer type	Clinical trial Phase	*n*	Dose and trial length	Adverse and/or toxic effects	Effect	Endpoints	References
	Prostate cancer	II	97	200 mg/day of orally administered EGCG for 1 year	Yes, one patient developed nausea	Daily intake of EGCG, accumulated in plasma, and was well tolerated, and did not produce treatment-related adverse effects in men with ASAP or HGPIN. The intervention was not associated with increased risk of detection of high-grade disease in the group of men at end of the study. A decrease in PSA levels was related to EGCG treatment in patients	Data provided evidence of the safety of 200 mg EGCG, which showed a reduction of PSA levels. EGCG remains a possible candidate to be further tested for prostate cancer prevention or treatment	Kumar et al. (2015, 2016)
	Ovarian cancer	300	II	200 mg/day of Indole-3-Carbinol (I3C) and 200 mg/day of EGCG for 60 months with or without neoadjuvant chemotherapy	No	After 5 years of follow-up, maintenance therapy dramatically prolonged progression-free survival and overall survival compared to control Median overall survival increased by 16 months in I3C and EGCG groups (from 44 to 60 months) Median progression-free survival was 40 months in I3C and EGCG groups, while in groups without natural compounds treatment, the average progression-free survival was 23 months. The rate of patients with recurrent ovarian cancer with ascites after combined treatment was significantly less in maintenance therapy groups compared to the control	The endpoints were overall survival, progression-free survival, and the rate of patients with recurrent ovarian cancer with ascites after combined treatment within 5 years of follow-up	Kiselev et al. (2018)
	High-risk oral premalignant lesions	41	II	500–1,000 mg/m^2 of orally administered TID EGCG for 12 weeks	Yes, some patients developed grade 1 or 2 insomnia, headache, nausea, and nervousness	The clinical response rate of patients with high-risk oral premalignant lesions (OPL) was higher in all EGCG groups compared to placebo, and such an effect seemed to be dose-dependent, but no statistical significance was found. EGCG treatment improved histology and was well tolerated. Higher mean baseline stromal VEGF correlated with clinical, but not with histologic, response. Other biomarkers (epithelial VEGF, p53, Ki-67, cyclin D1, and p16 promoter methylation) were not associated with a response or survival. p16 promoter methylation was associated with shorter cancer-free survival. Stromal VEGF and cyclin D1 expression were downregulated in clinically responsive EGCG-treated patients and upregulated in nonresponsive patients. EGCG may suppress OPL by reducing angiogenic stimulus (stromal VEGF). From the limited pharmacokinetic sampling available, there was no correlation between clinical or histologic response and levels of EGCG	Evaluation of the clinical and histologic response of high-risk OPL at 12 weeks with three different doses of EGCG. Qualitative and quantitative toxicities of EGCG, effects on the expression of biomarkers, and any correlation between treatment efficacy and/or toxicity with plasma concentrations of EGCG. Clinical and histological responses were assessed by complete or partial disappearance of lessons and by an increase of lesions	Tsao et al. (2009)
Resveratrol	Healthy volunteers	40	I	0.5–5.0 g/day orally administered for 29 days	Yes, 28 volunteers experienced mild nausea, flatulence, abdominal discomfort, and diarrhea	Resveratrol was safe and generally well tolerated by patients and showed mild gastrointestinal symptoms. Six metabolic conjugates in volunteers' plasma were found, and the most abundant circulating metabolite was resveratrol-3-O-sulfate. Resveratrol decreased levels of IGF-1 and IGFBP-3, and there was a hint of pharmacodynamic activity in terms of the effect on circulating IGF protein levels at the 2.5-g dose, with a plasma level of 1.45 μM. IGF proteins may be used as potential biomarkers of pharmacological activity of resveratrol in humans because high levels of IGF have been related to several cancers; IGF is known to have antiapoptotic and mitogenic activities	Determination of clinical safety, pharmacokinetics, and effect on insulin-like growth factor axis at 29 days with four different doses of resveratrol. Safety was assessed by meeting the National Cancer Institute Common Terminology Criteria for Adverse Events (CTCAE). Plasma samples collected between days 21 and 28 of patients, parent compound, and metabolites of resveratrol were determined by HPLC. Pharmacodynamics was assessed in serum measuring IGF-1 and IGFBP-3 levels by ELISA	Brown et al. (2010)
	Colon cancer	8	I	Resveratrol was administered at 20 and 80 mg/day. Grape extract (GE) was administered at 0.073 and 0.114 mg/day. Both treatments were taken orally	No	No toxic effects were related to resveratrol or GE treatments. Patients treated with resveratrol/GE had no change in *Wnt* target gene expression in colon cancer. Resveratrol and GE seemed to have different effects on normal colonic mucosa, whereas inhibition of *Wnt* target gene expression was determined by microarray and confirmed by qRT-PCR of cyclinD1 and axinII. Resveratrol or GE may play a beneficial role in colon cancer prevention	The safety of resveratrol and GE was established by the report of any gastrointestinal symptoms. Clinical effects of resveratrol or GE were determined by the expression of Fz receptors, Wnt ligands, Wnt inhibitors, Wnt targets in normal mucosa, and colon cancer	Holcombe et al. (2009)

(Continued on following page)

TABLE 1 | (*Continued*) Clinical trials of polyphenols-of-importance for cancer treatment.

Polyphenolic compound	Cancer type	Clinical trial Phase	*n*	Dose and trial length	Adverse and/or toxic effects	Effect	Endpoints	References
	Prostate cancer	14	I	500 up to 4,000 mg/day of Muscadine grape extract capsules MPX (containing 1.2 mg of ellagic acid, 9.2 μg of quercetin, and 4.4 μg of *trans*-resveratrol) administered orally for 28 days, with a follow-up of >2 years	Yes, four patients developed gastrointestinal symptoms, including grade 1 flatulence, soft stools, and eructation	Treatment was considered safe, and no tolerability issues were found in patients. At a 4,000 mg dose, ellagic acid, quercetin, and resveratrol were undetectable in the plasma. The lack of statistically significant within-patient change in PSADT and shortening in PSADT in 36% of the patients raise concerns about the efficacy of MPX. Median within-patient PSADT increased by 5.3 months (not significant). No patients experienced a maintained decline in serum PSA from baseline	Assessment of safety, tolerability, pharmacokinetic parameters, and efficient doses of resveratrol. Safety and tolerability were evaluated according to National Cancer Institute's CTCAE. Pharmacokinetics was estimated by UPLC-ESI-MS/MS. Clinical benefits were determined by measuring PSA and PASDT	Paller et al. (2015)
	Breast cancer	39	I	50–50 mg BID of orally administered resveratrol for 3 months	Not reported	Total *trans*-resveratrol levels were detectable in 6/30 (20%) samples at baseline. A dose-response tendency was found with high-dose resveratrol resulted in higher levels at 4 and 12 weeks than after low-dose treatment. Total *cis*-resveratrol was not detectable in any (0/32) of the baseline serum samples. Major metabolites comprised glucuronides (93–100%), whereas sulfates comprised the remainder. The fraction of methylated RASSF-1α DNA decreased, whereas that of APC increased for 3 of 4 women after high-dose resveratrol compared to before treatment. The change in RASSF-1α methylation was directly related to the change in PGE2	Quantification of resveratrol and related metabolites in plasma of breast cancer patients. Establishment of resveratrol activities on methylation patterns of p16, RASSF-1α, APC, and CCND2. Modulation of PGE2 was evaluated	Zhu et al. (2012)
Quercetin	Different cancers (large bowel, ovarian, pancreas, melanoma, stomach, hepatoma, non-small-cell lung cancer, and renal)	51	I	60–1,700 mg/m^2 every 3 weeks administered i.v.	No. However, patients had pain after injection of quercetin that lasted a few minutes. Three patients who received the dose of 1,700 mg/m^2 developed renal toxicity	Quercetin plasma levels achieved immediately after injection were in the range of 200–400 μM at a 945-mg/m^2 dose, with serum levels above 1 μM sustained up to 4 h. In 9 of 11 patients, lymphocyte protein tyrosine phosphorylation was inhibited following administration of quercetin at 1 h, which persisted to 16 h. Promising effects were observed in two patients. One patient with ovarian cancer refractory to Cisplatin (dose of 420 mg/m^2) had a reduction of the CA 125 from 295 to 55 units/ml. Another patient with hepatoma had a reduction in α-fetoprotein from (460–40 units/ml). Quercetin showed to be safe for i.v. administration, and the reduction of tyrosine kinase could be a promising approach to antitumor activity	Determination of safety, pharmacokinetics by HPLC of patients' plasma samples, and estimation of tyrosine kinase inhibition in lymphocytes isolated from patients by Western blot	Ferry et al. (1996)
	Blood malignancies; chemotherapy-derived oral mucositis	20	Pilot	250 mg capsule BID orally administered for 4 weeks	No	Patients received different chemotherapy regimens, but this was not related to the incidence of mucositis in the study population. The incidence of oral mucositis was lower in the quercetin group, but oral mucositis was more severe in the intervention group, which may be due to lower oral health status in the intervention group. No significant beneficial effect of quercetin was found in this study	Patients' oral health was checked by an oral medicine specialist before chemotherapy was initiated. The World Health Organization (WHO) oral toxicity scale was used to evaluate oral mucositis. The endpoints were preventing incidence and onset of OM and the severity of oral mucositis	Kooshyar et al. (2017)

clinical trial (NCT00609310) has suspended status with no results reported, and for kaempferol, no cancer clinical trials in any phase have been reported to date. Results evidence the importance of continuing the carrying out of studies in different clinical phases, permitting the support of the great amount of preclinical evidence that has been found to date for the bioactivities of polyphenols, with the main objective of demonstrating both their safety and efficacy for the prevention and treatment of different types of cancer. Safety and tolerability are demonstrated in numerous studies, and some of the clinical trials listed in **Table 1** include supporting evidence that curcumin, EGCG, resveratrol, and quercetin are safe for human clinical trials. Despite the problems related to the physicochemical properties of polyphenols, their administration route, pharmacokinetics, pharmacodynamics, and bioavailability, among others, involved factors that limit and impact their effectiveness and possible pharmacological action; these compounds may be considered serious candidates for cancer treatment. Because of the poor bioavailability of polyphenols and their extensive metabolism, high doses (up to a maximum of 12 g/day, depending on the type of compound tested) have been utilized by researchers in clinical trials. However, the results evidence the need for more research to increase the evidence and documentation of the bioactivities of these compounds in human subjects with well-controlled double-blind/placebo clinical trials for future therapeutic use, in order to establish their potential in terms of appropriate doses, the most effective routes of administration, in which types of cancer may they be most effective for treatment. Potential medicinal use, accessibility, low cost, safety, and toxicological profile, as well as multiple evidence from preclinical and clinical studies, make polyphenols important candidates for cancer treatment.

DISCUSSION

Polyphenols have gained attention as promising compounds with regulatory activities in several signaling pathways related to cancer development and progression. Understanding how polyphenols regulate cancer-associated mechanisms is important in the development of new therapies for cancer treatment. Polyphenols compose the third largest group of plant-derived chemical compounds after terpenes and alkaloids (Kennedy and Wightman, 2011), making them an important source of possible therapeutical agents given the great diversity of the compounds, from the simplest phenolic acids to polyphenols with a high degree of polymerization. The complexity of polyphenols will have an impact on their bioavailability and bioactivities. Oral administration is the most usual dosage form because it is safe, convenient for medication delivery, noninvasive, and painless, no sterile conditions are needed, both liquids and solids can be administered, it is cost-effective, and it can be self-administered. Nevertheless, oral drug delivery has disadvantages, including nonimmediate action (not suitable for emergency cases), patients must be conscious, absorption is variable among individuals, and some medications are not available in oral form because they are degraded in the GI tract and they may imply the transformation of the drug into a less active form or into toxic metabolites (Kerz et al., 2007; Vinarov et al., 2021). The absorption of polyphenols in GI differs according to their chemical nature. The main compounds to become absorbed are, in decreasing order, isoflavones, phenolic acids (caffeic and gallic), catechins, flavanones, and quercetin glucosides, whereas high-molecular-weight polyphenols, such as proanthocyanidins, catechins, and anthocyanins, are poorly absorbed (Manach et al., 2004). Functional groups may affect polyphenol absorption; glycosidic residues (the most common moieties) may render polyphenol absorption difficult in the small intestine or in the enzymatic activity of gut microbiota. However, this is not always true: some glycosylated metabolites of quercetin possess better bioavailability than aglycone itself (Velderrain-Rodríguez et al., 2014). All of these processes involved in polyphenol absorption may lead to changes in the molecular responses obtained *in vitro* and *in vivo* and must be considered in terms of their bioactivities; however, once absorbed and on their reaching target tissues, polyphenols may exert their bioactivities.

Nanotechnology has high importance in pharmaceutical formulations, targeted therapies, and high efficiency-controlled release. The use of nanotechnology may overcome the bioavailability issues of polyphenols and increase their bioactivity. The application of nanotechnology leads to an increase in the bioavailability and bioactivity of phytomedicine by reducing the size of the particles, by surface modification, and by entrapping the phytomedicine. Different types of compounds may be employed for nanoparticle formulations, including biopolymers, liposomes, quantum dots, polysaccharides, proteins, and metals. The efficiency of polyphenols may be enhanced by employing nanoparticles to reach specific tissues and diminish immunogenicity. The small sizes of nanoparticles (10–150 nm) ensure more efficient accumulation in tumors. Nanoparticles of <10 nm probably will be cleared by kidneys, whereas nanoparticles of >150 nm may be recognized and eliminated by macrophages (Kijanka et al., 2015). Nanoparticles significantly increase the efficiency of polyphenols against tumors. Curcumin-loaded nanoparticles have demonstrated better dose effectivity and bioactivity in cervical cancer cells (Zaman et al., 2016). Different nanoparticle-based therapies are approved by the FDA for the treatment of different cancers. As relevant examples, Myocet was approved in the year 2000 for the primary treatment of breast cancer, and VYXEOS was approved in August 2017 to treat acute myeloid leukemia. Therefore, the exploration of the use of polyphenol-loaded nanoparticles as novel anticancer therapies has a promising future.

Cancer represents a major public health concern around the globe, and despite the existence of a variety of therapies for its treatment, these therapies are often accompanied by adverse effects or toxicities in patients. Given the molecular complexity involved in cancer development and progression, novel treatments may be obtained using polyphenols. Polyphenolics are often recognized as safe products in several toxicity studies. According to reports of the European Food Safety Authority (EFSA), the daily recommended safe dose of curcumin is

0–3 mg/kg body weight (Kocaadam and Şanlier, 2017). The most promising polyphenols (curcumin, resveratrol, quercetin, and EGCG) and their use as possible therapeutic agents are being explored in clinical trials in different cancers including colon, breast, and prostate, to explore their clinical effects alone or in combination with chemotherapy.

p53 plays a central role in many cellular processes, can be activated by diverse stimuli, and is followed by its corresponding response, including apoptosis, senescence, cell-cycle arrest, DNA repair, metabolism regulation, and differentiation (Aubrey et al., 2016). Although *p53* is the most studied gene of all time (Dolgin, 2017), many questions on its regulation in cells that will determine cellular fate remain unclear. Regulation of *p53* may be achieved by posttranslational mechanisms, mRNA-level modulation, protein stability, etc. Dietary polyphenols have important regulatory activities on *p53* (**Figure 5**), including protein stabilization by its interaction with proteins (NQO1) in cells treated with curcumin (Patiño-Morales et al., 2020); EGCG evokes the regulation of mRNA and protein levels (Chu et al., 2017) or the epigenetic regulation induced by resveratrol, leading to the reestablishment of *p53* (Chatterjee et al., 2019). These features of polyphenols highlight their importance and their possible therapeutic action against cancer; however, there are many questions concerning the specific cancer type for which they must be used or on their molecular mechanisms of action, which are still poorly understood, as well as the synergistic effect they may have with conventional chemotherapy (**Figure 5**). Therefore, further research is required to answer these questions in order to move forward to the pharmacological use of polyphenols for cancer.

The PI3K/Akt/mTOR pathway plays a major role in survival, growth, metastasis, and drug chemoresistance in cancer. This pathway comprises a major node that is frequently mutated or amplified in a wide variety of solid tumors (Manning and Cantley, 2007). Several novel anticancer agents targeting the PI3K/Akt/mTOR pathway have been developed for the treatment of various malignancies. For this reason, inhibiting any component of this pathway comprises a promising therapeutic strategy. Wortmannin and LY294002 were the first-generation PI3K inhibitors that belong to the nonisoform-specific category. However, Wortmannin with irreversible inhibition lacks selectivity and adverse effects resulted in the termination of its clinical trials (Mishra et al., 2021). LY294002 has poor solubility, bioavailability, and several adverse effects, such as fatigue, nausea, vomiting, diarrhea, and hyperglycemia (Esposito et al., 2019).

Dietary polyphenols, such as the resveratrol present in peanuts, catechins in green tea, curcumin in turmeric, and apigenin in onions, have been widely demonstrated that polyphenols have antitumor effects with selective cytotoxicity to cancer cells and few adverse effects to the patient. Several preclinical experimental studies have been developed to highlight the antitumor effect of resveratrol, curcumin, apigenin, EGCG, and quercetin on several tumors. In this review, we describe that these polyphenols can alter the function of multiple molecules effective in PI3K signaling, such as Akt, mTOR, PTEN, and PDK-1, through different mechanisms, avoiding cancer progression, drug resistance, angiogenesis, and metastasis.

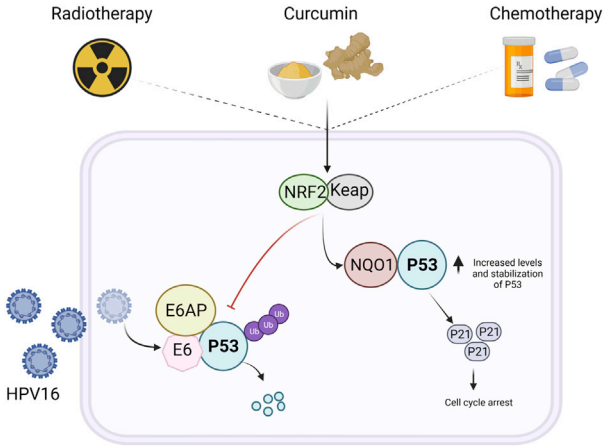

FIGURE 5 | p53 Stabilization by curcumin and synergy with routine therapy for the treatment of cervical cancer. Curcumin activates the Kelch-like ECH-associated protein 1-nuclear factor (erythroid-derived 2)-like 2 (Keap1/Nrf2) pathway, leading to an increase in the levels of NAD(P)H:quinone oxidoreductase 1 (NQO1). NQO1 binds to p53, promoting the loss of the interaction between p53 and E6AP, a negative regulator, promoting p53 stabilization in cancer cells with wild-type p53, such as cervical cancer cells. Moreover, a promising area of study is that of evaluating the synergistic effect of curcumin with routine chemotherapy, thus procuring a better response to treatment and fewer adverse effects.

Multiple *in vitro* and *in vivo* studies have shown that polyphenols decrease drug resistance. It was revealed that resveratrol decreases this drug resistance by reducing the expression of MRP1 and the efflux of Adriamycin in HL-60/ADR cells (Li F. et al., 2019) or by promoting cell death by autophagy. There is a catabolic process for bulk or selective encapsulated lysosomal degradation and the recycling of obsolete or damaged cytoplasmic cargo including proteins and organelles. Autophagy plays a dual role in cancer. On the one hand, the activation of autophagy in cancer cells promotes the efficacy of anticancer strategies, while on the other hand, it may promote cancer progression through the enhancement of cell survival (Tavakol et al., 2019). Resveratrol and curcumin induce autophagy and apoptosis through a decrease of the phosphorylation of Akt (S473) and AMPK or through *p53* activation (Chang et al., 2017). In contrast, in ovarian cancer, treatment with curcumin induces protective autophagy by inhibiting the Akt/mTOR pathway, resulting in resistance to chemotherapy. Interestingly, in these tumors, the inhibition of autophagy and curcumin therapy may provide a new perspective for clinical intervention (Liu Z. et al., 2019). However, more studies are needed to demonstrate the precise molecular mechanism and whether it is feasible to employ it in other types of cancer.

As mentioned previously, polyphenols inhibit the PI3K/Akt/mTOR pathway; however, these agents can interfere with other signaling cascades involved in cancer progression, such as MAPK and oncogenic RAS.

RAS proteins are small eukaryotic GTPases that cycle back and forth between the GDP-bound inactive state and the GTP-bound active state. The *KRAS* gene can simultaneously harbor multiple mutations that can potentiate tumor-promoting activity in several human cancers; thus, it is necessary to utilize a new therapeutic strategy to inhibit this oncoprotein and therefore the development of cancer (Mustachio et al., 2021). However, the *RAS* oncogene is particularly difficult to target with specific therapeutics. These *RAS*-mutated cancers respond poorly to standard chemotherapy; therefore, targeted approaches need to be found (Sheffels and Kortum, 2021).

Several studies both *in vitro* and *in vivo* have shown that polyphenols such as curcumin, resveratrol, and EGCG supplemented in a diet can prevent the formation and growth of tumors by downregulating *KRAS* expression (Limtrakul et al., 2001; Saud et al., 2014). EGCG inhibited cell proliferation induced by oncogenic RAS and exhibited a stronger inhibitory effect on cell proliferation in transformed cells than in nontransformed cells (Peng et al., 2006). Epicatechin reduced the GTP-bound active RAS protein level; moreover, it was demonstrated that this polyphenol decreased PI3K/Akt and MAPK signaling by inhibiting *KRAS* activity (Siddique et al., 2012). The ability of polyphenols to decrease RAS activity affords the possibility that polyphenols could be used for the targeting of many types of cancer that are caused by RAS activation, representing an attractive opportunity for the treatment of these tumors, which are characterized by being resistant to conventional chemotherapy. However, more studies are necessary to establish effectiveness either as monotherapy or as a combined therapy.

Despite the wide range of polyphenol health-related beneficial bioactivities in the regulation of cancer-related signaling pathways, we must consider the possible undesirable adverse effects caused by polyphenols. The similarity and ability of soy isoflavones to act as phytoestrogens may lead to undesired effects, principally in hormone-responsive diseases; Genistein treatment produces cell-cycle arrest and an improvement in mitochondrial functionality in T47D (low ERα/ERβ ratio), but not in MCF-7 (high ERα/ERβ ratio) and MDA-MB-231 (ER^-) (Pons et al., 2014). Polyphenols are not exempt from toxicological adverse effects. Despite the fact that curcumin is recognized as safe, patients given oral doses of curcumin 10–12 g exhibited minor grade-1 toxic effects according to the World Health Organization (WHO) toxicological classification (Vareed et al., 2008). Although extensive evidence supports the antioxidant protective effects of curcumin, high concentrations may induce an increase in intracellular ROS production. It has been demonstrated that curcumin (2.5–5 μg/ml) induces mitochondrial and nuclear DNA damage, which could raise questions concerning our safety (Cao et al., 2006; Burgos-Morón et al., 2010). Polyphenols such as quercetin inhibit CYP 1A2, 2C9, 2C19, 3A4, and 2D6 (Rastogi and Jana, 2014); therefore, we must take care when drugs metabolized through these CYP are coadministered with quercetin. Despite these possible adverse effects, the majority of the evidence supports the beneficial health effects of polyphenols. However, it is important to continue the development of experimental studies and clinical trials that allow us to understand the mechanisms that are fully involved and the specificity for the different types of cancer that can be treated with polyphenols.

In conclusion, this review has provided an overview of the principal strengths of the most promising polyphenolic compounds for the regulation of important key players in cancer, which control a wide variety of cellular processes such as differentiation, proliferation, apoptosis, cell-cycle arrest, and the responses to inflammatory processes or oxidative stress. Therapies in current use for cancer are associated with several adverse effects that reduce the overall quality of life or may cause the death of patients. Polyphenols have been attracting attention due to their multiple bioactivities and could be an interesting alternative as therapeutic agents with the aim of being more effective and less toxic for cancer treatment. Bioavailability is an important parameter to be considered in the use of polyphenols as therapeutics in patients with cancer, due to the biotransformation processes that modify their structure and, possibly, bioactivities along their passage through gut and liver metabolism. The anticancer effects of polyphenols are known to modulate several signaling pathways including MAPK and PI3K/Akt, important tumor suppressors such as p53, and oncoproteins such as RAS isoforms. Several polyphenols including curcumin, resveratrol, quercetin, kaempferol, EGCG, and apigenin may upregulate the expression of the key players in these signaling pathways in several cancer types through a variety of distinct mechanisms of action. All of these considerations make polyphenols a promising source of therapeutics for cancer treatment; however, further research is needed to elucidate the complete mechanisms involved in the polyphenol-induced regulation of cancer.

AUTHOR CONTRIBUTIONS

MC: conceptualization, resources, and writing. Kd: resources, writing, and figures. AG: conceptualization, review, editing, writing, and supervision.

FUNDING

The authors acknowledge continuous support from Subdirección de Investigación, Instituto Nacional de Cancerología, Mexico City, Mexico. MC (CVU 482843) is very grateful for his postdoctoral fellowship from Programa de Becas Posdoctorales en la UNAM (DGAPA) and CONACyT (Consejo Nacional de Ciencia y Tecnología, México). Kd (CVU 660667) is a doctoral student in the Programa de Doctorado en Ciencias Biomédicas, Universidad Nacional Autónoma de México (UNAM), and received fellowship 406537 from CONACyT.

ACKNOWLEDGMENTS

Figures were created with BioRender (Biorender.com).

REFERENCES

Agulló, V., Villaño, D., García-Viguera, C., and Domínguez-Perles, R. (2020). Anthocyanin Metabolites in Human Urine after the Intake of New Functional Beverages. *Molecules* 25 (2), 371. doi:10.3390/molecules25020371

Aherne, S. A., and O'Brien, N. M. (2002). Dietary Flavonols: Chemistry, Food Content, and Metabolism. *Nutrition* 18 (1), 75–81. doi:10.1016/S0899-9007(01)00695-5

Aubrey, B. J., Strasser, A., and Kelly, G. L. (2016). Tumor-suppressor Functions of the TP53 Pathway. *Cold Spring Harb Perspect. Med.* 6 (5), a026062. doi:10.1101/cshperspect.a026062

Aune, D., Giovannucci, E., Boffetta, P., Fadnes, L. T., Keum, N., Norat, T., et al. (2017). Fruit and Vegetable Intake and the Risk of Cardiovascular Disease, Total Cancer and All-Cause Mortality-A Systematic Review and Dose-Response Meta-Analysis of Prospective Studies. *Int. J. Epidemiol.* 46 (3), 1029–1056. doi:10.1093/ije/dyw319

Badciong, J. C., and Haas, A. L. (2002). MdmX Is a RING Finger Ubiquitin Ligase Capable of Synergistically Enhancing Mdm2 Ubiquitination. *J. Biol. Chem.* 277 (51), 49668–49675. doi:10.1074/jbc.M208593200

Bahrami, A., Jafari, S., Rafiei, P., Beigrezaei, S., Sadeghi, A., Hekmatdoost, A., et al. (2019). Dietary Intake of Polyphenols and Risk of Colorectal Cancer and Adenoma-A Case-Control Study from Iran. *Complement. Ther. Med.* 45, 269–274. doi:10.1016/j.ctim.2019.04.011

Barreca, D., Gattuso, G., Bellocco, E., Calderaro, A., Trombetta, D., Smeriglio, A., et al. (2017). Flavanones: Citrus Phytochemical with Health-Promoting Properties. *BioFactors* 43 (4), 495–506. doi:10.1002/biof.1363

Baugh, E. H., Ke, H., Levine, A. J., Bonneau, R. A., and Chan, C. S. (2018). Why Are There Hotspot Mutations in the TP53 Gene in Human Cancers? *Cell Death Differ* 25 (1), 154–160. doi:10.1038/cdd.2017.180

Bian, P., Hu, W., Liu, C., and Li, L. (2020). Resveratrol Potentiates the Anti-tumor Effects of Rapamycin in Papillary Thyroid Cancer: PI3K/AKT/mTOR Pathway Involved. *Arch. Biochem. Biophys.* 689, 108461. doi:10.1016/j.abb.2020.108461

Birt, D. F., and Jeffery, E. (2013). Flavonoids. *Adv. Nutr.* 4 (5), 576–577. doi:10.3945/an.113.004465

Bondonno, N. P., Dalgaard, F., Kyrø, C., Murray, K., Bondonno, C. P., Lewis, J. R., et al. (2019). Flavonoid Intake is Associated with Lower Mortality in the Danish Diet Cancer and Health Cohort. *Nat. Commun.* 10 (1), 1–10. doi:10.1038/s41467-019-11622-x

Borges, G. A., Elias, S. T., Amorim, B., de Lima, C. L., Coletta, R. D., Castilho, R. M., et al. (2020). Curcumin Downregulates the PI3K-AKT-mTOR Pathway and Inhibits Growth and Progression in Head and Neck Cancer Cells. *Phytother Res.* 34 (12), 3311–3324. doi:10.1002/ptr.6780

Bose, C., Zhang, H., Udupa, K. B., and Chowdhury, P. (2005). Activation of P-ERK1/2 by Nicotine in Pancreatic Tumor Cell Line AR42J: Effects on Proliferation and Secretion. *Am. J. Physiol. Gastrointest. Liver Physiol.* 289 (5), G926–G934. doi:10.1152/ajpgi.00138.2005

Bouayed, J., Hoffmann, L., and Bohn, T. (2011). Total Phenolics, Flavonoids, Anthocyanins and Antioxidant Activity Following Simulated Gastro-Intestinal Digestion and Dialysis of Apple Varieties: Bioaccessibility and Potential Uptake. *Food Chem.* 128 (1), 14–21. doi:10.1016/j.foodchem.2011.02.052

Brglez Mojzer, E., Knez Hrnčič, M., Škerget, M., Knez, Ž., and Bren, U. (2016). Polyphenols: Extraction Methods, Antioxidative Action, Bioavailability and Anticarcinogenic Effects. *Molecules* 21 (7), 1–38. doi:10.3390/molecules21070901

Brosh, R., and Rotter, V. (2009). When Mutants Gain New powers: News from the Mutant P53 Field. *Nat. Rev. Cancer* 9 (10), 701–713. doi:10.1038/nrc2693

Brown, V. A., Patel, K. R., Viskaduraki, M., Crowell, J. A., Perloff, M., Booth, T. D., et al. (2010). Repeat Dose Study of the Cancer Chemopreventive Agent Resveratrol in Healthy Volunteers: Safety, Pharmacokinetics, and Effect on the Insulin-like Growth Factor Axis. *Cancer Res.* 70 (22), 9003–9011. doi:10.1158/0008-5472.CAN-10-2364

Bueno, J. M., Sáez-Plaza, P., Ramos-Escudero, F., Jiménez, A. M., Fett, R., and Asuero, A. G. (2012). Analysis and Antioxidant Capacity of Anthocyanin Pigments. Part II: Chemical Structure, Color, and Intake of Anthocyanins. *Crit. Rev. Anal. Chem.* 42 (2), 126–151. doi:10.1080/10408347.2011.632314

Burgos-Morón, E., Calderón-Montaño, J. M., Salvador, J., Robles, A., and López-Lázaro, M. (2010). The Dark Side of Curcumin. *Int. J. Cancer* 126, 1771–1775. doi:10.1002/ijc.24967

Cao, J., Jia, L., Zhou, H. M., Liu, Y., and Zhong, L. F. (2006). Mitochondrial and Nuclear DNA Damage Induced by Curcumin in Human Hepatoma G2 Cells. *Toxicol. Sci.* 91 (2), 476–483. doi:10.1093/toxsci/kfj153

Cardona, F., Andrés-Lacueva, C., Tulipani, S., Tinahones, F. J., and Queipo-Ortuño, M. I. (2013). Benefits of Polyphenols on Gut Microbiota and Implications in Human Health. *J. Nutr. Biochem.* 24 (8), 1415–1422. doi:10.1016/j.jnutbio.2013.05.001

Castañeda-Ovando, A., Pacheco-Hernández, M. d. L., Páez-Hernández, M. E., Rodríguez, J. A., and Galán-Vidal, C. A. (2009). Chemical Studies of Anthocyanins: A Review. *Food Chem.* 113 (4), 859–871. doi:10.1016/j.foodchem.2008.09.001

Castillo-Pichardo, L., and Dharmawardhane, S. F. (2012). Grape Polyphenols Inhibit Akt/mammalian Target of Rapamycin Signaling and Potentiate the Effects of Gefitinib in Breast Cancer. *Nutr. Cancer* 64 (7), 1058–1069. doi:10.1080/01635581.2012.716898

Cerezo-Guisado, M. I., Zur, R., Lorenzo, M. J., Risco, A., Martín-Serrano, M. A., Alvarez-Barrientos, A., et al. (2015). Implication of Akt, ERK1/2 and Alternative p38MAPK Signalling Pathways in Human colon Cancer Cell Apoptosis Induced by Green tea EGCG. *Food Chem. Toxicol.* 84, 125–132. doi:10.1016/j.fct.2015.08.017

Chakrabarty, S., Nag, D., Ganguli, A., Das, A., Ghosh Dastidar, D., and Chakrabarti, G. (2019). Theaflavin and Epigallocatechin-3-Gallate Synergistically Induce Apoptosis through Inhibition of PI3K/Akt Signaling upon Depolymerizing Microtubules in HeLa Cells. *J. Cel Biochem.* 120 (4), 5987–6003. doi:10.1002/jcb.27886

Chan, K. K. L., Siu, M. K. Y., Jiang, Y. X., Wang, J. J., Leung, T. H. Y., and Ngan, H. Y. S. (2018). Estrogen Receptor Modulators Genistein, Daidzein and ERB-041 Inhibit Cell Migration, Invasion, Proliferation and Sphere Formation via Modulation of FAK and PI3K/AKT Signaling in Ovarian Cancer. *Cancer Cel Int* 18 (1), 65–14. doi:10.1186/s12935-018-0559-2

Chang, C. H., Lee, C. Y., Lu, C. C., Tsai, F. J., Hsu, Y. M., Tsao, J. W., et al. (2017). Resveratrol-induced Autophagy and Apoptosis in Cisplatin-Resistant Human Oral Cancer CAR Cells: A Key Role of AMPK and Akt/mTOR Signaling. *Int. J. Oncol.* 50 (3), 873–882. doi:10.3892/ijo.2017.3866

Chatterjee, B., Ghosh, K., and Kanade, S. R. (2019). Resveratrol Modulates Epigenetic Regulators of Promoter Histone Methylation and Acetylation that Restores BRCA1, P53, p21CIP1 in Human Breast Cancer Cell Lines. *BioFactors* 45 (5), 818–829. doi:10.1002/biof.1544

Chène, P. (2001). The Role of Tetramerization in P53 Function. *Oncogene* 20 (21), 2611–2617. doi:10.1038/sj.onc.1204373

Cheng, A. L., Hsu, C. H., Lin, J. K., Hsu, M. M., Ho, Y. F., Shen, T. S., et al. (2001). Phase I Clinical Trial of Curcumin, a Chemopreventive Agent, in Patients with High-Risk or Pre-Malignant Lesions. *Anticancer Res.* 21 (4B), 2895–2900.

Chen, M., Wang, X., Zha, D., Cai, F., Zhang, W., He, Y., et al. (2016). Apigenin Potentiates TRAIL Therapy of Non-small Cell Lung Cancer via Upregulating DR4/DR5 Expression in a P53-dependent Manner. *Sci. Rep.* 6 (1), 1–17. doi:10.1038/srep35468

Chiablaem, K., Lirdprapamongkol, K., Keeratichamroen, S., Surarit, R., and Svasti, J. (2014). Curcumin Suppresses Vasculogenic Mimicry Capacity of Hepatocellular Carcinoma Cells through STAT3 and PI3K/AKT Inhibition. *Anticancer Res.* 34 (4), 1857–1864.

Choi, J. B., Kim, J. H., Lee, H., Pak, J. N., Shim, B. S., and Kim, S. H. (2018). Reactive Oxygen Species and P53 Mediated Activation of P38 and Caspases Is Critically Involved in Kaempferol Induced Apoptosis in Colorectal Cancer Cells. *J. Agric. Food Chem.* 66 (38), 9960–9967. doi:10.1021/acs.jafc.8b02656

Chow, S. C. (2014). Bioavailability and Bioequivalence in Drug Development. *Wiley Interdiscip. Rev. Comput. Stat.* 6 (4), 304–312. doi:10.1002/wics.1310

Chowdhury, P., Jayroe, J. J., White, B. E., and Fenton, E. R. (2018a). Effects of a Natural Polyphenol on Nicotine-Induced Pancreatic Cancer Cell Proliferation. *Tob. Induc Dis.* 16 (October), 50–58. doi:10.18332/tid/95159

Chowdhury, P., Sahuc, M. E., Rouillé, Y., Rivière, C., Bonneau, N., Vandeputte, A., et al. (2018b). Theaflavins, Polyphenols of Black tea, Inhibit Entry of Hepatitis C Virus in Cell Culture. *PLoS One* 13, e0198226. doi:10.1371/journal.pone.0198226

Chu, Y. W., Liu, S. T., Yang, Y. L., Huang, S. M., and Wang, W. M. (2017). The Cytotoxic Mechanism of Epigallocatechin Gallate on Proliferative HaCaT Keratinocytes. *J. Biomed. Sci.* 24 (1), 55–58. doi:10.1186/s12929-017-0363-7

Cirkovic Velickovic, T. D., and Stanic-Vucinic, D. J. (2018). The Role of Dietary Phenolic Compounds in Protein Digestion and Processing Technologies to

Improve Their Antinutritive Properties. *Compr. Rev. Food Sci. Food Saf.* 17 (1), 82–103. doi:10.1111/1541-4337.12320

Clifford, M. N., and Scalbert, A. (2000). Review Ellagitannins-Nature, Occurrence and Dietary burden. *J. Sci. Food Agric.* 80, 1118–1125. doi:10.1002/(SICI)1097-0010(20000515)80:7<1118::AID-JSFA570>3.0.CO;2-9

Codrich, M., Dalla, E., Mio, C., Antoniali, G., Malfatti, M. C., Marzinotto, S., et al. (2021). Integrated Multi-Omics Analyses on Patient-Derived CRC Organoids Highlight Altered Molecular Pathways in Colorectal Cancer Progression Involving PTEN. *J. Exp. Clin. Cancer Res.* 40 (1), 1–17. doi:10.1186/s13046-021-01986-8

Cuadrado, A., and Nebreda, A. R. (2010). Mechanisms and Functions of P38 MAPK Signalling. *Biochem. J.* 429 (3), 403–417. doi:10.1042/BJ20100323

Das, L., and Vinayak, M. (2015). Long Term Effect of Curcumin in Restoration of Tumour Suppressor P53 and Phase-II Antioxidant Enzymes via Activation of Nrf2 Signalling and Modulation of Inflammation in Prevention of Cancer. *PLoS One* 10 (4), e0124000–22. doi:10.1371/journal.pone.0124000

Dasgupta, P., Rizwani, W., Pillai, S., Kinkade, R., Kovacs, M., Rastogi, S., et al. (2009). Nicotine Induces Cell Proliferation, Invasion and Epithelial-Mesenchymal Transition in a Variety of Human Cancer Cell Lines. *Int. J. Cancer* 124 (1), 36–45. doi:10.1002/ijc.23894

De, P., Baltas, M., and Bedos-Belval, F. (2011). Cinnamic Acid Derivatives as Anticancer Agents-A Review. *Curr. Med. Chem.* 18 (11), 1672–1703. doi:10.2174/092986711795471347

Delgado-Bellido, D., Serrano-Saenz, S., Fernández-Cortés, M., and Oliver, F. J. (2017). Vasculogenic Mimicry Signaling Revisited: Focus on Non-Vascular VE-Cadherin. *Mol. Cancer* 16 (1), 65–14. doi:10.1186/s12943-017-0631-x

Deprez, S., Mila, I., Huneau, J. F., Tome, D., and Scalbert, A. (2001). Transport of Proanthocyanidin Dimer, Trimer, and Polymer across Monolayers of Human Intestinal Epithelial Caco-2 Cells. *Antioxid. Redox Signal.* 3 (6), 957–967. doi:10.1089/152308601317203503

Dhar, S., Kumar, A., Rimando, A. M., Zhang, X., and Levenson, A. S. (2015). Resveratrol and Pterostilbene Epigenetically Restore PTEN Expression by Targeting oncomiRs of the miR-17 Family in Prostate Cancer. *Oncotarget* 6 (29), 27214–27226. doi:10.18632/oncotarget.4877

Dhillon, N., Aggarwal, B. B., Newman, R. A., Wolff, R. A., Kunnumakkara, A. B., Abbruzzese, J. L., et al. (2008). Phase II Trial of Curcumin in Patients with Advanced Pancreatic Cancer. *Clin. Cancer Res.* 14 (14), 4491–4499. doi:10.1158/1078-0432.CCR-08-0024

Di Matteo, V., Pierucci, M., Di Giovanni, G., and Esposito, E. (2007). "Prevention and Therapy of Neurodegenerative Disorders: Role of Nutritional Antioxidants," in *Oxidative Stress and Neurodegenerative Disorders*. Editors G. A. Qureshi and S. H. Parvez. 1st ed. (Amsterdam, The Netherlands: Elsevier Science), 621–661. doi:10.1016/B978-044452809-4/50168-X

Dibble, C. C., and Manning, B. D. (2013). Signal Integration by mTORC1 Coordinates Nutrient Input with Biosynthetic Output. *Nat. Cel Biol* 15 (6), 555–564. doi:10.1038/ncb2763

Dima, C., Assadpour, E., Dima, S., and Jafari, S. M. (2020). Bioavailability and Bioaccessibility of Food Bioactive Compounds; Overview and Assessment by *In Vitro* Methods. *Compr. Rev. Food Sci. Food Saf.* 19 (6), 2862–2884. doi:10.1111/1541-4337.12623

Ding, Z., Liang, J., Li, J., Lu, Y., Ariyaratna, V., Lu, Z., et al. (2010). Physical Association of PDK1 With AKT1 is Sufficient for Pathway Activation Independent of Membrane Localization and Phosphatidylinositol 3 Kinase. *PLoS One* 5 (3), e9910. doi:10.1371/journal.pone.0009910

Dolado, I., Swat, A., Ajenjo, N., De Vita, G., Cuadrado, A., and Nebreda, A. R. (2007). p38alpha MAP Kinase as a Sensor of Reactive Oxygen Species in Tumorigenesis. *Cancer Cell* 11 (2), 191–205. doi:10.1016/j.ccr.2006.12.013

Dolgin, E. (2017). The Most Popular Genes in the Human Genome. *Nature* 551 (7681), 427–431. doi:10.1038/d41586-017-07291-9

Dou, Y., Jiang, X., Xie, H., He, J., and Xiao, S. (2019). The Jun N-Terminal Kinases Signaling Pathway Plays a "seesaw" Role in Ovarian Carcinoma: a Molecular Aspect. *J. Ovarian Res.* 12 (1), 99–11. doi:10.1186/s13048-019-0573-6

Eblen, S. T. (2018). "Extracellular-Regulated Kinases: Signaling from Ras to ERK Substrates to Control Biological Outcomes," *Cancer Res.*. Editors K. D. Tew and P. B. Fisher. 1st ed (Academic Press Elsevier), Vol. 138, 99–142. doi:10.1016/bs.acr.2018.02.004

Edwards, R. L., Luis, P. B., Varuzza, P. V., Joseph, A. I., Presley, S. H., Chaturvedi, R., et al. (2017). The Anti-inflammatory Activity of Curcumin Is Mediated by its Oxidative Metabolites. *J. Biol. Chem.* 292 (52), 21243–21252. doi:10.1074/jbc.RA117.000123

Ekor, M. (2014). The Growing Use of Herbal Medicines: Issues Relating to Adverse Reactions and Challenges in Monitoring Safety. *Front. Pharmacol.* 4, 1–10. doi:10.3389/fphar.2013.00177

El Khawand, T., Courtois, A., Valls, J., Richard, T., and Krisa, S. (2018). A Review of Dietary Stilbenes: Sources and Bioavailability. *Phytochem. Rev.* 17 (5), 1007–1029. doi:10.1007/s11101-018-9578-9

El-Seedi, H. R., El-Said, A. M., Khalifa, S. A., Göransson, U., Bohlin, L., Borg-Karlson, A. K., et al. (2012). Biosynthesis, Natural Sources, Dietary Intake, Pharmacokinetic Properties, and Biological Activities of Hydroxycinnamic Acids. *J. Agric. Food Chem.* 60 (44), 10877–10895. doi:10.1021/jf301807g

Erdogan, S., Doganlar, O., Doganlar, Z. B., Serttas, R., Turkekul, K., Dibirdik, I., et al. (2016). The Flavonoid Apigenin Reduces Prostate Cancer CD44(+) Stem Cell Survival and Migration through PI3K/Akt/NF-κB Signaling. *Life Sci.* 162, 77–86. doi:10.1016/j.lfs.2016.08.019

Esposito, A., Viale, G., and Curigliano, G. (2019). Safety, Tolerability, and Management of Toxic Effects of Phosphatidylinositol 3-Kinase Inhibitor Treatment in Patients with Cancer: A Review. *JAMA Oncol.* 5 (9), 1347–1354. doi:10.1001/jamaoncol.2019.0034

Fernández-Medarde, A., De Las Rivas, J., and Santos, E. (2021). 40 Years of RAS-A Historic Overview. *Genes* 12 (5), 681. doi:10.3390/genes12050681

Ferry, D. R., Smith, A., Malkhandi, J., Fyfe, D. W., DeTakats, P. G., Anderson, D., et al. (1996). Phase I Clinical Trial of the Flavonoid Quercetin: Pharmacokinetics and Evidence for *In Vivo* Tyrosine Kinase Inhibition. *Clin. Cancer Res.* 2 (4), 659–668.

Fu, W., and Hall, M. N. (2020). Regulation of MTORC2 Signaling. *Genes (Basel)* 11 (9), 1–19. doi:10.3390/genes11091045

Fu, H., Wang, C., Yang, D., Wei, Z., Xu, J., Hu, Z., et al. (2018). Curcumin Regulates Proliferation, Autophagy, and Apoptosis in Gastric Cancer Cells by Affecting PI3K and P53 Signaling. *J. Cel Physiol* 233 (6), 4634–4642. doi:10.1002/jcp.26190

Gee, J. R., Saltzstein, D. R., Kim, K., Kolesar, J., Huang, W., Havighurst, T. C., et al. (2017). A phase II randomized, Double-Blind, Presurgical Trial of Polyphenon e in Bladder Cancer patients to Evaluate Pharmacodynamics and bladder Tissue Biomarkers. *Cancer Prev. Res. (Phila)* 10 (5), 298–307. doi:10.1158/1940-6207.CAPR-16-0167

Gencel-Augusto, J., and Lozano, G. (2020). p53 Tetramerization: At the center of the Dominant-Negative Effect of Mutant P53. *Genes Dev.* 34 (17–18), 1128–1146. doi:10.1101/gad.340976.120

Gerits, N., Kostenko, S., and Moens, U. (2007). *In Vivo* functions of Mitogen-Activated Protein Kinases: Conclusions from Knock-In and Knock-Out Mice. *Transgenic Res.* 16 (3), 281–314. doi:10.1007/s11248-006-9052-0

Giaccia, A. J., and Kastan, M. B. (1998). The Complexity of P53 Modulation: Emerging Patterns from Divergent Signals. *Genes Dev.* 12 (19), 2973–2983. doi:10.1101/gad.12.19.2973

Granato, M., Gilardini Montani, M. S., Santarelli, R., D'Orazi, G., Faggioni, A., and Cirone, M. (2017). Apigenin, by Activating P53 and Inhibiting STAT3, Modulates the Balance between Pro-apoptotic and Pro-survival Pathways to Induce PEL Cell Death. *J. Exp. Clin. Cancer Res.* 36 (1), 167–169. doi:10.1186/s13046-017-0632-z

Hassaninasab, A., Hashimoto, Y., Tomita-Yokotani, K., and Kobayashi, M. (2011). Discovery of the Curcumin Metabolic Pathway Involving a Unique Enzyme in an Intestinal Microorganism. *Proc. Natl. Acad. Sci. U S A.* 108 (16), 6615–6620. doi:10.1073/pnas.1016217108

Haytowitz, D. B., Wu, X., and Bhagwat, S. (2018). *USDA Database for the Flavonoid Content of Selected Foods Release 3.3 Prepared by*. Available at: https://www.ars.usda.gov/ARSUserFiles/80400525/Data/Flav/Flav3.3.pdf (Accessed April 1, 2021).

Hemmings, B. A., and Restuccia, D. F. (2012). PI3K-PKB/Akt Pathway. *Cold Spring Harb Perspect. Biol.* 4 (9), a011189–4. doi:10.1101/cshperspect.a011189

Hernandez-Valencia, J., Garcia-Villa, E., Arenas-Hernandez, A., Garcia-Mena, J., Diaz-Chavez, J., and Gariglio, P. (2018). Induction of P53 Phosphorylation at Serine 20 by Resveratrol Is Required to Activate P53 Target Genes, Restoring Apoptosis in MCF-7 Cells Resistant to Cisplatin. *Nutrients* 10 (9), 1148. doi:10.3390/nu10091148

Nguyen, A. V., Martinez, M., Stamos, M. J., Moyer, M. P., Planutis, K., Hope, C., et al. (2009). Results of a Phase I Pilot Clinical Trial Examining the Effect of

Plant-Derived Resveratrol and Grape Powder on Wnt Pathway Target Gene Expression in Colonic Mucosa and colon Cancer. *Cancer Manag. Res.* 1, 25–37. doi:10.2147/cmr.s4544

Hostetler, G. L., Ralston, R. A., and Schwartz, S. J. (2017). Flavones: Food Sources, Bioavailability, Metabolism, and Bioactivity. *Adv. Nutr.* 8 (3), 423–435. doi:10.3945/an.116.012948

Howells, L. M., Iwuji, C. O. O., Irving, G. R. B., Barber, S., Walter, H., Sidat, Z., et al. (2019). Curcumin Combined with FOLFOX Chemotherapy Is Safe and Tolerable in Patients with Metastatic Colorectal Cancer in a Randomized Phase IIa Trial. *J. Nutr.* 149 (7), 1133–1139. doi:10.1093/jn/nxz029

Huang, S., Wang, L. L., Xue, N. N., Li, C., Guo, H. H., Ren, T. K., et al. (2019). Chlorogenic Acid Effectively Treats Cancers through Induction of Cancer Cell Differentiation. *Theranostics* 9 (23), 6745–6763. doi:10.7150/thno.34674

Hui, L., Bakiri, L., Mairhorfer, A., Schweifer, N., Haslinger, C., Kenner, L., et al. (2007). p38alpha Suppresses normal and Cancer Cell Proliferation by Antagonizing the JNK-C-Jun Pathway. *Nat. Genet.* 39 (6), 741–749. doi:10.1038/ng2033

Igea, A., and Nebreda, A. R. (2015). The Stress Kinase P38α as a Target for Cancer Therapy. *Cancer Res.* 75 (19), 3997–4002. doi:10.1158/0008-5472.CAN-15-0173

Ikenoue, T., Inoki, K., Yang, Q., Zhou, X., and Guan, K. L. (2008). Essential Function of TORC2 in PKC and Akt Turn Motif Phosphorylation, Maturation and Signalling. *EMBO J.* 27 (14), 1919–1931. doi:10.1038/emboj.2008.119

Jia, L., Huang, S., Yin, X., Zan, Y., Guo, Y., and Han, L. (2018). Quercetin Suppresses the Mobility of Breast Cancer by Suppressing Glycolysis through Akt-mTOR Pathway Mediated Autophagy Induction. *Life Sci.* 208, 123–130. doi:10.1016/j.lfs.2018.07.027

Jiao, Y., Li, H., Liu, Y., Guo, A., Xu, X., Qu, X., et al. (2015). Resveratrol Inhibits the Invasion of Glioblastoma-Initiating Cells via Down-Regulation of the PI3K/Akt/NF-κB Signaling Pathway. *Nutrients* 7 (6), 4383–4402. doi:10.3390/nu7064383

Jin, L., Li, C., Xu, Y., Wang, L., Liu, J., Wang, D., et al. (2013). Epigallocatechin Gallate Promotes P53 Accumulation and Activity via the Inhibition of MDM2-Mediated P53 Ubiquitination in Human Lung Cancer Cells. *Oncol. Rep.* 29 (5), 1983–1990. doi:10.3892/or.2013.2343

Johnson, D. S., and Chen, Y. H. (2012). Ras Family of Small GTPases in Immunity and Inflammation. *Curr. Opin. Pharmacol.* 12 (4), 458–463. doi:10.1016/j.coph.2012.02.003

Jones, S. N., Roe, A. E., Donehower, L. A., and Bradley, A. (1995). Rescue of Embryonic Lethality in Mdm2-Deficient Mice by Absence of P53. *Nature* 378 (6553), 206–208. doi:10.1038/378206a0

Jung, W., Yu, O., Lau, S. M., O'Keefe, D. P., Odell, J., Fader, G., et al. (2000). Identification and Expression of Isoflavone Synthase, the Key Enzyme for Biosynthesis of Isoflavones in Legumes. *Nat. Biotechnol.* 18 (2), 208–212. doi:10.1038/72671

Kanai, M., Yoshimura, K., Asada, M., Imaizumi, A., Suzuki, C., Matsumoto, S., et al. (2011). A Phase I/II Study of Gemcitabine-Based Chemotherapy Plus Curcumin for Patients with Gemcitabine-Resistant Pancreatic Cancer. *Cancer Chemother. Pharmacol.* 68 (1), 157–164. doi:10.1007/s00280-010-1470-2

Karakostis, K., Ponnuswamy, A., Fusée, L. T., Bailly, X., Laguerre, L., Worall, E., et al. (2016). P53 mRNA and P53 Protein Structures Have Evolved Independently to Interact with MDM2. *Mol. Biol. Evol.* 33 (5), 1280–1292. doi:10.1093/molbev/msw012

Karimi, A., Majlesi, M., and Rafieian-Kopaei, M. (2015). Herbal versus Synthetic Drugs; Beliefs and Facts. *J. Nephropharmacol* 4 (1), 27–30. https://linkinghub.elsevier.com/retrieve/pii/S0167923615001189.

Katiyar, S. K., Pal, H. C., and Prasad, R. (2017). Dietary Proanthocyanidins Prevent Ultraviolet Radiation-Induced Non-melanoma Skin Cancer through Enhanced Repair of Damaged DNA-dependent Activation of Immune Sensitivity, *Semin. Cancer Biol.* 46, 138–145. doi:10.1016/j.semcancer.2017.04.003

Kaur, H., and Moreau, R. (2021). Curcumin Represses mTORC1 Signaling in Caco-2 Cells by a Two-Sided Mechanism Involving the Loss of IRS-1 and Activation of AMPK. *Cell Signal* 78, 109842. doi:10.1016/j.cellsig.2020.109842

Kennedy, D. O., and Wightman, E. L. (2011). Herbal Extracts and Phytochemicals: Plant Secondary Metabolites and the Enhancement of Human Brain Function. *Adv. Nutr.* 2 (1), 32–50. doi:10.3945/an.110.000117

Kerz, T., Paret, G., and Herff, H. (2007). "Routes of Drug Administration," in *Cardiac Arrest: The Science and Practice of Resuscitation Medicine* (Cambridge, United Kingdom: Cambridge University Press), 614–638. doi:10.1017/CBO9780511544828.035

Khan, M. K., Zill-E-Humaand Dangles, O. (2014). A Comprehensive Review on Flavanones, the Major Citrus Polyphenols. *J. Food Compost. Anal.* 33 (1), 85–104. doi:10.1016/j.jfca.2013.11.004

Khoo, H. E., Azlan, A., Tang, S. T., and Lim, S. M. (2017). Anthocyanidins and Anthocyanins: Colored Pigments as Food, Pharmaceutical Ingredients, and the Potential Health Benefits. *Food Nutr. Res.* 61 (1), 1361779. doi:10.1080/16546628.2017.1361779

Kijanka, M., Dorresteijn, B., Oliveira, S., and Van Bergen En Henegouwen, P. M. (2015). Nanobody-based Cancer Therapy of Solid Tumors. *Nanomedicine (Lond)* 10 (1), 161–174. doi:10.2217/nnm.14.178

Kim, J., and Guan, K. L. (2019). mTOR as a central Hub of Nutrient Signalling and Cell Growth. *Nat. Cel Biol* 21 (1), 63–71. doi:10.1038/s41556-018-0205-1

Kiselev, V. I., Ashrafyan, L. A., Muyzhnek, E. L., Gerfanova, E. V., Antonova, I. B., Aleshikova, O. I., et al. (2018). A New Promising Way of Maintenance Therapy in Advanced Ovarian Cancer: A Comparative Clinical Study. *BMC Cancer* 18 (1), 904–916. doi:10.1186/s12885-018-4792-9

Knobloch, T. J., Uhrig, L. K., Pearl, D. K., Casto, B. C., Warner, B. M., Clinton, S. K., et al. (2016). Suppression of Proinflammatory and Prosurvival Biomarkers in Oral Cancer Patients Consuming a Black Raspberry Phytochemical-Rich Troche. *Cancer Prev. Res. (Phila)* 9 (2), 159–171. doi:10.1158/1940-6207.CAPR-15-0187

Kocaadam, B., and Şanlier, N. (2017). Curcumin, an Active Component of Turmeric (Curcuma Longa), and its Effects on Health. *Crit. Rev. Food Sci. Nutr.* 57 (13), 2889–2895. doi:10.1080/10408398.2015.1077195

Koes, R. E., Quattrocchio, F., and Mol, J. N. M. (1994). The Flavonoid Biosynthetic Pathway in Plants: Function and Evolution. *BioEssays* 16 (2), 123–132. doi:10.1002/bies.950160209

Kooshyar, M. M., Mozafari, P. M., Amirchaghmaghi, M., Pakfetrat, A., Karoos, P., Mohasel, M. R., et al. (2017). A Randomized Placebo- Controlled Double Blind Clinical Trial of Quercetin in the Prevention and Treatment of Chemotherapy-Induced Oral Mucositis. *J. Clin. Diagn. Res.* 11 (3), ZC46–ZC50. doi:10.7860/JCDR/2017/23975.9571

Kozłowska, A., and Szostak-Wegierek, D. (2014). Flavonoids--food Sources and Health Benefits. *Roczniki Państwowego Zakładu Higieny* 65 (2), 79–85. Available at: https://www.ars.usda.gov/ARSUserFiles/80400525/Data/Flav/Flav3.3.pdf.

Křížová, L., Dadáková, K., Kašparovská, J., and Kašparovský, T. (2019). Isoflavones. *Molecules* 24 (6), 1–28. doi:10.3390/molecules24061076

Kumar, S., and Pandey, A. K. (2013). Chemistry and Biological Activities of Flavonoids: An Overview. *ScientificWorldJournal* 2013, 1–16. doi:10.1155/2013/162750

Kumar, N. B., Pow-Sang, J., Egan, K. M., Spiess, P. E., Dickinson, S., Salup, R., et al. (2015). Randomized, Placebo-Controlled Trial of Green Tea Catechins for Prostate Cancer Prevention. *Cancer Prev. Res. (Phila)* 8 (10), 879–887. doi:10.1158/1940-6207.CAPR-14-0324

Kumar, N. B., Pow-Sang, J., Spiess, P. E., Park, J., Salup, R., Williams, C. R., et al. (2016). Randomized, Placebo-Controlled Trial Evaluating the Safety of One-Year Administration of green tea Catechins. *Oncotarget* 7 (43), 70794–70802. doi:10.18632/oncotarget.12222

Laleh, G. H., Frydoonfar, H., Heidary, R., Jameei, R., and Zare, S. (2005). The Effect of Light, Temperature, pH and Species on Stability of Anthocyanin Pigments in Four Berberis Species. *Pakistan J. Nutr.* 5 (1), 90–92. doi:10.3923/pjn.2006.90.92

Laptenko, O., Shiff, I., Freed-Pastor, W., Zupnick, A., Mattia, M., Freulich, E., et al. (2015). The P53 C Terminus Controls Site-Specific DNA Binding and Promotes Structural Changes within the Central DNA Binding Domain. *Mol. Cel* 57 (6), 1034–1046. doi:10.1016/j.molcel.2015.02.015

Lee, H. S., Cho, H. J., Yu, R., Lee, K. W., Chun, H. S., and Park, J. H. (2014). Mechanisms Underlying Apoptosis-Inducing Effects of Kaempferol in HT-29 Human Colon Cancer Cells. *Int. J. Mol. Sci.* 15 (2), 2722–2737. doi:10.3390/ijms15022722

Lee, Y.-J., Lee, Y.-J., Park, I.-S., Song, J.-H., Oh, M.-H., Nam, H.-S., et al. (2015). Quercetin Exerts Preferential Cytotoxic Effects on Malignant Mesothelioma Cells by Inducing P53 Expression, Caspase-3 Activation, and Apoptosis. *Mol. Cel. Toxicol.* 11 (3), 295–305. doi:10.1007/s13273-015-0029-z

Lee, Y. J., Beak, S. Y., Choi, I., and Sung, J. S. (2018). Quercetin and its Metabolites Protect Hepatocytes against Ethanol-Induced Oxidative Stress by Activation of Nrf2 and AP-1. *Food Sci. Biotechnol.* 27 (3), 809–817. doi:10.1007/s10068-017-0287-8

Leopoldini, M., Russo, N., and Toscano, M. (2011). The Molecular Basis of Working Mechanism of Natural Polyphenolic Antioxidants. *Food Chem.* 125 (2), 288–306. doi:10.1016/j.foodchem.2010.08.012

Li, C., Zhao, Y., Yang, D., Yu, Y., Guo, H., Zhao, Z., et al. (2015). Inhibitory Effects of Kaempferol on the Invasion of Human Breast Carcinoma Cells by Downregulating the Expression and Activity of Matrix Metalloproteinase-9. *Biochem. Cel Biol* 93 (1), 16–27. doi:10.1139/bcb-2014-0067

Li, W., Li, C., Ma, L., and Jin, F. (2020). Resveratrol Inhibits Viability and Induces Apoptosis in the Small Cell Lung Cancer H446 Cell Line via the PI3K/Akt/c-Myc Pathway. *Oncol. Rep.* 44 (5), 1821–1830. doi:10.3892/or.2020.7747

Li, F., Wang, Y., Li, D., Chen, Y., and Dou, Q. P. (2019). Are We Seeing a Resurgence in the Use of Natural Products for New Drug Discovery? *Expert Opin. Drug Discov.* 14 (5), 417–420. doi:10.1080/17460441.2019.1582639

Li, Y., Guo, Y., Feng, Z., Bergan, R., Li, B., Qin, Y., et al. (2019). Involvement of the PI3K/Akt/Nrf2 Signaling Pathway in Resveratrol-Mediated Reversal of Drug Resistance in HL-60/ADR Cells. *Nutr. Cancer* 71 (6), 1007–1018. doi:10.1080/01635581.2019.1578387

Limtrakul, P., Anuchapreeda, S., Lipigorngoson, S., and Dunn, F. W. (2001). Inhibition of Carcinogen Induced C-Ha-Ras and C-Fos Proto-Oncogenes Expression by Dietary Curcumin. *BMC Cancer* 1 (1), 1. doi:10.1186/1471-2407-1-1

Liu, W., Zhai, Y., Heng, X., Che, F. Y., Chen, W., Sun, D., et al. (2016). Oral Bioavailability of Curcumin: Problems and Advancements. *J. Drug Target.* 24 (8), 694–702. doi:10.3109/1061186X.2016.1157883

Liu, R., Ji, P., Liu, B., Qiao, H., Wang, X., Zhou, L., et al. (2017). Apigenin Enhances the Cisplatin Cytotoxic Effect through P53-Modulated Apoptosis. *Oncol. Lett.* 13 (2), 1024–1030. doi:10.3892/ol.2016.5495

Liu, L. D., Pang, Y. X., Zhao, X. R., Li, R., Jin, C. J., Xue, J., et al. (2019). Curcumin Induces Apoptotic Cell Death and Protective Autophagy by Inhibiting AKT/mTOR/p70S6K Pathway in Human Ovarian Cancer Cells. *Arch. Gynecol. Obstet.* 299 (6), 1627–1639. doi:10.1007/s00404-019-05058-3

Liu, R., Chen, Y., Liu, G., Li, C., Song, Y., Cao, Z., et al. (2020). PI3K/AKT Pathway as a Key Link Modulates the Multidrug Resistance of Cancers. *Cell Death Dis* 11 (9), 797. doi:10.1038/s41419-020-02998-6

Liu, Z., Wu, X., Lv, J., Sun, H., and Zhou, F. (2019). Resveratrol Induces P53 in Colorectal Cancer through SET7/9. *Oncol. Lett.* 17 (4), 3783–3789. doi:10.3892/ol.2019.10034

Liu, Z., Hong, Z., and Qu, P. (2020). Proteomic Analysis of Human Endometrial Tissues Reveals the Roles of PI3K/AKT/mTOR Pathway and Tumor Angiogenesis Molecules in the Pathogenesis of Endometrial Cancer. *Biomed. Res. Int.* 2020, 1–10. doi:10.1155/2020/5273969

Lu, J., Zang, H., Zheng, H., Zhan, Y., Yang, Y., Zhang, Y., et al. (2020). Overexpression of P-Akt, P-mTOR and P-eIF4E Proteins Associates with Metastasis and Unfavorable Prognosis in Non-small Cell Lung Cancer. *PLOS ONE* 15 (2), e0227768. doi:10.1371/journal.pone.0227768

Lv, Q., Luo, F., Zhao, X., Liu, Y., Hu, G., Sun, C., et al. (2015). Identification of Proanthocyanidins from Litchi (Litchi Chinensis Sonn.) Pulp by LC-ESI-Q-TOF-MS and Their Antioxidant Activity. *PLOS ONE* 10 (3), e0120480. doi:10.1371/journal.pone.0120480

Manach, C., Scalbert, A., Morand, C., Rémésy, C., and Jiménez, L. (2004). Polyphenols: Food Sources and Bioavailability. *Am. J. Clin. Nutr.* 79 (5), 727–747. doi:10.1093/ajcn/79.5.727

Manna, S., Mukherjee, S., Roy, A., Das, S., and Panda, C. K. (2009). Tea Polyphenols Can Restrict Benzo[a]pyrene-Induced Lung Carcinogenesis by Altered Expression of P53-Associated Genes and H-Ras, C-Myc and Cyclin D1. *J. Nutr. Biochem.* 20 (5), 337–349. doi:10.1016/j.jnutbio.2008.04.001

Manning, B. D., and Cantley, L. C. (2007). AKT/PKB Signaling: Navigating Downstream. *Cell* 129 (7), 1261–1274. doi:10.1016/j.cell.2007.06.009

Marais, J. P. J., Deavours, B., Dixon, R. A., and Ferreira, D. (2006). "The Stereochemistry of Flavonoids," in *The Science of Flavonoids*. Editor E. Grotewold (New York, NY: Springer), 1–46. doi:10.1007/978-0-387-28822-2_1

Marín, L., Miguélez, E. M., Villar, C. J., and Lombó, F. (2015). Bioavailability of Dietary Polyphenols and Gut Microbiota Metabolism: Antimicrobial Properties. *Biomed. Res. Int.* 2015, 905215–905218. doi:10.1155/2015/905215

Maurya, A. K., and Vinayak, M. (2017). Quercetin Attenuates Cell Survival, Inflammation, and Angiogenesis via Modulation of AKT Signaling in Murine T-Cell Lymphoma. *Nutr. Cancer* 69 (3), 470–480. doi:10.1080/01635581.2017.1267775

Mekinić, I. G., Skroza, D., Ljubenkov, I., and Katalinić, V. (2016). Insight into the Presence of Stilbenes in Medicinal Plants Traditionally Used in Croatian Folk Medicine. *Nat. Prod. Commun.* 11 (6), 833–835. doi:10.1177/1934578x1601100634

Metzler, M., Pfeiffer, E., Schulz, S. I., and Dempe, J. S. (2013). Curcumin Uptake and Metabolism. *BioFactors* 39 (1), 14–20. doi:10.1002/biof.1042

Mishra, R., Patel, H., Alanazi, S., Kilroy, M. K., and Garrett, J. T. (2021). PI3K Inhibitors in Cancer: Clinical Implications and Adverse Effects. *Int. J. Mol. Sci.* 22 (7), 3464. doi:10.3390/ijms22073464

Moos, P. J., Edes, K., Mullally, J. E., and Fitzpatrick, F. A. (2004). Curcumin Impairs Tumor Suppressor P53 Function in colon Cancer Cells. *Carcinogenesis* 25 (9), 1611–1617. doi:10.1093/carcin/bgh163

Muñoz-Maldonado, C., Zimmer, Y., and Medová, M. (2019). A Comparative Analysis of Individual Ras Mutations in Cancer Biology. *Front. Oncol.* 9, 1088. doi:10.3389/fonc.2019.01088

Mustachio, L. M., Chelariu-Raicu, A., Szekvolgyi, L., and Roszik, J. (2021). Targeting KRAS in Cancer: Promising Therapeutic Strategies. *Cancers* 13 (6), 1204–1214. doi:10.3390/cancers13061204

Nagata, T., Shirakawa, K., Kobayashi, N., Shiheido, H., Tabata, N., Sakuma-Yonemura, Y., et al. (2014). Structural Basis for Inhibition of the MDM2: p53 Interaction by an Optimized MDM2-Binding Peptide Selected with mRNA Display. *PLoS ONE* 9 (10), e109163–19. doi:10.1371/journal.pone.0109163

Nie, J., Zhang, L., Zhao, G., and Du, X. (2019). Quercetin Reduces Atherosclerotic Lesions by Altering the Gut Microbiota and Reducing Atherogenic Lipid Metabolites. *J. Appl. Microbiol.* 127 (6), 1824–1834. doi:10.1111/jam.14441

Niesen, D. B., Hessler, C., and Seeram, N. P. (2013). Beyond Resveratrol: A Review of Natural Stilbenoids Identified from 2009-2013. *J. Berry Res.* 3 (4), 181–196. doi:10.3233/JBR-130062

Nishihara, R., Wang, M., Qian, Z. R., Baba, Y., Yamauchi, M., Mima, K., et al. (2014). Alcohol, One-Carbon Nutrient Intake, and Risk of Colorectal Cancer According to Tumor Methylation Level of IGF2 Differentially Methylated Region. *Am. J. Clin. Nutr.* 100 (6), 1479–1488. doi:10.3945/ajcn.114.095539

Noorolyai, S., Shajari, N., Baghbani, E., Sadreddini, S., and Baradaran, B. (2019). The Relation between PI3K/AKT Signalling Pathway and Cancer. *Gene* 698, 120–128. doi:10.1016/j.gene.2019.02.076

Nurgali, K., Jagoe, R. T., and Abalo, R. (2018). Editorial: Adverse Effects of Cancer Chemotherapy: Anything New to Improve Tolerance and Reduce Sequelae? *Front. Pharmacol.* 9, 245. doi:10.3389/fphar.2018.00245

Oi, N., Yuan, J., Malakhova, M., Luo, K., Li, Y., Ryu, J., et al. (2015). Resveratrol Induces Apoptosis by Directly Targeting Ras-GTPase-Activating Protein SH3 Domain-Binding Protein 1. *Oncogene* 34 (20), 2660–2671. doi:10.1038/onc.2014.194

Oya, Y., Mondal, A., Rawangkan, A., Umsumarng, S., Iida, K., Watanabe, T., et al. (2017). Down-Regulation of Histone Deacetylase 4, -5 and -6 as a Mechanism of Synergistic Enhancement of Apoptosis in Human Lung Cancer Cells Treated with the Combination of a Synthetic Retinoid, Am80 and green tea Catechin. *J. Nutr. Biochem.* 42, 7–16. doi:10.1016/j.jnutbio.2016.12.015

Paller, C. J., Rudek, M. A., Zhou, X. C., Wagner, W. D., Hudson, T. S., Anders, N., et al. (2015). A Phase I Study of Muscadine Grape Skin Extract in Men with Biochemically Recurrent Prostate Cancer: Safety, Tolerability, and Dose Determination. *Prostate* 75 (14), 1518–1525. doi:10.1002/pros.23024

Panche, A. N., Diwan, A. D., and Chandra, S. R. (2016). Flavonoids: An Overview. *J. Nutr. Sci.* 5, e47. doi:10.1017/jns.2016.41

Patiño-Morales, C. C., Soto-Reyes, E., Arechaga-Ocampo, E., Ortiz-Sánchez, E., Antonio-Véjar, V., Pedraza-Chaverri, J., et al. (2020). Curcumin Stabilizes P53 by Interaction with NAD(P)H:quinone Oxidoreductase 1 in Tumor-Derived Cell Lines. *Redox Biol.* 28, 101320. doi:10.1016/j.redox.2019.101320

Pérez-Jiménez, J., Neveu, V., Vos, F., and Scalbert, A. (2010). Identification of the 100 Richest Dietary Sources of Polyphenols: An Application of the Phenol-Explorer Database. *Eur. J. Clin. Nutr.* 64 Suppl 3, S112–S120. doi:10.1038/ejcn.2010.221

Peng, G., Wargovich, M. J., and Dixon, D. A. (2006). Anti-proliferative Effects of Green tea Polyphenol EGCG on Ha-Ras-Induced Transformation of Intestinal Epithelial Cells. *Cancer Lett.* 238 (2), 260–270. doi:10.1016/j.canlet.2005.07.018

Pereira, D., Valentão, P., Pereira, J., and Andrade, P. (2009). Phenolics: From Chemistry to Biology. *Molecules* 14 (6), 2202–2211. doi:10.3390/molecules14062202

M.Pevzner, A., A.Gaptulbarova, K., M.Tsyganov, M., K.Ibragimova, M., V.Vvedensky, A., G.Zhusina, Y., et al. (2021). Investigation of Somatic PIK3CA Gene Mutations in Breast Cancer Patients. *J. BUON* 26 (3), 747–752.

Piao, L., Mukherjee, S., Chang, Q., Xie, X., Li, H., Castellanos, M. R., et al. (2017). TriCurin, a Novel Formulation of Curcumin, Epicatechin Gallate, and Resveratrol, Inhibits the Tumorigenicity of Human Papillomavirus-Positive Head and Neck Squamous Cell Carcinoma. *Oncotarget* 8 (36), 60025–60035. doi:10.18632/oncotarget.10620

Pons, D. G., Nadal-Serrano, M., Blanquer-Rossello, M. M., Sastre-Serra, J., Oliver, J., and Roca, P. (2014). Genistein Modulates Proliferation and Mitochondrial Functionality in Breast Cancer Cells Depending on ERalpha/ERbeta Ratio. *J. Cel Biochem* 115 (5), 949–958. doi:10.1002/jcb.24737

Preedy, V. R. (2013). Isoflavones. Editor V. R. Preedy. 1st ed. (Cambridge, United Kingdom: RSC Publishing).

Psahoulia, F. H., Moumtzi, S., Roberts, M. L., Sasazuki, T., Shirasawa, S., and Pintzas, A. (2007). Quercetin Mediates Preferential Degradation of Oncogenic Ras and Causes Autophagy in Ha-RAS-Transformed Human colon Cells. *Carcinogenesis* 28 (5), 1021–1031. doi:10.1093/carcin/bgl232

Raj, N., and Attardi, L. D. (2017). The Transactivation Domains of the P53 Protein. *Cold Spring Harb Perspect. Med.* 7 (1), 1–18. doi:10.1101/cshperspect.a026047

Ramakrishna, R., Diamond, T. H., Alexander, W., Manoharan, A., and Golombick, T. (2020). Use of Curcumin in Multiple Myeloma Patients Intolerant of Steroid Therapy. *Clin. Case Rep.* 8 (4), 739–744. doi:10.1002/ccr3.2735

Rastogi, H., and Jana, S. (2014). Evaluation of Inhibitory Effects of Caffeic Acid and Quercetin on Human Liver Cytochrome P450 Activities. *Phytother Res.* 28 (12), 1873–1878. doi:10.1002/ptr.5220

Rathinaswamy, M. K., and Burke, J. E. (2019). Class I Phosphoinositide 3-kinase (PI3K) Regulatory Subunits and Their Roles in Signaling and Disease. *Adv. Biol. Regul.* 75, 100657. doi:10.1016/j.jbior.2019.100657

Rauf, A., Imran, M., Abu-Izneid, T., Iahtisham-Ul-HaqPatel, S., Pan, X., et al. (2019). Proanthocyanidins: A Comprehensive Review. *Biomed. Pharmacother.* 116, 108999. doi:10.1016/j.biopha.2019.108999

Revathidevi, S., and Munirajan, A. K. (2019). Akt in Cancer: Mediator and More. *Semin. Cancer Biol.* 59, 80–91. doi:10.1016/j.semcancer.2019.06.002

Riahi-Chebbi, I., Souid, S., Othman, H., Haoues, M., Karoui, H., Morel, A., et al. (2019). The Phenolic Compound Kaempferol Overcomes 5-fluorouracil Resistance in Human Resistant LS174 colon Cancer Cells. *Sci. Rep.* 9 (1), 1–20. doi:10.1038/s41598-018-36808-z

Rodríguez-Berriguete, G., Fraile, B., Martínez-Onsurbe, P., Olmedilla, G., Paniagua, R., and Royuela, M. (2012). MAP Kinases and Prostate Cancer. *J. Signal. Transduct.* 2012, 169170–169179. doi:10.1155/2012/169170

Rothwell, J. A., Perez-Jimenez, J., Neveu, V., Medina-Remón, A., M'hiri, N., García-Lobato, P., et al. (2013). Phenol-Explorer 3.0: A Major Update of the Phenol-Explorer Database to Incorporate Data on the Effects of Food Processing on Polyphenol Content. *Database (Oxford)* 2013, bat070–8. doi:10.1093/database/bat070

Rue, E. A., Rush, M. D., and van Breemen, R. B. (2018). Procyanidins: a Comprehensive Review Encompassing Structure Elucidation via Mass Spectrometry. *Phytochem. Rev.* 17 (1), 1–16. doi:10.1007/s11101-017-9507-3

Sabzichi, M., Hamishehkar, H., Ramezani, F., Sharifi, S., Tabasinezhad, M., Pirouzpanah, M., et al. (2014). Luteolin-loaded Phytosomes Sensitize Human Breast Carcinoma MDA-MB 231 Cells to Doxorubicin by Suppressing Nrf2 Mediated Signalling. *Asian Pac. J. Cancer Prev.* 15 (13), 5311–5316. doi:10.7314/APJCP.2014.15.13.5311

Saghatelyan, T., Tananyan, A., Janoyan, N., Tadevosyan, A., Petrosyan, H., Hovhannisyan, A., et al. (2020). Efficacy and Safety of Curcumin in Combination with Paclitaxel in Patients with Advanced, Metastatic Breast Cancer: A Comparative, Randomized, Double-Blind, Placebo-Controlled Clinical Trial. *Phytomedicine* 70, 153218. doi:10.1016/j.phymed.2020.153218

Saha, S., Buttari, B., Panieri, E., Profumo, E., and Saso, L. (2020). An Overview of Nrf2 Signaling Pathway and its Role in Inflammation. *Molecules* 25 (22), 1–31. doi:10.3390/molecules25225474

Santarpia, L., Lippman, S. M., and El-Naggar, A. K. (2012). Targeting the MAPK-RAS-RAF Signaling Pathway in Cancer Therapy. *Expert Opin. Ther. Targets* 16 (1), 103–119. doi:10.1517/14728222.2011.645805.Targeting

Saud, S. M., Li, W., Morris, N. L., Matter, M. S., Colburn, N. H., Kim, Y. S., et al. (2014). Resveratrol Prevents Tumorigenesis in Mouse Model of Kras Activated Sporadic Colorectal Cancer by Suppressing Oncogenic Kras Expression. *Carcinogenesis* 35 (12), 2778–2786. doi:10.1093/carcin/bgu209

Saxton, R. A., and Sabatini, D. M. (2017). mTOR Signaling in Growth, Metabolism, and Disease. *Cell* 168 (6), 960–976. doi:10.1016/j.cell.2017.02.004

Seleem, D., Pardi, V., and Murata, R. M. (2017). Review of Flavonoids: A Diverse Group of Natural Compounds with Anti-Candida Albicans Activity *In Vitro*. *Arch. Oral Biol.* 76, 76–83. doi:10.1016/j.archoralbio.2016.08.030

Sen, G. S., Mohanty, S., Hossain, D. M., Bhattacharyya, S., Banerjee, S., Chakraborty, J., et al. (2011). Curcumin Enhances the Efficacy of Chemotherapy by Tailoring p65NFκB-P300 Cross-Talk in Favor of P53-P300 in Breast Cancer. *J. Biol. Chem.* 286 (49), 42232–42247. doi:10.1074/jbc.M111.262295

Sheffels, E., and Kortum, R. L. (2021). The Role of Wild-Type RAS in Oncogenic RAS Transformation. *Genes (Basel)* 12 (5), 662. doi:10.3390/genes12050662

Shield, K. D., Ferlay, J., Jemal, A., Sankaranarayanan, R., Chaturvedi, A. K., Bray, F., et al. (2017). The Global Incidence of Lip, Oral Cavity, and Pharyngeal Cancers by Subsite in 2012. *CA Cancer J. Clin.* 67 (1), 51–64. doi:10.3322/caac.21384

Shimizu, C., Wakita, Y., Inoue, T., Hiramitsu, M., Okada, M., Mitani, Y., et al. (2019). Effects of Lifelong Intake of Lemon Polyphenols on Aging and Intestinal Microbiome in the Senescence-Accelerated Mouse Prone 1 (SAMP1). *Sci. Rep.* 9 (1), 3671. doi:10.1038/s41598-019-40253-x

Siddique, H. R., Liao, D. J., Mishra, S. K., Schuster, T., Wang, L., Matter, B., et al. (2012). Epicatechin-rich cocoa Polyphenol Inhibits Kras-Activated Pancreatic Ductal Carcinoma Cell Growth *In Vitro* and in a Mouse Model. *Int. J. Cancer* 131 (7), 1720–1731. doi:10.1002/ijc.27409

Sidhar, H., and Giri, R. K. (2017). Induction of Bex Genes by Curcumin Is Associated with Apoptosis and Activation of P53 in N2a Neuroblastoma Cells. *Sci. Rep.* 7, 41420. doi:10.1038/srep41420

Srivastava, S., Somasagara, R. R., Hegde, M., Nishana, M., Tadi, S. K., Srivastava, M., et al. (2016). Quercetin, a Natural Flavonoid Interacts with DNA, Arrests Cell Cycle and Causes Tumor Regression by Activating Mitochondrial Pathway of Apoptosis. *Sci. Rep.* 6, 24049. doi:10.1038/srep24049

Sudan, S., and Rupasinghe, H. P. (2014). Quercetin-3-O-glucoside Induces Human DNA Topoisomerase II Inhibition, Cell Cycle Arrest and Apoptosis in Hepatocellular Carcinoma Cells. *Anticancer Res.* 34 (4), 1691–1699.

Sun, X. X., and Dai, M. S. (2014). Deubiquitinating Enzyme Regulation of the P53 Pathway: A Lesson from Otub1. *World J. Biol. Chem.* 5 (2), 75–84. doi:10.4331/wjbc.v5.i2.75

Sung, H., Ferlay, J., Siegel, R. L., Laversanne, M., Soerjomataram, I., Jemal, A., et al. (2021). Global Cancer Statistics 2020: GLOBOCAN Estimates of Incidence and Mortality Worldwide for 36 Cancers in 185 Countries. *CA A. Cancer J. Clin.* 71 (3), 209–249. doi:10.3322/caac.21660

Takahashi, M., Nokihara, K., and Mihara, H. (2003). Construction of a Protein-Detection System Using a Loop Peptide Library with a Fluorescence Label. *Chem. Biol.* 10, 53–60. doi:10.1016/s10.1016/s1074-5521(02)00308-3

Tang, Y., Zhao, W., Chen, Y., Zhao, Y., and Gu, W. (2008). Acetylation Is Indispensable for P53 Activation. *Cell* 133 (4), 612–626. doi:10.1016/j.cell.2008.03.025

Tanigawa, S., Fujii, M., and Hou, D. X. (2008). Stabilization of P53 Is Involved in Quercetin-Induced Cell Cycle Arrest and Apoptosis in HepG2 Cells. *Biosci. Biotechnol. Biochem.* 72 (3), 797–804. doi:10.1271/bbb.70680

Tavakol, S., Ashrafizadeh, M., Deng, S., Azarian, M., Abdoli, A., Motavaf, M., et al. (2019). Autophagy Modulators: Mechanistic Aspects and Drug Delivery Systems. *Biomolecules* 9 (10), 530. doi:10.3390/biom9100530

Terahara, N. (2015). Flavonoids in Foods: A Review. *Nat. Prod. Commun.* 10 (3), 521–528. doi:10.1177/1934578x1501000334

Tsao, A. S., Liu, D., Martin, J., Tang, X. M., Lee, J. J., El-Naggar, A. K., et al. (2009). Phase II Randomized, Placebo-Controlled Trial of Green Tea Extract in Patients with High-Risk Oral Premalignant Lesions. *Cancer Prev. Res. (Phila)* 2 (11), 931–941. doi:10.1158/1940-6207.CAPR-09-0121

Tsuda, T. (2018). Curcumin as a Functional Food-Derived Factor: Degradation Products, Metabolites, Bioactivity, and Future Perspectives. *Food Funct.* 9 (2), 705–714. doi:10.1039/c7fo01242j

Vareed, S. K., Kakarala, M., Ruffin, M. T., Crowell, J. A., Normolle, D. P., Djuric, Z., et al. (2008). Pharmacokinetics of Curcumin Conjugate Metabolites in Healthy Human Subjects. *Cancer Epidemiol. Biomarkers Prev.* 17 (6), 1411–1417. doi:10.1158/1055-9965.EPI-07-2693

Vargas, A. J., and Thompson, P. A. (2012). Diet and Nutrient Factors in Colorectal Cancer Risk. *Nutr. Clin. Pract.* 27 (5), 613–623. doi:10.1177/0884533612454885

Velderrain-Rodríguez, G. R., Palafox-Carlos, H., Wall-Medrano, A., Ayala-Zavala, J. F., Chen, C. Y., Robles-Sánchez, M., et al. (2014). Phenolic Compounds: Their Journey after Intake. *Food Funct.* 5 (2), 189–197. doi:10.1039/c3fo60361j

Vidula, N., Yau, C., Li, J., Esserman, L. J., and Rugo, H. S. (2017). Receptor Activator of Nuclear Factor Kappa B (RANK) Expression in Primary Breast

Cancer Correlates with Recurrence-free Survival and Development of Bone Metastases in I-SPY1 (CALGB 150007/150012; ACRIN 6657). *Breast Cancer Res. Treat.* 165 (1), 129–138. doi:10.1007/s10549-017-4318-1

Vinarov, Z., Abrahamsson, B., Artursson, P., Batchelor, H., Berben, P., Bernkop-Schnürch, A., et al. (2021). Current Challenges and Future Perspectives in Oral Absorption Research: An Opinion of the UNGAP Network. *Adv. Drug Deliv. Rev.* 171, 289–331. doi:10.1016/j.addr.2021.02.001

Wang, W., Chen, J. X., Liao, R., Deng, Q., Zhou, J. J., Huang, S., et al. (2002). Sequential Activation of the MEK-Extracellular Signal-Regulated Kinase and MKK3/6-P38 Mitogen-Activated Protein Kinase Pathways Mediates Oncogenic Ras-Induced Premature Senescence. *Mol. Cel Biol* 22 (10), 3389–3403. doi:10.1128/MCB.22.10.3389-3403.2002

Wang, S., Yang, C., Tu, H., Zhou, J., Liu, X., Cheng, Y., et al. (2017). Characterization and Metabolic Diversity of Flavonoids in Citrus Species. *Sci. Rep.* 7, 10549. doi:10.1038/s41598-017-10970-2

Wang, W., Zhan, L., Guo, D., Xiang, Y., Tian, M., Zhang, Y., et al. (2019). Grape Seed Proanthocyanidins Inhibit Proliferation of Pancreatic Cancer Cells by Modulating microRNA Expression. *Oncol. Lett.* 17 (3), 2777–2787. doi:10.3892/ol.2019.9887

Wang, Z., Liu, F., Liao, W., Yu, L., Hu, Z., Li, M., et al. (2020). Curcumin Suppresses Glioblastoma Cell Proliferation by P-AKT/mTOR Pathway and Increases the PTEN Expression. *Arch. Biochem. Biophys.* 689, 108412. doi:10.1016/j.abb.2020.108412

Wei, X., Wu, S., Song, T., Chen, L., Gao, M., Borcherds, W., et al. (2016). Secondary Interaction between MDMX and P53 Core Domain Inhibits P53 DNA Binding. *Proc. Natl. Acad. Sci. U S A.* 113 (19), E2558–E2563. doi:10.1073/pnas.1603838113

Wei, R., Penso, N. E. C., Hackman, R. M., Wang, Y., and Mackenzie, G. G. (2019). Epigallocatechin-3-Gallate (EGCG) Suppresses Pancreatic Cancer Cell Growth, Invasion, and Migration Partly through the Inhibition of Akt Pathway and Epithelial-Mesenchymal Transition: Enhanced Efficacy when Combined with Gemcitabine. *Nutrients* 11 (8), 1856. doi:10.3390/nu11081856

Weiss, R. A. (2020). A Perspective on the Early Days of RAS Research. *Cancer Metastasis Rev.* 39 (4), 1023–1028. doi:10.1007/s10555-020-09919-1

Weng, J. K., Philippe, R. N., and Noel, J. P. (2012). The Rise of Chemodiversity in Plants. *Science* 336 (6089), 1667–1670. doi:10.1126/science.1217411

Weng, Y. P., Hung, P. F., Ku, W. Y., Chang, C. Y., Wu, B. H., Wu, M. H., et al. (2018). The Inhibitory Activity of Gallic Acid against DNA Methylation: Application of Gallic Acid on Epigenetic Therapy of Human Cancers. *Oncotarget* 9 (1), 361–374. doi:10.18632/oncotarget.23015

Xiao, K., Zhang, H.-J., Xuan, L.-J., Zhang, J., Xu, Y.-M., and Bai, D.-L. (2008). "Stilbenoids: Chemistry and Bioactivities," in *Studies in Natural Products Chemistry*. Editor A. u. Rahman (Amsterdam, The Netherlands: Elsevier B.V), Vol. 34, 453–646. doi:10.1016/S1572-5995(08)80032-4

Xiaokaiti, Y., Wu, H., Chen, Y., Yang, H., Duan, J., Li, X., et al. (2015). EGCG Reverses Human Neutrophil Elastase-Induced Migration in A549 Cells by Directly Binding to HNE and by Regulating α1-AT. *Sci. Rep.* 5, 11494. doi:10.1038/srep11494

Yamada, N., Matsushima-Nishiwaki, R., and Kozawa, O. (2020). Quercetin Suppresses the Migration of Hepatocellular Carcinoma Cells Stimulated by Hepatocyte Growth Factor or Transforming Growth Factor-α: Attenuation of AKT Signaling Pathway. *Arch. Biochem. Biophys.* 682, 108296. doi:10.1016/j.abb.2020.108296

Yang, L., Xian, D., Xiong, X., Lai, R., Song, J., and Zhong, J. (2018). Proanthocyanidins against Oxidative Stress: From Molecular Mechanisms to Clinical Applications. *Biomed. Res. Int.* 2018, 1–11. doi:10.1155/2018/8584136

Yang, Y., Wang, T., Chen, D., Ma, Q., Zheng, Y., Liao, S., et al. (2019). Quercetin Preferentially Induces Apoptosis in KRAS-Mutant Colorectal Cancer Cells via JNK Signaling Pathways. *Cell Biol Int* 43 (2), 117–124. doi:10.1002/cbin.11055

Yeo, C., Han, D.-S., Lee, H.-J., and Lee, E.-O. (2020). Epigallocatechin-3-gallate Suppresses Vasculogenic Mimicry through Inhibiting the twist/VE-Cadherin/AKT Pathway in Human Prostate Cancer PC-3 Cells. *Ijms* 21 (2), 439. doi:10.3390/ijms21020439

Young, L. F., Hantz, H. L., and Martin, K. R. (2005). Resveratrol Modulates Gene Expression Associated with Apoptosis, Proliferation and Cell Cycle in Cells with Mutated Human C-Ha-Ras, but Does Not Alter C-Ha-Ras mRNA or Protein Expression. *J. Nutr. Biochem.* 16 (11), 663–674. doi:10.1016/j.jnutbio.2005.03.004

Yu, X., Long, Y. C., and Shen, H. M. (2015). Differential Regulatory Functions of Three Classes of Phosphatidylinositol and Phosphoinositide 3-kinases in Autophagy. *Autophagy* 11 (10), 1711–1728. doi:10.1080/15548627.2015.1043076

Yuan, S. X., Wang, D. X., Wu, Q. X., Ren, C. M., Li, Y., Chen, Q. Z., et al. (2016). BMP9/p38 MAPK Is Essential for the Antiproliferative Effect of Resveratrol on Human colon Cancer. *Oncol. Rep.* 35 (2), 939–947. doi:10.3892/or.2015.4407

Zaheer, K., and Humayoun Akhtar, M. (2017). An Updated Review of Dietary Isoflavones: Nutrition, Processing, Bioavailability and Impacts on Human Health. *Crit. Rev. Food Sci. Nutr.* 57 (6), 1280–1293. doi:10.1080/10408398.2014.989958

Zaman, M. S., Chauhan, N., Yallapu, M. M., Gara, R. K., Maher, D. M., Kumari, S., et al. (2016). Curcumin Nanoformulation for Cervical Cancer Treatment. *Sci. Rep.* 6, 20051. doi:10.1038/srep20051

Zhang, P., and Zhang, X. (2018). Stimulatory Effects of Curcumin and Quercetin on Posttranslational Modifications of P53 during Lung Carcinogenesis. *Hum. Exp. Toxicol.* 37 (6), 618–625. doi:10.1177/0960327117714037

Zhang, Y., Liu, B., Chen, X., Zhang, N., Li, G., Zhang, L. H., et al. (2017). Naringenin Ameliorates Behavioral Dysfunction and Neurological Deficits in a D-Galactose-Induced Aging Mouse Model Through Activation of PI3K/Akt/Nrf2 Pathway. *Rejuvenation Res.* 20 (6), 462–472. doi:10.1089/rej.2017.1960

Zhang, Z., Yi, P., Tu, C., Zhan, J., Jiang, L., and Zhang, F. (2019). Curcumin Inhibits ERK/c-Jun Expressions and Phosphorylation against Endometrial Carcinoma. *Biomed. Res. Int.* 2019, 1–13. doi:10.1155/2019/8912961

Zhang, P., Meng, X., Liu, L., Li, S., Li, Y., Ali, S., et al. (2021). Identification of the Prognostic Signatures of Glioma with Different PTEN Status. *Front. Oncol.* 11, 633357. doi:10.3389/fonc.2021.633357

Zhao, G., Han, X., Cheng, W., Ni, J., Zhang, Y., Lin, J., et al. (2017). Apigenin Inhibits Proliferation and Invasion, and Induces Apoptosis and Cell Cycle Arrest in Human Melanoma Cells. *Oncol. Rep.* 37 (4), 2277–2285. doi:10.3892/or.2017.5450

Zhao, J., Blayney, A., Liu, X., Gandy, L., Jin, W., Yan, L., et al. (2021). EGCG Binds Intrinsically Disordered N-Terminal Domain of P53 and Disrupts P53-MDM2 Interaction. *Nat. Commun.* 12 (1), 1–11. doi:10.1038/s41467-021-21258-5

Zhao, W., Zhou, X., Qi, G., and Guo, Y. (2018). Curcumin Suppressed the Prostate Cancer by Inhibiting JNK Pathways via Epigenetic Regulation. *J. Biochem. Mol. Toxicol.* 32 (5), e22049. doi:10.1002/jbt.22049

Zhao, Y., Tang, H., Zeng, X., Ye, D., and Liu, J. (2018). Resveratrol Inhibits Proliferation, Migration and Invasion via Akt and ERK1/2 Signaling Pathways in Renal Cell Carcinoma Cells. *Biomed. Pharmacother.* 98, 36–44. doi:10.1016/j.biopha.2017.12.029

Zheng, A. W., Chen, Y. Q., Zhao, L. Q., and Feng, J. G. (2017). Myricetin Induces Apoptosis and Enhances Chemosensitivity in Ovarian Cancer Cells. *Oncol. Lett.* 13 (6), 4974–4978. doi:10.3892/ol.2017.6031

Zhou, Y. Y., Li, Y., Jiang, W. Q., and Zhou, L. F. (2015). MAPK/JNK Signalling: A Potential Autophagy Regulation Pathway. *Biosci. Rep.* 35 (3), 1–10. doi:10.1042/BSR20140141

Zhou, Y., Tang, J., Du, Y., Ding, J., and Liu, J. Y. (2016). The green tea Polyphenol EGCG Potentiates the Antiproliferative Activity of Sunitinib in Human Cancer Cells. *Tumour Biol.* 37 (7), 8555–8566. doi:10.1007/s13277-015-4719-x

Zhou, H., Ning, Y., Zeng, G., Zhou, C., and Ding, X. (2021). Curcumin Promotes Cell Cycle Arrest and Apoptosis of Acute Myeloid Leukemia Cells by Inactivating AKT. *Oncol. Rep.* 45 (4), 1–9. doi:10.3892/or.2021.7962

Zhu, W., Qin, K., Zhang, Y. C., Rottinghaus, E. R., Chen, Y. C., Kliethermes, B., et al. (2012). Trans-resveratrol Alters Mammary Promoter Hypermethylation in Women at Increased Risk for Breast Cancerr. *Nutr. Cancer* 64 (3), 393–400. doi:10.1080/01635581.2012.654926

Conflict of Interest: The authors declare that the research was conducted in the absence of any commercial or financial relationships that could be construed as a potential conflict of interest.

Publisher's Note: All claims expressed in this article are solely those of the authors and do not necessarily represent those of their affiliated organizations or those of the publisher, the editors, and the reviewers. Any product that may be evaluated in this article or claim that may be made by its manufacturer is not guaranteed or endorsed by the publisher.

frontiers in Pharmacology

ORIGINAL RESEARCH
published: 29 October 2021
doi: 10.3389/fphar.2021.713200

Saikosaponin A, a Triterpene Saponin, Suppresses Angiogenesis and Tumor Growth by Blocking VEGFR2-Mediated Signaling Pathway

Pan Zhang[1,2†], Xing Lai[3†], Mao-Hua Zhu[3], Mei Long[3], Xue-Liang Liu[3], Zi-Xiang Wang[1], Yifan Zhang[1], Run-Jie Guo[2], Jing Dong[3], Qin Lu[3], Peng Sun[4], Chao Fang[3] and Mei Zhao[1,2]**

[1]Department of Pharmacy, Shanghai University of Medicine and Health Sciences, Shanghai, China, [2]Graduate School, Shanghai University of Traditional Chinese Medicine, Shanghai, China, [3]Tongren Hospital and State Key Laboratory of Oncogenes and Related Genes, Department of Pharmacology and Chemical Biology, Hongqiao International Institute of Medicine, Shanghai Jiao Tong University School of Medicine (SJTU-SM), Shanghai, China, [4]Department of General Surgery, Tongren Hospital, SJTU-SM, Shanghai, China

OPEN ACCESS

Edited by:
Marne Carvalho De Vasconcellos, Federal University of Amazonas, Brazil

Reviewed by:
Lihui Wang, Shenyang Pharmaceutical University, China
Aling Shen, Fujian University of Traditional Chinese Medicine, China

***Correspondence:**
Mei Zhao
zhaom@sumhs.edu.cn
Chao Fang
fangchao32@sjtu.edu.cn

†These authors share first authorship

Specialty section:
This article was submitted to Pharmacology of Anti-Cancer Drugs, a section of the journal Frontiers in Pharmacology

Received: 22 May 2021
Accepted: 03 September 2021
Published: 29 October 2021

Citation:
Zhang P, Lai X, Zhu M-H, Long M, Liu X-L, Wang Z-X, Zhang Y, Guo R-J, Dong J, Lu Q, Sun P, Fang C and Zhao M (2021) Saikosaponin A, a Triterpene Saponin, Suppresses Angiogenesis and Tumor Growth by Blocking VEGFR2-Mediated Signaling Pathway. Front. Pharmacol. 12:713200. doi: 10.3389/fphar.2021.713200

Saikosaponin A (SSA), a main triterpenoid saponin component from *Radix Bupleurum*, has been revealed to have a variety of pharmacological activities. However, whether SSA can inhibit angiogenesis, a key step in solid tumor progression, remains unknown. In this study, we demonstrated that SSA could powerfully suppress the proliferation, migration, and tube formation of human umbilical vein endothelial cells. SSA also significantly inhibited angiogenesis in the models of the chick embryo chorioallantoic membrane and Matrigel plugs. Moreover, SSA was found to inhibit tumor growth in both orthotopic 4T1 breast cancer and subcutaneous HCT-15 colorectal tumor by the inhibition of tumor angiogenesis. Western blot assay indicated the antiangiogenic mechanism of SSA in the suppression of the protein phosphorylation of VEGFR2 and the downstream protein kinase including PLCγ1, FAK, Src, and Akt. In summary, SSA can suppress angiogenesis and tumor growth by blocking the VEGFR2-mediated signaling pathway.

Keywords: saikosaponin A, angiogenesis, VEGFR2, chick embryo chorioallantoic membrane, cancer therapy

INTRODUCTION

Saikosaponin A (SSA, **Figure 1A**), a main triterpenoid saponin component from *Radix Bupleurum*, has been widely investigated for its multiple pharmacological activities, such as antidepressant (Guo et al., 2020), immunoregulatory (Qi et al., 2021), and anti-inflammatory properties (He et al., 2016; Du et al., 2018; Zhou et al., 2019; Piao et al., 2020). The anticancer effects of SSA are also intriguing with diverse molecular mechanisms. Specifically, SSA can induce apoptosis or inhibit the proliferation of tumor cells through caspase-2, -4, and -8 activation (Kim and Hong, 2011; Kang et al., 2017); ERK signaling activation; or CXCR4 downregulation (Wang et al., 2019). SSA also regulates Th1/Th2 balance in tumors (Zhao et al., 2019) and generates microbicidal neutrophils to reduce cancer chemotherapy–induced neutropenia infection (Qi et al., 2021); both of them can benefit from antitumor therapy. However, it remains elusive whether SSA can directly suppress angiogenesis, the hallmark and a key step in solid tumor progression (Hanahan and Weinberg, 2011).

Angiogenesis, the development of new blood vessels from pre-existing ones, is a validated target in cancer clinics. More than 10 antiangiogenic drugs, including small kinase inhibitors (sunitinib, sorafenib, pazopanib, etc.), antibodies (bevacizumab and ramucirumab), and fusion proteins

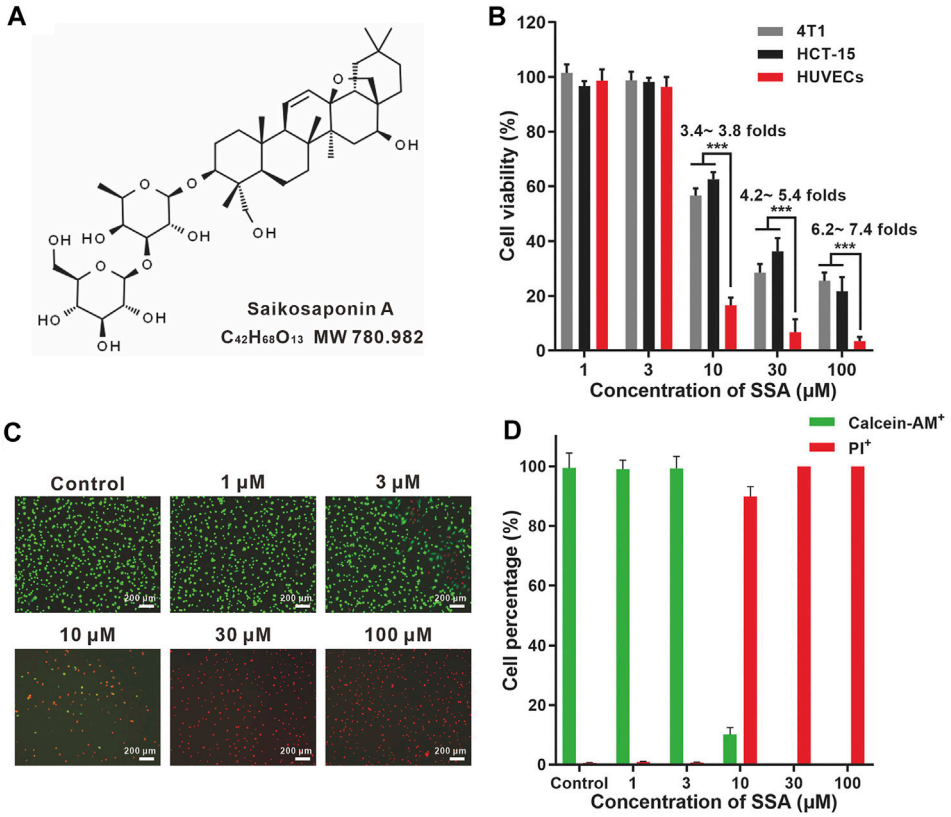

FIGURE 1 | SSA more efficiently suppressed the viabilities of HUVECs compared to those of HCT-15 and 4T1 cells. **(A)** Chemical structures of SSA. **(B)** Effect of SSA on cell viability. **(C)** Representative fluorescence photographs of HUVECs stained with calcein-AM/PI after treatment with SSA. **(D)** The live (calcein$^+$) and dead (PI$^+$) cell percentages of HUVECs after SSA treatments. All values were expressed as mean ± *s*.d. $n = 4$. $^{***}p < 0.001$.

(aflibercept), have been approved by the FDA and other countries for multiple cancer indicators (Jayson et al., 2016). However, low efficacy, toxic side effects, unsatisfied pharmacokinetic behavior, and high cost limit their wide use in cancer clinics (Jain et al., 2011; Jayson et al., 2016; Kim et al., 2019). It is urgent to develop new antiangiogenic agents. In recent years, exploring antiangiogenic natural products is emerging as an attractive research field. Many natural products with diverse molecular structures exerted potent antitumor actions via multiple antiangiogenic mechanisms (Guan et al., 2016).

In this work, the antiangiogenic effect of SSA and its molecular mechanism were revealed. SSA suppressed the proliferation, migration, and tube formation of human umbilical vascular endothelial cells (HUVECs, a classical *in vitro* cell model mimicking tumor vascular endothelial cells). SSA inhibited angiogenesis in the chick embryo chorioallantoic membrane (CAM) and Matrigel plug models. Moreover, SSA suppressed angiogenesis and tumor growth in orthotopic 4T1 breast cancer and subcutaneous HCT-15 xenograft in mice without overt toxicity. The underlying molecular mechanism of SSA is VEGFR2 signal blocking, which was proved in Western blot assay.

MATERIALS AND METHODS

Materials, Cells, and Animals

Saikosaponin A (SSA) was purchased from Push Bio-Technology Company (Chengdu, China). Dulbecco's modified Eagle medium (DMEM), RPMI 1640 medium, fetal bovine serum (FBS), penicillin, and streptomycin were provided by Basal Media Technologies (Shanghai, China). The recombinant human vascular endothelial growth factor ($VEGF_{165}$) was obtained from ProSpec-Tany TechnoGene (Ness Ziona, Israel). The Matrigel matrix was obtained from BD Biosciences (San Jose, CA, United States). Antibodies for Western blotting in the VEGFR2 signaling assay were supplied by Cell Signaling Technology (Shanghai, China). The antibodies were VEGF receptor 2 (55B11) rabbit mAb (#2479), phospho-VEGF receptor 2 (Tyr1175) rabbit mAb (#2478), PLCγ1 rabbit antibody (#2822), phospho-PLCγ1 (Ser1248) (D25A9) rabbit mAb (#8713), FAK rabbit antibody (#3285), phospho-FAK (Tyr397) (D20B1) rabbit mAb (#8556), Src rabbit antibody (#2108), phospho-Src Family (Tyr416) (E6G4R) rabbit mAb (#59548), Akt (pan) (11E7) rabbit mAb (#4685), and phospho-Akt (Ser473) (D9E) XP rabbit mAb (#4060). Goat

anti-rabbit IgG H&L (HRP) (ab205718) was supplied by Abcam (Shanghai, China).

Primary human umbilical vascular endothelial cells (HUVECs) were obtained from Lifeline Cell Technology (Frederick, MD). HUVECs were cultured in the VascuLife VEGF Cell Culture Medium (Frederick, MD), which contained supplements and growth factor cytokines, including VEGF, EGF, IGF-1, and bFGF. The HCT-15 human colorectal adenocarcinoma cell line and 4T1 mouse breast cancer cell line were purchased from American Type Culture Collection (Manassas, VA). They were all cultured at 37°C in humidified atmosphere containing 5% CO_2.

BALB/c mice or nude mice (20 ± 2 g) were provided by Shanghai Laboratory Animal Center (Chinese Academy of Sciences, Shanghai, China). All animal-associated experiments in this study were approved by the Ethical Committee of Shanghai Jiao Tong University School of Medicine.

Cell Viability Assay

The effect of SSA on cell viability was analyzed by using the Cell Counting Kit-8 (Dojindo Laboratories, Kumamoto, Japan). HUVECs, 4T1 or HCT-15 cells, were seeded at a density of 6×10^3 cells/well in 96-well plates (Corning, United States). After 24-h incubation, the cells were treated with various concentrations of SSA (1–100 μM) for 48 h. Then 10 μL CCK-8 solution was added for an additional 2-h incubation at 37°C. All experiments were performed in triplicate. Absorbance at 450 nm was measured using a microplate reader. Cell viability (%) was calculated against the control.

The LIVE/DEAD cell viability/cytotoxicity kit (Life technology, Carlsbad, CA) was also used to assess the viability of HUVECs. Calcein-AM can be transformed into calcein with green fluorescence in live cells, and propidium iodide (PI, red fluorescence) can stain the nuclei of dead cells. HUVECs (6×10^3 cells/well) were cultured in 96-well plates. After incubation at 37°C for 12 h, the medium was replaced by 200 μL of 1–100-μM SSA for 48-h incubation. Then the culture medium was replaced with 1 ml PBS containing 2 μM calcein-AM (Ex 488 nm and Em 515 nm) and 4.5μM PI (Ex 535 nm, Em 615 nm) for 15 min to stain live and dead cells.

Wound Healing Assay

HUVECs were seeded in 96-well plates (1×10^4 cells/well) and allowed to grow to confluence. Then the cells were scratched with WoundMaker (IncuCyte) and treated with various concentrations of SSA (1–100 μM) for 12 h. Then the cells were incubated with fresh medium till 48 h. After 48 h, the cells were observed and photographed using the IncuCyte Live-Cell Analysis System (Essen BioScience). Cell migration was quantified using Image-Pro Plus 8.0 software (Media Cybernetics, Bethesda, MD).

Transwell Migration Assay

The HUVEC migration assay was carried out in a 96-well Transwell Boyden chambers with a polycarbonate filter of a pore size of 8 μm and 6.5 mm diameter inserts (Corning Costar, MA). In brief, 5×10^5 cells suspended in 100-μL serum-free medium with various concentrations of SSA (1–100 μM) were added to the upper chamber. The bottom chambers were filled with 600 μL completed endothelial cell medium containing 20 ng/ml $VEGF_{165}$. The cells were cultured routinely in an incubator (37°C with 5% CO_2). After 10 h, the upper surface of the membrane was gently wiped with a cotton swab to remove non-migrating cells. The membrane was then fixed in 4% glutaraldehyde for 20 min and stained with crystal violet overnight at room temperature. After washing the Transwell chamber five times with PBS, the membrane was photographed using an EVOS microscope (Life Technologies, Grand Island, NY). The migrated cells were quantified using Image-Pro Plus 8.0 software.

Endothelial Cell Tube Formation Assay

Chilled Matrigel (BD Biosciences, CA) was thawed overnight at 4°C, dispensed into 96-well plates (70 μL/well), and then incubated at 37°C for 30 min for solidification. Then approximately 2×10^5 cells suspended in 100 μL medium containing various concentrations of SSA (1–100 μM) were seeded on Matrigel. After 8 h, the images of HUVEC tubular structures were photographed using the EVOS microscope, and the tube length and inhibition effect were analyzed using Image-Pro Plus 8.0 software.

Chick Embryo Chorioallantoic Membrane Assay

To evaluate the *in vivo* angiogenic effect of SSA, the chick embryo CAM assay was applied in this experiment (Liu et al., 2018). In brief, the fertilized eggs were placed in an incubator with approximately 60% humidity and 37.8°C. After 8 days, ~ a 1-cm^2 window was opened, and the shell membrane was removed to expose the CAM. A sterilized 5-mm diameter Whatman filter sheet as a drug carrier that was soaked with SSA of concentrations (1–100 μM) was placed on the CAM. The saline group was included as the control. Then the window was sealed with parafilm and returned to the incubator for additional 48 h. The images of CAM were captured through the windows using a digital camera (Nikon, Japan), and the neovascularization was quantified using Image-Pro Plus 8.0 software.

Matrigel Plug Assay

The *in vivo* antiangiogenic activity of SSA was also evaluated in the Matrigel plug model (Liu et al., 2015). Female BALB/c mice were divided into five groups ($n = 4$) and subcutaneously injected with 500-μL Matrigel that contained 30 U heparin with recombinant human $VEGF_{165}$ (50 ng/ml) and various concentrations of SSA (0, 3, 10, 30 μM). Matrigel containing no $VEGF_{165}$ (50 ng/ml) was set as control. After 12 days, the mice were euthanized. The Matrigel plugs were harvested, fixed in 4% glutaraldehyde overnight, and processed for CD31 immunofluorescence staining. The images of microvessels were photographed under the EVOS microscope, and microvessel density (MVD) was quantified using Image-Pro Plus 8.0 software.

Anticancer Therapy of SSA in Orthotopic 4T1 Tumor in Mice

One million 4T1 cells were injected into the right mammary fat pad of female BALB/c mice to establish the orthotopic tumor model. When the tumor grew to approximately 100 mm^3, 16 mice were divided into two groups and treated intraperitoneally with saline or SSA (10 mg/kg/day) for consecutive 15 days. The tumor volume and body weight were recorded every day. The tumor volume was calculated as follows: volume = (length×$width^2$)/2. On the final day, the mice were euthanized, and the tumors were removed and weighted. The tumors were fixed in 4% paraformaldehyde solution and processed for frozen sections. Then the slices were stained with rat anti-mouse CD31 antibody (1: 200, BD Biosciences, Shanghai, China) and Cy3 conjugated goat anti-rat IgG (H + L) (1:300, Servicebio, Wuhan, China) (Ex 550 nm, Em 570 nm) for microvessel density (MVD) assay. The tumor tissues were also processed for paraffin sections for pathological examination. The sections were then stained with anti-Ki-67 rabbit pAb (1:500, Servicebio, Wuhan, China) and HRP-conjugated goat anti-rabbit IgG (H + L) (1:200, Servicebio, Wuhan, China). Then the slices were photographed under a confocal laser scanning microscope (Leica TCS-SP8) or photomicroscope (Leica DFC 320), and the images were analyzed for microvessel density (MVD), Ki-67–positive tumor cells, and tumor necrosis area using Image-Pro Plus 8.0 software.

Anticancer Therapy of SSA in Subcutaneous HCT-15 Tumor in Nude Mice

Three million HCT-15 cells were subcutaneously injected into the right anterior axillary of the six-week-old BALB/c nude mice to establish the xenograft tumor model. When the tumor volume reached ~100 mm^3, 16 mice were randomly divided into two groups. Then the mice were treated intraperitoneally with saline or SSA (10 mg/kg) every day consecutively for 15 days. The methods for antitumor evaluation are same as those in the aforementioned anti-4T1 tumor experiment.

Western Blot

Western blot assay was used to investigate the antiangiogenic mechanism of SSA. In brief, HUVECs (2×10^5 cells per well) were seeded in 6-well plates and incubated for 2 days until they reached 80% confluence. Then the cells were incubated with various concentrations of SSA for 30 min and stimulated with 50 ng/ml $VEGF_{165}$ for 4 min. Subsequently, RIPA lysis buffer (Beyotime, Shanghai, China) supplemented with PMSF (Sangon Biotech, Shanghai, China) and phosphatase inhibitor cocktail (EpiZyme, Shanghai, China) were added to each well to extract whole cell lysates. The BCA Protein Quantification Kit (Yeasen biotech, Shanghai, China) was used to determine the protein concentration. Equal amounts of protein (30 μg) were applied to 10% SDS-PAGE, and they were transferred onto a PVDF membrane (Millipore, Bill-erica, MA). The membrane was then blocked in 5% non-fat milk blocking buffer for 1 h and incubated with specific primary antibodies (1:1,000, Cell Signaling Technology, Shanghai, China) followed by exposure to HRP-conjugated secondary antibody (1:5,000, Abcam, Shanghai). All experiments were carried out at least three times.

Statistical Analysis

All data obtained were presented as mean ± *s*.d. Statistical analysis was performed using GraphPad Prism 8.0 (GraphPad Software, San Diego, CA). Differences between the groups were examined using one-way ANOVA with Bonferroni's multiple comparison tests or Student's t test. The differences were considered significant when the p value was below 0.05.

RESULTS

SSA Inhibited the Viability of Human Umbilical Vascular Endothelial Cells More Efficiently Than That of 4T1 and HCT-15

HUVEC is a normal cell line that can mimic tumor endothelial cells well. (Guan et al., 2015). SSA efficiently suppressed HUVEC viability in a dose-dependent manner (**Figure 1B**). The viabilities of HUVECs were completely suppressed when SSA concentrations exceeded 30 μM. Similar observations were obtained in the calcein-AM and PI dual staining assay (**Figures 1C,D**). Compared to HUVECs, tumor cells (4T1 and HCT-15) were less sensitive to SSA. 3.4- ~ 7.4-fold higher viability of the 4T1 and HCT-15 cells was maintained after treatment with 10–100 μM SSA. Generally, the activated tumor endothelial cells are more sensitive to chemotherapeutic drugs than tumor cells, offering a choice for specific antiangiogenic therapy (Kerbel and Kamen, 2004). We also examined the cytotoxicity of SSA in two normal cell lines, L-02 (human fetal hepatocyte line) and ARPE-19 (a human retinal pigment epithelial cell line). It showed that compared to HUVECs, L-02 and ARPE-19 were less sensitive to SSA (**Supplementary Figure S1**), suggesting the potential safety of SSA when used *in vivo*.

SSA Inhibited Human Umbilical Vascular Endothelial Cell Migration and Tube Formation

The wound healing test is a representative method for the evaluation of HUVEC migration (Guan et al., 2015; Li et al., 2019). HUVECs were pretreated with SSA for 12 h and then incubated in fresh medium till 48 h. After 12-h incubation, more than 65% cells were still alive even at the highest test concentration (100 μM) (**Supplementary Figure S2**). The inhibition of the horizontal migration of HUVECs in the wound healing test was obtained in a dose-dependent manner. ~40% migration inhibition was obtained under 10 μM SSA, and this effect increased to nearly 80% when 30 μM or higher (100 μM) SSA was used (**Figure 2A**). It is noted that 30 μM SSA decreased 30% cell viability (**Supplementary Figure S2**),

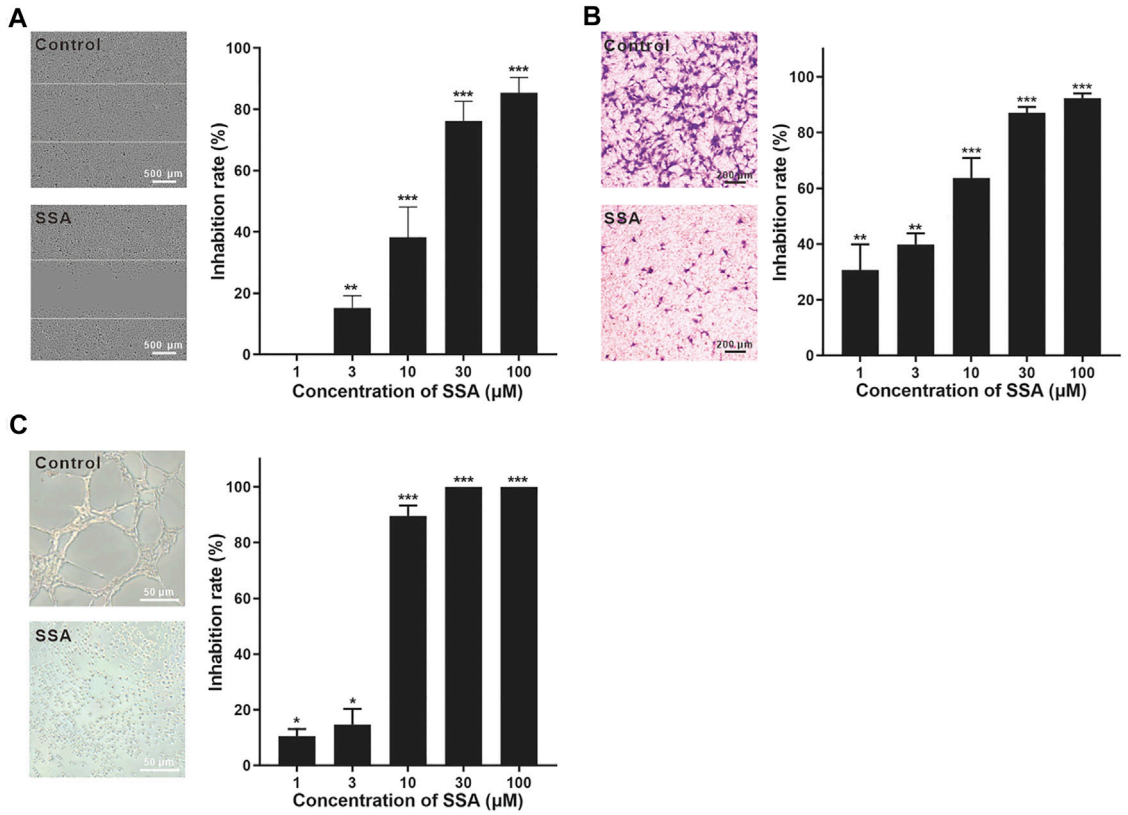

FIGURE 2 | SSA significantly suppressed HUVEC migration and tube formation. **(A)** SSA suppressed the horizontal migration of HUVECs in the wound healing test. The line indicated the initial boundary of the cells. **(B)** SSA inhibited HUVEC migration in the Transwell assay. The migrated cells were stained with crystal violet and quantified using Image-Pro plus 8.0 software. **(C)** SSA inhibited HUVEC tube formation. The length of the tubular structures was photographed and quantified using Image-Pro plus 8.0 software. The photos of the control and SSA groups (30 μM) were shown in each panel. The values are expressed as mean ± *s*.d. $n = 3$. $^{*}p < 0.05$, $^{**}p < 0.01$, and $^{***}p < 0.001$. SSA suppressed angiogenesis in the chick embryo CAM.

while increased nearly 80% inhibition of the migration. Thus, the antiangiogenic effect of SSA would be from both direct cytotoxicity and the specific interference to the cell function in migration.

HUVEC migration was also investigated using the Transwell test (Luan et al., 2014). The cells were treated with SSA for 10 h. During this time, ~80% cells were still alive even at the highest test concentration (100 μM) (**Supplementary Figure S3**). After 10 μM SSA treatment for 10 h, more than 90% HUVECs were alive. Under this treatment condition, more than 60% cell migration was suppressed (**Figure 2B**). This observation reflected the specific interference of SSA to the cell function in migration. More than 90% migration was suppressed when the cells were treated with 30 and 100 μM SSA (**Figure 2B**).

The tube formation of HUVECs is a classical *in vitro* angiogenesis assay (Luan et al., 2014). The endothelial cells differentiate and form tube-like structures on the extracellular matrix (Matrigel). In contrast to the well-formed tube-like pattern, SSA exhibited strong antiangiogenic potency with more than 90–100% inhibition when concentrations went above 10 μM with 8-h treatment (**Figure 2C**). Specifically, the cells were individually spread on the Matrigel with almost no connection between them.

SSA Suppressed Angiogenesis in Chick Embryo Chorioallantoic Membrane

We then investigate the antiangiogenic activity of SSA *in vivo* using the classic chick embryo CAM model (Liu et al., 2018). After 48-h treatment, the formation of new blood vessels was dramatically suppressed by SSA compared to that in the control, demonstrating the potent antiangiogenic activity *in vivo* (**Figure 3**).

SSA Inhibited Vascularization in the Matrigel Plugs in Mice

The Matrigel plug model was also used for the *in vivo* antiangiogenic evaluation of SSA (Liu et al., 2015). Matrigel containing 30 U heparin, $VEGF_{165}$ (0 or 50 ng/ml), or SSA (3, 10, and 30 μM) was subcutaneously injected into female BALB/c mice. After 12 days, the formed Matrigel plugs were harvested and photographed (**Figure 4A**). The immunofluorescent

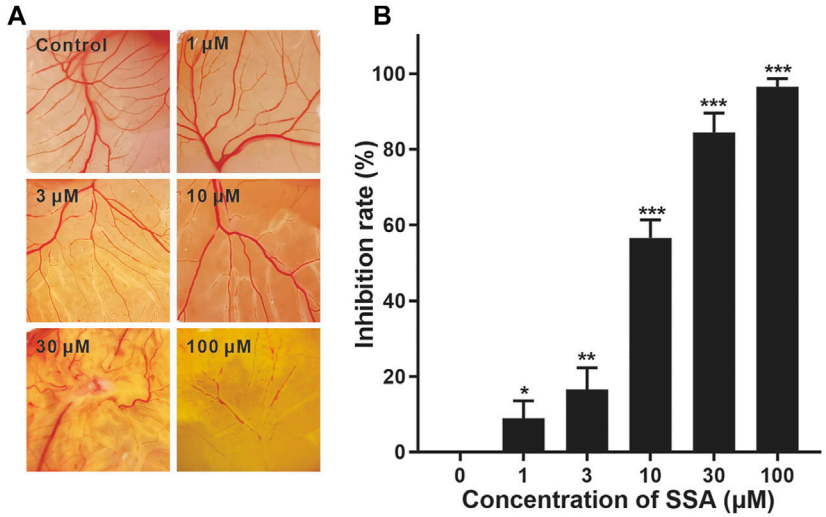

FIGURE 3 | Effect of SSA on angiogenesis in the CAM. CAMs were treated for 48 h with a 6.5-mm diameter Whatman filter disk previously immersed in various concentrations of SSA (1–100 μM). CAM angiogenesis was photographed using a digital camera **(A)** and quantified using Image-Pro Plus 8.0 software **(B)**. Data were expressed as mean ± *s*.d. $n = 3$. $^{*}p < 0.05$, $^{**}p < 0.01$, and $^{***}p < 0.001$ as compared with the control group. SSA inhibited vascularization in the Matrigel plugs in mice.

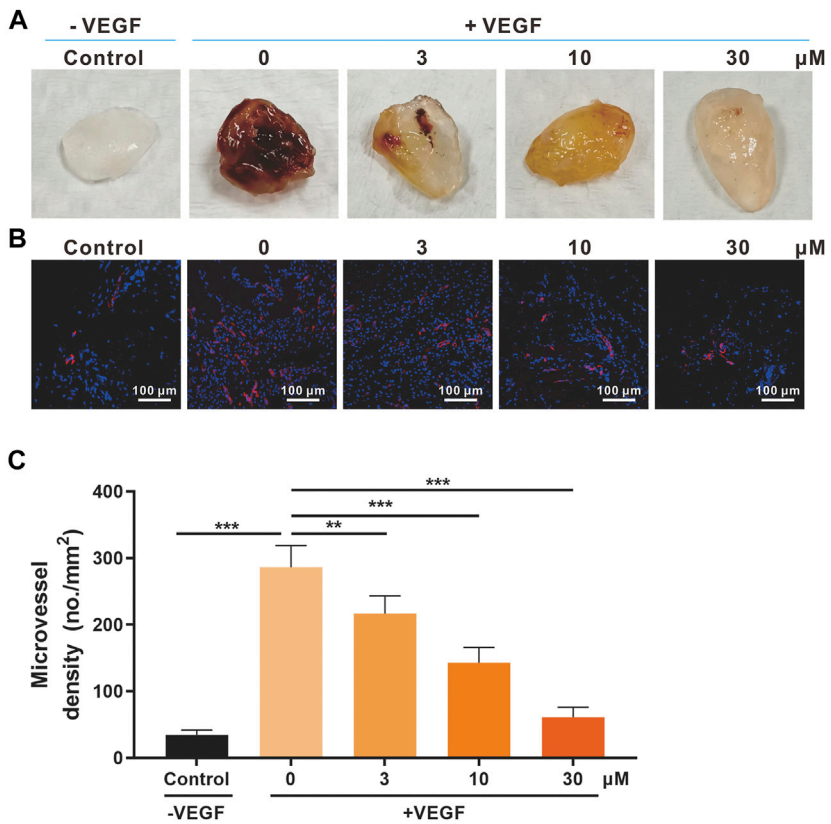

FIGURE 4 | Effects of SSA on *in vivo* angiogenesis evaluated in the Matrigel plug model. **(A)** Photographs of the Matrigel plugs of different groups on day 12. **(B)** Immunofluorescence staining of CD31-positive microvessels (red) in the Matrigel plugs. Representative images were shown. **(C)** Quantified microvessel density (MVD). All values were shown as mean ± *s*.d. $n = 5$. $^{**}p < 0.01$ and $^{***}p < 0.001$. SSA inhibited angiogenesis and growth of orthotopic 4T1 tumors in mice.

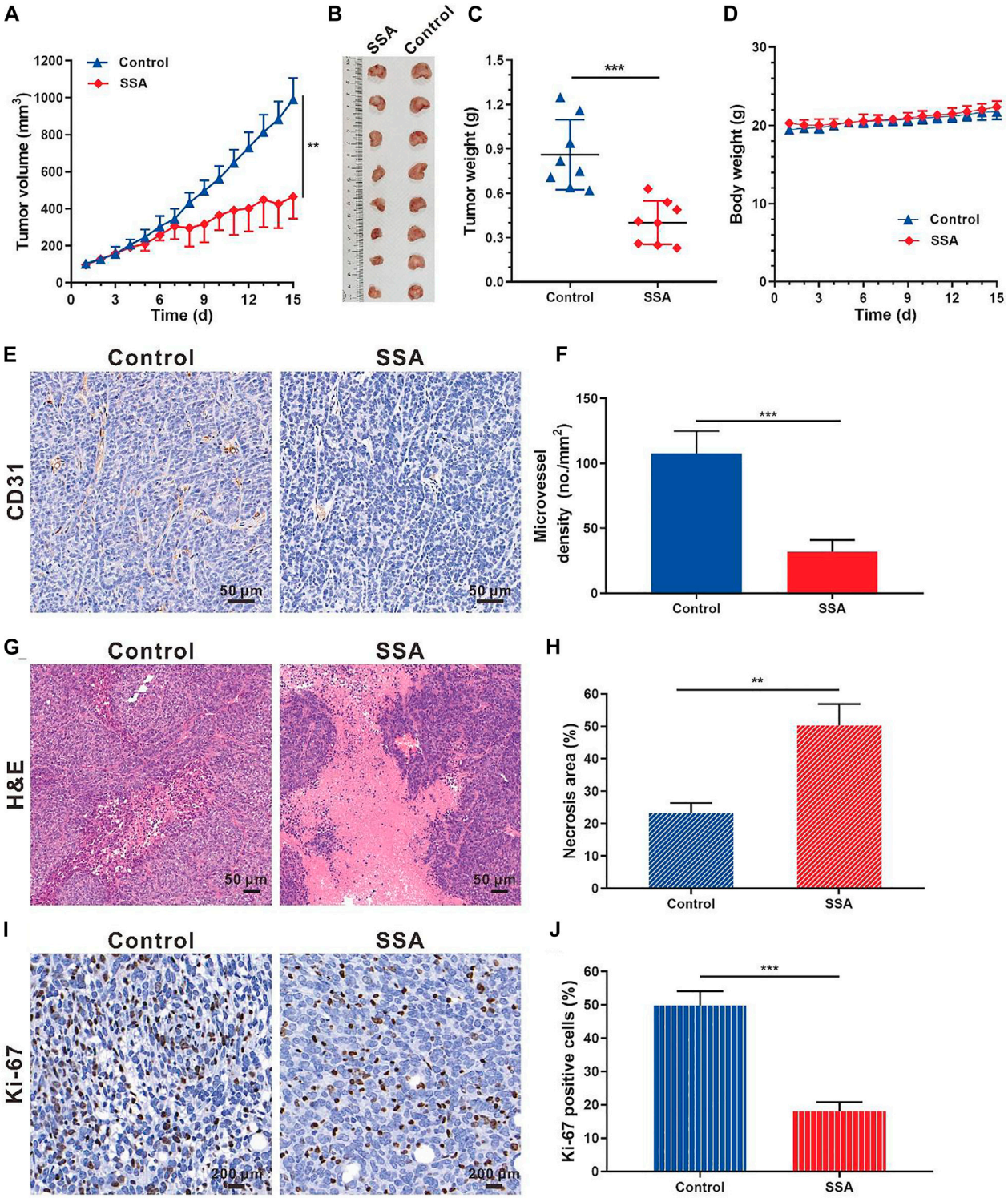

FIGURE 5 | SSA inhibited orthotopic 4T1 tumor growth and angiogenesis in BALB/c mice. When the tumor grew to approximately 100 mm^3, the mice were treated intraperitoneally with saline or SSA (10 mg/kg/day) for consecutive 15 days. **(A)** Tumor growth curve. **(B)** Photographs of the excised tumor on day 15. **(C)** Tumor weight on day 15. **(D)** Mouse body weight during the therapy. **(E)** Representative images of the immunohistochemical staining of $CD31^+$ tumor vessels. **(F)** Quantified analysis of tumor microvessel density (MVD). **(G)** H&E staining of the tumors showed the necrosis region. **(H)** Quantified necrosis area assay. **(I)** The brown nuclei of proliferative tumor cells were stained with anti-Ki-67 antibody. **(J)** Statistical assay of the Ki-67 positive tumor cells in panel I. All values were shown as mean ± *s*.d. $n = 8$ in A, C, and D. $n = 5$ in F, H, and J. $^{**}p < 0.01$, $^{***}p < 0.001$. SSA suppressed angiogenesis and growth of subcutaneous HCT-15 tumors in mice.

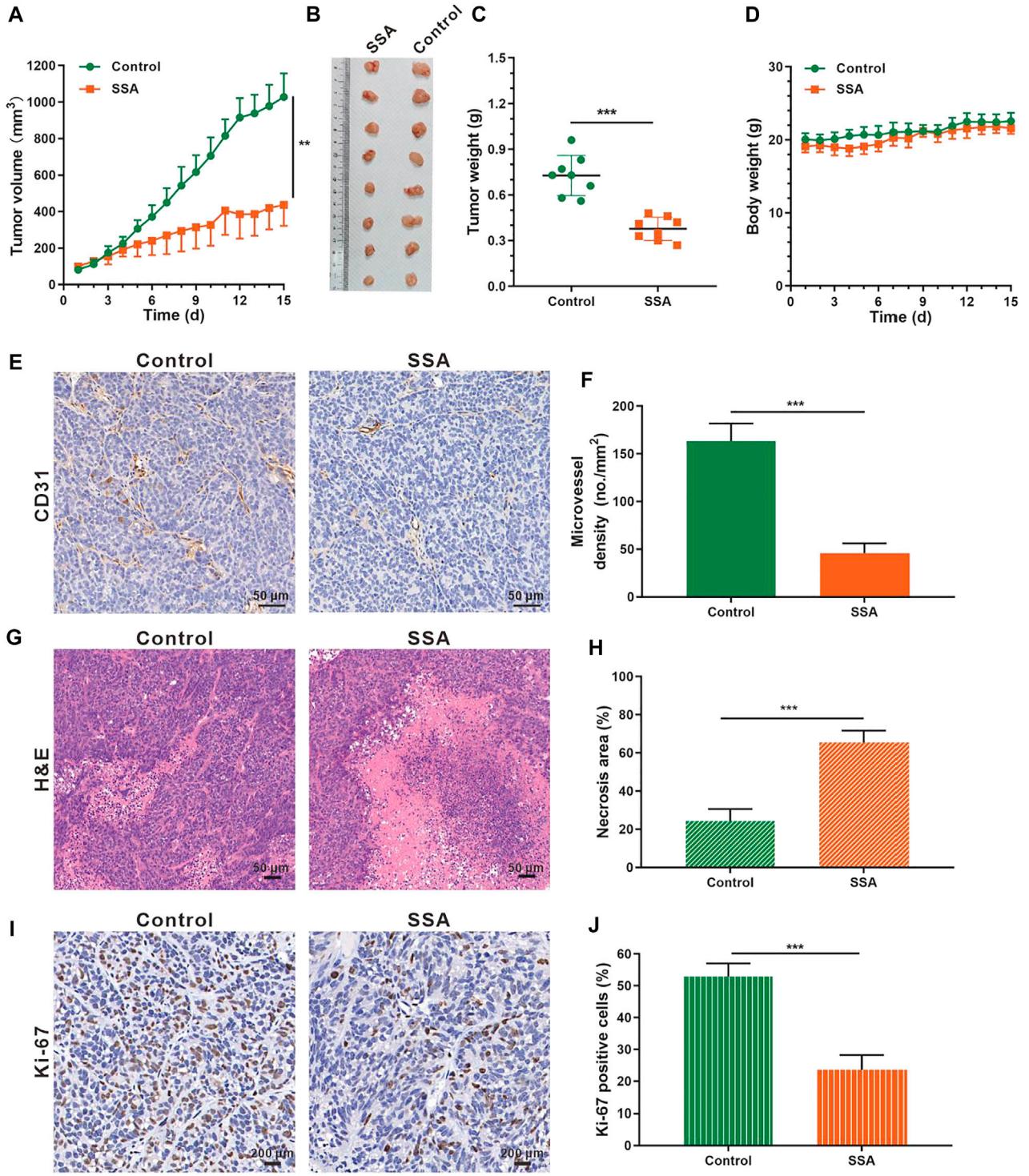

FIGURE 6 | SSA suppressed HCT-15 tumor growth by inhibiting tumor angiogenesis. When the tumor volume reached ~100 mm^3, the mice were treated intraperitoneally with saline or SSA (10 mg/kg) every day for consecutive 15 days. **(A)** Tumor growth curve. **(B)** Photographs of the excised tumor on day 15. **(C)** Tumor weight on day 15. **(D)** Mouse body weight during the therapy. **(E)** Representative images of the immunohistochemical staining of $CD31^+$ tumor vessels. **(F)** Quantified analysis of tumor microvessel density (MVD). **(G)** H&E staining of the tumors showed the necrosis region. **(H)** Quantified necrosis area assay. **(I)** The brown nuclei of proliferative tumor cells were stained with anti–Ki-67 antibody. **(J)** Statistical assay of the Ki-67 positive tumor cells in panel I. All values were shown as mean ± s.d. $n = 8$ in A, C, and D. $n = 5$ in F, H, and I. $^{**}p < 0.01$, $^{***}p < 0.001$. SSA inhibited angiogenesis by suppressing the VEGFR2 signaling pathway and Its downstream proteins.

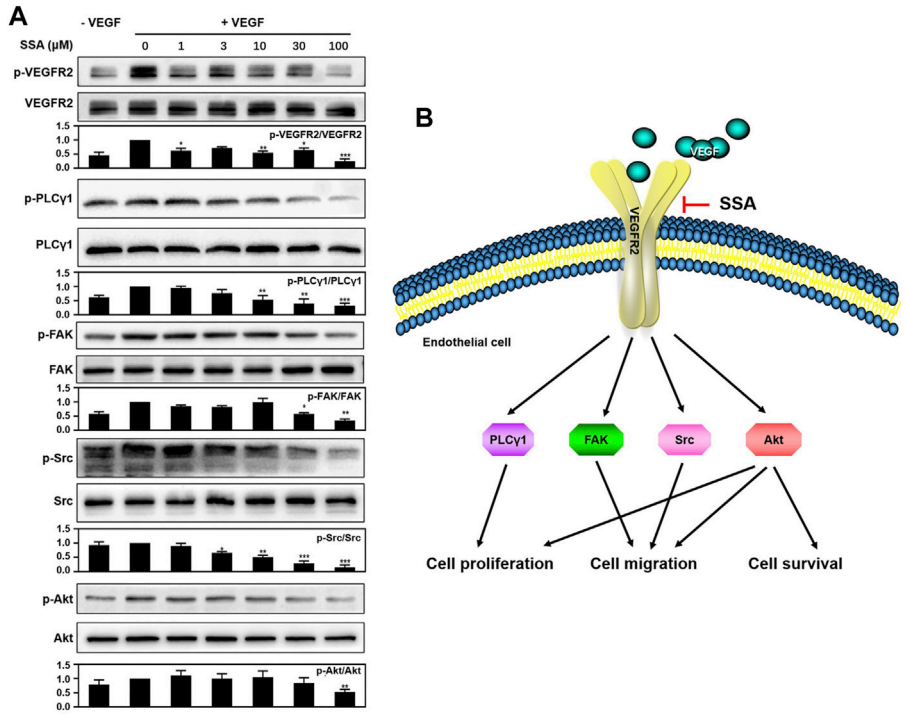

FIGURE 7 | SSA suppressed the phosphorylation of VEGFR2 and downstream signaling molecules in HUVECs. (**A**) SSA inhibited the activation of VEGFR2 and its downstream signaling kinases in HUVECs. The activation of VEGFR2 and its downstream proteins, such as PLCγ1, FAK, Src, and Akt was examined by Western blot. The gray scale ratio of the phosphorylated protein to the total protein was shown. Comparisons to the control group (cell treated only with $VEGF_{165}$) were performed. n = 3. (**B**) Diagram of the SSA-mediated antiangiogenic signaling pathway. $^{*}p < 0.05$, $^{**}p < 0.01$, and $^{***}p < 0.001$. n = 3.

staining of CD31-positive blood vessels in the plugs indicated that SSA effectively inhibits angiogenesis in a dose-dependent manner (**Figures 4B,C**).

SSA Inhibited Angiogenesis and Growth of Orthotopic 4T1 Tumors in Mice

Based on the antiangiogenic performance of SSA in chick embryo CAM and Matrigel plug models, we hypothesized that SSA would inhibit tumor growth by suppressing angiogenesis. The orthotopic 4T1 tumor breast tumor model was adopted for this test. Starting from the seventh day, the tumor growth rate of the SSA-treated group slowed down significantly. On day 15 (the end of the test), the tumor volume treated by SSA was 465.1 mm^3, 53.1% smaller than that (991.4 mm^3) of the control group (**Figures 5A,B**). Correspondingly, the tumor weight (0.40 g) of the SSA group was 39.6% less than that (0.86 g) of the control group (**Figure 5C**). The mouse body weight was well-maintained, indicating good tolerance of the therapeutic regimen (**Figure 5D**). Immunohistochemical and pathological assays showed that SSA treatment obviously decreased MVD and dramatically elevated the necrosis area than that in the control group (**Figures 5E–H**). The antitumor effect was also reflected in the percentage of proliferative cells in tumors. It showed that SSA treatment pronounceably reduced the Ki-67–positive tumor cells (**Figures 5I,J**).

SSA Suppressed Angiogenesis and Growth of Subcutaneous HCT-15 Tumors in Mice

The antiangiogenic activity of SSA was also examined in HCT-15 tumors in mice. Similar antitumor effects like those in 4T1 tumors were obtained. At the end of the test (day 15), the HCT-15 tumor volume treated by SSA was 436.9 mm^3, 57.5% smaller than that (1,028.2 mm^3) of the control group (**Figures 6A,B**). Correspondingly, the tumor weight (0.35 g) of the SSA group was 52.1% less than that (0.73 g) of the control group (**Figure 6C**). No obvious loss of mouse body weight appeared, demonstrating good safety (**Figure 6D**). Tumor vessels indicated as MVD were largely inhibited in the SSA-treated group, and the necrosis area of tumor tissues was dramatically increased (**Figures 6E–H**). Same as the observation as in 4T1 tumors, the proliferative Ki-67–positive cells in HCT-15 tumors were dramatically decreased after SSA treatment, indicating significant antitumor efficacy (**Figures 6I,J**).

SSA Inhibited Angiogenesis by Suppressing VEGFR2 Signaling Pathway and Its Downstream Proteins

To explore the mechanism of SSA-mediated antiangiogenic activity in HUVECs, Western blot assay was used to examine whether SSA could inhibit the phosphorylation of VEGFR2 and

its downstream proteins, the most important angiogenic signal pathway that regulates the endothelial cell function in angiogenesis. It showed that VEGFR2 activation and the downstream signaling, including PLCγ1, FAK, Src, and Akt, were decreased when treated with different concentrations of SSA in a concentration-dependent manner (**Figure 7A**).

DISCUSSION

Antiangiogenic therapy is a major therapeutic modality in cancer clinics. More than 10 antiangiogenic agents have been approved worldwide, and the small molecular kinase inhibitors account for the majority (Jayson et al., 2016). However, the clinical benefits are compromised by the therapy-associated side effects and resistance (Jayson et al., 2016). Moreover, unsatisfied pharmacokinetic behavior and high cost limit their wide use in cancer clinics (Jain et al., 2011; Kim et al., 2019). Exploring novel natural products with antiangiogenic activity is an emerging attractive field (Yang and Wu, 2015; Guan et al., 2016; Kotoku et al., 2016; Lu et al., 2016). Besides similar therapeutic potential, natural products are generally inexpensive and less toxic (Lu et al., 2016).

SSA is a triterpenoid saponin extracted from the traditional Chinese medicinal herb *Radix Bupleurum*. Its diverse pharmacological activities including antitumor effects have been revealed. However, the antiangiogenic potency of SSA still remains unknown. In this work, the antiangiogenic activity of SSA was carefully characterized. Compared to the tumor cells (4T1 and HCT-15), HUVEC viability was more efficiently inhibited by SSA, indicating higher sensitivity of the tumor vascular endothelial cells. SSA also suppressed HUVEC migration and tube formation in a dose-dependent manner. The good antiangiogenic activities are also well-observed in *in vivo* models of the chick embryo CAM and Matrigel plugs. The potent antiangiogenic activity resulted in significant antitumor effects in two solid tumor models, orthotopic 4T1 breast cancer, and subcutaneous HCT-15 colorectal cancer. Over 50% of tumor repression was obtained at dose of 10 mg/kg/day for consecutive 15 injections. Further dose escalation and antitumor effects are warranted.

VEGFR2 signaling is the most important pathway for tumor angiogenesis (Kerbel, 2008). Western blot assay indicated that SSA could decrease the VEGF-induced VEGFR2 phosphorylation and its downstream signaling pathways, including PLCγ1, FAK, Src, and Akt, in a dose-dependent manner. The downregulation of PLCγ1 can be responsible for the inhibition of human vascular endothelial cell (HUVEC) proliferation (Sase et al., 2009). The inactivation of FAK and Src can compromise endothelial cell migration (Guan et al., 2015). Akt involves multiple cellular functions, including cell survival, proliferation, migration, and protein synthesis (Liu et al., 2018). The antiangiogenic molecular mechanism of SSA is summarized in **Figure 7B**. It is noted that other triterpenoid natural products, such as Raddeanin A (Guan et al., 2015), Platycodin D (Luan et al., 2014), Cucurbitacin E (Dong et al., 2010), and acetyl-11-keto-β-boswellic acid (AKBA) (Pang et al., 2009), also exert antiangiogenic roles via blocking of VEGFR2 signaling. The study of the structure–activity relationship will help reveal the mechanism of action of these compounds in depth.

In conclusion, our findings first revealed that SSA possesses potent antiangiogenic activities, thereby suppressing tumor growth by blocking VEGFR2 signaling pathways. These observations demonstrate that SSA may be a potential drug candidate or lead compound for antiangiogenic cancer therapy.

DATA AVAILABILITY STATEMENT

The raw data supporting the conclusions of this article will be made available by the authors, without undue reservation.

ETHICS STATEMENT

The animal study was reviewed and approved by the Ethical Committee of Shanghai Jiao Tong University School of Medicine.

AUTHOR CONTRIBUTIONS

MZ and CF conceived and designed the experiments. PZ, XL, M-HZ, ML, X-LL, and Z-XW performed the experiments. YZ, R-JG, JD, QL, and PS participated in discussions of data analysis. PZ wrote the article. CF and MZ edited the manuscript. All authors approved the final version for submission to this journal. We also thank the Core Facility of Basic Medical Sciences (SJTU-SM) for frozen section making and scanning.

FUNDING

This work is supported by the National Natural Science Foundation of China (81602729, 81773274, 82073379).

SUPPLEMENTARY MATERIAL

The Supplementary Material for this article can be found online at: https://www.frontiersin.org/articles/10.3389/fphar.2021.713200/full#supplementary-material

REFERENCES

Dong, Y., Lu, B., Zhang, X., Zhang, J., Lai, L., Li, D., et al. (2010). Cucurbitacin E, a Tetracyclic Triterpenes Compound from Chinese Medicine, Inhibits Tumor Angiogenesis through VEGFR2-Mediated Jak2-STAT3 Signaling Pathway. *Carcinogenesis* 31, 2097–2104. doi:10.1093/carcin/bgq167

Du, Z. A., Sun, M. N., and Hu, Z. S. (2018). Saikosaponin a Ameliorates LPS-Induced Acute Lung Injury in Mice. *Inflammation* 41, 193–198. doi:10.1007/s10753-017-0677-3

Guan, Y. Y., Liu, H. J., Luan, X., Xu, J. R., Lu, Q., Liu, Y. R., et al. (2015). Raddeanin A, a Triterpenoid Saponin Isolated from Anemone Raddeana, Suppresses the Angiogenesis and Growth of Human Colorectal Tumor by Inhibiting VEGFR2 Signaling. *Phytomedicine* 22, 103–110. doi:10.1016/j.phymed.2014.11.008

Guan, Y. Y., Luan, X., Lu, Q., Liu, Y. R., Sun, P., Zhao, M., et al. (2016). Natural Products with Antiangiogenic and Antivasculogenic Mimicry Activity. *Mini Rev. Med. Chem.* 16, 1290–1302. doi:10.2174/1389557516666160211115507

Guo, J., Zhang, F., Gao, J., Guan, X., Liu, B., Wang, X., et al. (2020). Proteomics-based Screening of the Target Proteins Associated with Antidepressant-like Effect and Mechanism of Saikosaponin A. *J. Cel. Mol. Med.* 24, 174–188. doi:10.1111/jcmm.14695

Hanahan, D., and Weinberg, R. A. (2011). Hallmarks of Cancer: the Next Generation. *Cell* 144, 646–674. doi:10.1016/j.cell.2011.02.013

He, D., Wang, H., Xu, L., Wang, X., Peng, K., Wang, L., et al. (2016). Saikosaponin-a Attenuates Oxidized LDL Uptake and Prompts Cholesterol Efflux in THP-1 Cells. *J. Cardiovasc. Pharmacol.* 67, 510–518. doi:10.1097/FJC.0000000000000373

Jain, L., Woo, S., Gardner, E. R., Dahut, W. L., Kohn, E. C., Kummar, S., et al. (2011). Population Pharmacokinetic Analysis of Sorafenib in Patients with Solid Tumours. *Br. J. Clin. Pharmacol.* 72, 294–305. doi:10.1111/j.1365-2125.2011.03963.x

Jayson, G. C., Kerbel, R., Ellis, L. M., and Harris, A. L. (2016). Antiangiogenic Therapy in Oncology: Current Status and Future Directions. *Lancet* 388, 518–529. doi:10.1016/S0140-6736(15)01088-0

Kang, S. J., Lee, Y. J., Kang, S. G., Cho, S., Yoon, W., Lim, J. H., et al. (2017). Caspase-4 Is Essential for Saikosaponin A-Induced Apoptosis Acting Upstream of Caspase-2 and γ-H2AX in colon Cancer Cells. *Oncotarget* 8, 100433–100448. doi:10.18632/oncotarget.22247

Kerbel, R. S., and Kamen, B. A. (2004). The Anti-angiogenic Basis of Metronomic Chemotherapy. *Nat. Rev. Cancer* 4, 423–436. doi:10.1038/nrc1369

Kerbel, R. S. (2008). Tumor Angiogenesis. *N. Engl. J. Med.* 358, 2039–2049. doi:10.1056/NEJMra0706596

Kim, B. M., and Hong, S. H. (2011). Sequential Caspase-2 and Caspase-8 Activation Is Essential for Saikosaponin A-Induced Apoptosis of Human colon Carcinoma Cell Lines. *Apoptosis* 16, 184–197. doi:10.1007/s10495-010-0557-x

Kim, J. J., Mcfarlane, T., Tully, S., and Wong, W. W. L. (2019). Oncologist.Lenvatinib versus Sorafenib as First-Line Treatment of Unresectable Hepatocellular Carcinoma: A Cost-Utility Analysis

Kotoku, N., Arai, M., and Kobayashi, M. (2016). Search for Anti-angiogenic Substances from Natural Sources. *Chem. Pharm. Bull. (Tokyo)* 64, 128–134. doi:10.1248/cpb.c15-00744

Li, J., Peng, J., Zhao, S., Zhong, Y., Wang, Y., Hu, J., et al. (2019). Tussilagone Suppresses Angiogenesis by Inhibiting the VEGFR2 Signaling Pathway. *Front. Pharmacol.* 10, 764. doi:10.3389/fphar.2019.00764

Liu, Y. R., Cai, Q. Y., Gao, Y. G., Luan, X., Guan, Y. Y., Lu, Q., et al. (2018). Alantolactone, a Sesquiterpene Lactone, Inhibits Breast Cancer Growth by Antiangiogenic Activity via Blocking VEGFR2 Signaling. *Phytother. Res.* 32, 643–650. doi:10.1002/ptr.6004

Liu, Y. R., Guan, Y. Y., Luan, X., Lu, Q., Wang, C., Liu, H. J., et al. (2015). Delta-like Ligand 4-targeted Nanomedicine for Antiangiogenic Cancer Therapy. *Biomaterials* 42, 161–171. doi:10.1016/j.biomaterials.2014.11.039

Lu, K., Bhat, M., and Basu, S. (2016). Plants and Their Active Compounds: Natural Molecules to Target Angiogenesis. *Angiogenesis* 19, 287–295. doi:10.1007/s10456-016-9512-y

Luan, X., Gao, Y. G., Guan, Y. Y., Xu, J. R., Lu, Q., Zhao, M., et al. (2014). Platycodin D Inhibits Tumor Growth by Antiangiogenic Activity via Blocking VEGFR2-Mediated Signaling Pathway. *Toxicol. Appl. Pharmacol.* 281, 118–124. doi:10.1016/j.taap.2014.09.009

Pang, X., Yi, Z., Zhang, X., Sung, B., Qu, W., Lian, X., et al. (2009). Acetyl-11-keto-beta-boswellic Acid Inhibits Prostate Tumor Growth by Suppressing Vascular Endothelial Growth Factor Receptor 2-mediated Angiogenesis. *Cancer Res.* 69, 5893–5900. doi:10.1158/0008-5472.CAN-09-0755

Piao, C. H., Song, C. H., Lee, E. J., and Chai, O. H. (2020). Saikosaponin A Ameliorates Nasal Inflammation by Suppressing IL-6/ROR-γt/STAT3/IL-17/NF-κB Pathway in OVA-Induced Allergic Rhinitis. *Chem. Biol. Interact.* 315, 108874. doi:10.1016/j.cbi.2019.108874

Qi, X., Liu, J., Li, X., Fan, M., Huang, N., and Sun, R. (2021). Saikosaponin a Contributed to CCIN Treatment by Promoting Neutrophil Bactericidal Activity via Activation CBL-dependent ERK Pathway. *Phytomedicine* 82, 153444. doi:10.1016/j.phymed.2020.153444

Sase, H., Watabe, T., Kawasaki, K., Miyazono, K., and Miyazawa, K. (2009). VEGFR2-PLCgamma1 axis Is Essential for Endothelial Specification of VEGFR2+ Vascular Progenitor Cells. *J. Cel Sci.* 122, 3303–3311. doi:10.1242/jcs.049908

Wang, Y., Zhao, L., Han, X., Wang, Y., Mi, J., Wang, C., et al. (2019). Saikosaponin A Inhibits Triple-Negative Breast Cancer Growth and Metastasis through Downregulation of CXCR4. *Front. Oncol.* 9, 1487. doi:10.3389/fonc.2019.01487

Yang, X., and Wu, X. Z. (2015). Main Anti-tumor Angiogenesis Agents Isolated from Chinese Herbal Medicines. *Mini Rev. Med. Chem.* 15, 1011–1023. doi:10.2174/1389557515121507311132 42

Zhao, X., Liu, J., Ge, S., Chen, C., Li, S., Wu, X., et al. (2019). Saikosaponin A Inhibits Breast Cancer by Regulating Th1/Th2 Balance. *Front. Pharmacol.* 10, 624. doi:10.3389/fphar.2019.00624

Zhou, F., Wang, N., Yang, L., Zhang, L. C., Meng, L. J., and Xia, Y. C. (2019). Saikosaponin A Protects against Dextran Sulfate Sodium-Induced Colitis in Mice. *Int. Immunopharmacol.* 72, 454–458. doi:10.1016/j.intimp.2019.04.024

Conflict of Interest: The authors declare that the research was conducted in the absence of any commercial or financial relationships that could be construed as a potential conflict of interest.

Publisher's Note: All claims expressed in this article are solely those of the authors and do not necessarily represent those of their affiliated organizations, or those of the publisher, the editors, and the reviewers. Any product that may be evaluated in this article, or claim that may be made by its manufacturer, is not guaranteed or endorsed by the publisher.

frontiers in Pharmacology

ORIGINAL RESEARCH
published: 05 November 2021
doi: 10.3389/fphar.2021.706220

OPEN ACCESS

Edited by:
Cecilia Veronica Nunez,
National Institute of Amazonian Research (INPA), Brazil

Reviewed by:
Sahil Sharma,
Sloan Kettering Institute, United States
Patrícia Sartorelli,
Federal University of São Paulo, Brazil
Massuo Jorge Kato,
University of São Paulo, Brazil

***Correspondence:**
Chang Li
lichang661@126.com
Yue-Hu Pei
Peiyh@163.vip.com
Shu-Lin Liu
slliu@hrbmu.edu.cn

†Present address:
Yu-Jie Zhou,
Advanced Innovation Center for Human Brain Protection, Beijing Key Laboratory for Cancer Invasion and Metastasis, Department of Immunology, School of Basic Medical Sciences, Department of Oncology, Capital Medical University, Beijing, China

‡These authors have contributed equally to this work

Specialty section:
This article was submitted to Pharmacology of Anti-Cancer Drugs, a section of the journal Frontiers in Pharmacology

Received: 27 May 2021
Accepted: 29 September 2021
Published: 05 November 2021

Citation:
Wang Q, Wang Y, Wang Y-J Ma N, Zhou Y-J Zhuang H, Zhang X-H Li C, Pei Y-H and Liu S-L (2021) Dissection of the Functional Mechanism of Human Gut Bacterial Strain AD16 by Secondary Metabolites' Identification, Network Pharmacology, and Experimental Validation. Front. Pharmacol. 12:706220. doi: 10.3389/fphar.2021.706220

Dissection of the Functional Mechanism of Human Gut Bacterial Strain AD16 by Secondary Metabolites' Identification, Network Pharmacology, and Experimental Validation

Qin Wang[1‡], Yao Wang[2‡], Ya-Jing Wang[1], Nan Ma[1], Yu-Jie Zhou[2†], He Zhuang[2], Xing-Hua Zhang[2], Chang Li[1], Yue-Hu Pei[1]* and Shu-Lin Liu[2,3]**

[1]Department of Medicinal Chemistry and Natural Medicine Chemistry, College of Pharmacy, Harbin Medical University, Harbin, China, [2]Genomics Research Center (State-Province Key Laboratories of Biomedicine-Pharmaceutics of China), College of Pharmacy, Harbin Medical University, Harbin, China, [3]Department of Microbiology, Immunology and Infectious Diseases, University of Calgary, Calgary, AB, Canada

Gut microbiota plays important roles in several metabolic processes, such as appetite and food intake and absorption of nutrients from the gut. It is also of great importance in the maintenance of the health of the host. However, much remains unknown about the functional mechanisms of human gut microbiota itself. Here, we report the identification of one anticancer gut bacterial strain AD16, which exhibited potent suppressive effects on a broad range of solid and blood malignancies. The secondary metabolites of the strain were isolated and characterized by a bioactivity-guided isolation strategy. Five new compounds, streptonaphthalenes A and B (1-2), pestaloficins F and G (3-4), and eudesmanetetraiol A (5), together with nine previously known compounds, were isolated from the effective fractions of AD16. Structures of the new compounds were established by 1D and 2D NMR and MS analysis, and the absolute configurations were determined by the CD method. The analysis of network pharmacology suggested that 3, 2, and 13 could be the key components for the anti-NSCLC activity of AD16. In addition to the PI3K–Akt signaling pathway, the proteoglycans in cancer pathway could be involved in the anti-NSCLC action of AD16.

Keywords: gut bacterial, secondary metabolites, network pharmacology, anticancer, AD16

INTRODUCTION

The human gut microbiota is composed of an enormous diversity of microorganisms, including bacteria, fungi, and other microbes, which together play important roles in maintaining the dynamic homeostatic and healthy micro-environment of the host (Johnson et al., 2016; Thomas et al., 2017; Liang et al., 2018). In recent years, numerous discoveries have been reported on the human gut bacteria affecting human health and diseases, such as cardiovascular diseases, inflammatory diseases, obesity, and especially cancer (Hasan et al., 2020; Moritz et al., 2020). There has been mounting evidence supporting the roles of the gut bacteria in response to cancer (Johnson et al., 2016; Li et al.,

2019), such as producing anticancer metabolites (Zhou et al., 2017). Although several bioactive metabolites from animal gut bacteria have been reported, such as sannastatin (Yang et al., 2011), few therapeutic metabolites have been identified from human gut bacteria (Rahim et al., 2019).

Our previous research suggested that the composition of the gut microbiota in lung cancer patients was radically different from that of healthy individuals, which had a higher abundance of bacteria of phylum Actinobacteria compared to the lung cancer patients (Zhuang et al., 2019). This finding prompted us to isolate more Actinobacteria from the human gut (Zhou et al., 2017). Strain AD16 was determined to belong to the Actinobacteria genus *Streptomyces* and showed potent cytotoxic activities against several cancer cell lines both *in vitro* and *in vivo*. Based on the promising results, AD16 was selected for phytochemical studies with a focus on its secondary metabolites responsible for the observed anticancer properties. We identified five new compounds, including streptonaphthalenes A and B (1-2), pestaloficins F and G (3-4), and eudesmanetetraiol A (5), along with nine previously known ones, cyclo-(leucyl-histidyl) (6) (Furukawa et al., 2012), 4,10-dihydroxy-10-methyl-undec-2-en-1, 4-olide (7) (Cho et al., 2001), 4-acetyl-benzoxazolin-2-one (8) (Fielder et al., 1994), cinnamic acid (9) (Ai et al., 2010), indole-3-carboxylic acid (10) (Qian et al., 2014), 1-(1H-indol-3-yl)-ethanone (11) (Kamble et al., 2020), DBP (12) (Chang et al., 2013), 4-hydroxy-8-[6-hydroxy-1,3,7-trimethyl-2-oxo-oct-3-enyl]-5-methyl-oxocan-2-one (13) (Tapiolas et al., 1991), and 1,2,4-triazolenucleoside (14) (Zhou et al., 2010). We also applied network pharmacology analysis to investigate the underlying mechanisms of the anticancer effects of AD16.

In this paper, we describe the anticancer activities of gut bacterial strain AD16, the isolation and structural elucidation of five new compounds, along with nine known ones *via* bioactivity-guided isolation, and the network analysis of the compounds from AD16. The chemical structures of the isolated compounds were deduced by means of their physico-chemical properties, as well as the analysis of their spectroscopic data. This work demonstrated that gut microbiota is a rich source of potential cancer therapeutics for further studies and future clinical applications.

MATERIALS AND METHODS

General Experimental Procedures

Optical rotations were measured on a Nicolet iS5 (Thermo, United States) spectrometer, and UV spectra were recorded on an Evolution 220 (Thermo, United States) UV/Vis spectrometer. IR spectra were obtained using a JASCO FT/IR-480 plus spectrometer. ^{1}H-NMR and 2D NMR spectra were measured on a Bruker AV-600 spectrometer, while ^{13}C-NMR spectra were measured on a Bruker AV-400 spectrometer. CD spectra were recorded on MOS 450 (Bio-Logic, France). HRESIMS data were determined by an Agilent Q-TOF 6520 mass spectrometer. Open column chromatography (CC) was performed using silica gel (200–300 mesh, Qingdao Haiyang Chemical Group Corp., Qingdao, China), ODS (50 μm, YMC, Japan), and HW-40 (Tosoh, Japan). Thin-layer chromatography (TLC) was performed using precoated silica gel plates (silica gel GF254, 1 mm, Yantai).

Isolation and Identification of AD16

The detailed collection and isolation procedures of the bacteria from human fecal specimens were done as previously reported (Zhuang et al., 2019). A colony of bacteria that showed potent anticancer activities was identified as closely related to *Streptomyces* and was given the strain name AD16 (gene bank No. KU883604.1). This strain was isolated from the fecal specimen of a healthy girl (5 years old) and stocked in the Laboratory of Genomics Research Center of Harbin Medical University (Harbin, China). All the experiments of the study were consistent with standard biosecurity and institutional safety procedures. All microbes were handled in the BSL-2 laboratory.

Cell Culture and CCK-8 Assay

Human solid cancer cell lines, including cervical cancer HeLa, ovarian cancer A2780, lung cancer A549, and colorectal cancer HCT116, were cultured in Dulbecco's modified Eagle's medium (DMEM) with 10% fetal bovine serum. Ovarian cancer cell lines ES-2 and OV-90 were cultured in McCoy's 5A medium with 10% fetal bovine serum. All the cultures were maintained in an incubator at 37°C with 5% CO_2 in a humidified atmosphere.

Cell viability was measured by the Cell Counting Kit (CCK)-8 (Dojindo, Tokyo, Japan) assay. A549 cells (5.0×10^3 cells per well) were seeded into 96-well plates (Corning, NY) and cultured for 24 h. The cells were then incubated with fresh media containing the compounds under study at various concentrations for 24, 48, or 72 h. After incubation, the media were removed and the wells were washed twice with PBS to remove non-adherent cells. Then, 100 μL fresh medium and 10 μL CCK-8 were added to each well at the indicated time points. The cells were further incubated at 37°C for 60 min. The absorbance of the samples was measured at 492 nm using a Bio-Rad model 3550 microplate reader (Richmond, CA).

Morphological Assessment

Morphological changes of cells treated with AD16 supernatant or metabolites were inspected by phase-contrast inverted microscopy (Zeiss Axiocam ERc 5s, Germany). The performance of the experiments and the determination of experimental results were completed blindly and separately by at least two different persons.

Cell Apoptosis Analysis

The cells were incubated in the medium containing culture supernatant of AD16 for 6 h. The cells were harvested, washed twice with cold 1 × PBS, and re-suspended in 100 μL 1 × binding buffer at a density of 1×10^5 cells/mL. The cells were then stained with 5 μL Annexin V and 5 μL PI (BD Biosciences) for 15 min in dark condition at room temperature. After staining, we added 400 μL of 1 × binding buffer to each tube. The samples were subjected to analysis by flow cytometry (BD FACSCanto^{TM} II). The early apoptosis was evaluated based on the percentage of Annexin V–positive and PI-negative cells, while the late apoptosis

was evaluated based on the percentage of Annexin V–positive and PI-positive cells.

Statistical Analysis

Statistical analysis was presented as the mean ± standard deviation (SD) of at least three independent experiments. Student's t-test, chi-square test, and Spearman's rank correlation analysis were used to assess the means of the different samples with SPSS statistical software version 17.0 and GraphPad Prism software. The statistical significance was accepted at $p < 0.05$. Our study closely followed the line of randomness and preciseness to ensure reproducibility.

Fermentation, Extraction, and Isolation of AD16

Strain AD16 was inoculated in 500 ml conical flasks (497 bottles in total) containing 300 ml GRC1 medium (20 g of soluble starch, 1 g of KNO_3, 0.5 g of KH_2PO_4, 0.5 g of $MgSO_4$ $7H_2O$, and 0.5 g of NaCl in 1 L of distilled water) for 15 days at 150 rpm/min at room temperature. D101 macroporous resin was soaked with the whole culture for 24 h and then eluted with water and EtOH–H_2O (95:5, V/V), respectively. The EtOH–H_2O eluate was concentrated by a rotary evaporator in vacuum to afford 33.8 g of dry material. An aliquot (31.7 g) was applied to an ODS column (3.5*46 cm; 50 μm) and eluted with MeOH–H_2O in gradient to give 13 fractions (K1–K13).

Fraction K4 [MeOH–H_2O (20:80, V/V) eluate, 0.7 g] was subjected to HW-40 CC, eluted with MeOH–H_2O in gradient, to yield 11 subfractions (K4A–K4K). Subfraction K4J [MeOH–H_2O (100:0, V/V) eluate, 15.6 mg] was purified by preparative HPLC (Cosmosil C18, 5 μm, 20 × 250 mm, Cosmosil) with MeOH–H_2O (15:85, V/V) to afford compound 6 (5.2 mg, t_R = 22.5 min).

Fraction K8 [MeOH–H_2O (25:75–30:70, V/V) eluate, 0.9 g] was subjected to HW-40 CC, eluted with MeOH–H_2O in gradient, to yield 11 subfractions (K8A–K8K). Subfraction K8D [MeOH–H_2O (10:90, V/V) eluate, 158.8 mg] was subjected to silica-gel CC eluted with CH_2Cl_2–MeOH in gradient to yield nine subfractions (K8D1–K8D9). Subfraction K8D2 [CH_2Cl_2–MeOH (25:1, V/V) eluate, 49.9 mg] was subjected to Sephadex LH-20 CC eluted with MeOH to yield three subfractions (K8D2A–K8D2C). K8D2B (MeOH eluate, 9.3 mg) was purified by silica-gel CC with a cyclohexane–acetone gradient to yield four subfractions (K8D2B1–K8D2B4). After combining K8D2B2 [cyclohexane–acetone (7:2, V/V) eluate, 4.8 mg] and K8D2C (MeOH eluate, 4.8 mg) to the new fraction, it was further purified by preparative HPLC (Cosmosil C18, 5 μm, 10 × 250 mm, Cosmosil) with MeOH–H_2O (18:82, V/V) to afford compound 4 (2.8 mg, t_R = 54 min). Fraction K8K [MeOH–H_2O (50:50–100:0, V/V) eluate, 12.6 mg] was purified by Sephadex LH-20 CC eluted with MeOH to afford compound 10 (1.3 mg).

Fraction K9 [MeOH–H_2O (30:70–50:50, V/V) eluate, 0.6 g] was subjected to HW-40 CC, eluted with MeOH–H_2O in gradient, to yield 12 subfractions (K9A–K9L). Subfraction K9B [MeOH–H_2O (15:85, V/V) eluate, 49.6 mg] was subjected to silica-gel CC with cyclohexane–acetone to yield three subfractions (K9B1–K9B3). The fine fraction K9B2 [cyclohexane–acetone (1:1, V/V) eluate, 10.0 mg] was purified by Sephadex LH-20 CC eluted with MeOH to afford compound 5 (3.0 mg). Fraction K9C [MeOH–H_2O (30:70, V/V) eluate, 25.5 mg] was purified by preparative HPLC (Cosmosil C18, 5 μm, 10 × 250 mm, Cosmosil) with MeOH–H_2O (20:80, V/V) to afford compound 14 (4.7 mg, t_R = 66.0 min). Fraction K9H [MeOH–H_2O (30:70, V/V) eluate, 24.8 mg] was purified by Sephadex LH-20 CC eluted with MeOH to afford compound 8 (3.1 mg).

Fraction K10 [MeOH–H_2O (50:50–70:30, V/V) eluate, 1.5 g] was subjected to HW-40 CC, eluted with MeOH–H_2O in gradient, to yield 17 subfractions (K10A–K10Q). Subfraction K10J [MeOH–H_2O (30:70, V/V) eluate, 18.9 mg] was subjected to silica-gel CC eluted with a CH_2Cl_2–MeOH gradient to afford compound 2 [CH_2Cl_2–MeOH (25:1, V/V) eluate, 2.0 mg]. Subfraction K10M [MeOH–H_2O (50:50, V/V) eluate, 23.2 mg] was subjected to silica-gel CC with cyclohexane–acetone (7:1, V/V) to afford compound 11 (2.4 mg) and yield two subfractions (K10M1-K10M2). The fine fraction K10M1 [cyclohexane–acetone (7:1, V/V) eluate, 7 mg] was purified by preparative TLC with CH_2Cl_2–MeOH (20:1, V/V) to afford compound 9 (3.5 mg).

Fraction K11 [MeOH–H_2O (70:30, V/V) eluate, 6.9 g] was subjected to HW-40 CC, eluted with MeOH–H_2O in gradient, to yield nine subfractions (K11A–K11I). Subfraction K11C [MeOH–H_2O (40:60, V/V) eluate, 1.3 g] was subjected to HW-40 CC eluted with an MeOH–H_2O gradient to yield nine subfractions (K11C1–K11C9). Fraction K11C4 [MeOH–H_2O (15:85, V/V) eluate, 159.5 mg] was subjected to Sephadex LH-20 CC eluted with MeOH to yield 10 subfractions (K11C4A–K11C4J). Subfraction K11C4C (MeOH eluate, 24.2 mg) was purified by preparative HPLC (Cosmosil C18, 5 μm, 10 × 250 mm, Cosmosil) with MeOH–H_2O (48:52, V/V) to afford compound 13 (2.0 mg, t_R = 115.0 min). Subfraction K11C4D (MeOH eluate, 18.3 mg) was purified by preparative HPLC (Cosmosil C18, 5 μm, 10 × 250 mm, Cosmosil) with MeOH–H_2O (48:52, V/V) to afford compound **7** (2.4 mg, t_R = 39.0 min). Subfraction K11C4F (MeOH eluate, 21.7 mg) was purified by preparative HPLC (Cosmosil C18, 5 μm, 20 × 250 mm, Cosmosil) with MeOH–H_2O (43:57, V/V) to afford compound 3 (2.1 mg, t_R = 46.0 min). Subfraction K11C9 [MeOH–H_2O (50:50, V/V) eluate, 82.4 mg] was subjected to silica-gel CC with a cyclohexane–acetone gradient to yield eight subfractions (K11C9A–K11C9H). The fine fraction K11C9D [cyclohexane–acetone (4:1, V/V) eluate, 3.4 mg] was purified by preparative TLC with cyclohexane–acetone (1:1, V/V) to afford compound 1 (1.8 mg). Fraction K11F [MeOH–H_2O (60:40, V/V) eluate, 0.8 g] was purified by preparative HPLC (Cosmosil C18, 5 μm, 20 × 250 mm, Cosmosil) with MeOH–H_2O (77:23, V/V) to afford compound 12 (22.1 mg, t_R = 40.0 min).

Streptonaphthalene A (1)

White amorphous solid; $[\alpha]^{20}_D$ 98 (*c* 0.1, MeOH); UV (MeOH) λ_{max} (log) 230 (4.22) nm, 275 (3.94) nm; CD (MeOH) 230

TABLE 1 | ^{1}H-NMR (600 MHz) and ^{13}C-NMR (100 MHz) data for compounds 1 and 2 (in CD_3OD).

Position	Compound 1		Compound 2	
	δ_H	δ_C	δ_H	δ_C
1		198.7		198.8
2	2.60 (1H, dd, *J* = 16.3, 8.0 Hz, 2α) 2.82 (1H, dd, *J* = 16.3, 3.8 Hz, 2β)	50.1	2.61 (1H, dd, *J* = 16.2, 7.8 Hz, 2α) 2.86 (1H, dd, *J* = 16.2, 3.5 Hz, 2β)	50.1
3	4.24 (1H, m)	66.5	4.25 (1H, m)	66.5
4	2.92 (1H, dd, *J* = 15.9, 7.5 Hz, 4α) 3.16 (1H, dd, *J* = 15.9, 3.8 Hz, 4β)	40.5	2.92 (1H, dd, *J* = 16.1, 7.6 Hz, 4α) 3.16 (1H, dd, *J* = 16.1, 3.6 Hz, 4β)	40.5
4a		147.3		147.4
5	6.63 (1H, s)	114.6	6.63 (1H, s)	114.7
6		158.5		158.8
7		132.0		132.0
8		145.5		145.2
8a		124.0		124.0
9		207.7		207.7
10	2.47 (3H, s)	32.6	2.48 (3H, s)	32.6
11	2.89 (1H, m) 2.83 (1H, m)	30.5	2.89 (2H, m)	30.0
12	1.35 (2H, m)	41.3	1.51 (1H, m) 1.32 (1H, m)	35.8
13	1.62 (1H, m)	30.0	1.66 (1H, m)	37.5
14	0.92 (3H, d, *J* = 6.7 Hz)	22.6	3.35 (1H, m) 3.48 (1H, m)	68.1
15	0.92 (3H, d, *J* = 6.7 Hz)	22.6	0.96 (3H, d, *J* = 6.7 Hz)	16.8

TABLE 2 | ^{1}H-NMR (600 MHz) and ^{13}C-NMR (100 MHz) data for compounds 3–5 (in CD_3OD).

Position	Compound 3		Compound 4		Position	Compound 5	
	δ_H	δ_C	δ_H	δ_C		δ_H	δ_C
2		172.8		172.8	1	3.20 (1H, t, *J* = 7.1 Hz)	78.7
3		131.5		131.6	2	1.75 (2H, m)	35.0
4		160.2		160.2	3	3.67 (1H, m)	72.1
5	5.84 (1H, s)	99.7	5.84 (1H, s)	99.2	4	2.39 (1H, m)	34.0
1′	4.47 (1H, t, *J* = 6.7 Hz)	67.2	4.52 (1H, t, *J* = 6.3 Hz)	66.9	5	1.12 (1H, dd, *J* = 10.6, 4.1 Hz)	51.0
2′	1.76 (2H, m)	34.3	1.74 (2H, m)	37.0	6	4.01 (1H, t, *J* = 10.6 Hz)	70.1
3′	1.32 (1H, m) 1.17 (1H, m)	35.5	1.39 (1H, m) 1.48 (1H, m)	21.3	7	1.46 (1H, m)	55.4
4′	1.56 (1H, m)	28.9	1.49 (2H, m)	44.3	8	1.62 (1H, dq, *J* = 13.3, 3.5 Hz) 1.17 (1H, m)	23.4
5′	0.91 (3H, d, *J* = 6.6 Hz)	22.8		71.2	9	1.83 (1H, dt, *J* = 12.8, 3.5 Hz) 1.04 (1H, dt, *J* = 12.8, 3.5 Hz)	40.7
6′	0.91 (3H, d, *J* = 6.6 Hz)	22.7	1.17 (3H, s)	29.0	10		40.5
7′	2.10 (3H, s)	11.5	1.17 (3H, s)	28.9	11		75.5
8′			2.11 (3H, s)	11.5	12	1.21 (3H, s)	29.8
					13	1.27 (3H, s)	24.1
					14	0.91 (3H, d, *J* = 7.4 Hz)	8.5
					15	0.88 (3H, s)	15.6

(Δε −2.63), 296 (Δε −1.07) nm; IR 3354 cm^{-1}, 2,957 cm^{-1}, 2,930 cm^{-1}, 2,868 cm^{-1}, 1,694 cm^{-1}; HRESIMS *m/z* 289.1448 $[M-H]^-$ (calcd. for $C_{17}H_{21}O_4$, 289.1434); for ^{1}H-NMR (CD_3OD, 600 MHz) and ^{13}C-NMR (CD_3OD, 100 MHz) data, see **Table 1**.

Streptonaphthalene B (2)

White amorphous solid; $[\alpha]^{20}_D$ −34 (*c* 0.1, MeOH); UV (MeOH) λ_{max} (log) 226 (4.33) nm, 278 (4.17) nm; CD (MeOH) 226 (Δε −3.76), 286 (Δε −1.33) nm; IR 3393 cm^{-1}, 2,955 cm^{-1}, 2,926 cm^{-1}, 2,874 cm^{-1}, 1,697 cm^{-1}; HRESIMS *m/z* 305.1396 $[M-H]^-$ (calcd. for $C_{17}H_{21}O_5$, 305.1383); for ^{1}H-NMR (CD_3OD, 600 MHz) and ^{13}C-NMR (CD_3OD, 100 MHz) data, see **Table 1**.

Pestaloficin F (3)

Colorless oil; $[\alpha]^{20}_D$ 73 (*c* 0.1, MeOH); UV (MeOH) λ_{max} (log) 202 (4.26) nm, 231 (3.61) nm; CD (MeOH) 202 (Δε −5.63), 231 (Δε 1.81) nm; IR 3287 cm^{-1}, 2,955 cm^{-1}, 2,868 cm^{-1}, 1749 cm^{-1}; HRESIMS *m/z* 213.1127 $[M-H]^-$ (calcd. for $C_{11}H_{17}O_4$, 213.1121); for ^{1}H-NMR (CD_3OD, 600 MHz) and ^{13}C-NMR (CD_3OD, 100 MHz) data, see **Table 2**.

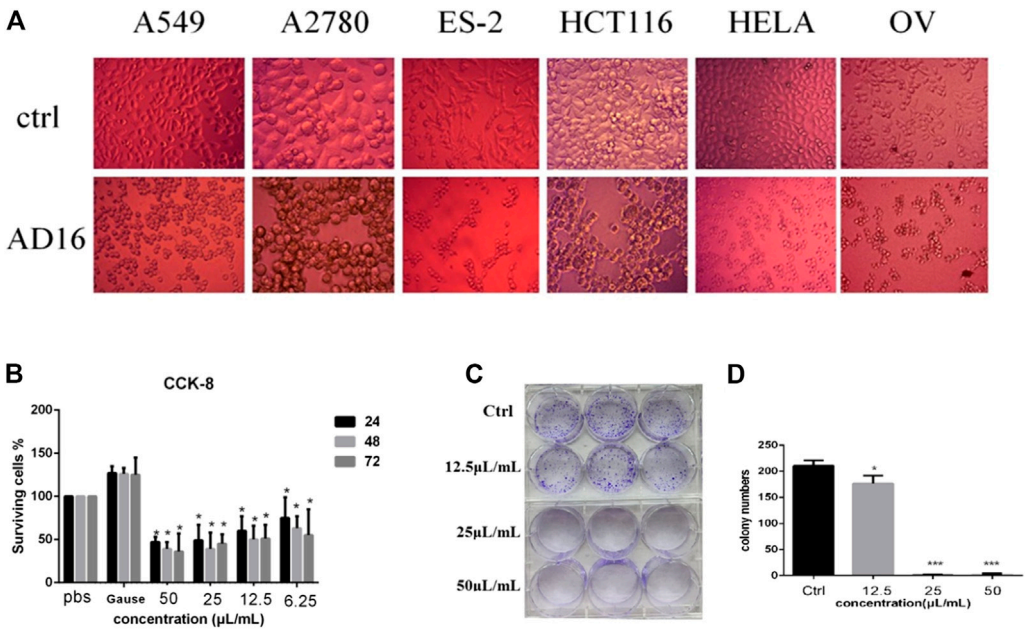

FIGURE 1 | (A) Significant changes in cell morphology were observed under the microscope after AD16 metabolites were added in various cancer cells (×400). **(B)** CCK-8 assay results of AD16 metabolites in A549 cells. **(C)** Results of colony formation of A549 cells incubated with AD16 metabolites for 12 h. **(D)** The paired-sample t-test was used to analyze whether there was a significant difference in the number of colony formation between each AD16-added group and control (*$p < 0.05$, ***$p < 0.001$). Ctrl, control.

Pestaloficin G (4)

Colorless oil; [α] $^{20}_{D}$ 117 (*c* 0.1, MeOH); UV (MeOH) λ_{max} (log) 206 (4.06) nm, 229 (3.54) nm; CD (MeOH) 206 (Δε −8.60), 229 (Δε 5.33) nm; IR 3372 cm^{-1}, 2,928 cm^{-1}, 2,860 cm^{-1}, 1,599 cm^{-1}; HRESIMS *m/z* 243.1236 $[M-H]^-$ (calcd. for $C_{12}H_{19}O_5$, 243.1227); for ^{1}H-NMR (CD_3OD, 600 MHz) and ^{13}C-NMR (CD_3OD, 100 MHz) data, see **Table 2**.

Eudesmanetetraiol A (5)

Yellow crystal; [α] $^{20}_{D}$ 96 (*c* 0.1, MeOH); IR 3443 cm^{-1}; HRESIMS *m/z* 295.1873 $[M + Na]^+$ (calcd. for $C_{15}H_{28}O_4Na$, 295.1880); for ^{1}H-NMR (CD_3OD, 600 MHz) and ^{13}C-NMR (CD_3OD, 100 MHz) data, see **Table 2**.

Target Network Analysis

The ingredients isolated were imported into the PubChem database and ChemBio3D Ultra 14.0, and the 3D molecular structures were exported in the form of SDFs. The targets were retrieved from the online target prediction platform PharmMapper (http://www.lilab-ecust.cn/pharmmapper/). Human species was used for target prediction, and the targets with Norm Fit ≥ 0.75 were collected. Thereafter, the targets were converted to gene names using the UniProt Knowledgebase (UniProtKB, http://www.uniprot.org/), and species were restricted to "*Homo sapiens*." Meanwhile, the NSCLC-related targets were obtained from the DisGeNET database (http://www.disgenet.org/) and TTD (http://database.idrb.cqu.edu.cn/TTD/). The STRING database (version 11.0, https://string-db.org/) was used to explore the protein–protein interactions (PPIs), and protein interactions with a confidence score > 0.4 were selected in the designed setting after eliminating duplicates and independent ones. Cytoscape software (version 3.7.2) was applied to construct the chemical–target network and protein–protein interaction (PPI) network. All genes were subjected to pathway enrichment analysis (KEGG analysis) using DAVID Bioinformatics Resources 6.8, and those pathway terms with a *p*-value < 0.05 were regarded as significant and interesting (Zhang et al., 2021).

RESULTS AND DISCUSSIONS

Cytotoxic Effects of the Extract of AD16

The anticancer activity of the EtOAc extract of AD16 was investigated. Strain AD16 exhibited a broad killing spectrum of cancers including lung cancer (A549), ovarian cancer (A2780, ES-2/OV-90), colorectal cancer (HCT116), and cervical cancer (HeLa) at the concentration of 5 μL/ml (**Figure 1A**). The CCK-8 result of A549 cells incubated with AD16 demonstrated that the effects of AD16 were dose- and time-dependent against A549 as judged by cell proliferation percentages in comparison with the control (**Figure 1B**). The colony formation activity against A549 cells was also investigated, which indicated that AD16 could strongly inhibit colony formation of the A549 cell line (**Figures 1C,D**). To determine the possible mechanism of the anticancer effects of AD16, we detected the induction to apoptosis after treatment with AD16. Six hours after treatment with different concentrations, cells were double-stained with Annexin V and PI and subjected to flow cytometry to quantitatively analyze the apoptotic effects. As

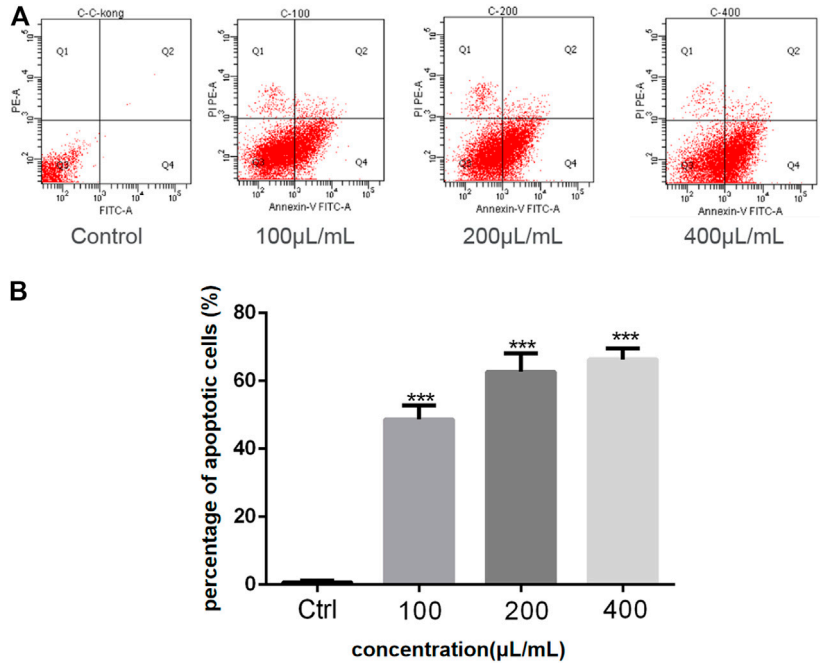

FIGURE 2 | (A) The percent of apoptosis in A549 cells was evaluated by flow cytometry; **(B)** Student's t-test was used to analyze the differences between the control group and the AD16 group (***$p < 0.001$). Ctrl, control.

illustrated in **Figure 2A**, the percentages of total apoptotic cells, including the early apoptotic portion (Annexin V positive) and the late apoptotic portion (Annexin V and PI positive), were dose-dependently increased with increasing concentrations of AD16 in the A549 cell line (**Figure 2B**). These results suggested that the AD16 culture could suppress cell proliferation by inducing cell apoptosis.

Cytotoxic Effect of the Subfractions

Based on bioactivity-guided isolation, a large quantity of the AD16 extract was partitioned with ODS by MeOH–H_2O gradients. All the fractions were examined to determine their anticancer effects at 100 μl/ml (**Figures 3A,B**). When compared to other fractions, fractions 9–11 showed the highest inhibitory activities (**Figure 3B**). Eventually, we isolated and identified 14 compounds, including five new compounds and nine previously known ones.

Structural Determination of Compounds From AD16

Compound 1 was isolated as a white amorphous solid. The negative-ion ESIMS spectrum showed a peak at *m/z* 289.1448 [M-H]$^-$, so its molecular formula was unambiguously assigned as $C_{17}H_{22}O_4$ on the basis of HRESIMS data (**Supplementary Figure S1-3**). The ^{1}H NMR spectrum of compound 1 showed one aromatic proton at δ_H 6.63 (1H, s, H-5), an oxygenated methine proton at δ_H 4.24 (1H, m, H-3), and three methyl groups at δ_H 2.47 (3H, s, H-10) and δ_H 0.92 (6H, d, J = 6.7 Hz, H-14/15). ^{13}C NMR spectroscopic data revealed the presence of 17 carbon atoms, including two ketone carbonyls atδ_C 198.7 (C-1), 207.7 (C-9) and six aromatic carbon atoms at δ_C 158.5 (C-6), 147.3 (C-4a), 145.5 (C-8), 132.0 (C-7), 124.0 (C-8a), and 114.6 (C-5). The ^{1}H NMR and ^{13}C NMR data of 1 were very similar to those of the known compound 7-acetyl-3,6-dihydroxy-8-propyl-3,4-dihydronaphthalen-1(2H)-one (Yeo et al., 1998) (**Supplementary Figures S1-1,2**), except that the propyl moiety was replaced by the isopentyl moiety in 1 (**Figure 4**). Moreover, the ^{1}H–^{1}H COSY correlations between δ_H 2.89, 2.83 (H-11) and δ_H 1.35(H-12), δ_H 1.35 (H-12) and δ_H 1.62 (H-13), δ_H 1.62 (H-13), and δ_H 0.92 (H-14/15), as well as the HMBCs between H-14/15 (δ_H 0.92) and C-13 (δ_C 30.0), suggested the isopentyl fragment in 1. The HMBCs between H-11 (δ_H 2.89, 2.83) and C-8 (δ_C 145.5) suggested the isopentyl fragment to be located at C-8 in 1 (**Figure 5**) (**Supplementary Figures S1-4,5,6**). The configuration of the chiral carbon C-3 was assigned as *R* by comparing the CD spectrum (**Figure 6**) (negative Cotton effects at 230 and 296 nm) with that of 7-acetyl-3,6-dihydroxy-8-propyl-3,4-dihydronaphthalen-1(2H)-one (Huasin et al., 2012). Thus, compound 1 was named streptonaphthalene A.

Compound 2 was obtained as a white amorphous solid. Its molecular formula was determined as $C_{17}H_{22}O_5$ on the basis of HRESIMS data, which gave a peak at *m/z* 305.1396 [M-H]$^-$ (**Supplementary Figure S2-3**). The ^{1}H NMR spectrum of compound 2 also showed one aromatic proton at δ_H 6.63 (1H, s, H-5), an oxygenated methine proton at δ_H 4.25 (1H, m, H-3), and two methyl groups at δ_H 2.48 (3H, s, H-10) and δ_H 0.96 (3H, d, J = 6.7 Hz, H-15) (**Supplementary Figure S2-1**). ^{13}C NMR spectroscopic data revealed the presence of 17 carbon atoms. Analysis of ^{1}H NMR and ^{13}C NMR data

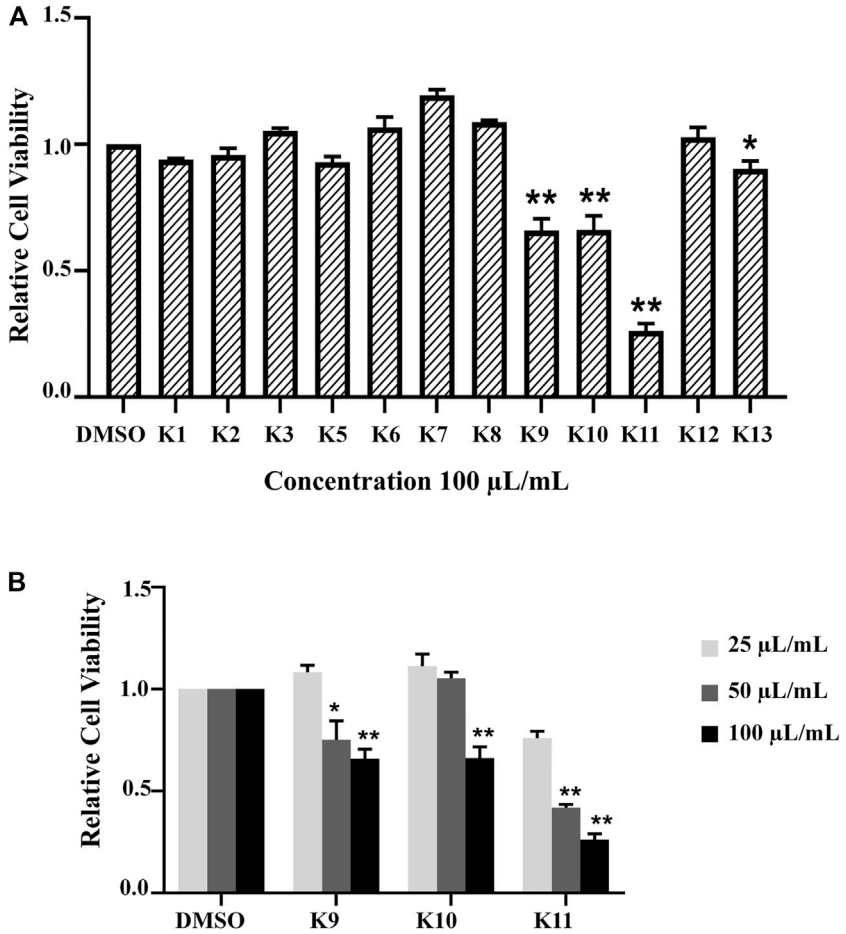

FIGURE 3 | (A) All fractions showed different effects in the A549 cell line according to the CCK-8 assay 24 h after treatment with 100 μL/ml of K1–K13. **(B)** The activity was determined by the OD_{492} value compared with the control group. K9, K10, and K11 inhibited cancer cell activity in a concentration-dependent manner significantly (*$p < 0.05$, **$p < 0.01$).

indicated that compound 2 was similar to 1, except that the methyl group was replaced by the hydroxymethyl moiety (**Supplementary Figures S2-2,4,5,6**). The configuration of the carbon C-3 was deduced to be *R* by comparing the structure with that of 1, which might be derived from the same biosynthesis pathway. Unfortunately, because of its limited amount, the configuration of C-13 was not further determined by the chemical method. Compound 2 was named streptonaphthalene B.

Compound 3 was obtained as colorless oil. Its molecular formula was deduced as $C_{11}H_{18}O_4$, from the HRESIMS signal at *m/z* 213.1127 $[M\text{-}H]^-$ (calcd. for $C_{11}H_{17}O_4$, 213.1121) (**Supplementary Figure S3-3**). The ^1H NMR spectrum of compound 3 showed two oxygenated methine protons at δ_H 5.84 (1H, s, H-5) and δ_H 4.47 (1H, t, J = 6.7 Hz, H-1′) (**Supplementary Figure S3-1**). The ^{13}C NMR spectrum revealed the presence of 11 carbon atoms (**Supplementary Figure S3-2**). Its NMR spectra contained resonances reminiscent of a 5-hydroxy-2(5H)-furanone skeleton carrying an alkane moiety. The furanone moiety was determined by the chemical shifts of the two quaternary carbon atoms δ_C 131.5 (C-3), δ_C 160.2 (C-4), the carboxy carbon (δ_C 172.8, C-2), and the methylene carbon (δ_C 99.7, C-5), as well as the HMBCs of δ_H 5.84 (H-5) with δ_C 172.8 (C-2). ^1H–^1H COSY correlations of δ_H 4.47 (H-1′)/δ_H 1.76 (H-2′), δ_H 1.76 (H-2′)/δ_H 1.32, 1.17 (H-3′), δ_H 1.32, 1.17 (H-3′)/δ_H 1.56 (H-4′), and δ_H 1.56 (H-4′)/δ_H 0.91 (H-5′/6′) enabled the deduction of the C-6 alkane moiety. The HMBCs of δ_H 4.47 (H-1′) with δ_C 131.5 (C-3)/172.8 (C-2)/160.2 (C-4), δ_H 1.76 (H-2′) with δ_C 131.5 (C-3), and δ_H 2.10 (H-7′) with δ_C 160.2 (C-4)/131.5 (C-3)/99.7 (C-5) confirmed the location of the alkane moiety at C-3 and the methyl moiety at C-4 (**Supplementary Figures S3-4,5,6**). In the NOESY spectrum, the correlations of δ_H 2.10 (7′-CH_3) with δ_H 4.47 (H-1′) and δ_H 5.84 (H-5) indicated that the two protons H-1′ and H-5 were in the same orientation (**Supplementary Figure S3-7**). The negative Cotton effect at 202 nm (**Figure 6**) was in good agreement with those of the model compound with 5*R* configuration, indicating the 5*R*, 1′*R* configuration of 3 (Song et al., 2018). Thus, the structure of 3 was assigned as shown in **Figure 4**, named pestaloficin F.

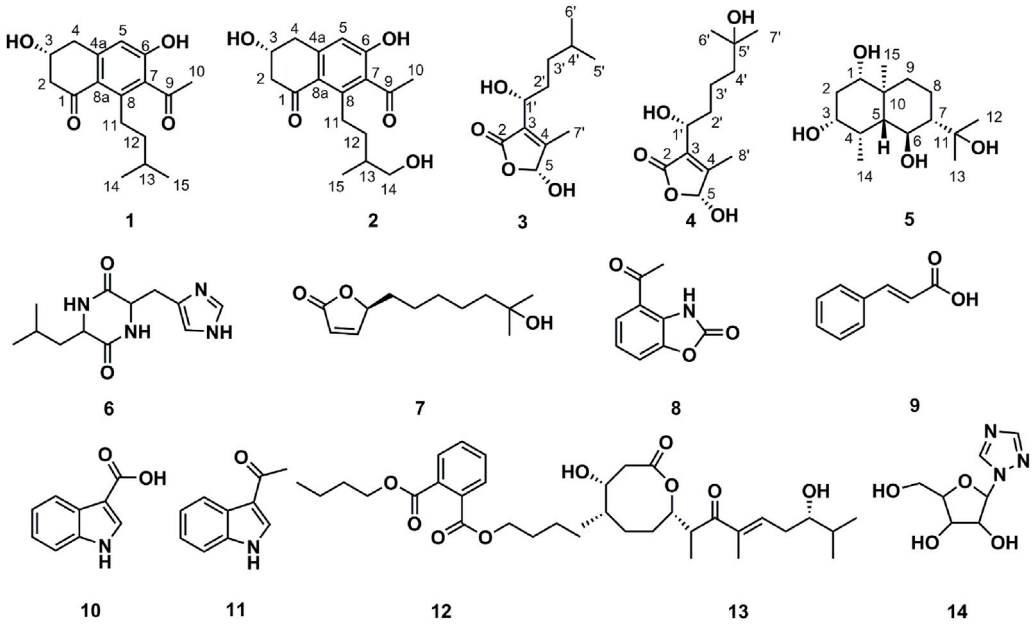

FIGURE 4 | Chemical structures of compounds isolated from AD16.

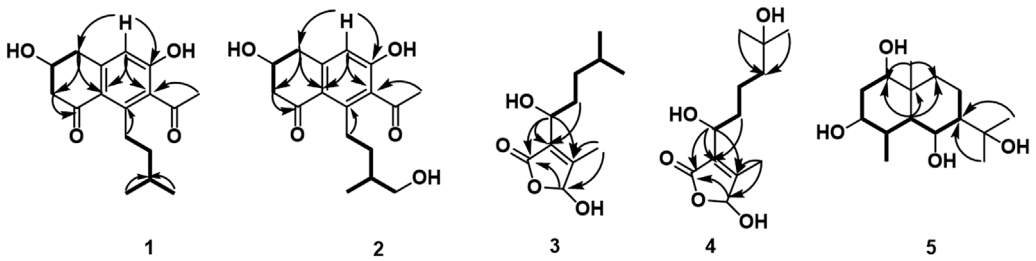

FIGURE 5 | Key ^{1}H–^{1}H COSY (▬) and HMBC (⟶) correlations of compounds 1–5.

Compound 4 was obtained as colorless oil. Its molecular formula was deduced as $C_{12}H_{20}O_5$ by analysis of its HRESIMS data (*m/z* 243.1236 [M-H]$^-$, calcd. for $C_{12}H_{19}O_5$, 243.1227) (**Supplementary Figure S4-3**). The comparison of the NMR spectroscopic data of 4 with those of 3 indicated that 4 also had one butenolide moiety (**Supplementary Figures S4-1,2**). The ^{1}H–^{1}H COSY correlations of δ_H 4.52 (H-1′)/δ_H 1.74 (H-2′), δ_H 1.74 (H-2′)/δ_H 1.39 (H-3′), δ_H 1.39 (H-3′)/δ_H 1.49 (H-4′) and HMBCs of δ_H 1.17 (H-6′/H-7′)/δ_C 71.2 (H-5′), δ_H 1.49 (H-4′)/δ_C 71.2 (H-5′) enabled the deduction of the alkyl moiety (**Figure 5**) (**Supplementary Figure S4-4**). The HMBCs of δ_H 4.52 (H-1′) with δ_C 131.6 (C-3)/172.8 (C-2), δ_H 1.74 (H-2′) with δ_C 131.6 (C-3), and δ_H 2.11 (H-8′) with δ_C 160.2 (C-4)/131.6 (C-3)/99.2 (C-5) confirmed the location of the alkane moiety at C-3 and the methyl moiety at C-4 (**Supplementary Figures S4-5,6,7**). The CD spectrum of 4 showed similar CEs to 3 (**Figure 6**), indicating the 5*R*, 1′*R* configuration of 4. Compound 4 was named pestaloficin G.

Compound 5 was obtained as yellow gum. Its molecular formula was deduced as $C_{15}H_{28}O_4$ by analysis of its HRESIMS data (*m/z* 295.1873 [M + Na]$^+$, calcd. for $C_{15}H_{28}O_4Na$, 295.1880) (**Supplementary Figure S5-3**). The ^{1}H NMR spectrum of 5 showed signals of three three-proton singlets at δ_H 0.88 (3H, s), 1.21 (3H, s), and 1.27 (3H, s) for methyl groups attached to quaternary carbon atoms, one three-proton doublet at δ_H 0.91 (3H, d, *J* = 7.4 Hz) for the methyl group attached to methine carbon, three methylene protons at δ_H 1.04 (1H, dt, *J* = 12.8, 3.5 Hz) and 1.83 (1H, dt, *J* = 12.8, 3.5 Hz), 1.17 (1H, m) and 1.62 (1H, dq, *J* = 13.5, 3.5 Hz), and 1.75 (2H, m), three methine proton (bearing hydroxyl groups) signals at δ_H 3.20 (1H, t, *J* = 7.1 Hz), 3.67 (1H, m), and 4.01 (1H, t, *J* = 10.6 Hz), and three methine proton signals at δ_H 1.12 (1H, dd, *J* = 10.6, 4.1 Hz), 1.46 (1H, m), and 2.39 (1H, m) (**Supplementary Figure S5-1**). The ^{13}C-NMR and DEPT spectra of 5 showed 15 carbon signals (**Supplementary Figure S5-2**). C-1 (δ_C 78.7) was connected to C-2 (δ_C 35.0) to C-8 (δ_C 23.4) based on the ^{1}H–^{1}H COSY correlations of H-1 (δ_H 3.20)/H-2 (δ_H 1.75)/H-3 (δ_H 3.67)/H-4 (δ_H 2.39)/H-5 (δ_H 1.12)/

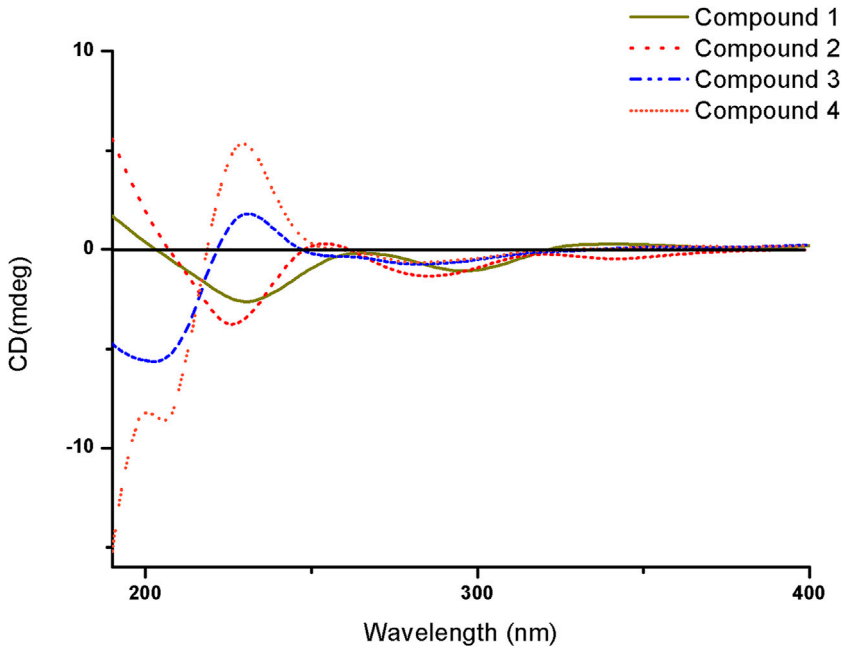

FIGURE 6 | CD spectra of compounds 1–4.

H-6 (δ_H 4.01)/H-7 (δ_H 1.46)/H-8 (δ_H 1.62), and HMBC of H-5 (δ_H 1.12) with C-1 (δ_C 78.7), C-9 (δ_C 40.7), and C-10 (δ_C 40.5), CH_3-15 (δ_H 0.88) with C1 (δ_C 78.7) and C9 (δ_C 40.7), and CH_3-12/13 (δ_H 1.21/1.27) with C7 (δ_C 55.4) enabled the deduction of the planner structure of compound 5 (**Figure 5**) (**Supplementary Figures S5-4,5,6,7**), which had an eudesmane skeleton of sesquiterpene (Katsutani et al., 2020).

The relative stereochemistry of 5 was deduced from the analysis of its NOESY correlations. H-6 (δ_H 4.01) showed strong NOE interactions with CH_3-13 (δ_H 1.27), CH_3-14 (δ_H 0.91), and CH_3-15 (δ_H 0.88); at the same time, NOE correlations were observed in H-1 (δ_H 3.20) with H-3 (δ_H 3.67) and H-5 (δ_H 1.12), but H-1 and H-3 showed no correlations with H-14 and H-15, suggesting that H-6 (δ_H 4.01), CH_3-13 (δ_H 1.27), CH_3-14 (δ_H 0.91), and CH_3-15 (δ_H 0.88) should be placed as α orientation and H-1 (δ_H 3.20), H-3 (δ_H 3.67), H-4 (δ_H 2.39), H-5 (δ_H 1.12), and H-7 (δ_H 1.46) should be placed as β orientation. Thus, the structure of 5 was established unambiguously. Compound 5 was named eudesmanetetraiol A.

Network Pharmacology Analysis

Network pharmacology is a systems biology–based methodology focused on the complex interaction network composed of diseases, genes, protein targets, and drugs using holistic and systemic views in a biological system, offering an effective strategy to uncover the overall action mode of multiple compounds (Bu et al., 2021; Tu et al., 2021). Therefore, to predict the underlying mechanism of AD16, a network pharmacology approach was applied. All the isolated compounds were used for target prediction, and the targets with the probability more than 0.75 were used for analysis. As a result, a total of 89 targets were summarized. The target–compound network was constructed as well (**Figure 7A**). The DisGeNET database and TTD search was performed to predict 592 targets associated with NSCLC. Then, eleven targets were screened out by looking for the overlapping targets from the compound-related targets and NSCLC-related targets (**Figure 7B**). The connections of the targets are shown in **Figure 7C**. Ten targets were identified in the PPI network based on their topological parameters. The gene products AURKA, CHEK1, PGR, ESR1, MAPK1, CASP3, FGFR1, CDK2, KDR, and NOS3 with high node degree were considered the key targets of AD16 against NSCLC. Among them, three targets with a higher degree value among the anti-NSCLC activity of AD16 are caspase 3 (CASP3), estrogen receptor 1 (ESR1), and mitogen-activated protein kinase 1 (MAPK1).

It can be seen from the results of the interactions between components of AD16 and NSCLC targets (**Figure 7D**) that 12 in 14 ingredients could correspond to multiple targets within multiple pathways, which were responsible for the anti-NSCLC effect of AD16. The compounds pestaloficin F (3), streptonaphthalene B (2), and 4-hydroxy-8-[6-hydroxy-1,3,7-trimethyl-2-oxo-oct-3-enyl]-5-methyl-oxocan-2-one (13) having the highest degree value (6, 5, 5), which attribute nodes in the network graph, could be considered the core ingredients in the network with a major anti-NSCLC effect. Over the years, butenolides and tetralones have played an important role in drug discovery, design, and development of plentiful pharmacologically active moieties. A lot of natural butenolides have been isolated from endophytic fungus and other microbial sources, which covered a broad range of therapeutic activities,

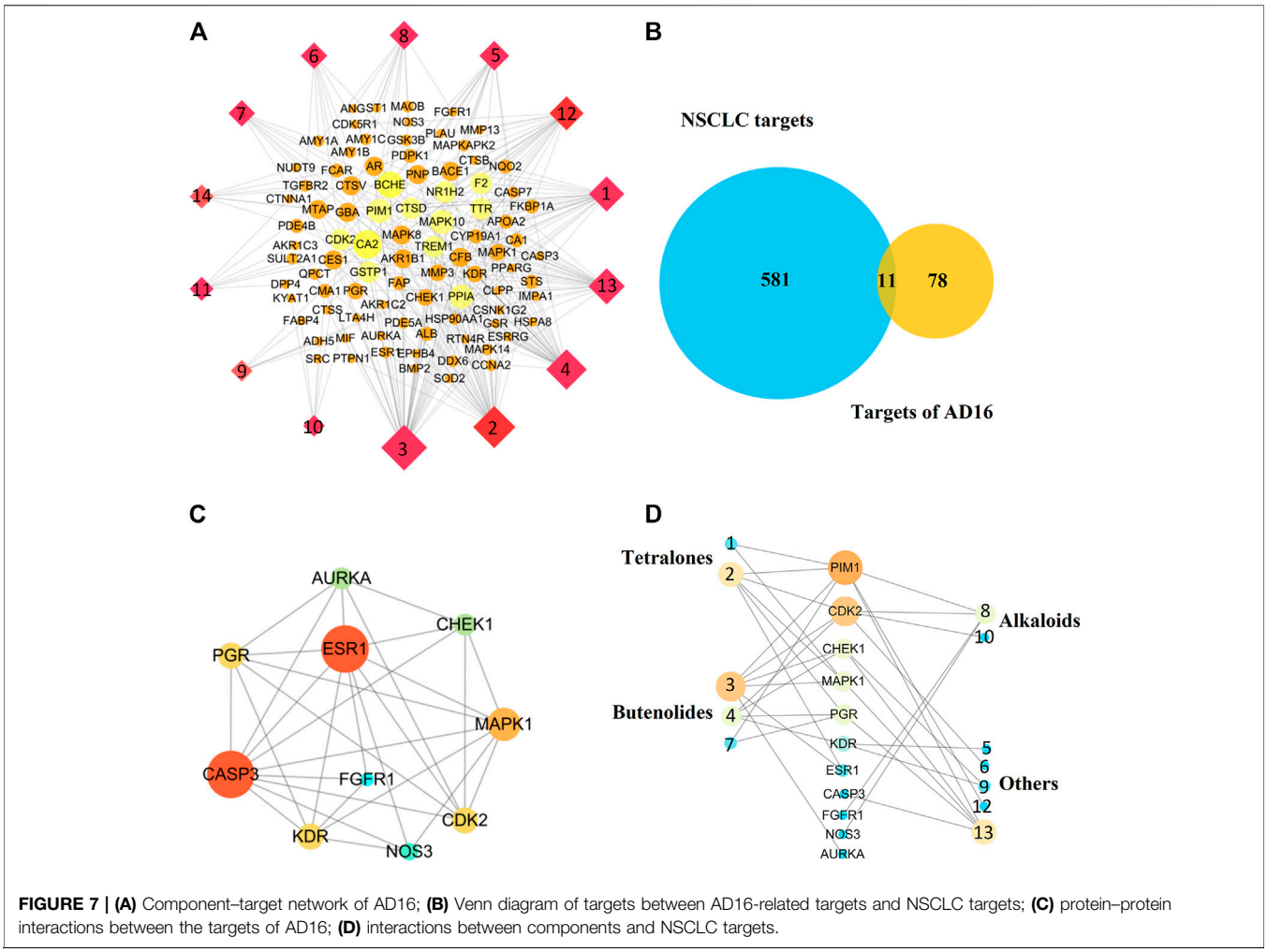

FIGURE 7 | (A) Component–target network of AD16; **(B)** Venn diagram of targets between AD16-related targets and NSCLC targets; **(C)** protein–protein interactions between the targets of AD16; **(D)** interactions between components and NSCLC targets.

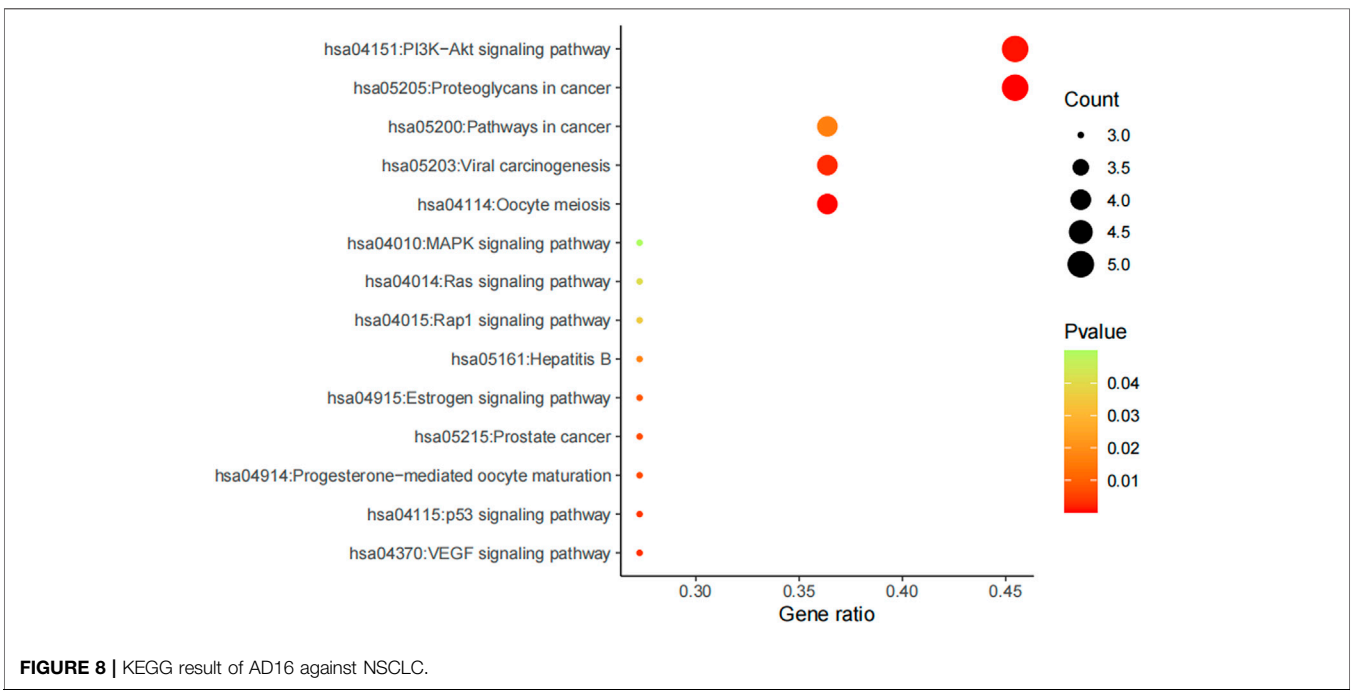

FIGURE 8 | KEGG result of AD16 against NSCLC.

including anticancer effects (Kornsakulkarn.et al., 2011; Kil et al., 2018; Husain et al., 2019; Wang et al., 2019; Yang et al., 2019). Compounds 3 (a new butenolide) and 2 (a new tetralone), proposed to be active constituents of AD16 herein, could act as leading compounds for further structural modification and drug design.

In addition, our result showed that cinnamic acid (9) played function on the target KDR. According to the references, 9 significantly increased the ratio of tumor growth inhibition, mean survival time, and percentage of the lifespan of the treated mice (Almeer et al., 2019). Furthermore, 9 induced angiogenesis *in vivo* and *in vitro*, which is related to VEGF and Flk-1/KDR expressions of endothelial cells (Choi et al., 2009). It was also reported that DBP (12) could inhibit the PI3K/Akt signaling pathway in INS-1 cells to induce cell apoptosis (Li et al., 2021). These results partially supported these biological processes predicted by network pharmacology.

Furthermore, potential regulated biological processes and signaling pathways of AD16 treatment were predicted by KEGG analysis, and anti-NSCLC–related signal pathways were summarized (**Figure 8**). In addition to the PI3K–Akt signaling pathway and proteoglycans in cancers, pathways in cancer, viral carcinogenesis, and oocyte meiosis were the other main patterns for AD16 to achieve its anti-NSCLC effects (Zhang et al., 2017; Chen et al., 2018; Kim et al., 2018).

To summarize, we isolated one bacterial strain AD16 from human gut microbiota that had significant cytotoxic effects on A549. Fourteen compounds were isolated and identified by various chromatographic methods. Among them, five compounds were new, and their structures were determined by NMR, HRESIMS, and CD methods. However, as the amount of components isolated was limited, we inferred the anti-NSCLC mechanism of the AD16 compounds mainly based on network pharmacology. Network pharmacology analysis revealed that the regulation of AD16 on NSCLC could be via acting on multiple targets, multiple pathways, and multiple biological processes. Compounds 3, 2, and 13 might possibly be the key components of AD16 for its anti-NSCLC effects. In addition, the PI3K–Akt signaling pathway and proteoglycans in cancer pathway were the main patterns for AD16 to achieve its anti-NSCLC effects. Our work demonstrated the function mechanism of the human gut bacterial strain AD16 by secondary metabolites' identification, network pharmacology, and experimental validation. It not only expanded the chemical and pharmacological diversities of metabolites from gut microbiota but also recommended that gut microbiota is of great potential for the discovery of new anticancer agents.

DATA AVAILABILITY STATEMENT

We obtained a written informed consent from participant or their guardian, consistent with the 1975 Declaration of Helsinki. All experimental protocols were reviewed and approved by The Ethics Committee, Harbin Medical University, and all experiments were performed in accordance with relevant guidelines and regulations.

ETHICS STATEMENT

The animal study was reviewed and approved by the Harbin Medical University Ethics Review Committee.

AUTHOR CONTRIBUTIONS

CL, S-LL, and Y-HP were responsible for conception and research design. QW, Y-JW, and NM conducted the chemical experiments. YW, Y-JZ, HZ, and X-HZ discussed biological function. All authors read and approved the final manuscript.

FUNDING

This work was supported by Young Talents Start-up Funding (2019-QD-04), National Natural Science Foundation of China (82020108022, 81871623).

SUPPLEMENTARY MATERIAL

The Supplementary Material for this article can be found online at: https://www.frontiersin.org/articles/10.3389/fphar.2021.706220/full#supplementary-material

REFERENCES

Abdul Rahim, M. B. H., Chilloux, J., Martinez-Gili, L., Neves, A. L., Myridakis, A., Gooderham, N., et al. (2019). Diet-induced Metabolic Changes of the Human Gut Microbiome: Importance of Short-Chain Fatty Acids, Methylamines and Indoles. *Acta Diabetol.* 56, 493–500. doi:10.1007/s00592-019-01312-x

Ai, F., Zhang, S., and Li, Y. (2010). Chemical Constituents in Root of Typhoniumgiganteum. *Zhongcaoyao* 41 (2), 201–203.

Almeer, R. S., Aref, A. M., Hussein, R. A., Othman, M. S., and Abdel Moneim, A. E. (2019). Antitumor Potential of Berberine and Cinnamic Acid against Solid Ehrlich Carcinoma in Mice. *Anticancer Agents Med. Chem.* 19, 356–364. doi:10.2174/1871520618666181116162441

Bu, H., Li, X., Hu, L., Wang, J., Li, Y., Zhao, T., et al. (2021). The Anti-inflammatory Mechanism of the Medicinal Fungus Puffball Analysis Based on Network Pharmacology. *Inform. Med. Unlocked* 23, 100549. doi:10.1016/j.imu.2021.100549

Chang, R., Wang, C., Zeng, Q., Guan, B., Zhang, W., and Jin, H. (2013). Chemical Constituents of the Stems of Celastrus Rugosus. *Arch. Pharm. Res.* 36 (11), 1291–1301. doi:10.1007/s12272-013-0145-z

Chen, J., Dong, X., Lei, X., Xia, Y., Zeng, Q., Que, P., et al. (2018). Non-small-cell Lung Cancer Pathological Subtype-Related Gene Selection and Bioinformatics Analysis Based on Gene Expression Profiles. *Mol. Clin. Oncol.* 8, 356–361. doi:10.3892/mco.2017.1516

Cho, K. W., Lee, H. S., Rho, J. R., Kim, T. S., Mo, S. J., and Shin, J. (2001). New Lactone-Containing Metabolites from a marine-derived Bacterium of the Genus Streptomyces. *J. Nat. Prod.* 64 (5), 664–667. doi:10.1021/np000599g

Choi, D. Y., Baek, Y. H., Huh, J. E., Ko, J. M., Woo, H., Lee, J. D., et al. (2009). Stimulatory Effect of Cinnamomum cassia and Cinnamic Acid on Angiogenesis

through Up-Regulation of VEGF and Flk-1/KDR Expression. *Int. Immunopharmacol* 9, 959–967. doi:10.1016/j.intimp.2009.04.001

Fielder, D. A., Collins, F. W., Blackwell, B. A., Bensimon, C., and ApSimon, J. W. (1994). Isolation and Characterization of 4-Acetyl-Benzoxazolin-2-One (4-ABOA), a New Benzoxazolinone from Zea mays. *Tetrahedron Lett.* 35 (4), 521–524. doi:10.1016/s0040-4039(00)75827-8

Furukawa, T., Akutagawa, T., Funatani, H., Uchida, T., Hotta, Y., Niwa, M., et al. (2012). Cyclic Dipeptides Exhibit Potency for Scavenging Radicals. *Bioorg. Med. Chem.* 20 (6), 2002–2009. doi:10.1016/j.bmc.2012.01.050

Hasan, R. A., Koh, A. Y., and Zia, A. (2020). The Gut Microbiome and Thromboembolism. *Thromb. Res.* 189, 77–87. doi:10.1016/j.thromres.2020.03.003

Husain, A., Khan, S. A., Iram, F., Iqbal, M. A., and Asif, M. (2019). Insights into the Chemistry and Therapeutic Potential of Furanones: A Versatile Pharmacophore. *Eur. J. Med. Chem.* 171, 66–92. doi:10.1016/j.ejmech.2019.03.021

Husain, S. M., Schätzle, M. A., Röhr, C., Lüdeke, S., and Müller, M. (2012). Biomimetic Asymmetric Synthesis of (R)-GTRI-02 and (3S,4R)-3,4-Dihydroxy-3,4-Dihydronaphthalen-1(2h)-Ones. *Org. Lett.* 14 (14), 3600–3603. doi:10.1021/ol301305p

Johnson, C. H., Spilker, M. E., Goetz, L., Peterson, S. N., and Siuzdak, G. (2016). Metabolite and Microbiome Interplay in Cancer Immunotherapy. *Cancer Res.* 76 (21), 6146–6152. doi:10.1158/0008-5472.CAN-16-0309

Kamble, N. R., Pawar, H. R., and Kamble, V. T. (2020). NbCl5 and AgClO4 Promoted Regio-Selective Acylation of Indoles. *Asian J. Chem.* 32 (2), 317–321. doi:10.14233/ajchem.2020.22419

Katsutani, K., Sugimoto, S., Yamano, Y., Otsuka, H., Matsunami, K., and Mizuta, T. (2020). Eudesmane-type Sesquiterpene Glycosides: Sonneratiosides A-E and Eudesmol β-D-glucopyranoside from the Leaves of Sonneratia alba. *J. Nat. Med.* 74, 119–126. doi:10.1007/s11418-019-01353-0

Kil, Y. S., So, Y. K., Choi, M. J., Han, A. R., Jin, C. H., and Seo, E. K. (2018). Cytoprotective Dihydronaphthalenones from the wood of Catalpa Ovata. *Phytochemistry* 147, 14–20. doi:10.1016/j.phytochem.2017.12.009

Kim, Y., Pierce, C. M., and Robinson, L. A. (2018). Impact of Viral Presence in Tumor on Gene Expression in Non-small Cell Lung Cancer. *BMC Cancer* 18, 843. doi:10.1186/s12885-018-4748-0

Kornsakulkarn, J., Dolsophon, K., Boonyuen, N., Boonruangprapa, T., Rachtawee, P., Prabpai, S., et al. (2011). Dihydronaphthalenones from Endophytic Fungus *Fusarium* Sp. BCC14842. *Tetrahedron* 67, 7540–7547. doi:10.1016/j.tet.2011.07.078

Li, L., Wang, F., Zhang, J., Wang, K., De, X., Li, L., et al. (2021). Typical Phthalic Acid Esters Induce Apoptosis by Regulating the PI3K/Akt/Bcl-2 Signaling Pathway in Rat Insulinoma Cells. *Ecotoxicol Environ. Saf.* 208, 111461. doi:10.1016/j.ecoenv.2020.111461

Li, W., Deng, Y., Chu, Q., and Zhang, P. (2019). Gut Microbiome and Cancer Immunotherapy. *Cancer Lett.* 447, 41–47. doi:10.1016/j.canlet.2019.01.015

Liang, D., Leung, R. K., Guan, W., and Au, W. W. (2018). Involvement of Gut Microbiome in Human Health and Disease: Brief Overview, Knowledge Gaps and Research Opportunities. *Gut Pathog.* 10, 3. doi:10.1186/s13099-018-0230-4

Moritz, V. W., Hilde, H., Judith, A. W., Maarten, R. S., Daniel, H. V., and Max, N. (2020). Gut Microbiota: a Promising Target against Cardiometabolic Diseases. *Expert Rev. Endocrinolmetab* 15 (1), 13–27.

Qian, C. D., Fu, Y. H., Jiang, F. S., Xu, Z. H., Cheng, D. Q., Ding, B., et al. (2014). Lasiodiplodia Sp. ME4-2, an Endophytic Fungus from the floral Parts of Viscum Coloratum, Produces Indole-3-Carboxylic Acid and Other Aromatic Metabolites. *BMC Microbiol.* 14, 297. doi:10.1186/s12866-014-0297-0

Song, Y.-P., Miao, F.-P., Fang, S.-T., Yin, X.-L., and Ji, N.-Y. (2018). Halogenated and Nonhalogenated Metabolites from the Marine-Alga-Endophytic Fungus Trichoderma Asperellum Cf44-2. *Mar. Drugs* 16, 266. doi:10.3390/md16080266

Tapiolas, D. M., Roman, M., Fenical, W., Stout, T. J., and Clardy, J. (1991). Octalactins A and B: Cytotoxic Eight-Membered-Ring Lactones from a marine Bacterium, Streptomyces Sp. *J. Am. Chem. Soc.* 113, 4682–4683. doi:10.1021/ja00012a048

Thomas, S., Izard, J., Walsh, E., Batich, K., Chongsathidkiet, P., Clarke, G., et al. (2017). The Host Microbiome Regulates and Maintains Human Health: a Primer and Perspective for Non-microbiologists. *Cancer Res.* 77 (8), 1783–1812. doi:10.1158/0008-5472.CAN-16-2929

Tu, Y. B., Wang, K., Jia, X. J., Tan, L. H., Han, B., Zhang, Q. W., et al. (2021). Isolation and Identification of Antiarthritic Constituents fromGlycine Tabacina and Network Pharmacology-Based Prediction of Their Protective Mechanisms against Rheumatoid Arthritis. *J. Agric. Food Chem.* 68, 10664–10677. doi:10.1021/acs.jafc.0c00878

Wang, Z., Hu, X., Li, Y., Mou, X., Wang, C., Chen, X., et al. (2019). Discovery and SAR Research for Antivirus Activity of Novel Butenolide on Influenza A Virus H1N1 *In Vitro* and *In Vivo*. *ACS omega* 4 (8), 13265–13269. doi:10.1021/acsomega.9b01421

Yang, B., Tong, Q., Lin, S., Guo, J., Zhang, J., Liu, J., et al. (2019). Cytotoxic Butenolides and Diphenyl Ethers from the Endophytic Fungus *Pestalotiopsis* Sp. *Phytochemistry Lett.* 29, 186–189. doi:10.1016/j.phytol.2018.11.021

Yang, S. X., Gao, J. M., Zhang, A. L., and Laatsch, H. (2011). RETRACTED: Sannastatin, a Novel Toxic Macrolactam Polyketide Glycoside Produced by Actinomycete Streptomyces Sannanensis. *Bioorg. Med. Chem. Lett.* 21 (13), 3905–3908. doi:10.1016/j.bmcl.2011.05.028

Yeo, W. H., Yun, B. S., Kim, S. S., Park, E. K., Kim, Y. H., Yoo, I. D., et al. (1998). GTRI-02, a New Lipid Peroxidation Inhibitor from Micromonospora Sp. SA246. *J. Antibiot. (Tokyo)* 51, 952–953. doi:10.7164/antibiotics.51.952

Zhang, F. X., Li, Z. T., Li, M., Yuan, Y. L., Cui, S. S., Chen, J. X., et al. (2021). Dissection of the Potential Anti-influenza Materials and Mechanism of Lonicerae Japonicae Flos Based on *In Vivo* Substances Profiling and Network Pharmacology. *J. Pharm. Biomed. Anal.* 193, 113721. doi:10.1016/j.jpba.2020.113721

Zhang, M., Sai, B., Cao, P., Li, Z., Zhang, L., Shuai, C., et al. (2017). Iron Oxide Nanoparticles Synergize with Erlotinib to Suppress Refractory Non-small Cell Lung Cancer Cell Proliferation through the Inhibition of ErbB/PI3K/AKT and PTEN Activation. *J. Biomed. Nanotechnol* 13, 458–468. doi:10.1166/jbn.2017.2358

Zhou, X., Xu, T., Wen, K., Yang, X. W., Xu, S. H., and Liu, Y. (2010). New N-Acyl Taurine from the Sea Urchin Glyptocidaris Crenularis. *Biosci. Biotechnol. Biochem.* 74 (5), 1089–1091. doi:10.1271/bbb.90848

Zhou, Y. J., Zhao, D. D., Liu, H., Chen, H. T., Li, J. J., Mu, X. Q., et al. (2017). Cancer Killers in the Human Gut Microbiota: Diverse Phylogeny and Broad Spectra. *Oncotarget* 8 (30), 49574–49591. doi:10.18632/oncotarget.17319

Zhuang, H., Cheng, L., Wang, Y., Zhang, Y. K., Zhao, M. F., Liang, G. D., et al. (2019). Dysbiosis of the Gut Microbiome in Lung Cancer. *Front Cel Infect Microbiol* 9, 112. doi:10.3389/fcimb.2019.00112

Conflict of Interest: The authors declare that the research was conducted in the absence of any commercial or financial relationships that could be construed as a potential conflict of interest.

Publisher's Note: All claims expressed in this article are solely those of the authors and do not necessarily represent those of their affiliated organizations, or those of the publisher, the editors, and the reviewers. Any product that may be evaluated in this article, or claim that may be made by its manufacturer, is not guaranteed or endorsed by the publisher.

Advantages of publishing in Frontiers

OPEN ACCESS
Articles are free to read for greatest visibility and readership

FAST PUBLICATION
Around 90 days from submission to decision

HIGH QUALITY PEER-REVIEW
Rigorous, collaborative, and constructive peer-review

TRANSPARENT PEER-REVIEW
Editors and reviewers acknowledged by name on published articles

Frontiers
Avenue du Tribunal-Fédéral 34
1005 Lausanne | Switzerland

Visit us: www.frontiersin.org
Contact us: frontiersin.org/about/contact

REPRODUCIBILITY OF RESEARCH
Support open data and methods to enhance research reproducibility

DIGITAL PUBLISHING
Articles designed for optimal readership across devices

FOLLOW US
@frontiersin

IMPACT METRICS
Advanced article metrics track visibility across digital media

EXTENSIVE PROMOTION
Marketing and promotion of impactful research

LOOP RESEARCH NETWORK
Our network increases your article's readership